TRANSPORTATION RESEARCH
RECORD

No. 1462

Soils, Geology, and Foundations

Compaction of Difficult Soils and Resilient Modulus Testing

A peer-reviewed publication of the Transportation Research Board

TRANSPORTATION RESEARCH BOARD
NATIONAL RESEARCH COUNCIL

NATIONAL ACADEMY PRESS
WASHINGTON, D.C. 1994

Transportation Research Record 1462
ISSN 0361-1981
ISBN 0-309-06068-0
Price: $27.00

Subscriber Category
IIIA soils, geology, and foundations

Printed in the United States of America

Sponsorship of Transportation Research Record 1462

GROUP 2—DESIGN AND CONSTRUCTION OF TRANSPORTATION FACILITIES
Chairman: Charles T. Edson, Greenman Pederson, Inc.

Soil Mechanics Section
Chairman: Michael G. Katona, U.S. Air Force Armstrong Laboratory

Committee on Transportation Earthworks
Chairman: Richard P. Long, University of Connecticut
Loren R. Anderson, Arnold Aronowitz, Jerry A. DiMaggio, Said M. Easa, Eugene C. Geiger, Raymond L. Gemme, John B. Gilmore, Robert D. Holtz, Ilan Juran, Philip C. Lambe, Victor A. Modeer, Jr., K. Jeff Nelson, T. Skep Nordmark, Subal K. Sarkar, Cliff J. Schexnayder, Walter C. Waidelich

Committee on Modelling Techniques in Geomechanics
Chairman: Deborah J. Goodings, University of Maryland
Sreenivas Alampalli, Sangchul Bang, Richard D. Barksdale, Richard J. Bathurst, Joseph A. Caliendo, Jack I. Clark, K. P. George, Mary E. Hynes, William M. Isenhower, Ilan Juran, Victor N. Kaliakin, Stephen Ketcham, Kenneth J. Larsson, Rita B. Leahy, Glen E. Miller, Victor A. Modeer, Jr., Reed L. Mosher, Yacoub M. Najjar, Clifford J. Roblee, Raymond L. Sterling, Harry E. Stewart, Tien H. Wu

Geology and Properties of Earth Materials Section
Chairman: Robert D. Holtz, University of Washington

Committee on Soil and Rock Properties
Chairman: Mehmet T. Tumay, National Science Foundation
Robert C. Bachus, Dario Cardoso de Lima, Umakant Dash, Don J. De Groot, Eric C. Drumm, David J. Elton, Kenneth L. Fishman, Paul M. Griffin, Jr., Robert D. Holtz, An-Bin Huang, Mary E. Hynes, Steven L. Kramer, Rodney W. Lentz, Emir Jose Macari, Paul W. Mayne, Kenneth L. McManis, Victor A. Modeer, Jr., Priscilla P. Nelson, Peter G. Nicholson, Norman I. Norrish, Samuel G. Paikowsky, Sibel Pamukcu, Kaare Senneset, Sunil Sharma, Timothy D. Stark

Transportation Research Board Staff
Robert E. Spicher, Director, Technical Activities
G. P. Jayaprakash, Engineer of Soils, Geology, and Foundations
Nancy A. Ackerman, Director, Reports and Editorial Services
Luanne Crayton, Editor

Sponsorship is indicated by a footnote at the end of each paper. The organizational units, officers, and members are as of December 31, 1993.

Transportation Research Record 1462

Contents

Foreword

The 12 papers in this volume are arranged in two groups. The first six papers present information on various issues that relate to compaction of soils, including the impact of the rock correction equation method on construction control of engineered fills when the material being compacted contains gravel; the importance of properly addressing the purpose of a project in the contract specifications in achieving the desired end results on construction projects; the results of an investigation of instability of embankments built with silty clay, and steps taken to mitigate the problem; the findings from a review and comparison of the compaction criteria used for construction of soil hydraulic barriers, and a discussion of the advantages and disadvantages of the different criteria; the mechanical properties of expanded polystyrene, which is used as a lightweight fill and embankment earth material; and the results of an investigation of the effects of construction methods on widening of roads on soft soils using a small centrifuge.

The second group of six papers covers resilient modulus testing. These papers present information on the effects of overall testing procedures and location of internal deformation measurement devices on resilient modulus values; use of the technique of specimen grouting to the end platens to improve the external deformation measurement; the results of a laboratory investigation of field cores to determine the factors that affect the selection of a design resilient modulus value for the subgrade; findings from a comparative study on bulk stress and universal modeling (the two well-known constitutive equations) of granular subgrade soils; the results of a comparative study of resilient modulus determined by laboratory testing, back calculation using deflection measurements, and using the estimation equation given in the 1986 *AASHTO Guide*.

PART 1

Compaction of Difficult Soils

Rock Correction Issues in Compaction Specifications for High Gravel Content Soil

KENNETH D. WALSH, SANDRA L. HOUSTON, AND GREGORY P. WILSON

Construction control for engineered fills is usually provided by a specification requirement that the in-place dry density of the fill be at least a specified percentage of a reference dry density. The reference dry density is usually measured by a laboratory compaction test, such as the ASTM D698 (Standard Proctor) moisture-density relationship test. The use of laboratory determination of the reference dry density for construction control is based on the implicit assumption that the material compacted in the lab is substantially equivalent to the material compacted in the field. However, when the fill material contains gravel (material coarser than the No. 4 sieve), this assumption is generally not correct. Therefore the contractor and engineer must rely on experience with the performance of high gravel content fills at certain specified percentages of a reference dry density, selecting specification requirements appropriate to individual circumstances. Several methods are available to account for the effect of the coarse fraction on the reference dry density, including various rock correction equations and laboratory scalp-and-replace techniques. Each method may provide a different reference dry density. The impact of the rock-correction method on construction control is addressed. The results of a survey of several large construction companies in the southwestern United States revealed that contractors have a great deal of experience with scalp-and-replace rock correction methods and apparently not as much experience with rock correction equations, particularly in highway work. Although contractors may tend to have most of their experience with scalp-and-replace methods, many engineering testing firms tend toward the use of rock correction equations. Given the significant variation in computed relative compaction that can arise from the different rock correction methods, well-written compaction specifications for high gravel content soils, explicitly stating the technique for rock correction in compaction control, are a must. An understanding of the potential differences in rock correction methods, by contractors and engineers alike, should reduce conflicts and future problems with the compacted fill.

The use of laboratory determination of reference dry density for construction compaction control is based on the implicit assumption that the material compacted in the lab is substantially equivalent to the material compacted in the field. However, when the fill material contains gravel or rock (material coarser than the No. 4 sieve), this assumption is generally not correct. The laboratory molds place a physical restriction on the maximum particle size that can be conveniently tested. Fills containing material with large aggregate can be successfully constructed, but the effect of the coarse fraction on the reference dry density must be considered.

Because several methods are available to account for the effect of the coarse fraction on the reference dry density, the particular technique assumed (or preferred) by the engineer should be clearly stated in the compaction specifications to reduce the potential for conflict with the contractor. The method for accounting for the rock fraction may have a significant impact on the reference density. Because the required compacted fill density is expressed as a percentage of the reference dry density, the rock correction method selected can have a significant impact on the ease with which the contractor can meet a particular specification. Modifications to compaction standards, such as the new ASTM D698–91, could significantly affect compactive effort for soils with high rock content unless required relative compactions are adjusted to account for the differences in methods used to adjust the maximum dry density for rock. Therefore contractors, construction inspectors, and designers should be consistent in the method adopted for rock correction, following the procedure outlined as a part of a well-written specification. The technique for rock correction is often not clearly addressed in compaction specifications, leading to inconsistencies between rock correction techniques assumed for design and those adopted for construction.

K. D. Walsh, Thomas-Hartig and Associates, 7031 W. Oakland St., Chandler, Ariz. 85226. S. L. Houston, Center for Advanced Transportation System Research, Arizona State University, Tempe, Ariz. 85287. G. P. Wilson, Dept. of Construction, Louisiana State University, Baton Rouge, La. 70808–8752.

METHODS FOR OBTAINING A REFERENCE DRY DENSITY

Several methods are available to account for the effect of the coarse fraction on the reference dry density. The available methods may be categorized as rock correction equations and laboratory testing modifications. In rock correction equations, the maximum density of the fine (passing the No. 4 sieve) fraction, the percentage of the fill that is gravel sized, and perhaps the character of the fine fraction are used to produce a mathematical approximation of the maximum dry density of the total soil. In the laboratory, the maximum dry density of the field soil is usually estimated by testing a modified soil in which the gravel fraction is removed from the sample and replaced with material between the No. 4 and 19-mm (0.75-in.) screens (e.g., AASHTO T99, Method C, or the "scalp-and-replace" method). Only in specialized research applications is the maximum dry density obtained by laboratory or field compaction of large samples that include the entire gravel fraction.

Any of the above methods could be used to write an acceptable specification for compaction of materials containing up to about 60 percent large aggregate. However, not all methods produce the same maximum dry density and optimum water content for use as the reference value (*1*). Furthermore the difference from one method to another varies depending on the characteristics, such as the Plasticity Index, of the material passing the No. 4 sieve (*2*).

New ASTM compaction procedures D698–91 and D1557–91 no longer include the scalp-and-replace option. The potential impact of compaction standard modifications on engineering and construction practice must be understood to avoid eventual conflict.

Commonly used rock correction equations are presented in detail in Table 1. These methods require laboratory testing to determine the maximum dry density of the minus No. 4 fraction. As an alter-

TABLE 1 Rock Correction Equations

Equation Designation	Reference	Equation*	Comments
AASHTO-1	AASHTO T224	$D = (1 - P_c)D_f + 0.9P_c(62.4)G_m$	D_f is determined using Method A or B, AASHTO T99 or T180
AASHTO-2	AASHTO T224	$D = \dfrac{62.4}{\dfrac{P_c}{G_m} + \dfrac{62.4(1 - P_c)}{r_a D_f}}$	D_f determined using Method A or B, AASHTO T99 or T180. r_a depends on rock content
ASTM-1	ASTM D4718	$D = \dfrac{62.4}{\dfrac{P_c}{G_m} + \dfrac{62.4(1 - P_c)}{D_f}}$	D_f determined using ASTM D698 or D1557
USBR-1	USBR 5515-89	$D = \dfrac{62.4}{\dfrac{P_c}{G_m} + \dfrac{62.4(1 - P_c)}{r_u D_f}}$	D_f determined using USBR Method 5500-89. r_u depends on rock content and plasticity of fines

*Definitions:

D_f = Maximum dry density of finer material (pcf)

D = Maximum dry density of finer soil (pcf)

P_c = Percent rock by weight (decimal)

G_m = Bulk specific gravity of rock

r_a = Correction factor in AASHTO equation to account for interference of large aggregate

r_u = Correction factor in USBR equation to account for interference of large aggregate

native to using one of the rock correction equations, small-scale compaction tests on material containing particle sizes up to 19 mm (0.75 in.) may be used to determine a reference dry density. The most common laboratory procedure is the scalp-and-replace method, sometimes referred to as the procedure for replacement of oversized aggregate. Scalp-and-replace methods involve the removal of all material larger than 19 mm and replacement with an equal weight of No. 4 to 19-mm material. Commonly used scalp-and-replace methods are ASTM procedure D698–78, Method D, and ASTM D1557–78, Method D, using a mold 15 cm (6 in.) in diameter; AASHTO T99, Method C, using a 10-cm (4-in.) mold; or AASHTO 180, using a mold 15 cm in diameter. The ASTM procedures for scalp-and-replace are no longer included in the ASTM D698–91 and D1557–91 standards, but have been used extensively in the recent past for compaction of fills.

COMPARISON OF REFERENCE DENSITIES

In general, the effect of increasing the rock content of a given soil is to increase the maximum dry density. This occurs because the specific gravity of the rock is usually much higher than that of the bulk material between the rock fragments. The percentage increase in maximum dry density (relative to zero rock content) as a function of percent rock is shown in Figure 1 (*2–4*). Several methods are available for determining maximum dry density of soils containing large aggregate.

The differences among the various methods for obtaining reference dry density have been found to be most significant for clayey soils (*2*). The rock correction equations presented in Table 1 were used to estimate the maximum dry density for five medium- to high-plasticity clayey soils. The maximum dry densities computed using the rock correction equations were compared to each other and to maximum dry densities obtained using the scalp-and-replace procedure (ASTM D698–78, Method D). Rock contents were varied in the laboratory from 10 to 60 percent, and the rock gradations consisted of material between the No. 4 and 19-mm sieves. When the rock contents were changed in the laboratory, the gradation of the minus No. 4 material was left unchanged, and the percentage by weight of the plus No. 4 material was increased or decreased as required.

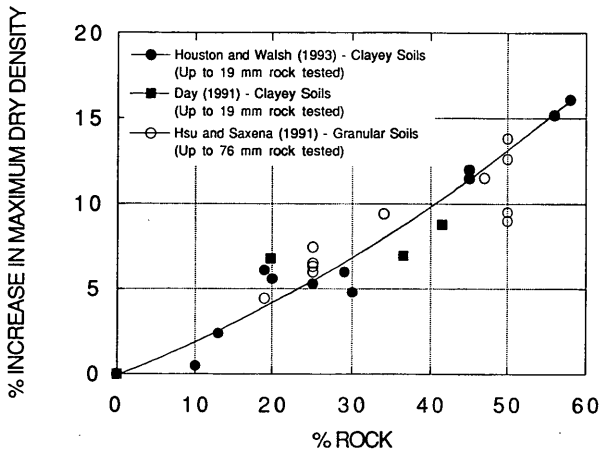

FIGURE 1 Effect of rock on maximum dry density.

In all cases the maximum dry density estimated from the rock correction equations was greater than the maximum dry density obtained from the scalp-and-replace compaction method. The percentage difference by which the rock correction equation exceeds the maximum dry density obtained from ASTM Method D increases with increasing rock content for equations AASHTO-1 and ASTM-1, as shown in Figure 2 and Figure 3. The AASHTO-2 equation incorporates a factor that provides a correction for the increased interference of the coarse aggregate on the compaction of the fine fraction as rock content increases. The AASHTO-2 equation estimates were 1.5 to 3.5 percent higher than the scalp-and-replace at all rock contents. The USBR-1 equation includes different correction factors based on the character of the minus No. 4 fraction. Estimates using the USBR-1 equation were higher than the scalp-and-replace estimates by about 3.0 to 6.5 percent at all rock contents.

The scalp-and-replace dry density was selected as a convenient basis for comparison. This selection should not be construed as an endorsement of the scalp-and-replace method over the other methods. The emphasis here is not on determining which value is the "correct" maximum density for a given fill soil containing large aggregate. In fact, it may well be that the whole question of the "correct" value is without meaning for such fills. The point of a compaction specification written in terms of a maximum density is to achieve a suitably dense fill, and not to achieve a given fraction of the maximum point on a curve developed with a testing method that arguably bears little resemblance to the actual compaction method in the field.

Specifications are written in terms of relative compaction instead of absolute density only because the performance of different soil types tends to be normalized by the maximum dry density. However, when considering the compaction of soils with large aggregate, selection of the rock correction method to establish maximum densities will likely be based on the experience of the designer with rock correction methods and related performance. Equally good specifications could be written with any rock correction method, as long as the differences between the results obtained with the differ-

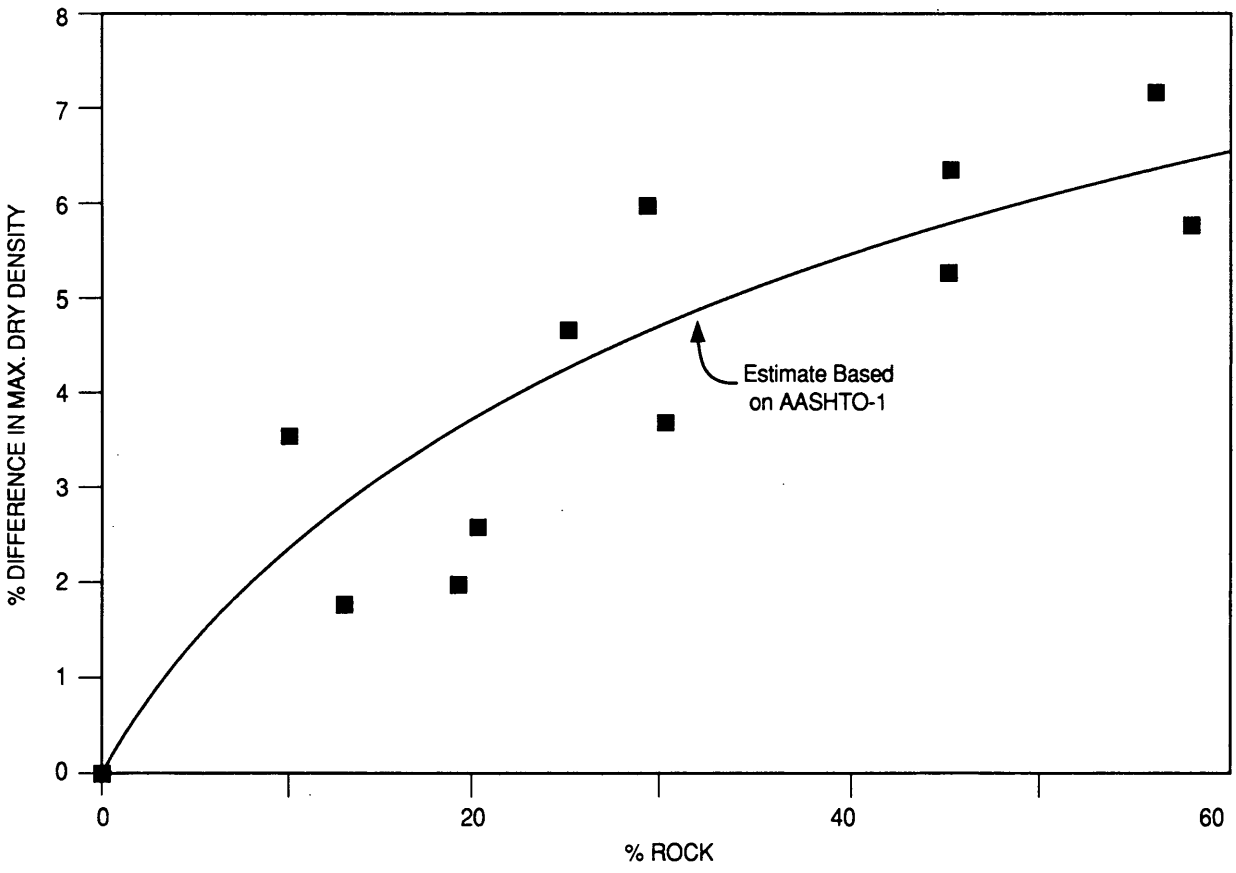

FIGURE 2 Comparison of maximum dry density estimates using scalp-and-replace method and AASHTO-1.

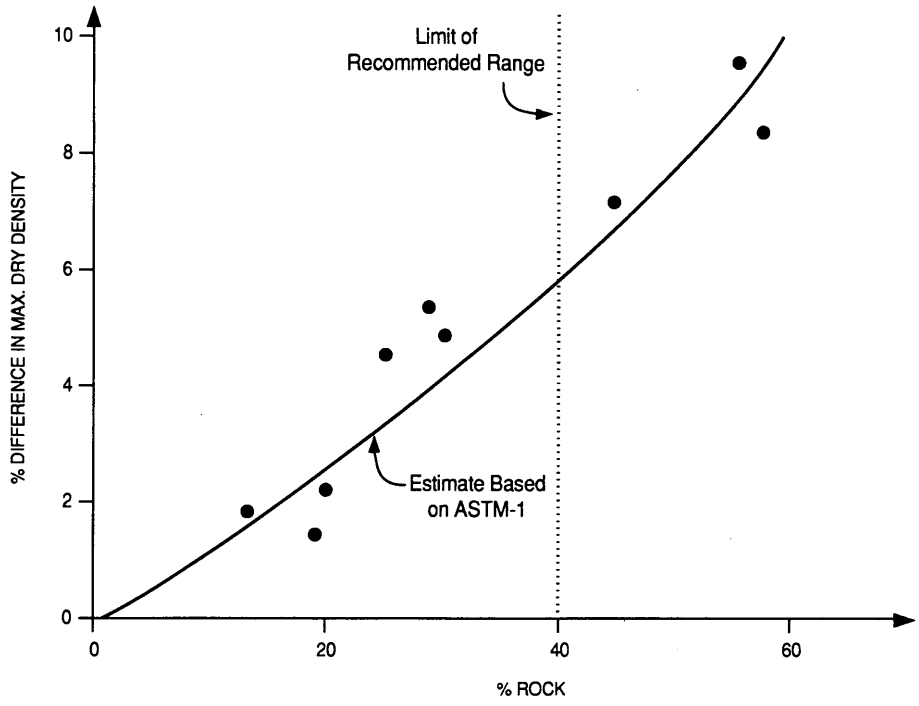

FIGURE 3 Comparison of maximum dry density using scalp-and-replace method and ASTM equation.

ent methods are understood. Therefore although arguments can be made about which method is better, this discussion is dedicated only to pointing out that the methods are different.

IMPLICATIONS FOR CONSTRUCTION

The maximum dry density of a clayey soil was determined at several rock contents, ranging from 0 to 60 percent, using several rock correction equations. The maximum dry density of this clayey soil was also determined using ASTM D698–78, Method D, scalp-and-replace. The clayey soil tested exhibited moderate expansive characteristics, having a plasticity index of 35. A compaction specification of 95 percent of the maximum dry density was selected for discussion purposes. This specification was applied to the maximum dry densities computed using the different rock correction methods to develop the actual required density to be accomplished in the field. The results are shown in Figure 4.

The actual required field density depends significantly on the rock correction method. At about 60 percent rock, for example, the required fill densities range from about 17.9 kN/m^3 (114 pcf) to about 19.6 kN/m^3 (125 pcf). These differences in required fill density amount to differences in the compactive effort that would be required to meet a specification. A contractor with experience with field control by scalp-and-replace methods would therefore experience greater than the expected difficulty in meeting specification requirements when completing a project to be controlled by AASHTO-1, for example. Therefore it is in the contractor's best interest to be aware of the differences and bid accordingly.

IMPLICATIONS FOR FORENSICS

Another area in which the differences between the various large aggregate correction methods can have an impact is in forensic investigations. In the case of fill failure, the issue of compliance with specification will almost certainly arise. It is likely that the in-place density of the fill will be evaluated and compared to the reference dry density to determine the relative compaction of the fill. If the method selected for rock correction in the forensic study is different from that used for construction control, very different conclusions could be reached regarding compliance with the specification.

The differences that could arise in a forensic study are shown in Table 2. The hypothetical 95 percent compaction specification for the clayey soil described in the previous section (Figure 3) was used to produce the estimate of maximum dry density required in situ for the various rock correction methods. The differences in relative compaction that would be attained if a different rock correction procedure were assumed are indicated for 40 percent rock and for 60 percent rock. Note that the entries along the diagonal of Table 2 are all 95 percent because the field control and forensic evaluation are performed with the same rock correction method.

Table 2 shows the differences in the various methods of rock correction. In the hypothetical case, the fill under consideration just reached the specified density by the control method used at the location of the test. Of course, only one actual field density exists for a given test sample. However, depending on the combination of field control and forensic investigation rock correction methods chosen, the computed relative compaction can vary from 89.6 to 100.7 percent at 40 percent rock. For the 60 percent rock case, the computed relative compaction can vary from 86.4 to 104.5 percent, although the actual dry density in situ has only one value. In real fills, sampling difficulties in coarse-grained materials and test scatter could easily widen the range.

The problem created by this variation is that different forensic investigators could come to very different conclusions regarding the degree to which the contractor met, or failed to meet, the specifications for a given project. What's more, these investigators would all

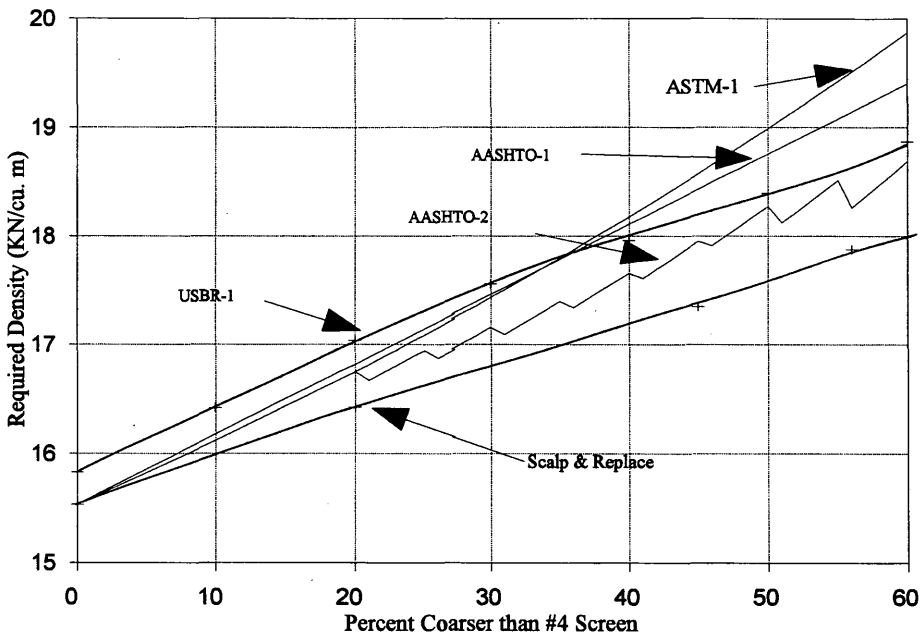

FIGURE 4 Maximum dry density estimates for various rock correction methods.

be considering a fill that passed the specification by the construction control method, at least in this hypothetical case.

As another example, consider a designer experienced with AASHTO-1 who produced a specification recommendation of 95 percent relative compaction and then discovered that the compaction control was monitored by others using the scalp-and-replace method. Because of the differences in the rock correction methods, the fill would be placed at only 88.5 percent relative compaction by AASHTO-1. The behavior of fill materials is closely related to the dry density, and therefore the discrepancy in dry density could have serious consequences with regard to the long-term fill behavior. In general, the use of rock correction equations for determining reference dry density will lead to denser compacted fills for a given specified relative compaction, as compared with scalp-and-replace. In addition, some rock correction equations produce higher reference values than other equations.

ROCK CORRECTIONS IN CONSTRUCTION PRACTICE

Several major construction companies, operating primarily in the southwestern United States, were surveyed to determine typical practices and specifications encountered by contractors dealing with soils containing large aggregate. Contractors surveyed reported that 20 to 90 percent of their compaction projects were on soils containing large aggregate. Thus the technique employed for handling rock correction may have a significant impact on their work.

According to contractors surveyed, compaction specifications often do not address the method to be used for rock correction. However, particularly in regions dominated by gravelly, high rock-content soils, the most common rock correction technique specified is the scalp-and-replace method. For highway applications, AASHTO T99, Method C, is typical, but most private-industry project specifications have used reference dry densities obtained using ASTM D698–78, Method D, scalp-and-replace. The authors have observed essentially no difference in reference dry densities obtained using the AASHTO and the ASTM scalp-and-replace methods for soils containing up to 19 mm (0.75 in.) particle size (*3*).

Contractors reported that the use of rock correction equations was infrequent compared with scalp-and-replace, particularly in highway work. Therefore much of the contractors' experience can be assumed to be with reference dry densities obtained using the laboratory scalp-and-replace method. Further, the rock correction technique (whether explicitly specified or assumed) did not affect the contractors' bids, implying that bidding is done primarily on the basis of experience with similar soils instead of in response to a particular specification. The required percent relative compaction (e.g., 90 versus 95 percent), or whether standard or modified compactive effort is specified, was more likely to affect bidding by contractors than the method specified for rock correction.

Contractors reported that in-place densities were normally determined by nuclear gauge or sand cone methods. Although several government agencies require sand cone tests, the majority of field compaction control is performed using nuclear density determinations. One contractor noted that when scalp-and-replace rock corrections are used, often there is insufficient laboratory testing for determining reference maximum dry density when there are radically changing soil conditions on a given project. The problem arises when numerous soil-type changes occur and there are insufficient laboratory compaction tests (scalp-and-replace) to provide appropriate reference values for all soil types. An inappropriate reference dry density may lead to problems in meeting specifications.

Based on the authors' studies, the scalp-and-replace method has been found to provide lower reference dry densities than any of the rock correction equations evaluated. Therefore contractors accustomed to field control on the basis of scalp-and-replace would likely find it more difficult to meet the specified relative compaction when the reference dry density is based on rock correction equations, such as those called for in the new ASTM D698 and D1557 standard pro-

cedures. The more clayey the fine fraction of material, the greater the differences in rock correction methods are likely to be.

There is a trend with engineering testing firms away from scalp-and-replace rock correction methods in favor of rock correction equations. One advantage to using rock correction equations is that, for a given specified relative compaction, a denser fill tends to be achieved compared to scalp-and-replace methods. However, contractors must recognize the potential differences in compactive effort that may arise from changes in rock correction specifications. In addition, the various rock correction equations lead to different reference dry densities. Ultimately the relative compaction specification specified for any reference dry density should be related to field performance.

The use of nuclear density testing for compaction control is quite prevalent. When nuclear gauges are used to determine in situ densities, it is good practice to calibrate the results with occasional sand cone density tests. In addition, when a nuclear gauge is used to obtain density, the percent rock (e.g., material retained on the No. 4 sieve) should be measured at each density test location so that an appropriate reference dry density (by the selected rock correction method) can be determined. Percent rock at field density test locations is not always measured. Failure to adjust the reference dry density for the appropriate rock content could lead to problems in fill performance if the reference dry density is too low (rock content underestimated), or it may make compaction specifications difficult for the contractor to meet if the reference density is too high (rock content overestimated).

Failure to directly address rock correction in compaction specifications, or failure to apply rock corrections to laboratory determination reference dry density during field inspection, can lead to poor field performance. The density of a compacted fill increases with increasing rock content. Therefore the use of a reference dry density determined at a lower-than-average rock content may result in loose compacted fill with poor engineering performance.

A case history of a rocky compacted fill that experienced hydrocollapse is presented by Kropp, McMahon, and Houston (*5*). The compacted fill contained a high percentage of rock and gravel-sized fragments, with the fine-grained portion of the soil consisting primarily of granular materials with some clayey fines. The compaction specifications were based on laboratory testing using ASTM D1557–78 (Modified Proctor), requiring 90 percent relative compaction. Although the rock contents (plus No. 4) varied widely in situ from 10 to 80 percent, only three soil types were identified for reference dry density. The three soils were described by the project engineer as brown silty, sandy, broken rock (GM); brown, silty, with broken rock (SM); and brown, silty, sandy gravel (GM), having maximum dry densities by ASTM D1557–78 of 20.4 kN/m^3 (130 pcf), 20 kN/m^3 (127 pcf), and 20.8 kN/m^3 (132 pcf). Field den-

TABLE 2 Hypothetical Forensic Results

Forensic Study with Rock Corrections Below for Relative Compaction	a) Field Control at 95% of the maximum density corrected for 40% oversize aggregate using: Scalp & Replace	AASHTO-2	USBR-1	AASHTO-1	ASTM-1
Scalp & Replace	95.0%	97.8%	99.5%	100.3%	100.7%
AASHTO-2	92.1%	95.0%	96.5%	97.4%	97.7%
USBR-1	90.6%	93.3%	95.0%	95.8%	96.1%
AASHTO-1	89.9%	92.6%	94.1%	95.0%	95.3%
ASTM-1	89.6%	92.3%	93.8%	94.7%	95.0%

Forensic Study with Rock Corrections Below for Relative Compaction	b) Field Control at 95% of the maximum density corrected for 60% oversize aggregate using: Scalp & Replace	AASHTO-2	USBR-1	AASHTO-1	ASTM-1*
Scalp & Replace	95.0%	98.3%	99.2%	102.1%	104.5%
AASHTO-2	91.8%	95.0%	95.8%	98.6%	101.0%
USBR-1	91.0%	94.2%	95.0%	97.8%	100.2%
AASHTO-1	88.5%	91.5%	92.3%	95.0%	97.3%
ASTM-1*	86.4%	89.4%	90.2%	92.8%	95.0%

* Beyond Recommended Range

sities were determined using a nuclear gauge. In all field tests, the contractor met or exceeded the required 90 percent relative compaction, averaging about 93 to 94 percent, but typically below optimum water content. Because percent rock was not determined in the field to correct reference dry densities, there was no way to determine whether the reference dry density was consistent with engineering expectations. Given the apparent ease with which the contractor met specification on this project, it is likely that the percent rock in the laboratory specimens was lower, on average, than that in the field. The fill material that resulted in this case was loose, and significant building damage resulted from the wetting-induced differential settlements. In general, any compacted fill, whether rocky or not, may collapse on wetting when compacted to 90 percent of Modified Proctor, particularly when compacted dry of optimum. However, fills containing high rock content may be particularly susceptible to poor performance when inappropriate specifications and field control (relative to the rock content) are used.

CONCLUSIONS AND RECOMMENDATIONS

The method used to account for the coarse fraction (material larger than 19 mm) in a fill can have a significant impact on the reference dry density used to evaluate a fill. The presence of the coarse fraction can be accounted for by

- The scalp-and-replace method where the material greater than 19 mm is replaced by an equal weight of material between the No. 4 and 19-mm sieves; or
- The use of a rock correction equation and compaction test results, usually on the fine fraction (material passing the No. 4 sieve) only, although ASTM D698–91 and 1557–91 call for testing of particles up to 19 mm (0.75 in.) to obtain densities to be corrected by equation for large aggregate.

The rock correction equation methods generally give higher estimates of the maximum dry density than the scalp-and-replace method.

Differences between the maximum dry densities determined from the various rock correction methods have been observed. The required density to pass a compaction specification (as a function of rock content) was determined for one clayey soil, and a significant variation depending on the rock correction method selected was obtained. Because the density achieved for a given fill soil is related to the compactive effort expended, the rock correction method used for field control can have a significant effect on the difficulty in complying with a given specification. This effect should be clearly understood by the contractor producing a bid to complete earthwork.

Further, the differences in rock correction methods were shown to create a range of conclusions regarding the adequacy of fill in a forensic study. Because of the possible range in computed relative compaction using different rock correction methods, the forensic engineer could conceivably arrive at almost any conclusion, depending on the combination of methods employed for correcting for the effects of large aggregate in construction control and forensic study. Such a possibility is clearly not desirable for achieving an understanding of the problem being studied.

Because of the potential variation implicit in the application of different rock correction techniques, recommendations for fill compaction and well-written specifications should include the intended rock correction method. Based on a survey of contractors, the practice of specifying the rock correction method is apparently not consistently used. Further, the rock correction method to be used does not appear to affect contractor bids.

A well-written compaction specification should include the desired percent compaction for different classes of fill material and the intended rock correction method. The effect of the rock correction method on compactive effort and performance of compacted soils must be recognized by engineers and contractors alike to avoid conflict.

REFERENCES

1. Donaghe, R. T., and F. C. Townsend. Sealing and Replacement Effects on the Compaction Characteristics of Earth-Rock Mixtures. *STP 599: Soil Specimen Preparation for Laboratory Testing.* ASTM, Philadelphia, Pa., 1976, pp. 348–377.
2. Houston, S. L., and J. D. Vann. Methods of Evaluating the Expansion Potential of Compacted Soils with Significant Fractions of Large Aggregate. *Geotechnical Testing Journal,* Vol. 10, No. 2, 1987, pp. 59–70.
3. Houston, S. L., and K. D. Walsh. Comparison of Rock Correction Methods for Compaction of Clayey Soils. *Journal of Geotechnical Engineering,* Vol. 119, No. 4, 1993, pp. 763–778.
4. Hsu, T. S., and S. K. Saxena. A General Formula for Determining Density of Compacted Soils with Oversize Particles. *Soils and Foundations,* Vol. 31, No. 3, 1991, pp. 91–96.
5. Kropp, A., D. McMahon, and S. Houston. Field Wetting Tests of a Collapsible Compacted Fill. *Proc., First International Symposium on Arid Soils,* London, July 6–8, 1993.
6. Day, R. W. Expansion of Compacted Gravelly Clay. *Journal of Geotechnical Engineering,* Vol. 117, No. 6, June 1991, pp. 968–972.

Publication of this paper sponsored by Committee on Transportation Earthworks.

Compaction Specifications for Low Hydraulic Conductivity Clay Embankments

CLIFF J. SCHEXNAYDER

Communication of regulatory and engineering decisions by the project specifications contractually establishes the parameters of project acceptance and sets forth how performance will be validated. If contract specifications fail to properly address the purpose of the project, it is difficult to properly perform the work. With a material such as kaolin clay the precision or variance associated with the results of commonly accepted testing procedures may be of a magnitude greater than that normally assumed. During a design-test program only two-thirds of the individual construction water-content tests fell within a desired wet-of-optimum range. Yet infiltrometer tests proved the hydraulic quality of the test panels. During project construction more than two-thirds of the individual water-content tests fell within the contracturally specified range, yet 50 percent of the work was rejected because there was no provision in the construction specifications to allow for the outliers. Construction techniques used for clay pulverization, moisture conditioning, and compaction on a full production basis in the construction of a 53-acre kaolin clay liner having a specified in situ permeability are described.

The project clay specifications reported here were developed with the intention of ensuring that the constructed kaolin clay cap would have an in situ permeability of less than 1×10^{-7} cm/sec. The purpose of this impermeable clay cap barrier was to prevent rainfall and surface runoff water from percolating downward through buried nuclear waste.

Because in situ sealed double-ring infiltrometer tests can take from 3 to 5 months to perform, another test method had to be specified to allow cap construction to proceed on a production basis. For clay materials there is a good correlation between placement water content and density, and in situ permeability. This is well known to geotechnical engineers and is documented in the literature (*1–4*). Therefore the project specifications used that relationship to define the acceptance standard for the compacted clay. However, problems were encountered during the execution of the work because the owner's field construction managers did not understand these geotechnical relationships.

DESIGN-TEST PROGRAM

The design-test program, conducted before preparation of the project specifications, examined both construction techniques and resulting clay cap properties for tertiary and cretaceous age kaolin. Tertiary and cretaceous clay from three different active mines in South Carolina was used to construct nine test panels. Panels were constructed at both standard (ASTM D698) optimum water content and at two to three percentage points wet of optimum with clay from each of the three sources. The construction technique for eight panels was to add water to the clay in a separate material conditioning area and then to transport the moisture-conditioned clay to the panel for placement and compaction. However, for the ninth panel a procedure of moisture conditioning the next lift of clay directly on the previously placed panel lift was used. This eliminated having to transport moisture-conditioned clay.

Early in the program it became obvious that the cretaceous kaolin was a sandier and less plastic material. Therefore only two test panels were constructed of the cretaceous clay. Both panels had field infiltrometer test and laboratory permeability test results exhibiting a hydraulic conductivity above the required minimum in situ permeability of $\leq 1 \times 10^{-7}$ cm/sec, thus proving that it would be difficult or impossible to meet the design criteria using cretaceous kaolin. The cretaceous clay was therefore eliminated from project consideration.

The tertiary clay used in the test program had natural water contents in the range of 20 to 25 percent. The average liquid limit and plastic limit values were 69 percent and 32 percent, respectively. The percent fines, < No. 200 sieve, was 98 percent or greater. Standard compaction test optimum water-content values ranged from 24 to 29 percent. In almost all cases, the natural clay was dry of optimum, thus making it necessary to add water to achieve the desired placement water content.

During the test program a stationary clay shredder and a traveling recycler were used to break down the blocky chunks of clay that were delivered from the mines. A recycler is a piece of highway construction equipment designed for pulverizing and mixing asphalt pavements and base materials. This size-reduction operation yielded a material having a maximum size of 38 mm (1½ in.). The purpose of the size reduction was to speed the water absorption of the clay by creating more contact surface area and to enhance the kneading effect of the rollers during compaction.

The 38-mm (1½-in.) minus particle size clay was spread in a lift 0.15 to 0.23 m (6 to 9 in.) thick and water was added by alternating passes of a water wagon and the recycler. The water wagon was not driven over the clay lift. It was equipped with a pressure system and nozzle that permitted water to be sprayed onto the clay while the wagon moved along the side of the conditioning area. The water content of the clay was raised to the desired percentage by this spraying-mixing procedure.

This approach of adding water while not having to actually traverse the clay was only possible because of the limited width of the test panels. That method, however, failed to model applicable construction procedures when faced with placing clay over large areas, as the actual project would require.

Del E. Webb School of Construction, Arizona State University, Tempe, Ariz. 85287.

After moisture adjustment the clay was covered with plastic and allowed to cure overnight. After this moisture conditioning period, the clay was picked up and transported to the panel by a 272-kW (365-hp) elevating wheel tractor scraper. On the panel, motor graders spread the clay in a uniform lift. Compaction was performed with a 161-kW (216-hp), 20 055-kg (44,175-lb) tamping foot soil compactor. The pads of a tamping foot roller are tapered with an oval or rectangular shape, as opposed to those of a sheepsfoot roller, which are uniformly cylindrical from base to pad face.

Trautwein-type, sealed double-ring infiltrometers were used to test the in situ permeability of both the tertiary and cretaceous kaolin panels. A test was conducted in each completed panel for 98 to 158 days. The results of those permeability tests, presented in Table 1, demonstrated that in situ permeabilities of less than the 1×10^{-7} cm/sec could be expected if the tertiary kaolin was compacted at water contents 2 to 4 percentage points wet of optimum as determined by standard compaction tests (*5*). The average compacted dry density for the individual test panels varied from 94 to 100 percent of standard maximum dry density.

PROJECT SPECIFICATIONS

The design-test program provided the water content and density parameters that could produce the desired low-hydraulic-conductivity clay layer without the need for in situ permeability testing during construction. The critical parts of the original project specifications that were developed on the basis of the test program data are summarized here:

1. Cretaceous kaolin shall not be used (but no identification criteria were specified).
2. The clay shall be tertiary kaolin clay with the following properties:
   a. Liquid Limit per ASTM D4318–84 shall be between 75 percent maximum and 55 percent minimum.
   b. Plasticity Index per ASTM D4318–84 shall be between 44 percent maximum and 26 percent minimum.
   c. Percent passing a No. 200 sieve per ASTM D422–63 shall be 90 percent minimum.
3. Clay blocks shall be broken before moisture conditioning to a maximum size of 38-mm (1½-in.) chunks to ensure uniform wetting (no specific testing procedure was specified).
4. Clay shall be placed in a 0.15-m (6-in.) maximum thickness unconditioned, loose lift.
5. Moisture conditioning of the kaolin shall be conducted before compaction to achieve 2 to 4 percent wet of the standard compaction optimum water content. To ensure uniformity of water content before placement and compaction, one water-content test, ASTM D2216-81, is required for every 250 m^2 (300 yd^2) of clay in the conditioning area.
6. The kaolin clay shall be compacted to a minimum of 95 percent of standard maximum dry density (ASTM D698–78).
7. A minimum of 12 passes with a CAT 815B roller is required.
8. The initial water-content placement range will be 2 to 4 percent wet of the average optimum water content as determined from a minimum of six moisture-density relationships (ASTM D698-78). Three moisture-density relationship determinations will be from kaolin samples taken at the borrow pit before commencement of mining, and three other determinations will be from kaolin samples from the initial 454 Mg (500 tons) of material delivered to the project.
9. In the placement area, uniformity of compaction is confirmed with in-place nuclear densities, a minimum of one per 383 m^3 (500 yd^3).

TABLE 1 Summary of Infiltrometer Test Data, Design-Test Program (*5*)

Panel Number	Kaolin Clay Type	Number of Test Days	Average $w_f - w_{opt}$, percent	Average percent Standard Proctor Density	Final Field Permeability K (field) cm/sec × 10^{-7}	Average Lab Permeability K (lab) cm/sec × 10^{-7}
A1	Tertiary	134	-1.3	105	1.60	0.81
A2	Tertiary	98	2.0	100	0.32	0.28
B1	Tertiary	141	3.5	94	0.61	0.34
B2	Tertiary	124	3.6	98	0.56	0.25
B3	Tertiary	101	2.9	98	0.91	0.27
C1	Tertiary	158	0.4	103	1.20	0.34
C2	Tertiary	106	2.7	100	0.49	0.43
D1	Cretaceous	117	3.4	98	3.60	1.60
D2	Cretaceous	141	2.0	97	5.00	1.70

All infiltrometer tests performed with a sealed double ring infiltrometer with 3.7 m (12 ft) outer ring and a 1.5 m (5 ft) square inner ring.

10. No after-compaction moisture-content testing was specified.
11. To determine whether the average optimum water content is valid, one moisture-density relation is required for each 3825 m^3 (5,000 yd^3 of clay placed.

A few items in the initial specifications deserve special notice. The compaction specification dictated both the method and the result: 12 passes with a CAT 815B roller and 95 percent of maximum dry density. The basis for establishing the acceptable water-content range was an average of the optimum water content as determined from the standard moisture-density relation. The acceptance water content was to be taken in the conditioning area before compaction. Density was to be confirmed by in-place nuclear methods. There was no provision for handling outliers when making an acceptance decision with regard to an individual water-content or density test. In addition, there was no provision to drop old data when calculating the average optimum water content.

CONSTRUCTION REALITY AND SPECIFICATIONS

Quality control (QC), testing, and acceptance of the clay was undertaken by a third-party QC organization reporting to the owner's project construction management organization. Neither the construction manager nor the QC organization had the authority to change or even interpret the project specifications. To be accepted, the moisture-conditioned and compacted kaolin clay had to meet the specifications exactly.

Changes or interpretations of the specifications could only be accomplished by authority of the permitting agencies. Therefore any modification of the original specifications was a lengthy process involving layers of technical and regulatory bureaucracy.

Design engineers must realize the contractual and, in many cases, the regulatory implications of project specifications. The relationship between the nature of the materials being handled and the limitations concerning testing processes and precision must be understood and embodied in the specifications. The specifications must address each individual element of the construction process in a realistic manner. No engineer can foresee every possible situation; consequently provisions should be incorporated into the specifications that establish procedures to resolve unique situations.

Unique situations can occur during any project. In one specific area on this project, density could not be obtained on the initial clay lifts. At first the problem was attributed to the contractor exceeding the specified lift thickness; then the quality of the kaolin was questioned. After many days of effort, it was realized that the background radiation from the nuclear waste was slightly greater in this area. The nuclear density meters used to test compaction were being affected by the background radiation. The larger problem was that there was no provision in the specifications to use another method to verify compaction.

Compaction difficulties were encountered on the project because of the double specification, specifying both method and result. At higher water contents, 12 passes with the specified roller caused overrolling. The specified density could not be achieved when more than eight roller passes were made. By the specification, density was an imposed critical parameter. However, in the case of compaction wet of optimum, density alone may not be a good gauge of resulting hydraulic conductivity. It has been found that even though the dry density of a compacted soil did not measurably increase with the application of more compactive energy, the hydraulic conductivity could be lowered by a factor as high as 100 (*3*). This has been attributed to the additional kneading action. A double specification will always cause problems. The design engineer must determine the important parameters, and those parameters must be carefully addressed in the specifications.

Early in the project the 152-mm (6-in.) maximum lift thickness specification was a problem. When a 152-mm (6-in.) kaolin clay lift was laid down as the first lift on top of the existing red silty soil of the site, the kaolin would become contaminated with the underlying material during processing and compaction. The tines of the mixing equipment would cut into the lower material in any spots where the lift thickness was less than 152 mm (6 in.). The feet of the rollers would likewise puncture through the kaolin and pull the red silt up into the white clay. Because of the color difference between the two materials, contamination was easy to discern.

The specifications limited the lift thickness and required full-depth mixing and compaction. Mixing could have been achieved on top of other panels of clay and the conditioned material hauled to the initial placement panel as was done during the test program, but such a procedure would not have solved the compaction problem. An alternative solution would have been to compact the initial lift with a smooth drum roller, but that would have eliminated the important kneading action during compaction.

A technical review at the design team level, not at the construction management level, determined that an initial thick lift would not be in violation of the permit. Therefore the adopted solution was to allow a 254-mm (10-in.) initial lift, to condition the lift to a depth of 203 mm (8 in.), and to retain the use of the specified kneading roller.

VARIABILITY AND ACCEPTABLE RANGE

Both the project and the design-test program panels B1, B2, and B3 used kaolin clay from the same source. The variability of the test results for those three design-test program panels is particularly relevant to the interpretation of the earthwork specifications.

Test Panel Data

The kaolin's average optimum water content from all standard compaction tests for the three panels was 26.8 percent. Individual test optimums varied from 24.2 to 29.2 percent, a range of 5 percent. At the same time, the individual water-content tests on samples taken from the field-compacted test panels varied from 26.4 to 32.8 percent. Those water-content values from the field samples were reported to be from 1.7 to 6.8 percent above the average optimum water content for the respective panel. Moreover, the standard deviations of the water-content tests on field samples from the panels ranged from 1.1 to 1.3 percent.

The significance of the standard deviations is that approximately two-thirds of the test results should be expected to be within one standard deviation of the mean value. This means that for test panel B3, for which $(w_f - w_{opt})$ had a mean of 2.9 percent and a standard deviation of 1.1 percent, only about two-thirds of the measured water contents were 2 to 4 percent wet of optimum. For the other two panels, the mean values and standard deviations of $(w_f - w_{opt})$ indicate that significantly less than two-thirds of the measured water contents were in the range of 2 to 4 percent wet of optimum. It is important to note that all of these test panels satisfied the perme-

ability criteria for the clay cap (Table 1), and permeability was the true critical parameter.

Project Data

Because of its dimensions [15.3 m × 61 m (50 ft × 200 ft], a typical project panel required, by specification, four water-content tests. During a 1-month period early in the project, more than 50 percent of the clay panels constructed were rejected because one or more of the four individual water-content tests taken from a panel were not within the specified range of 2 to 4 percent wet of the average optimum. In every case, conformance of the compacted density and water content to the specifications was evaluated on the basis of an average optimum water content of 25.6 percent and a maximum dry density of 1.54 Mg/m^3 (95.9 lb/ft^3).

An analysis of the 300 water-content tests taken by QC during the first 3 months of clay construction showed a mean water-content value of 28.6 percent and a standard deviation of 1.1 percent. The mean value for the tests was exactly 3.0 percent wet of the established optimum, and when the water-content values were rounded to the nearest 0.5 percent, 76 percent of the values were within the 2- to 4-percent wet-of-optimum range specified. Thus the constructed clay fill was at least as uniform as the design-test panels.

Specification Range

Had the specifications been written consistent with the realities of the design-test program, the project would have proceeded smoothly, as field construction mirrored the program very well. However, the specifications did not allow for the reality that only about two-thirds of the individual water-content tests for controlled construction conditions, the design-test program, actually fell within a 2- to 4-percent range above an average optimum water-content value. Researchers realized that general statements from the test program report had become the specifications, which had to be followed exactly.

Variability

An important factor that the writers of the specifications failed to recognize was the natural variability of the kaolin clay. The standard compaction test, performed by the QC organization, had shown optimum water-content values from 24.1 to 27.0 percent. The chosen average optimum value for construction was 25.6 percent, which in turn set the acceptability limits at between 27.6 (plus 2 percent) and 29.6 percent (plus 4 percent).

This decision to use the average as a benchmark presents several problems. Consider the case of a batch of clay actually having an optimum of 24.1 percent. To provide the required permeability based on the 2 to 4 percent wet-of-optimum criteria, this clay should be placed at a water content of between 26.1 and 28.1 percent. However, according to the specifications, any panels having tests below 27.6 percent would be rejected, thus forcing unnecessary rework of clay that was actually acceptable from a permeability standpoint. Now consider a case on the other extreme: in order to meet the minimum-plus-2 percent criteria, a batch of clay actually having an optimum of 27 percent would have to be placed at a water content of 29 percent. In this second case, clay that was not even conditioned to the plus 2 percent of its natural optimum would be accepted by the average criteria. These facts are diagramed in Figure 1 on the basis of the project data previously discussed.

The correct criteria for a specification is the moisture-density relationship to permeability. Plotting a test point, as in Figure 1, will prove whether the conditioned clay is acceptable considering the permeability standard. An acceptable test must fall within the band of the line of optimums and the saturation line. Such a specification criteria would be consistent with recommendations by Daniel (*6*) and Daniel and Benson (*7*). "The recommended procedure involves establishing $\omega - \gamma_d$ ranges needed to achieve the required hydraulic conductivity, and then modifying these ranges to account for other factors besides k" (*7*). Using this procedure allows for consideration of clay variability, yet the time to make an acceptance decision is minimal and would not restrict production-oriented construction operations.

Engineer's Intent

Additional moisture-density compaction tests were required by the specification to determine if the average optimum water content is valid. However, when a test did not confirm the validity of the average, it was not stated how the information was to be used. Should it alter the accepted water-content acceptance range for future clay placement? This section of the specifications shows that someone had considered the fact that there would be variability, but a complete statement of how to apply the validation information never made it into the specifications.

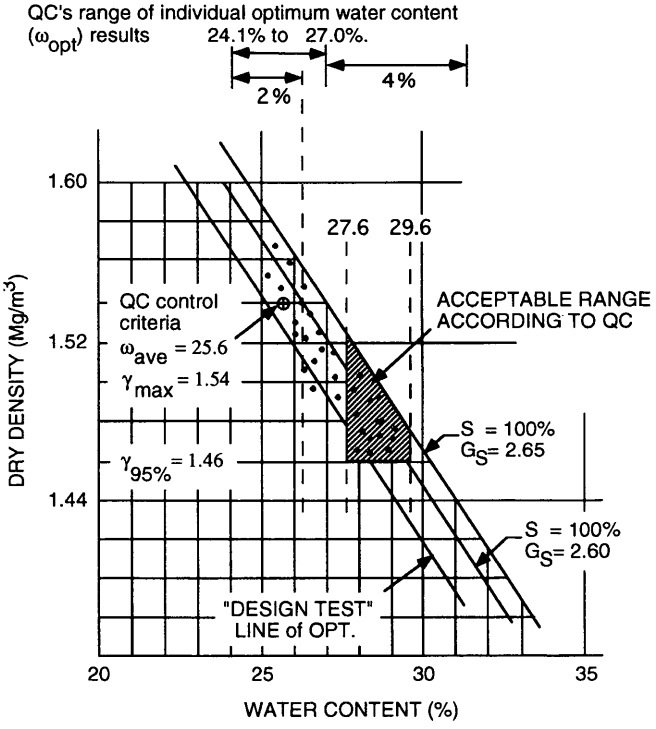

FIGURE 1 Project moisture-density data for the first 3 months of kaolin clay construction (QC-established average optimum water content was 25.6 percent and maximum dry density criteria was 1.54 Mg/m^3 for the period).

Sensitivity of Kaolin

During the first 6 months of clay placement the average optimum water content steadily dropped from 25.6 percent to just over 22 percent. Because no other properties of the clay displayed change, questions were raised about this significant difference. Work by Daniels and Ming-Tai Chao at the University of Texas, using samples of kaolin from the project pit, has shown that there is a correlation between optimum water content of a standard compaction test and the drying of the clay during test processing before compaction. It appears that QC caused the optimum moisture to be lowered over the first part of the project. This in turn meant that processed clay was accepted when it was actually dry of the specified water-content range necessary to ensure low hydraulic conductivity. Therefore a change order had to be issued to the contractor to remove and rework approximately 36,280 Mg (40,000 tons) of previously accepted clay.

Precision

The precision of testing procedures for clay material needs to be understood and could well be the subject of additional research. By specification, microwave water-content testing of 100-gram minimum clay samples was the standard for acceptance. As a result of the problems experienced on the project, both the contractor and the construction manager performed limited research into using microwave methods for water-content determination in kaolin clay.

Because most of the panel rejections were attributed to nonconforming water-content tests, this was the main area investigated. Clay samples from the field were split when they were taken and separate water-content tests were performed on each half, with the values calculated to the nearest tenth. Differences as great as 3.7 percent were noted. The average difference was about 1.8 percent. If the water-content values were rounded to the nearest half of a percent, the average difference was 1.5 percent.

A specification that is strictly enforced, makes no allowance for outliers, and limits the acceptance range to 2 percent, in combination with a test procedure that has a precision range of 1.5 percentage points, is going to cause problems. Geotechnical engineers have a responsibility to inform owners and specification writers concerning the limits of testing methods and procedures.

CONSTRUCTION TECHNIQUES AND EQUIPMENT

The critical construction operations when working with a clay are as follows:

- The clay must be broken into small clods to create surface area for water contact so that the material can be remolded into a new homogeneous mass (*1*).
- Water must be added and thoroughly mixed with the clay in a manner that will ensure a homogeneous material of uniform moisture content.
- The moisture-conditioned clay should be compacted by a kneading method.

These requirements were recognized, and several different pieces of heavy construction equipment and construction techniques were investigated in the field on a full production basis.

Clay Pulverization

The first task is to break down the large clay clods that come from the borrow pit. Excavation and loading at the pit was done by a hydraulic hoe excavator. When the hydraulic hoe loaded the clay into dump trucks for hauling to the fill area, the excavated material had many large chunks. These chunks from the pit normally had a maximum long dimension of about 0.46 m (18 in.).

Bulldozer

A 104-kW (140-hp) bulldozer was used to level the clay after it was dumped from the trucks, as shown in Figure 2. The dozer spread the clay out in a lift 0.15 m (6 in.) thick. Major size reduction was accomplished during the leveling, as chunks were crushed by the weight and motion of the dozer. The tracks of the dozer would bridge across low spots and place all the machine contact pressure on the largest chunks, which were the high points causing the bridging. Thus the largest chunks were crushed in the spreading process.

The use of a track dozer allowed the accomplishment of two material-handling requirements in one process: lift leveling and size reduction. After leveling by the dozer, the material could be classified as 0.15 m (6 in.) minus; therefore further size reduction was still necessary.

Rotavator

Rotavators proved to be efficient in accomplishing final size reduction and were used for that purpose for the entire project duration. A rotavator is nothing more than an oversized garden tiller pulled by a farm tractor. With a rotavator, clod reduction is accomplished by mechanical pulverization. The power for turning the rotavator tines, which do the actual chopping, is supplied by the tractor's power takeoff.

A 104-kW (140-hp) tractor could pull a 2.4-m (8-ft) wide rotavator at an average speed of 53 m/min (2 mph) through clay having a natural water content of about 22 percent and a maximum clod size of 0.15 m (6 in.). Depth of tine penetration was normally 0.20 to 0.25 m (8 to 10 in.). With the rotavators, average throughput of material meeting the maximum clod size specification [38 mm (1½ in.)], was about 180 Mg per hour (200 tons/hr).

At water contents above optimum the rotavators were not effective because of traction problems. They were therefore not used for final moisture-conditioning operations, but did perform initial blending of raw clay and water.

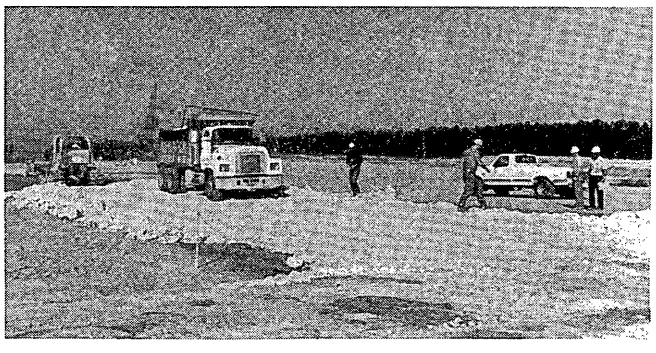

FIGURE 2 A 104-kW bulldozer leveling kaolin clay.

Shredder

The use of a clay shredder was investigated for a short time in the field. A shredder is a revolving blade with teeth; it cuts or shaves the clay into the desired size in the same manner as a meat slicer.

The drawback and reason it was not used for mass production was the shredder's passthrough tonnage limitation. With the blade set to operate at 38 mm (1½ in.) maximum size, the passthrough production was only 127 Mg/hr (140 tons/hr). A second reason for rejecting the shredder was that it adds material-handling steps to the production process. Material must be loaded and hauled to the machine, loaded into the machine, and loaded and hauled a second time after processing.

Soil Stabilization Machines

A soil stabilizer is a completely self-contained machine consisting of a power unit and a mixing chamber, as shown in Figure 3. Stabilizers are specifically designed for soil pulverization and mixing. They are common to highway construction work for inplace stabilization of lime or cement with soils.

As with the rotavators, when used for pulverization on this project, the stabilizers were not used until the raw clay had been leveled into a 0.15-m (6-in.) lift by a dozer. The stabilizers had a working speed of 27 m/min (1 mph), or about half that of the farm tractor-pulled rotavators, but pulverization could be accomplished in half the number of passes.

Experiments were conducted with machines having both up-cutting and down-cutting tine rotation. The best results were obtained using L-shaped chopper tines and up-cut rotation with the stabilizer box rear doors closed. Maximum clod size would increase as the door opening was increased. Operators want to increase the door opening because it allows them to increase forward speed. Typically, two passes with a stabilizer were necessary to reduce the 0.15-m (6-in.) minus clay down to 38 mm (1½ in.) minus. However, three passes were necessary on occasion, usually on grades. In such situations the operator was forced to increase the rear-door opening, which in turn affected size reduction.

On a highway soil stabilization project, the specific type of stabilizer that was used on this project will operate at an average propel hydraulic pressure of about 15 500 kPa (2,250 psi). Working kaolin, which lies relatively horizontal, with the machine in the up-cut mode, the propel pressure was 24 100 kPa (3,500 psi). On a 7-percent grade the pressure would go up to 25 500 kPa (3,700 psi). The machine has a pressure override valve set at 25 500 kPa (3,700 psi); therefore, when going up the grade, the operator had to increase the opening of the rear door to avoid stalling. The down-cut mode would have been easier on the machine, only 15 160 kPa (2,200 psi) up grade, but pulverization was not good and the clay would stick to the rear door, causing other problems. In fact, even operating up-cut, severe pressure was placed on the rear door. Rear-door cylinders had an average life of only 850 operating hours.

Moisture Conditioning

Once the clay had been processed so that the maximum clod size was 38 mm (1½ in.) or less, moisture conditioning began. The first method tried was to use a standard water truck with a pump-driven spray bar. Multiple passes were made over the pulverized clay until

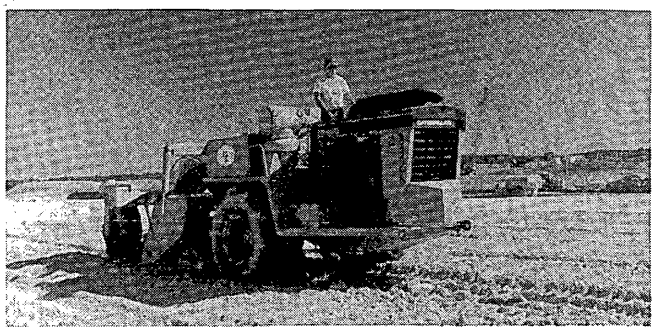

FIGURE 3 Soil stabilizer mixing moisture-conditioned kaolin clay.

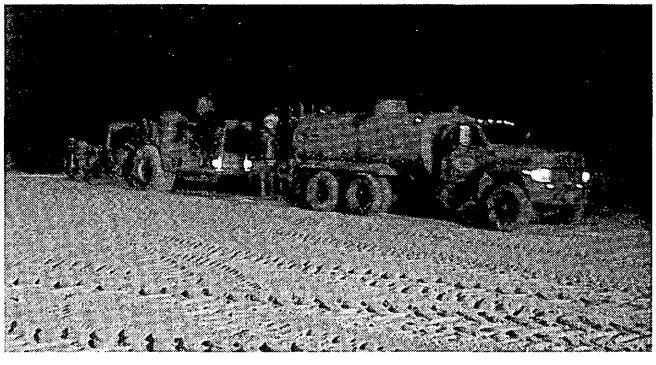

FIGURE 4 Water truck being followed by stabilizer during moisture conditioning of kaolin clay.

the material became so slippery the truck could not maneuver. At that point the farm tractor-pulled rotavator would make a couple of passes to mix the water and clay clods. After this mixing the water truck could make additional passes.

This procedure failed to produce a uniform moisture-conditioned clay. The tire ruts from the water truck tended to collect water before the mixing and became permanent streaks of high moisture content in the clay panel. The standard spray bar does not provide a uniform application of water. More water came out at the point where the bar connected to the pump than at the ends.

To overcome these deficiencies modifications were made to both the equipment and the construction techniques. The water truck spray-bar system was modified to form a continuous loop with a circulating pump so that the pressure at each nozzle was approximately the same. To eliminate the problem of water collecting in the ruts, it became standard procedure to operate a rotavator or stabilizer directly behind the water truck during moisture application, as shown in Figure 4. Once the required amount of water had been applied, two additional passes were made with the stabilizers to complete the mixing.

The water trucks all had metering systems to control the quantity of water applied. The amount of water that had to be added to the clay could easily be calculated based on the difference between the moisture-content tests of the pulverized clay and the specified water-content range. The problem was not in making the calculation or with the metering system, but in figuring the total amount of water to add, considering a necessary correction for the amount of evaporation that would take place in the time interval required to

add the water, condition the clay, and complete compaction. During day shifts in hot summer weather, the amount of extra conditioning water necessary to make up for evaporation loss was about 13.4 L/Mg (3.2 gal/ton). Operating at night during the summer required only 3.3 L/Mg (0.8 gal/ton) extra. Direct sunshine and wind were factors that greatly affected the amount of extra water needed.

Compaction

Tamping foot compactors of both 161 kW (216 hp), 20 055 kg (44,175 lb) and 235 kW (315 hp), 32 429 kg (71,429 lb) were tried at the beginning of construction. Tamping foot compactors can develop all four forces of compaction: pressure, impact, vibration, and manipulation. When dealing with a clay wet of optimum, however, pressure and manipulation are the important forces. Field trials revealed that there is an upper limit to acceptable pressure.

Considering the drum width and weight of each machine, the contact pressure of the larger machine was about 1.4 times that of the smaller machine. When the kaolin clay was conditioned to 2 percent or greater above optimum water content, the feet of the larger compactor would be pushed completely down into the moisture-conditioned clay and the roller would be supported by drum contact. The clay would then stick to the drum, and the upper lift of clay would be pulled up from the previous lift by the forward motion of the roller. This result was not satisfactory, so all production compaction was with a 20 055-kg (44,175-lb) tamping foot compactor.

CONCLUSIONS

The following conclusions were drawn on the basis of the project experience:

1. Standard highway construction equipment is appropriate for manipulating kaolin clay in constructing low-hydraulic-conductivity liners and caps.
2. Project specifications must be structured to account for testing precision and natural material variability.
3. No designer can anticipate all possible field situations; therefore it is important that specifications include procedures for resolving unique situations.
4. Most environmentalists and regulators are not familiar with earthwork or construction. It is therefore necessary for engineers to be alert to the consequences of poorly drafted specifications or controls.

If contract specifications fail to address the purpose of the project, it is difficult to properly perform the work. In fact, the constructor and the engineer may be forced to rely on their expertise instead of the specifications to complete the project.

REFERENCES

1. Lambe, T. W. The Permeability of Compacted Fine Grained Soils. *Special Technical Publication No. 163,* ASTM, Philadelphia, Pa., 1955.
2. Lambe, T. W., and R. V. Whitman. *Soil Mechanics.* John Wiley and Sons, Inc., New York, 1969, Chapter 19.
3. Mitchell, J. K., D. R. Hooper, and R. G. Campanello. Permeability of Compacted Clay. *Journal of the Soil Mechanics and Foundation Division,* Vol. 91, No. SM4, 1965, pp. 41–65.
4. Mitchell, J. K., and M. Jaber. Factors Controlling the Long-Term Properties of Clay Liners. In *Waste Containment Systems: Construction, Regulation, and Performance.* ASCE, Geotechnical Special Publication No. 26, 1990, pp. 85–105.
5. *Clay Cap Test Section Evaluation Report, Mixed Waste Management Facility (MWMF) Closure, Savannah River Plant.* Mueser Rutledge Consulting Engineers, New York, 1988, Table K-21.
6. Daniel, D. E. Summary Review of Construction Quality Control for Compacted Soil Liners. In *Waste Containment Systems: Construction, Regulation, and Performance.* ASCE, Geotechnical Special Publication No. 26, 1990, pp. 175–189.
7. Daniel, D. E., and C. H. Benson. Water Content-Density Criteria for Compacted Soil Liners. *Journal of Geotechnical Engineering,* Vol. 116, No. 12, 1990, pp. 1,811–1,830.

Publication of this paper sponsored by Committee on Transportation Earthworks.

Compacted Clay Embankment Failures

ZENON G. KYFOR AND RAYMOND L. GEMME

Embankment instability that occurred along several completed sections of a major interstate highway located in the western part of New York State is described. The affected embankments ranged in height from 4.6 m (15 ft) to 9.15 m (30 ft) and were constructed of silty clay over a silty clay foundation. Field investigations revealed that movements were taking place within the embankments and were not a result of the foundation soil. These movements were consistent with an undrained mode of failure. The embankment material was obtained from borrow excavations made outside the project limits and classified as a medium to highly plastic clay. The moisture contents of the borrow ranged from 25 to 55 percent and the plasticity index ranged from 15 to 32 percent. Drill holes progressed through the affected fills indicated that the embankment moisture contents at the time of distress exceeded the optimum moisture content (20 percent) by 5 to 10 percent based on a standard Proctor compactive effort. The undrained shear strengths at these moisture contents were not sufficient to provide for internal stability of the embankments. The results of the field and laboratory investigations are presented. They consist of inclinometer results of embankment monitoring, compaction curves for material used, and moisture contents and densities of fills obtained during construction and after movement began. A relationship between moisture content and undrained shearing strength is also shown. Stabilization consisted of flattening all embankments greater than 4.6 m (15 ft) from a 1 (vertical) on 2 (horizontal) to a 1 (vertical) on 3.5 (horizontal) side slope.

The current New York State Department of Transportation specifications require embankment material be compacted to at least 90 percent of the maximum Standard Proctor Density. The contractor determines the type and size of compaction equipment, selects lift thickness, and exerts proper control over the moisture content of the material and other details necessary to obtain satisfactory results.

Many hundreds of miles of embankments have been constructed with few serious problems, indicating for the most part that the earthwork specifications currently in use are effective. This can be attributed primarily to the following factors:

- Many of the embankments constructed in New York State are built out of granular materials.
- Contractors will often opt to waste highly plastic excavation materials and substitute granular or low-plasticity materials for embankment construction whenever economically feasible.
- The majority of the embankments constructed do not exceed 6.1 m (20 ft) in height. Although embankments exceed this height at many bridge approaches, the material used at the abutment locations is mostly a select granular material.

Notable problems have all been related to embankment construction using plastic soils. The problems have ranged from the "during construction" type, such as difficulty in handling and placing material, rutting, and weaving, to internal instability of the embankment soon after construction is completed. The internal stability of embankments is the subject of this paper.

The failure of compacted clay embankments containing low-plasticity [plasticity index (PI) = 8 to 13] soils in New York State has previously been reported (*1*). These failures were attributed to the condition in which the moisture contents of the fill material exceeded the optimum moisture content for standard compaction.

The present paper deals with the instability of highway embankments that occurred in the fall of 1982 on a major Interstate project. The embankments were constructed of higher-plasticity soils (PI = 15 to 35). The type of embankment failures that occurred on this project were short-term failures in which the undrained soil strength parameters would govern. The results of the investigation and recommendations for remedial treatment of the problem areas and for use of similar embankment materials on future projects are presented.

BACKGROUND

Project Description

The project is located in Erie County just northeast of Buffalo (Figure 1). A closeup of the location of the problem areas is shown in Figure 2.

Site Geology

Geomorphologically the project area is a broad, flat, glacial lake bed dissected by several streams. The soils consist mainly of lacustrine bottom deposits, with alluvial deposits found on the flood plains of the streams.

General Foundation Conditions

The general foundation conditions in the project area consist of up to 1.5 m (5 ft) of sandy silt, underlain by 1.5 m (5 ft) of stiff red/brown clay over 3.1 m (10 ft) of soft red/brown clay. The soft clay is underlain by compact glacial till extending to rock. Figure 3 diagrams the embankment geometry showing embankment distress. Figure 4 shows the stress history and undrained shear strengths of the foundation soils.

Embankment Material

The embankment material was obtained from borrow excavations made outside of the project limits and is classified as medium to highly plastic clay (Unified Soil Classification System: CL to CH).

New York State Department of Transportation, Soil Mechanics Bureau, Bldg. 7, State Campus, 1220 Washington Avenue, Albany, N.Y. 12232.

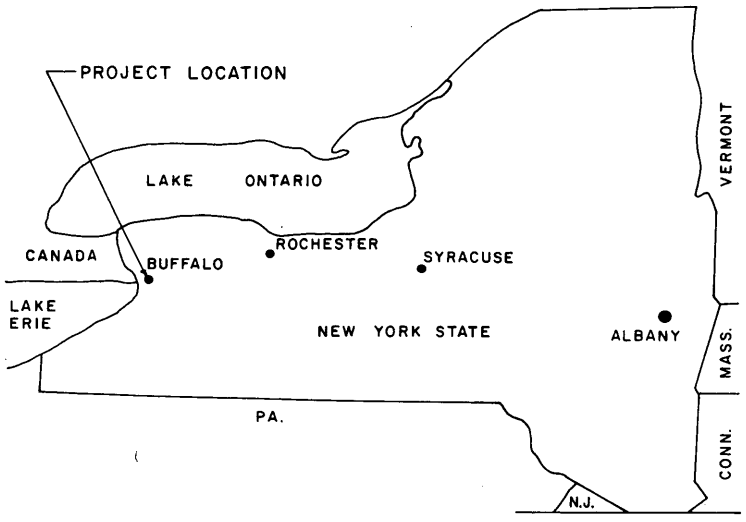

FIGURE 1 Project location.

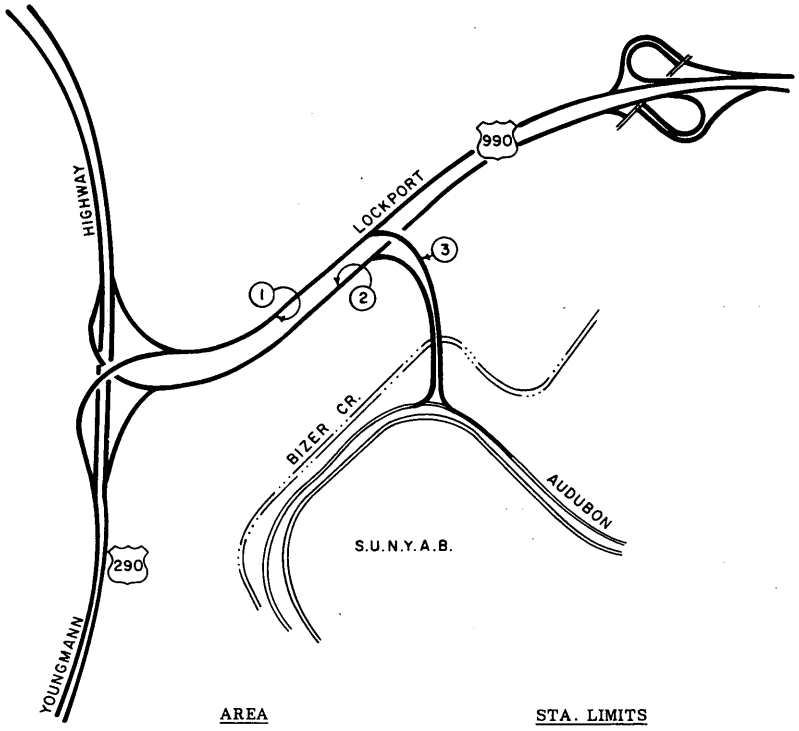

AREA	STA. LIMITS
1-SOUTHBOUND LANES	'SB' 127+50 - 'SB' 135+00
2-NORTHBOUND LANES	'NB' 140+00 - 'NB' 142+00
3-'UWLS' RAMP	'UWLS' 156+00 - 'UWLS' 158+50

FIGURE 2 Project plan and location of problem areas.

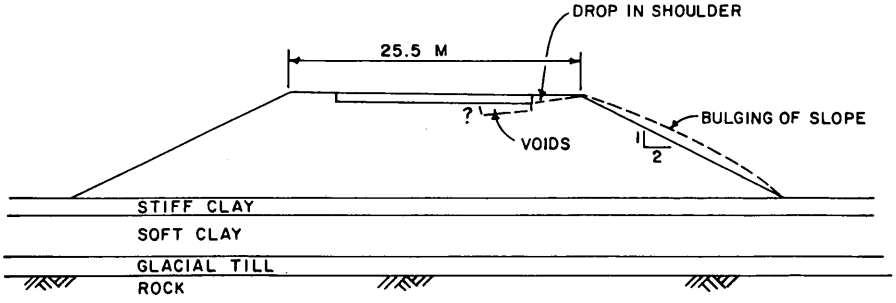

FIGURE 3 Embankment geometry showing embankment distress.

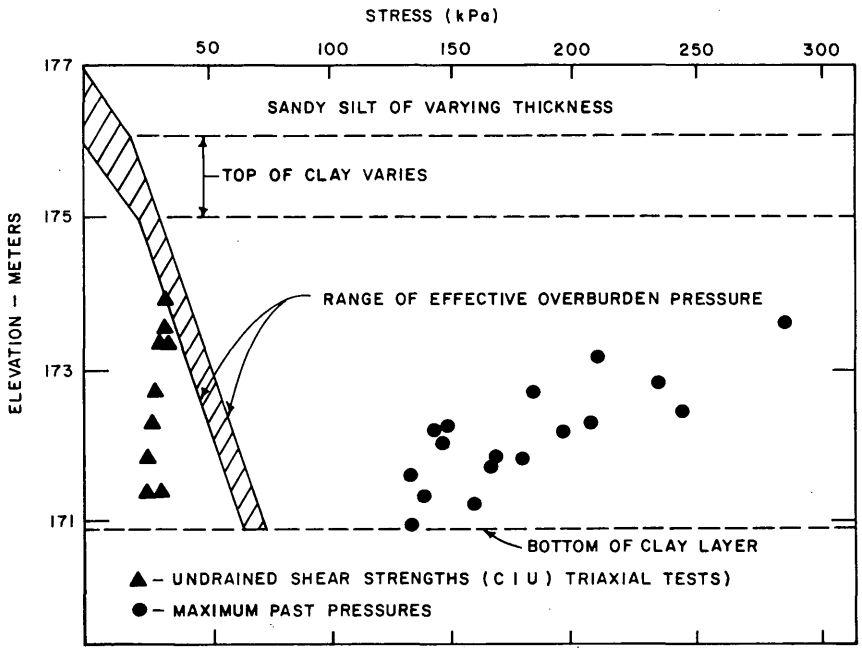

FIGURE 4 Stress history and undrained shear strengths of foundation soils.

The moisture content of the borrow ranged from 25 to 55 percent and the plasticity index ranged from 15 to 32 percent. The optimum moisture content at the standard Proctor compactive effort was determined to be ±20 percent (Figure 5). As indicated, the natural moisture content of the material from these excavations was wetter than optimum.

Earthwork Construction Method

Where necessary a working platform of granular material was established above the original ground surface up to 1 m (3 ft) in depth. The wet silty clay excavated from the borrow sources was placed in approximately 0.23-m (9-in.) lifts and then aerated with discs and tractors for 2 to 3 days, depending on weather conditions. The material was then compacted using a sheepsfoot roller until the roller effectively walked out of the lift with an approximate 76.2-mm (3-in.) rebound behind the roller. Compaction tests were performed for the lifts to be approved.

INVESTIGATION OF FAILURES

Description of Problem Areas

Several months after project embankments were completed and pavements were in place, three embankment areas (Figure 2) began experiencing unexplained movements (Figure 3). Eventually all embankments greater than 4.6 m (15 ft) in height would experience similar movements. The southbound (Area 1) and northbound (Area 2) lanes of the project mainline were paved with concrete, whereas the third, designated the UWLS ramp (Area 3), was paved with asphalt. The fill heights of the southbound lanes, northbound lanes, and UWLS ramp were 7.6 m (25 ft), 6.1 m (20 ft), and 9.2 m (30 ft), respectively. During the design phase of this project it was determined that the foundation clay was not capable of supporting the UWLS embankment for its full height (2). Stabilizing berms were selected as the most cost-effective way of preventing embankment foundation failure. The berms were 2.4 m (8 ft) high and 22.9 m (75 ft) wide and placed on both sides of the embankment.

On one side of the southbound lanes it was noticed that a drop of less than 25 mm (1 in.) had occurred in the asphalt shoulder relative to the concrete pavement. No bulging of the side slopes was noticeable. It could not be determined visually whether this movement was due to the foundation soils or to the materials used in constructing the embankments. By coincidence, an instrumentation program for monitoring embankment foundation performance, initiated during the project design phase, was in place at this particular location. The instrumentation consisted of piezometers, settlement gauges, and inclinometers. The information obtained from this instrumentation indicated that the foundation soils had completely consolidated and gained strength under the weight of the embankment.

The northbound lanes had experienced movements similar to those on the southbound lanes; however, they were more pronounced. The asphalt shoulder had dropped vertically 51 mm (2 in.) to 76 mm (3 in.). A separation between the shoulder and concrete pavement was measured to be 25 mm (1 in.).

Of the three embankments, the movements that had occurred on the UWLS ramp were the most visually dramatic. In October of 1982, a crack 30.5 m (100 ft) long was noted along the centerline of the ramp (Figure 6) and a small bulge existed along the bottom portion of the embankment slope above the berm. The initial crack was approximately 25 mm (1 in.) wide and 77 mm (3 in.) deep. By February 1983, the crack was 61.0 m (200 ft) long and the asphalt pavement had dropped vertically 0.8 m (2.5 ft) (Figure 7). By this time, a large bulge was apparent in the slope.

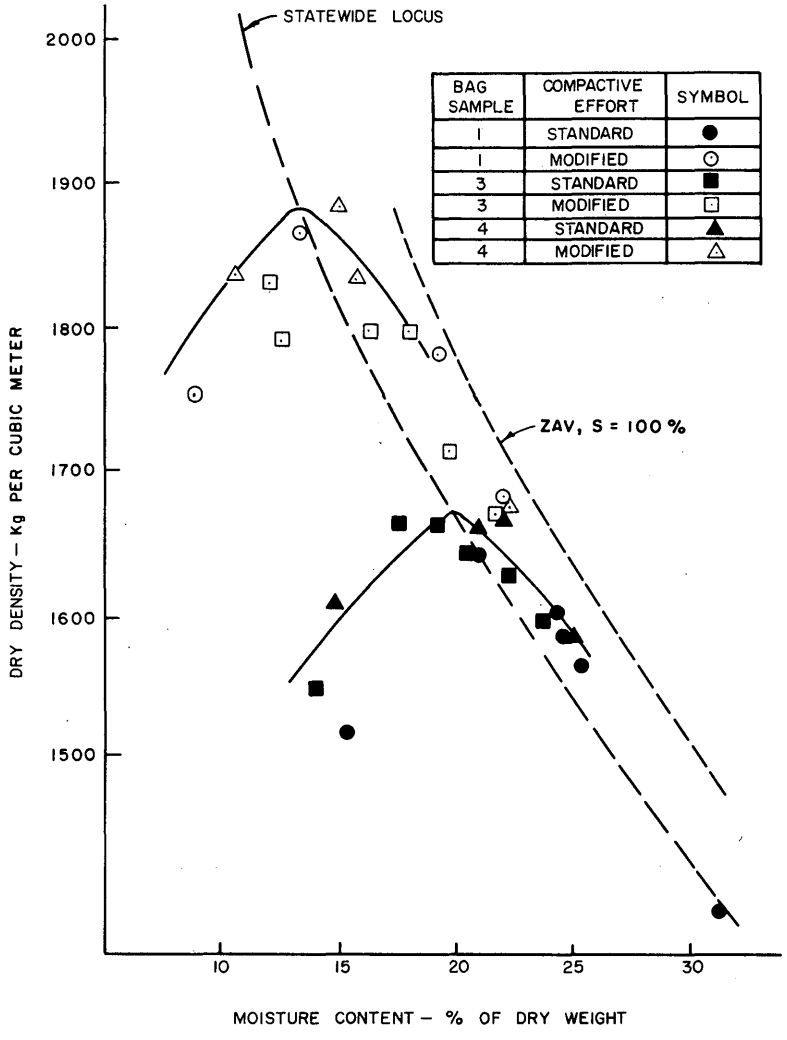

FIGURE 5 Dry density versus moisture content for bag samples.

Investigation Program

The investigation program of the distressed areas consisted of the following:

- Laboratory classification, consolidation, and triaxial compression tests performed on undisturbed Shelby tube samples of the foundation soils.
- Laboratory classification, density, moisture content, and triaxial compression (unconsolidated-undrained) tests performed on brass liner samples of the embankment materials taken after the failures. (It was difficult to press Shelby tubes through the embankment materials, therefore a split barrel-driven sampler having a thin-wall, 76.2-mm (3-in.) diameter brass liner was used to obtain representative samples. After sampling, the liner was sealed in a manner similar to a Shelby tube: capped with plastic caps, coated over with wax, and sent directly to the laboratory.)
- Comparison studies of standard and modified laboratory compaction with unconsolidated-undrained triaxial compression tests performed on bag samples of the silty clay embankment materials taken after the failures.
- The results of field density tests performed during construction of the embankments before the failures.
- The results of several inclinometers installed to measure horizontal movements of the embankments and foundation soils both before and after the failures.
- Optical surveys to detect both vertical and horizontal movements of embankment pavements and slopes after the failures.
- Visual observations made during several field inspections after the failures.

RESULTS OF INVESTIGATION— VERIFICATION OF CAUSE OF MOVEMENTS

Inclinometer Borings and Optical Surveys

Inclinometers were installed at the problem sites to determine the location of the zones of movement. At the mainline locations (northbound and southbound lanes) the inclinometers were progressed through the fills into the foundation soils and at the toe of slope. The inclinometer at the UWLS ramp was progressed at the

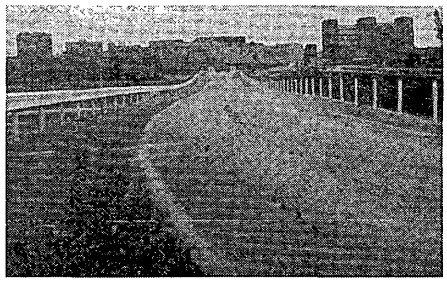

FIGURE 6 Crack developing on UWLS ramp, October 1983.

FIGURE 7 Drops of 2 to 3 ft on one side of UWLS ramp, February 1983.

toe of the ramp slope, through the berm and into the foundation soil. Figure 8 shows the results of the inclinometer monitoring. The data indicate that the movements were all occurring within the embankments. The inclinometer progressed through the berm at the toe of the UWLS ramp slope indicated no movement.

A series of optical survey points were established on the pavement and along the side slope at the UWLS ramp site. The edge of asphalt pavement dropped at a relatively uniform rate (102 mm per month) since the start of the optical survey in mid-October. During this period, the slope moved out horizontally 0.3 m (1 ft). No significant vertical movements were detected on hubs located on top of the berm.

Strength of Fill Material

Laboratory Testing

Bag samples of the clay material used to construct the embankments were obtained to perform laboratory compaction and strength tests. The samples were compacted under both standard and modified compactive efforts, and the results are shown in Figure 5. At the standard compactive effort, the optimum moisture content was 20 percent and the maximum dry density was 1 681 kg/m^3 (105 pcf). An optimum moisture content of 13 percent and a maximum dry density of 1 874 kg/m^3 (117 pcf) was obtained for this material compacted at the modified effort.

On completion of the compaction tests, each sample was taken out of the compaction mold and full-diameter unconsolidated-undrained triaxial compression tests were performed at 100 percent saturation. A confining pressure of 172.5 kPa (25 psi) was applied to each sample. A relationship between moisture content and undrained shear strength was developed and is shown in Figure 9.

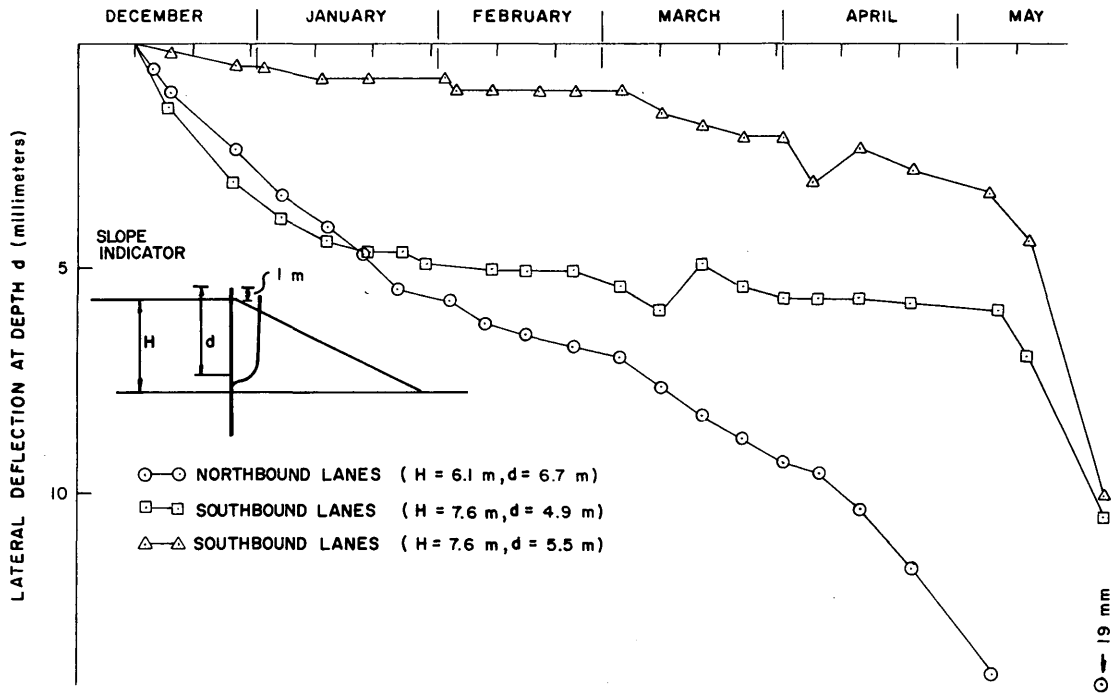

FIGURE 8 Slope indicator monitoring results within fill.

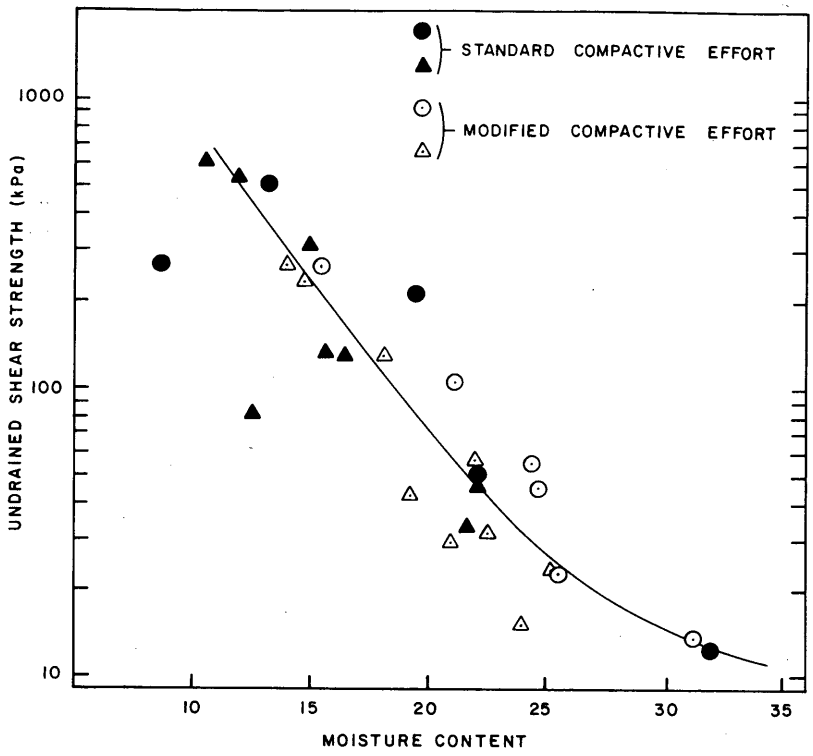

FIGURE 9 Undrained shear strength versus moisture content for bag samples.

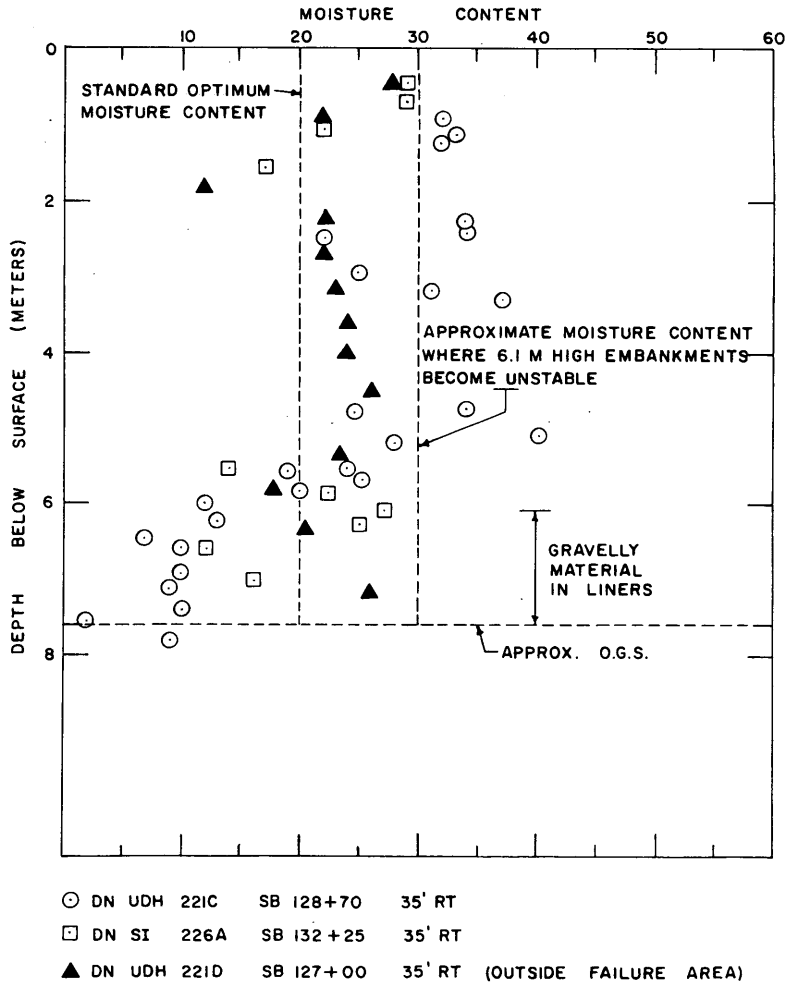

FIGURE 10 Depth versus moisture content for southbound lanes.

As can be seen, strengths as low as 14.4 kPa (300 psf) were obtained at a ±30 percent moisture content. It made no significant difference whether the samples were compacted at the standard or the modified effort.

Density, moisture content, and strength determinations were made on the brass liner samples of the embankment material obtained from borings progressed through the problem embankments. Moisture content profiles are shown in Figures 10–12. Density versus moisture content relationships are shown in Figure 13. As can be seen, the densities of the embankment samples were determined to be above the minimum required 90 percent standard Proctor density and the moisture contents were considerably wetter than optimum. The relationship between moisture content and undrained shear strength is shown in Figure 14. As indicated, the shear strengths obtained from tests performed on the brass liner samples of the embankments were generally higher than those for the bag samples. An explanation for this is that most of the material in the embankments had a chance to gain strength after placement. The sampling procedure may also have had an effect on the strengths obtained. The bag samples, on the other hand, were tested soon after they were compacted and thus were not allowed to gain strength with time (i.e., no thixotropic strength gain). The bag sample shear strengths are more typical of the shear strengths of embankments experiencing movement. This is true because along the active plane of movement, within the embankment, the soil has not had a chance to gain strength because of its constant movement and remolding action. This view is in agreement with other investigators (*3–6*) who have performed research on the strength characteristics of compacted clay embankments. Therefore, shear strengths obtained from the bag samples were used in analyzing the stability of the embankments.

Field Testing

The results of recorded field density tests in which moisture contents were obtained during construction are shown in Figure 13. The densities obtained were all above the minimum required 90 percent standard density, and the majority of the moisture contents were at or below the optimum moisture content of 20 percent as determined in the laboratory. The moisture contents determined during construction of the embankments are considerably lower than the moisture contents determined after construction. Some possible reasons for this are

- Field density test time and location (i.e., selective testing);
- Infiltration of water into previously accepted embankment lifts;
- Material placed wetter than optimum; and
- Sampling disturbance.

Strength of Fill Used in Stability Analyses

The engineering behavior of compacted cohesive soils is affected by moisture content, degree of saturation, method of compaction,

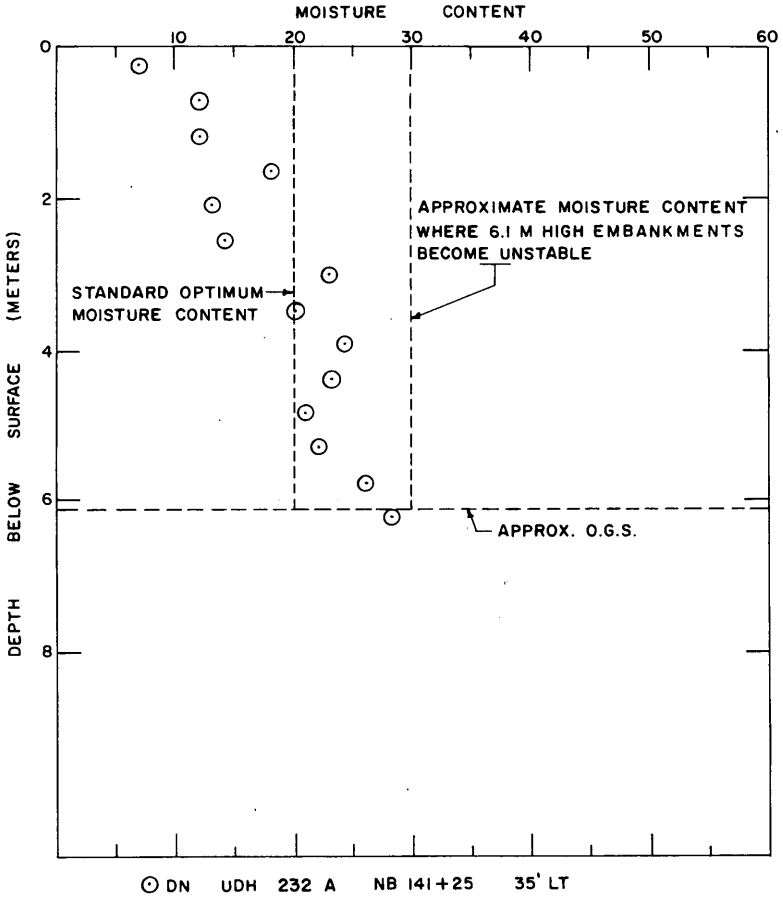

FIGURE 11 Depth versus moisture content for northbound lanes.

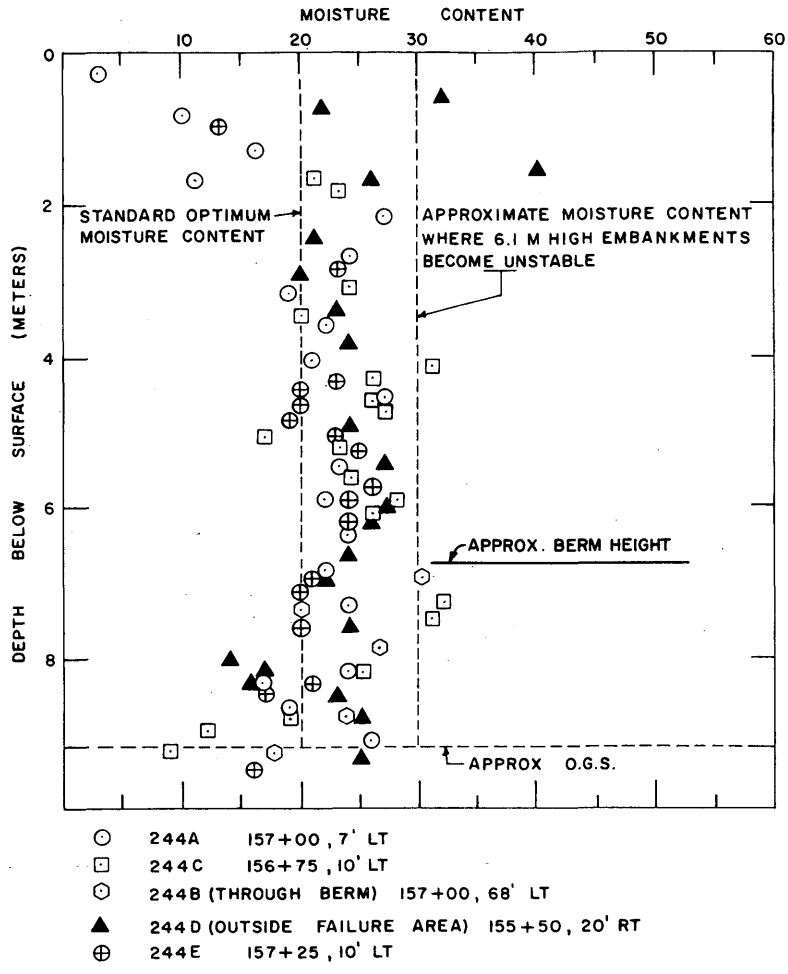

FIGURE 12 Depth versus moisture content for UWLS ramp.

and compactive effort. Of all these factors, moisture content appears to play the most important role in the strength of the soil, as indicated from the plot of moisture content versus shear strength shown in Figure 9.

In addition, a distinction must be made between long-term stability and short-term stability, as this affects the selection of soil strength parameters used in the analyses of these embankment failures. Long-term failure starts to take place a relatively long period of time (perhaps years) after completion of embankment construction. Failure usually takes place close to the surface of the slope [less than 2.4 m (8 ft.)] deep as a result of loss of shear strength as the soil swells and takes on water to reach a point of equilibrium with respect to the elements. Shear cracks usually first show up in the slope or outer portions of the shoulder. Long-term drained soil strength parameters are used in the stability analyses of embankments failing in this manner.

In the short-term case, failure starts to take place deep within the embankment (verified by inclinometers) and within a short time (days or months) after completion of embankment construction. Failure is associated with a deep outward squeezing of soil from within the lower portions of the embankments due to the overlying loads from the upper portions of the embankments. Because the movements are initially deep within an embankment, the movement cracks first show up in the shoulder or pavement. Because the movements exhibited in the embankments were consistent with what would be expected for the short-term case, undrained soil strength parameters were used in all stability analyses.

Figures 10–12 show the moisture content profiles found to exist in borings progressed through the roadway embankments. These figures indicate that moisture contents approached or exceeded 30 percent at the time of failure in these embankments. Using these moisture content profiles, undrained shear strengths were selected for analysis from the relationship of moisture content versus shear strength obtained from Figure 9. From this relationship a shear strength of 14.4 kPa (300 psf) was used for analysis in the lower portions of the compacted embankments.

Stability Analyses

Slope stability analyses were performed to equate safe fill heights to shear strength using the simplified Bishop analysis. A fill height of 6.1 m (20 ft) was used for the problem embankments for the following reasons:

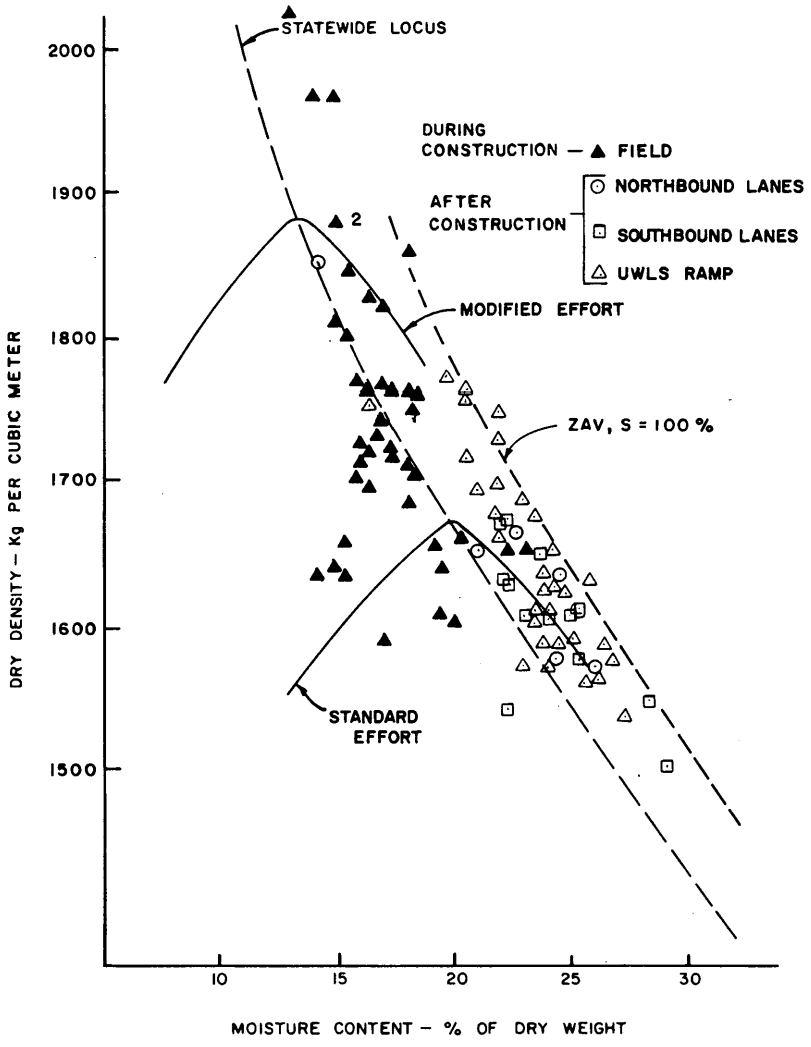

FIGURE 13 Dry density versus moisture content for field and laboratory testing.

- The bottom 1.5 m (5 ft) of the 7.6-m (25-ft) high southbound embankment contained granular material.
- The fill height was actually 6.1 m (20 ft) for the northbound embankment, and the maximum moisture content occurred at the bottom.
- The fill height above the berm was 6.1 m (20 ft) for the UWLS ramp.

When incorporated with the results of laboratory testing, the results of these analyses show that embankments constructed of this material possessing an undrained shear strength of 14.4 kPa (300+ psf) can be built safely [factor of safety (F.S.) = 1.25] to a height of approximately 4.6 m (15 ft) and that the effective fill heights of 6.1 m (20 ft) in these areas run a high risk of failure, as actually happened. Figure 15 shows the results of a stability analysis performed on the UWLS ramp. An undrained shear strength of 26.3 kPa (550 psf) would have been required in order to ensure short-term stability of the embankment. Based on the relationship developed in Figure 9, the undrained shear strength required for stability (F.S. = 1.25) corresponds to a moisture content of 25 percent. The moisture content found to exist in the lower portion of the fill (above the berm) approached 29 percent, corresponding to an undrained shear strength of 19.2 kPa (400+ psf).

REMEDIAL TREATMENTS

Recommendations were made to stabilize all the project embankments that were greater than 4.6 m (15 ft) high. Stabilization consisted of flattening the embankment side slopes because material was readily available and right-of-way was not a problem. Based on an average fill height of 6.1 m (20 ft), a required F.S. of 1.25, and an undrained shear strength of 14.4 kPa (300 psf), the slopes were flattened to 1 (vertical) on 3.5 (horizontal).

CONCLUSIONS

The results of the investigations into the embankment failures that occurred on this project revealed that the moisture contents in the fills exceeded the optimum moisture content at the standard effort

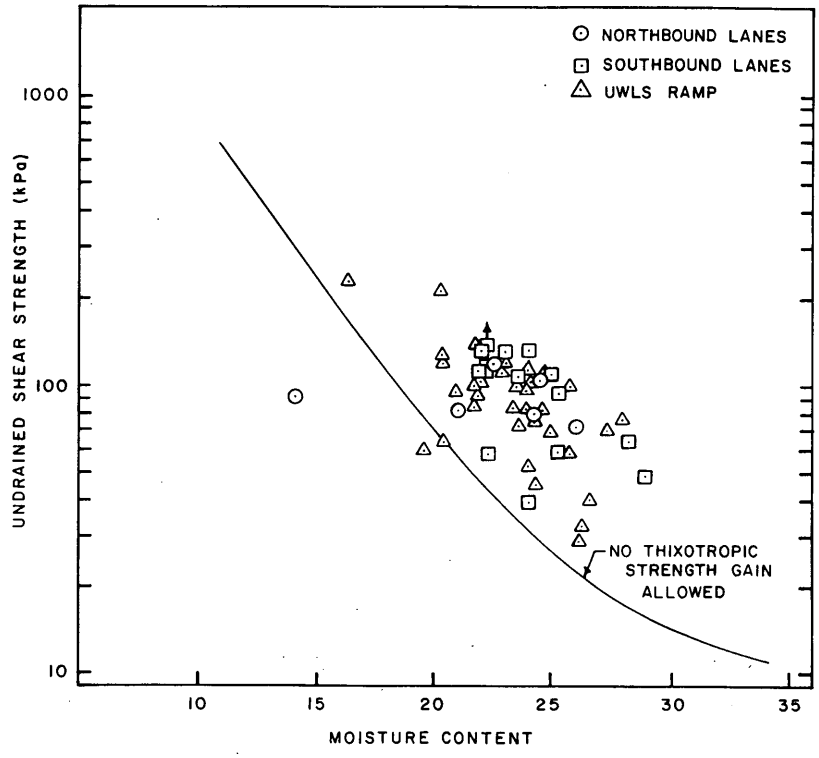

FIGURE 14 Undrained shear strength versus moisture content for brass liner samples.

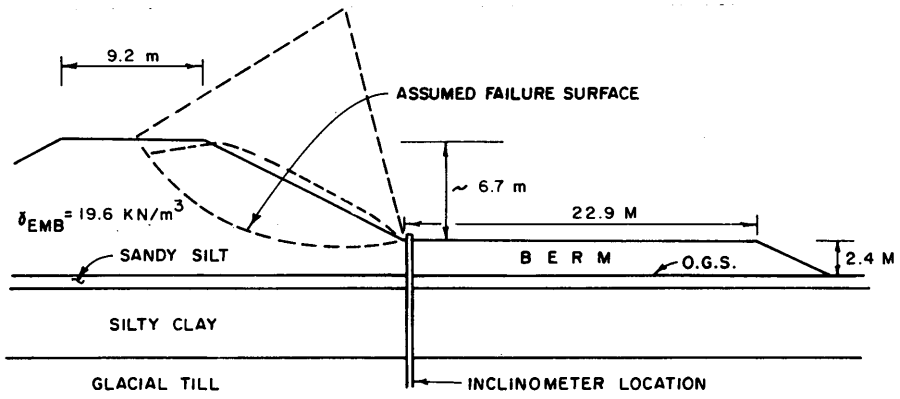

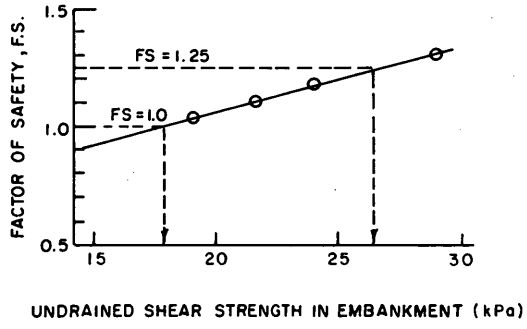

FIGURE 15 Stability analyses for UWLS ramp.

by as much as 10 percent. These moisture contents corresponded to undrained shear strengths deemed inadequate in ensuring stable embankments greater than 4.6 m (15 ft) high.

Moisture control would appear to be the answer if it were not for the fact that construction records showed that for the most part the fill met the density and moisture content requirements for the particular soil used. The difference between the construction records and post-failure results could not be adequately explained.

Since these high-plasticity clays are not used all that often in embankments of any great height, perhaps it would be better to assume that moisture contents in completed fills will exceed those desired by a certain percent and then design accordingly.

EMBANKMENT DESIGN IN NEW YORK STATE

The New York State Soil Mechanics Bureau seldom designs, in the strict sense, highway embankments. It has been the position of the bureau that strict adherence to the standard specification requirements will produce internally stable embankments constructed with side slopes of 1 vertical on 2 horizontal. For the most part this approach has worked quite well. Experiences in recent years have caused the bureau to modify its operating procedure concerning the use of low- to high-plasticity soils as embankment construction material. Embankments that are to be constructed 4.6 m (15 ft) or higher and have a strong probability of being constructed out of plastic soils are now more closely evaluated and, if deemed necessary, designed to prevent problems during construction. Provided right-of-way is not a problem, flattening the embankment side slopes is a common approach. Other methods might be the inclusion of geosynthetic reinforcement, stabilization of embankment soil with chemicals, or zoned construction (placement of granular materials in selected areas of the embankment).

REFERENCES

1. Gemme, R. L. *Undrained Failure of Compacted Plastic Embankments.* In *Transportation Research Record 897,* TRB, National Research Council, Washington, D.C., 1982, pp. 22–26.
2. McGuffey, V., D. Grivas, J. Iori, and Z. Kyfor. Conventional and Probabilistic Embankment Design. *Journal of the Geotechnical Engineering Division,* ASCE, Vol. 108, GT10, Oct. 1982.
3. Seed, H., J. Mitchell, and C. Chan. The Strength of Compacted Cohesive Soils. *ASCE Research Conference on Shear Strength of Cohesive Soils,* Boulder, Colo., 1960, pp. 877–964.
4. Seed, H., and C. Chan. Structure and Strength Characteristics of Compacted Clays. *Journal, Soil Mechanics Bureau and Foundation Division,* ASCE, Vol. 85, No. SM5, 1959, pp. 87–125.
5. *Soil Compaction. Investigation: Compaction Studies on Silty Clay.* Report No. 2, Technical Memorandum No. 3–271. U.S. Corps of Engineers Waterways Experiment Station, Vicksburg, Miss., 1949.
6. Weitzel, D. W., and C. W. Lovell. The Effect of Laboratory Compaction on the Unconsolidated-Undrained Strength Behavior of a Highly Plastic Clay. In *Transportation Research Record 754,* TRB, National Research Council, Washington, D.C., 1980.

Publication of this paper sponsored by Committee on Transportation Earthworks.

Compaction Control Criteria for Clay Hydraulic Barriers

MAJDI A. OTHMAN AND SCOTT M. LUETTICH

Compacted clays are commonly used as hydraulic barriers. In the construction of a clay hydraulic barrier it is important to use a water content–dry unit weight criterion that results in low hydraulic conductivity. Recently several compaction criteria have been proposed for the construction of soil hydraulic barriers. Discrepancies exist, however, in the acceptable water content–dry unit weight zones defined by these criteria. Three of these criteria are reviewed and compared. The advantages and disadvantages of each criterion are discussed with emphasis on efficiency, effectiveness, and practicality of use during construction. An evaluation is presented that suggests that a criterion based on achieving a minimum initial degree of saturation (i.e., the leftmost boundary of the water content–dry unit weight zone is a contour of constant degree of saturation) has desirable attributes and has several advantages over the other approaches. Laboratory and field data on compaction and hydraulic conductivity of several clay soils are examined to evaluate the validity of the degree-of-saturation approach. The data show that this approach provides good control over the quality of compacted clays in the field and is more accommodating to natural variations in soil composition and compaction characteristics than are the other approaches. A case history is presented that illustrates the degree-of-saturation compaction criterion.

Compacted clays are commonly used as hydraulic barriers. Examples include the cores of earth dams, liners and covers of landfills, and liners of surface impoundments. Because the main purpose of a hydraulic barrier is to minimize flow, its hydraulic conductivity is of paramount importance.

Traditionally clay hydraulic barriers have been compacted in the field to achieve a minimum dry unit weight within a specified range of water content (typically wetter than the optimum water content). This approach has been criticized because it is unnecessarily restrictive and does not ensure low hydraulic conductivity (*1,2*). This approach is based primarily on achieving a minimum dry unit weight for adequate strength and limited compressibility instead of achieving a low hydraulic conductivity. Therefore the traditional compaction criterion is not considered acceptable for construction of hydraulic barriers and thus is not addressed further in this paper. For the clay hydraulic barrier to perform well, it must have a low hydraulic conductivity. Therefore a compaction criterion that is primarily based on hydraulic conductivity should be used for its construction.

Recently new criteria for the compaction of clay hydraulic barriers have been proposed that require defining a water content–dry unit weight zone that corresponds to the required hydraulic conductivity. Discrepancies exist, however, in the approaches proposed to determine the acceptable water content–dry unit weight zone. Three of these approaches are reviewed and compared in this paper. The advantages and disadvantages of each criterion are discussed with emphasis on efficiency, effectiveness, and practicality of use during construction. It should be noted that these criteria are based on hydraulic conductivity only. Other considerations such as shear strength and resistance to desiccation or freeze-thaw also need to be considered as part of the compaction criteria, but are not addressed in detail in this paper.

The first criterion defines the water content–dry unit weight zone corresponding to the required hydraulic conductivity graphically from laboratory compaction data for a range of compactive effort. The second criterion is based on the line of optimums, which identifies the leftmost boundary of the acceptable water content–dry unit weight zone. In the third criterion, the leftmost boundary of the zone is a contour of constant degree of saturation.

Background information on the effects of compaction variables on the hydraulic conductivity of soils is summarized. The three modern criteria described previously are presented and discussed, and an evaluation of these criteria is presented that suggests that the degree-of-saturation approach has desirable attributes and has several advantages over the other approaches.

Laboratory and field data on compaction and hydraulic conductivity of many clays are examined to evaluate the validity of the degree-of-saturation approach. The data show that this approach provides good control over the quality of compacted clays in the field, and is more accommodating to natural variations in soil composition and compaction characteristics than are the other approaches. A case history that illustrates the degree-of-saturation compaction criterion is presented.

COMPACTION VARIABLES AND HYDRAULIC CONDUCTIVITY

Factors affecting the hydraulic conductivity of compacted clays have been studied extensively (*3–7*). All studies have shown that molding water content and compactive effort have the greatest effect on hydraulic conductivity. Typical relationships among water content, compactive effort, dry unit weight, and hydraulic conductivity are shown in Figure 1 (*4*). Figure 1(*b*) shows that the dry unit weight of the soil reaches a maximum value at an "optimum water content" for a certain compactive effort. The line connecting the optimum water content points on compaction curves for various compaction efforts is commonly referred to as the "line of optimums." This line is usually almost parallel to the line of full saturation (i.e., the zero air void line).

The hydraulic conductivity of the soil decreases with the increase of water content or compactive effort, as shown in Figure 1 (*a*). For water contents dry of optimum, the hydraulic conductivity is large and it decreases sharply as water content approaches optimum water content. When the soil is wetter than optimum, the hydraulic con-

GeoSyntec Consultants, 5775 Peachtree Dunwoody Road, Suite 200F, Atlanta, Ga. 30342.

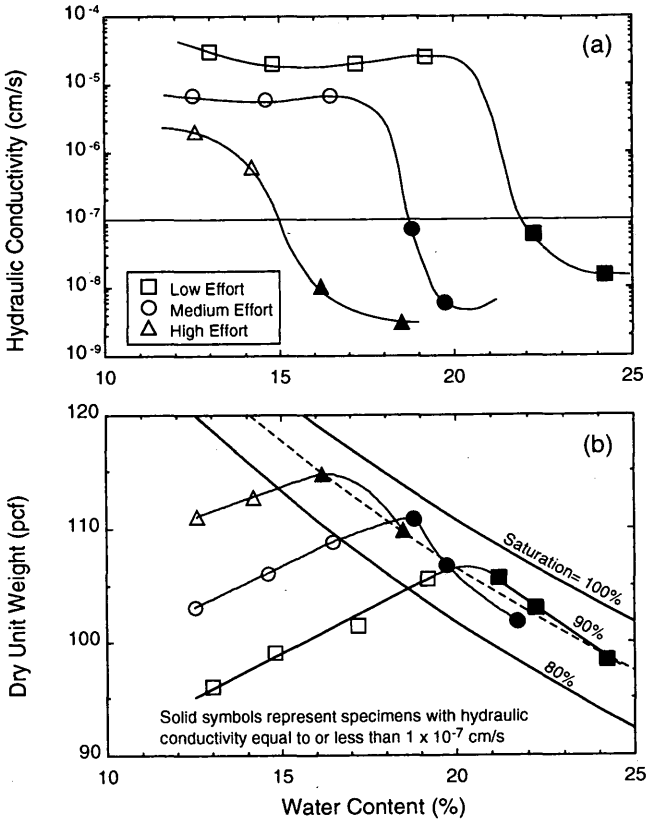

FIGURE 1 Data from Mitchell et al. (*4*) for silty clay soil: (*a*) hydraulic conductivity versus molding water content; (*b*) dry unit weight versus molding water content (1 pcf = 0.157 kN/m³).

ductivity is low. The hydraulic conductivity also decreases significantly with the increase in the compactive effort.

The cause of the change in hydraulic conductivity from high to low with dry to wet-of-optimum water content and with the increase of compactive effort is due to the change in the pore size distribution. On the dry side of optimum water content, the clay aggregates have higher strength and thus are more resistant to deformation during compaction. As a result, the clay has a heterogeneous network of macroscopic pore and hence high hydraulic conductivity (*5,7,8*). On the wet side of optimum, the clay aggregates deform easily during compaction, which results in a dense, relatively homogeneous mass with a very fine pore size (*7,9,10*). The fine (perhaps microscopic) pore size limits the conduction of fluid.

To further demonstrate the effects of compaction variables on hydraulic conductivity, all data points in Figure 1 corresponding to an arbitrarily selected maximum hydraulic conductivity of 1×10^{-7} cm/sec have been represented by solid symbols (a design hydraulic conductivity of 1×10^{-7} cm/sec is typical for hydraulic barriers and therefore is used throughout this paper). As shown in Figure 1 (*b*), these data points plot in a narrow zone that extends almost parallel to the line of full saturation (i.e., zero air void line) and the line of optimums. The leftmost boundary of the zone coincides with the 83 percent degree-of-saturation contour line. Therefore for this particular soil, to achieve a maximum hydraulic conductivity of 1×10^{-7} cm/sec, the soil must be compacted to an initial degree of saturation in excess of 83 percent.

Throughout the paper, reference is made to degree of saturation. This is the initial (i.e., as compacted) degree of saturation and not the degree of saturation of the soil during or after permeation.

MODERN COMPACTION CONTROL CRITERIA

Graphical Approach

Daniel and Benson (*1*) proposed a graphical approach for determining the acceptable water content–dry unit weight zone. This approach is illustrated in Figure 2 for the data of Mitchell et al. (*4*). The approach consists of the following steps:

1. Specimens are compacted using three broad compactive efforts that are representative of efforts used in construction. Approximately five to six different specimens are compacted with each effort.
2. The compacted specimens are permeated to determine their hydraulic conductivity. The compaction curves and water content–hydraulic conductivity curves are plotted as shown in Figure 2.
3. Different symbols are used to distinguish between specimens with hydraulic conductivity greater than the maximum acceptable value and specimens with hydraulic conductivity less than or equal to the maximum acceptable value. In Figure 2, the maximum acceptable hydraulic conductivity is arbitrarily shown as 1×10^{-7} cm/sec.

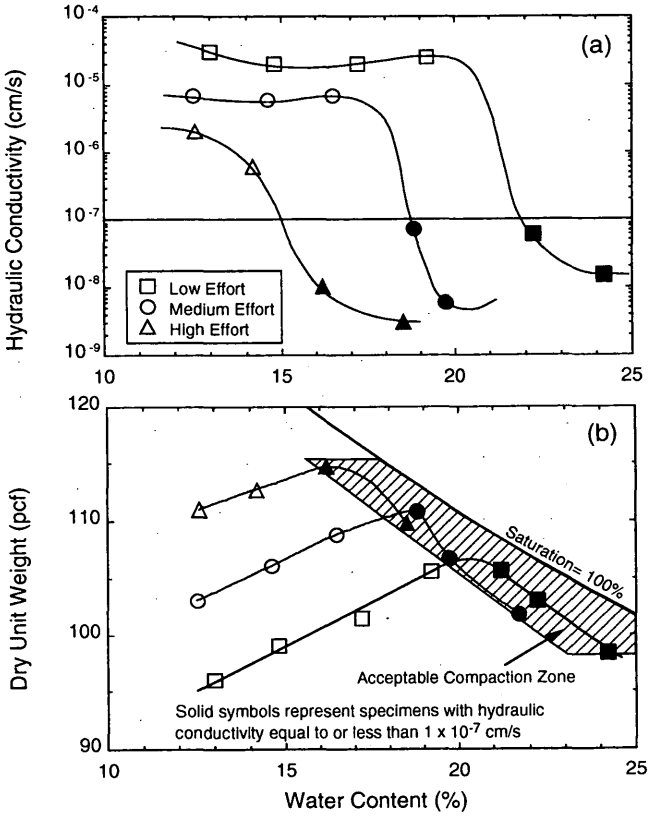

FIGURE 2 Graphical approach illustrated for data of Mitchell et al. (*4*): (*a*) hydraulic conductivity versus molding water content; (*b*) dry unit weight versus molding water content showing acceptable compaction zone (1 pcf = 0.157 kN/m³).

4. The "acceptable" water content–dry unit weight zone is drawn to encompass the data points representing specimens with hydraulic conductivity equal to or less than the maximum acceptable hydraulic conductivity.
5. Although not addressed in this paper, Daniel and Benson (*1*) do make provisions to limit the acceptable zone to account for other considerations such as shear strength, shrinkage, swelling, and desiccation or settlement cracking.

This approach is clearly superior to the traditional approach because it is based primarily on hydraulic conductivity. This criterion can be used effectively in the construction of hydraulic barriers with low hydraulic conductivity as long as the soil used to construct the hydraulic barrier does not exhibit significant variability in compaction characteristics. It is the experience of the authors and several researchers (*11,12*), however, that in many cases the compaction characteristics of soil from the same borrow source may vary considerably because of slight changes in sand or gravel contents.

In these cases construction quality assurance technicians in the field find that the water content—dry unit weight relationship (i.e., the compaction curve) shifts during the course of construction, even when soil from one borrow source is used. Therefore the previously established acceptable water content–dry unit weight zone may not be valid for all soils excavated from the same borrow area. A new acceptable zone must be established for each soil excavated. Establishing a new zone can be expensive and may delay construction.

Problems can also arise from the inability to detect variations in the soils used to construct the hydraulic barrier in cases where testing frequencies are inadequate and soil variations are not visually recognized. In these cases using the established criterion may be restrictive or may not ensure low hydraulic conductivity. Even if all soils from the borrow area to be used in the construction of the hydraulic barrier were identified and an acceptable zone were defined for each one of them, having several compaction zones may be confusing to the technician in the field. The technician must be able to identify new soils excavated with certainty to determine which of the acceptable compaction zones should be used for its construction.

Line-of-Optimums Approach

Mundell and Bailey (*13*) and Benson and Boutwell (*2*) proposed criteria that are based primarily on compacting the soil wet of the line of optimums. On the wet side of optimum the soil has lower shear strength and thus the clods are easier to remold. This results in a dense, relatively homogeneous mass with a very fine pore size and thus low hydraulic conductivity (*7,9,10*). On the dry side of optimum the clods are harder and thus are typically more difficult to remold. Therefore soil compacted on the dry side of optimum contains larger pores, and as a result the hydraulic conductivity is higher.

In many cases, however, the maximum allowable hydraulic conductivity can still be achieved if the soil is compacted on the dry side of optimum. Figure 3 shows the acceptable water content–dry unit weight zone based on the line-of-optimums approach for the data of Mitchell et al. (*4*). The solid symbols represent soil specimens with hydraulic conductivity less than or equal to 1×10^{-7} cm/sec. As shown in Figure 3, four of the eight specimens that have hydraulic conductivity less than or equal to 1×10^{-7} cm/sec plot outside the acceptable zone based on the line-of-optimums approach. Other laboratory and field data presented in this paper also suggest that, depending on the type of clay, low hydraulic conductivity can be achieved by compaction on the dry side of the line of optimums.

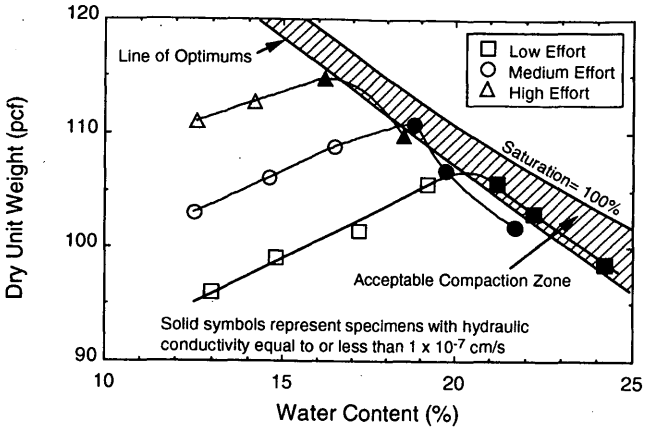

FIGURE 3 Line-of-optimums approach illustrated for data of Mitchell et al. (*4*) (1 pcf = 0.157 kN/m³).

Therefore the line-of-optimums approach may be restrictive in some cases. It is especially restrictive when considerations other than achieving low hydraulic conductivity, such as adequate shear strength or resistance to desiccation or freeze-thaw cracking, are also significant. For example, a soil liner placed on a steep slope may need to be compacted as dry as possible, while still achieving the required hydraulic conductivity, in order to gain the necessary shear strength for its stability. Similarly, recent research has shown that compacting the soil as dry as possible increases its resistance to desiccation and freeze-thaw damage (*14,15*).

Degree-of-Saturation Approach

As discussed earlier, the hydraulic conductivity of a compacted soil decreases with increasing degree of saturation. The degree of saturation combines the effects of water content and dry unit weight in one parameter. As the molding water content and dry unit weight are increased, so is the degree of saturation, and thus hydraulic conductivity decreases. An examination of Figure 1 suggests that degree of saturation can be used as a criterion for the compaction of clay hydraulic barriers. For the data shown in Figure 1, to achieve a hydraulic conductivity equal to or less than 1×10^{-7} cm/sec, the soil must be compacted to a minimum degree of saturation of 83 percent.

Several researchers found strong correlations between hydraulic conductivity and degree of saturation for specimens obtained from compacted clay liners. Boutwell and Hedges (*16*) performed regression analyses on hydraulic conductivity data for Shelby tube specimens taken from liners from several sites. They found the logarithm of hydraulic conductivity to be inversely proportional to the degree of saturation to the third power. Similarly, Benson et al. (*17*) collected and analyzed data from more than 50 sites to identify variables with the greatest effect on hydraulic conductivity. They also found the hydraulic conductivity to decrease with the increase of degree of saturation. They found that at degrees of saturation greater than 90 percent, nearly all specimens had hydraulic conductivities of less than 1×10^{-7} cm/sec.

Lahti et al. (*18*) performed laboratory and field hydraulic conductivity tests on a liner constructed using low-plasticity clay till at the Keele Valley Landfill at Maple, Ontario. The liner was required to achieve a hydraulic conductivity of 1×10^{-8} cm/sec. The soil was compacted at water contents 2 to 3 percent wetter than optimum water content and to a dry unit weight greater than 95 percent of the maximum dry unit weight based on the standard Proctor (ASTM D698) compactive effort. Laboratory tests performed on Shelby tube specimens obtained from the liner showed a geometric mean hydraulic conductivity of 8×10^{-9} cm/sec. Field hydraulic conductivity tests consisted of six 15-m × 15-m lysimeters. The geometric mean hydraulic conductivity calculated from flow rates in the lysimeters was 9×10^{-9} cm/sec. Lahti et al. (*18*) concluded that to achieve the acceptable hydraulic conductivity of 1×10^{-8} cm/sec, the clay till must be compacted at water contents greater than the optimum water content based on the standard Proctor compactive effort and to a degree of saturation of 95 percent or more.

On the basis of the findings of these researchers and others, it appears that the degree-of-saturation approach can be used to control and predict hydraulic conductivity of compacted clay barriers. The degree-of-saturation approach has several desirable practical characteristics. First, with this approach one parameter—degree of saturation—replaces the two parameters used in the other approaches—water content and dry unit weight.

The second advantage of this approach is that it is numerical. The technician in the field can easily and accurately determine whether the soil passes or fails the compaction criteria by comparing the actual degree of saturation to the minimum required degree of saturation. Nuclear moisture/density gauges, which are commonly used to measure water content and dry unit weight in the field, can also be programmed by manufacturers to calculate and display degree of saturation.

The third advantage of this approach is that the minimum degree of saturation required to achieve the maximum design hydraulic conductivity is not sensitive to natural variations in soil composition. A small change in sand or gravel content has little effect on saturation–hydraulic conductivity relationships as long as the sand and gravel fractions are not dominant (*11*). Therefore, unlike the graphical approach, where variability in soil compaction characteristics may require defining multiple acceptance zones, with the degree-of-saturation approach, one criterion can be used for soils with only small variations in composition.

LABORATORY DATA

Compaction and hydraulic conductivity data from several laboratory studies have been analyzed to establish a relationship between hydraulic conductivity and degree of saturation. Table 1 summarizes the properties of the soils used in these studies and shows that the soils vary in composition and compaction characteristics.

Figures 4 through 6 show the compaction and hydraulic conductivity–water content relationships for Wisconsin soils A, B, and C studied by Othman and Benson (*19*). These relationships are similar to those shown in Figure 1 and are typical of clays. The solid symbols in the figures represent specimens with hydraulic conductivity equal to or less than 1×10^{-7} cm/sec. As shown in Figures 4 (*b*), 5 (*b*), and 6 (*b*), these data points plot generally parallel to the line of full saturation.

The effect of degree of saturation on hydraulic conductivity of the Wisconsin soils is shown in Figure 7. The two lines shown in Figure 7 encompass the data points and assist in showing the trend exhibited by the data. Although the three clays are significantly different in composition and compaction characteristics, they demon-

TABLE 1 Characteristics of Soils Used in Laboratory Studies and Soil Specimens from Liners of Several Landfills

Reference	Soil	USCS Classification	LL(%)[a]	PI(%)[a]	P_{200}(%)[b]	5μm Clay Fraction (%)	Optimum Water Content[c] (%)	Maximum Dry Unit Weight (pcf)[c]
			Laboratory Studies					
19	Wisconsin A	CL	34	16	85	58	16.0	114.5
	Wisconsin B	CL	42	19	99	77	18.5	107.0
	Wisconsin C	CH	84	60	71	58	26.0	93.5
20	Wisconsin A	CL	36	19	88	61	15.0	116.0
1	Type A	-	55	27	-	-	29.0	92.0
	Type B	-	34	18	-	-	17.0	109.0
4	Silty Clay	CL	37	14	-	-	-	-
			Field Soil Specimens					
	1	CL	45	24	82	42	18.8	106.6
	2	CL	35	12	57	-	14.3	116.8
	3	CH	63	42	96	53	20.5	103.9
	4	ML	37	12	64	33	-	-
	5	GC	26	8	16	5	-	-
	6	SC	32	10	14	5	-	-
	7	SW-SM	30	7	10	3	-	-

[a]LL = Liquid Limit; PI = Plasticity Index
[b]Percent Passing No. 200 Sieve (0.075 mm)
[c]Standard Proctor (ASTM D698), 1 pcf = 0.157 kN/m^3

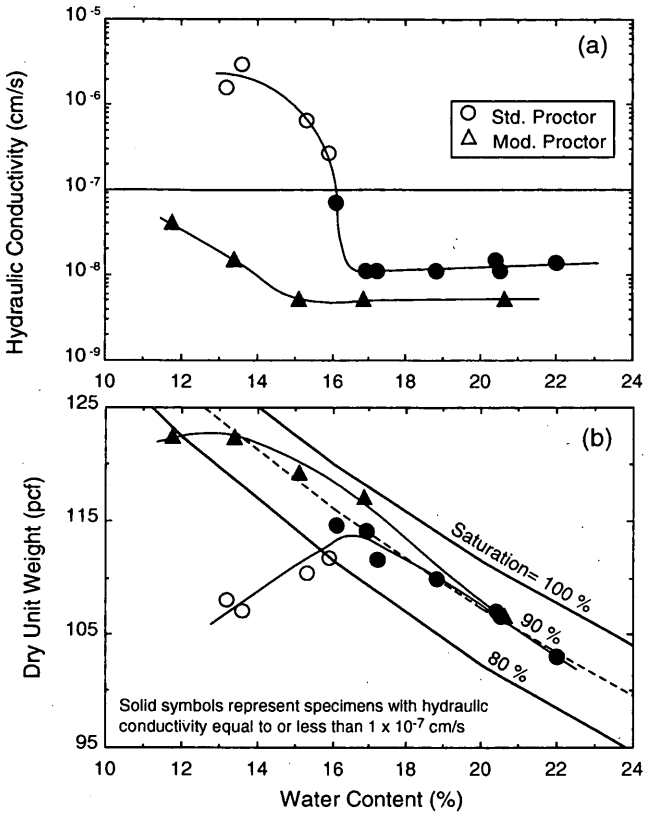

FIGURE 4 Data from Othman and Benson (*19*) for Wisconsin soil A: (*a*) hydraulic conductivity versus molding water content; (*b*) dry unit weight versus molding water content (1 pcf = 0.157 kN/m³).

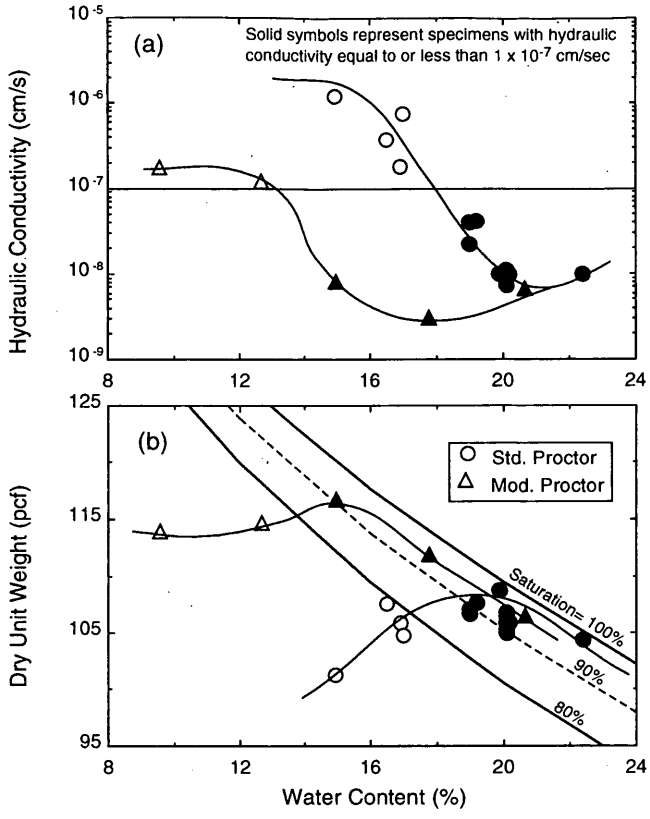

FIGURE 5 Data from Othman and Benson (*19*) for Wisconsin soil B: (*a*) hydraulic conductivity versus molding water content; (*b*) dry unit weight versus molding water content (1 pcf = 0.157 kN/m³).

strate almost the same relationship between hydraulic conductivity and degree of saturation. As the degree of saturation increases, hydraulic conductivity decreases. For the three clays, maximum hydraulic conductivities of 1×10^{-6}, 1×10^{-7}, and 1×10^{-8} cm/sec are achieved at degrees of saturation of approximately 77, 88, and 100 percent, respectively. Therefore, to ensure that the hydraulic conductivity of any of these soils is less than 1×10^{-7} cm/sec, for example, the soil must be compacted to a degree of saturation greater than 88 percent.

Figure 8 (*a*) shows the relationship between hydraulic conductivity and degree of saturation for data from laboratory studies on all the soils listed in Table 1. As shown, some variability exists in the data; however, a trend of decreasing hydraulic conductivity with increasing degree of saturation is evident.

FIELD DATA

Hydraulic conductivity tests were conducted on specimens obtained from compacted clay liners at several sites, and the data were collected and analyzed to evaluate the degree-of-saturation approach and to confirm findings based on the laboratory data. Table 1 summarizes the properties of the soils used at the different sites and shows that the soils vary in composition and compaction characteristics.

Figure 8(*b*) shows the relationship between degree of saturation and hydraulic conductivity for all of the field and laboratory specimens. Laboratory and field data show similar degree of saturation–hydraulic conductivity relationships. There is a clear trend in Figure 8 (*b*) of decreasing hydraulic conductivity with increasing degree of saturation.

CASE HISTORY

A test fill program was performed for a landfill in the western United States to fulfill permit conditions that require that a compacted clay liner test fill be constructed before secure cell construction. In accordance with Environmental Protection Agency (EPA) guidance documents, construction of the test fill was performed using the same soil, equipment, and procedures that will be used to construct the compacted clay components of the secure cell liner system. The EPA guidance documents also required that the hydraulic conductivity of the test fill be evaluated using field testing techniques.

The test fill program consisted of the following steps:

1. A preconstruction laboratory testing program was performed to quantify index properties of the soil and to establish an acceptable compaction zone (ACZ) on the basis of laboratory hydraulic conductivity tests conducted on laboratory-compacted (i.e., remolded) specimens.
2. A construction-phase laboratory testing program was conducted to confirm index properties of the soil and to evaluate the ACZ on the basis of laboratory hydraulic conductivity tests conducted on samples obtained from the test fill.

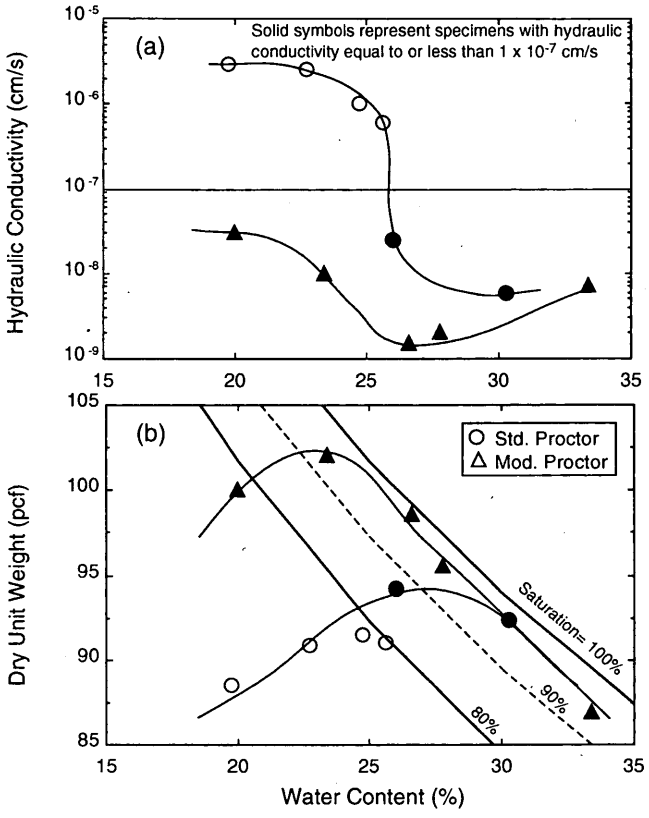

FIGURE 6 Data from work by Othman and Benson (*19*) for Wisconsin soil C: (*a*) hydraulic conductivity versus molding water content; (*b*) dry unit weight versus molding water content (1 pcf = 0.157 kN/m³).

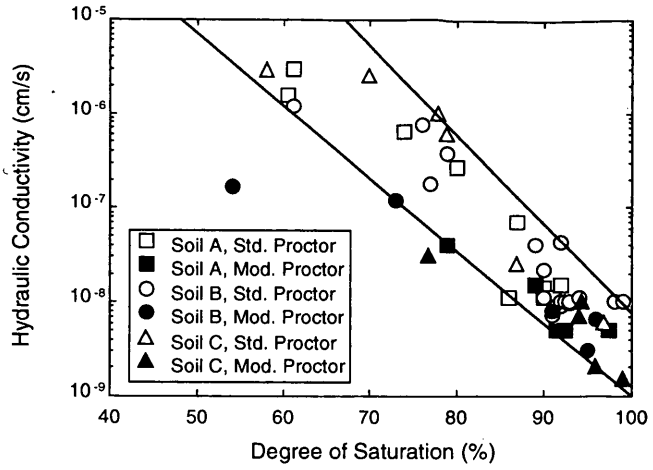

FIGURE 7 Effect of degree of saturation on hydraulic conductivity of three Wisconsin clays.

3. A field-scale testing program was performed to evaluate the field-measured hydraulic conductivity of a prototype compacted soil liner.

Results of the preconstruction laboratory testing program indicated that the soil is classified as a clay of high plasticity according to the Unified Soil Classification System. The composition and index properties of the soil are shown in Table 1 (Soil 3). The ACZ established during the preconstruction laboratory testing program (i.e., the "lab ACZ"), shown in Figure 9, indicates that the soil achieves a hydraulic conductivity less than 1×10^{-7} cm/sec when compacted in the laboratory to a wide range of water content–dry unit weight conditions. Preliminary boundaries were also established for the zone shown in Figure 9 to account for shrinkage and shear strength.

Results of the construction-phase laboratory testing program indicated that the ACZ determined from undisturbed field samples (i.e., the "field ACZ") is relatively similar to the lab ACZ established during the preconstruction testing program. Figure 10 shows the relationship between degree of saturation and hydraulic conductivity for the laboratory and field specimens. Clearly both sets of data can be described using the same relationship. Figure 10 indicates that a minimum degree of saturation of approximately 78 percent is required to achieve a hydraulic conductivity of less than 1×10^{-7} cm/sec.

Information obtained during the preconstruction and construction laboratory testing programs was used to select a set of target compaction (i.e., water content–dry unit weight) conditions for construction of a prototype soil liner. The target conditions, shown in Figure 9, were selected to be within the field ACZ. A prototype soil liner was constructed using the clay soil and the target compaction conditions. Field testing of the hydraulic conductivity of the prototype compacted soil liner was conducted using a sealed double-ring infiltrometer (SDRI). The field-measured hydraulic conductivity of the prototype soil liner from the SDRI test was approximately 2×10^{-8} cm/sec. This value corresponded well with the hydraulic conductivity that would be predicted from both the lab and field ACZ, as shown in Figure 10.

Results of the test fill program conducted using the clay soil were used to establish an ACZ to be used during actual construction of the clay components of the liner system. The ACZ represents the compaction conditions that will yield a high probability of achieving a hydraulic conductivity during construction that is less than 1×10^{-7} cm/sec. In addition, lower-side boundaries were established for the ACZ based on minimum shear strength and workability requirements of the compacted clay component of the liner system.

From the test fill program it is concluded that the acceptable compaction zone may be most efficiently defined in terms of the minimum degree of saturation required to achieve a low hydraulic conductivity. Agreement between laboratory and field data suggests that the degree-of-saturation approach is valid and effective in predicting and controlling hydraulic conductivity of clay hydraulic barriers.

SUMMARY AND CONCLUSIONS

In this paper, criteria currently used for compacting soil hydraulic barriers are reviewed. Compaction criteria define an acceptable water content–dry unit weight zone. The paper examines three modern compaction criteria that require defining a water content–dry unit weight zone that corresponds to the maximum required hydraulic conductivity. The modern criteria reviewed are the graphical approach, the line-of-optimums approach, and the degree-of-saturation approach. The advantages and deficiencies of each approach are discussed with emphasis on efficiency, effectiveness, and practicality of use in construction. It was concluded

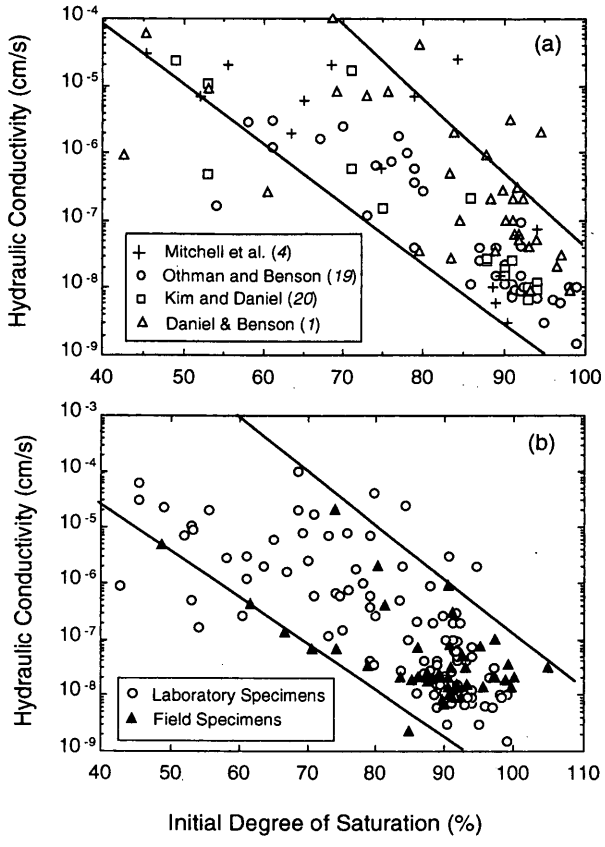

FIGURE 8 Effect of degree of saturation on hydraulic conductivity of (*a*) laboratory specimens; (*b*) laboratory and field specimens combined.

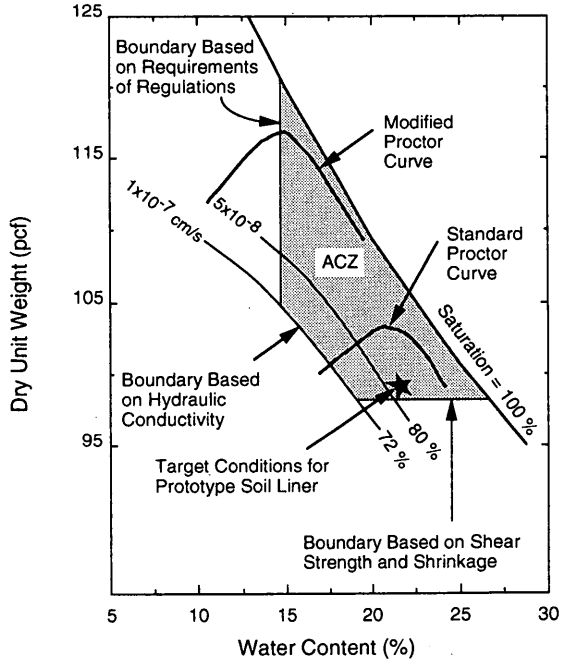

FIGURE 9 Acceptable compaction zone determined from laboratory testing program (1 pcf = 0.157 kN/m³).

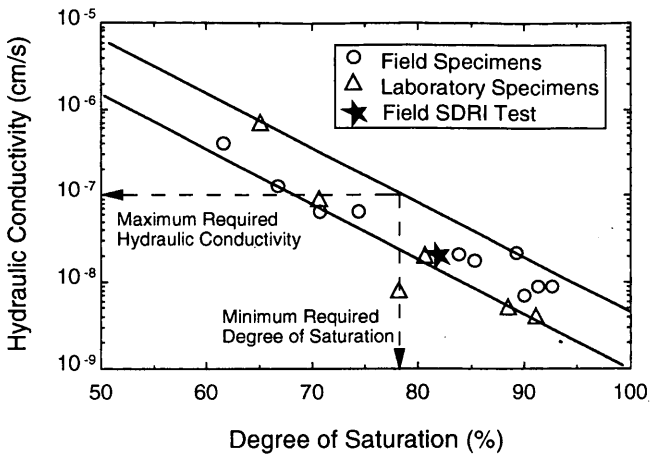

FIGURE 10 Hydraulic conductivity as a function of degree of saturation from tests on laboratory and field specimens and from a field SDRI test.

that the graphical approach may be impractical when the soils in the field exhibit significant variability in compaction characteristics. The line-of-optimums approach may be too restrictive, since the maximum required hydraulic conductivity may be achieved on the dry side of optimum.

The degree-of-saturation approach appears to have desirable attributes and has several advantages over the two other approaches. Only one parameter—the degree of saturation—is used to control and predict hydraulic conductivity. This factor, and the fact that this approach is numerical, makes construction quality control in the field easier and more efficient. Furthermore, unlike the compaction curve, the hydraulic conductivity–degree of saturation relationship is typically not sensitive to the natural variations of soil composition. Therefore, one criterion can be used for soils with small variations in composition.

Laboratory and field data on compaction and hydraulic conductivity of many soils were examined to evaluate the degree-of-saturation approach. The data show that degree of saturation can be used to accurately predict and control hydraulic conductivity. Hydraulic conductivity decreased with increasing degree of saturation for all soils examined. This result is consistent with the findings of other investigators (*16–18*). A case history that illustrates the use of the degree-of-saturation compaction criterion in the construction of a landfill liner is presented. It is concluded that degree of saturation can be used as a compaction control criterion during construction of clay hydraulic barriers.

ACKNOWLEDGMENTS

The authors thank Rudy Bonaparte for his review of the manuscript and Nader Rad for providing some of the data used in this paper. Thanks are also expressed to Karen Rich and Mitzi Jiles for their help with typing the manuscript.

REFERENCES

1. Daniel, D. E., and C. H. Benson. Water Content–Density Criteria for Compacted Soil Liners. *Journal of Geotechnical Engineering,* ASCE, Vol. 116, No. 12, 1990, pp. 1811–1830.

2. Benson, C. H., and G. P. Boutwell. Compaction Control and Scale-Dependent Hydraulic Conductivity of Clay Liners. *Proc., 15th Annual Madison Waste Conference,* Madison, Wis., 1992, pp. 62–83.
3. Lambe, T. Special Technical Publication 163: *The Permeability of Compacted Fine-Grained Soils.* ASTM, Philadelphia, Pa., 1954, pp. 56–67.
4. Mitchell, J. K., D. R. Hooper, and R. G. Campanella. Permeability of Compacted Clay. *Journal of the Soil Mechanics and Foundations Division,* ASCE, Vol. 91, No. SM4, 1965, pp. 41–65.
5. Garcia-Bengochea, I., C. W. Lovell, and A. G. Altschaeffl. Pore Distribution and Permeability of Silty Clay. *Journal of Geotechnical Engineering,* ASCE, Vol. 105, No. 7, July 1979, pp. 839–856.
6. Elsbury, B. R., D. E. Daniel, G. A. Sraders, and D. C. Anderson. Lessons Learned from Compacted Clay Liner. *Journal of Geotechnical Engineering,* ASCE, Vol. 116, No. 11, Nov. 1990, pp. 1641–1660.
7. Benson, C. H., and D. E. Daniel. Influence of Clods on Hydraulic Conductivity of Compacted Clay. *Journal of Geotechnical Engineering,* ASCE, Vol. 116, No. 8, Aug. 1990, pp. 1231–1248.
8. Lambe, T. W. Foundation Engineering. In *Soil Stabilization* (G. A. Leonards, ed.), McGraw Hill, New York, 1962, pp. 351–437.
9. Shackelford, C., and F. Javed. Large-Scale Laboratory Permeability Testing of a Compacted Clay Soil. *Geotechnical Testing Journal,* Vol. 14, No. 2, 1991, pp. 171–179.
10. Haug, M., and L. Wong. Impact of Molding Water Content on Hydraulic Conductivity of Compacted Sand-Bentonite. *Canadian Geotechnical Journal,* Vol. 29, No. 2, 1992, pp. 253–262.
11. Shelley, T. L., and D. E. David. Effect of Gravel on Hydraulic Conductivity of Compacted Soil Liners. *Journal of Geotechnical Engineering,* ASCE, Vol. 119, No. 1, Jan. 1993, pp. 54–68.
12. Houston, S. L., and K. D. Walsh. Comparison of Rock Correction Methods for Compaction of Clayey Soils. *Journal of Geotechnical Engineering,* ASCE, Vol. 119, No. 4, April 1993, pp. 763–778.
13. Mundell, J., and B. Bailey. The Design and Testing of a Compacted Clay Barrier to Limit Percolation Through Landfill Covers. In *Special Technical Publication 874: Hydraulic Barriers in Soil and Rock* (Johnson et al., eds.), ASTM, Philadelphia, 1985, pp. 246–262.
14. David, D. E., and Y.-K. Wu. Compacted Clay Liners and Covers for Arid Sites. *Journal of Geotechnical Engineering,* ASCE, Vol. 119, No. 2, Feb. 1993, pp. 223–237.
15. Bowders, J. J., and M. A. Othman. Molding Water Content and Hydraulic Conductivity of Compacted Soils Subjected to Freeze-Thaw. In *Transportation Research Record 1434,* TRB, National Research Council, Washington, D.C., 1994.
16. Boutwell, G. P., and C. Hedges. Evaluation of Waste-Retention Liners by Multivariate Statistics. *Proc., 12th International Conference on Soil Mechanics and Foundation Engineering,* Rio de Janeiro, Brazil, 1989, pp. 815–818.
17. Benson, C. H., H. Zhai, and X. Wang. Estimating Hydraulic Conductivity of Compacted Clay Liners. *Journal of Geotechnical Engineering,* ASCE, Vol. 120, No. 2, Feb. 1994, pp. 366–387.
18. Lahti, L. R., K. S. King, D. W. Reades, and A. Bacopoulos. Quality Assurance Monitoring of a Large Clay Liner. In *Geotechnical Practice for Waste Disposal '87* (R. D. Woods, ed.), American Society of Civil Engineers, New York, 1987, pp. 641–654.
19. Othman, M. A., and C. H. Benson. Effect of Freeze-Thaw on the Hydraulic Conductivity of Three Compacted Clays from Wisconsin. In *Transportation Research Record 1369,* TRB, National Research Council, Washington, D.C., 1992, pp. 118–125.
20. Kim, W.-H. and D. E. Daniel. Effects of Freezing on Hydraulic Conductivity of Compacted Clay. *Journal of Geotechnical Engineering,* ASCE, Vol. 118, No. 7, July 1992, pp. 1083–1097.

Publication of this paper sponsored by Committee on Transportation Earthworks.

Behavior of Expanded Polystyrene Blocks

T. PREBER, S. BANG, Y. CHUNG, AND Y. CHO

An innovative construction material, expanded polystyrene blocks (EPS blocks), has been introduced in geotechnical engineering in recent years. Because of its extremely light weight and ease in handling, it provides an alternative to conventional backfill, embankment earth materials, and lightweight fill. It is anticipated that the use of EPS blocks in the construction industry may result in substantial cost savings. New applications of EPS blocks as structural elements are expected to emerge as engineers learn more about this material. A series of laboratory tests were conducted to determine the mechanical properties of EPS blocks. Included are the results of undrained triaxial tests with volume change measurements for the determination of a constitutive relationship, a repeated loading test, punching shear tests, and a long-term creep test. The test results show several distinctive material characteristics, including a bilinear stress-strain relationship and negative Poisson's ratio that are not common in conventional construction materials. The results of this study can readily be incorporated in detailed analyses of various geotechnical engineering structures constructed with EPS blocks.

The geotechnical engineering and construction industries have been seeking inexpensive, lightweight construction materials for backfill against retaining structures, fill for embankments on soft ground and beneath pavements, and replacement material for slope stabilization. The use of lightweight materials has been considered a technically acceptable and economical solution to many instability and settlement problems related to weak and highly compressible soils.

Super-light expanded polystyrene blocks (EPS blocks) have been used in the road construction industry as a lightweight material for nearly three decades (*1,2*). The literature indicates that the Norwegian Road Research Laboratory has successfully used EPS blocks on more than 100 projects (*1,3,4*). It has been reported that the EPS blocks produce almost no lateral pressure on the bridge abutment walls. EPS blocks have also been used extensively as frost-proofing layers in highways in Europe and North America (*5*).

One of the first projects in which EPS blocks were used in the United States was a bridge near Pickford, Michigan, where a large portion of the abutment fill was replaced with EPS blocks. Another large-scale project in the United States was the 1987 reconstruction of a failed 60-m long section of U.S.-160 near Durango, Colorado (*6*). EPS blocks were selected mainly because the fragile slope could not support any more weight than the highway itself.

Expanded polystyrene has typically been used as insulation and packaging material. Its density is approximately 0.15 to 0.3 kN/m^3, equivalent to 1/60 to 1/30 the density of water (*7*). It is therefore extremely light, producing almost no gravity-induced stress, and is easy to handle. It also has extremely low thermal conductivity and can therefore be used as an insulation material in cold regions with frost-susceptible soils. It is stable chemically, and it is not subject to decay. However, it must be protected from petroleum distillates, fire, ultraviolet light, and vandalism. Because of its light weight, the cost of conventional earth work can be dramatically reduced if EPS blocks are used under certain circumstances. Engineering structures constructed with EPS blocks are expected to experience lower stresses than those constructed with conventional materials, resulting in smaller structural sections and thereby substantial cost savings.

Department of Civil and Environmental Engineering, South Dakota School of Mines and Technology, 501 East St. Joseph Street, Rapid City, S.D. 57701–3995

DETERMINATION OF MATERIAL BEHAVIOR

A series of laboratory tests was performed on samples cut from EPS blocks for determination of the constitutive relationship, punching shear resistance, material characteristic under a repeated loading, and long-term creep characteristic. The stress-strain relationship was determined from uniaxial compression tests and four sets of undrained triaxial tests on EPS samples of different densities. Each set consisted of four different confining pressures (0, 21, 41, and 62 kPa). The volume change behavior of the EPS samples was also observed during the triaxial tests. The creep behavior of the EPS material was monitored from a sample under an axial load of 24 kPa. The EPS material is identified by its unit weight [i.e., pounds per cubic foot (pcf)], which also represents the product name.

The details of the EPS samples and the stress conditions applied in various laboratory tests are presented in Table 1. The maximum confining pressure applied in undrained triaxial testing was limited to less than 62 kPa because the samples deformed excessively under confining pressures greater than 62 kPa.

Uniaxial Compressive and Undrained Triaxial Tests

Figures 1 through 3 show typical results obtained from the unconfined compression and undrained triaxial tests. The shapes of the stress-strain curves are similar regardless of the material unit weight and confining pressure. The stress-strain relationship is typically bilinear.

The test results indicate that, in general, as the unit weight of the EPS blocks increases, both the initial and plastic moduli increase, with the plastic modulus increasing at a lower rate. The test results also indicate that the material strength increases with unit weight. With increasing confining pressure, the initial modulus decreases but the plastic modulus increases.

Stress-Strain Relationship of EPS Blocks

To establish a detailed stress-strain relationship, four parameters were selected, as shown in Figure 4. These parameters are defined as follows:

TABLE 1 Summary of Laboratory Tests

Type of Test	Uniaxial Compression	Triaxial Compression	Punch Shear	Creep
Type of Material(pcf)	1,1.25 1.5,2.0	1,1.25 1.5,2.0	1,1.25 1.5,2.0	1.5
Confining Pressure(kPa)		0,21 41,62		
Axial Stress (kPa)				24 71

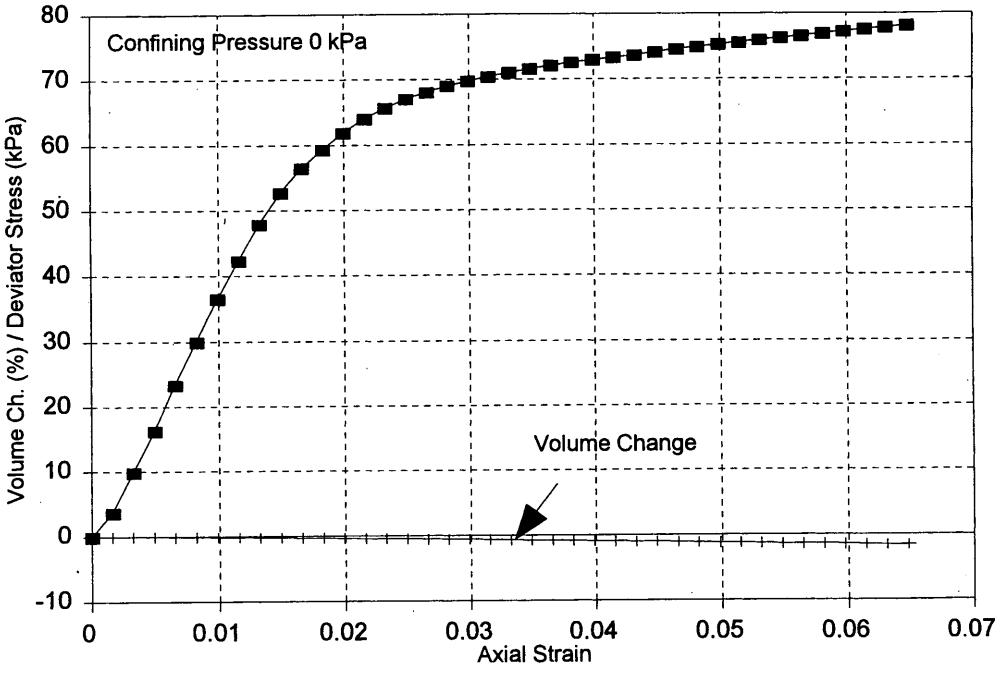

FIGURE 1 Undrained triaxial test on 1.25-pcf EPS.

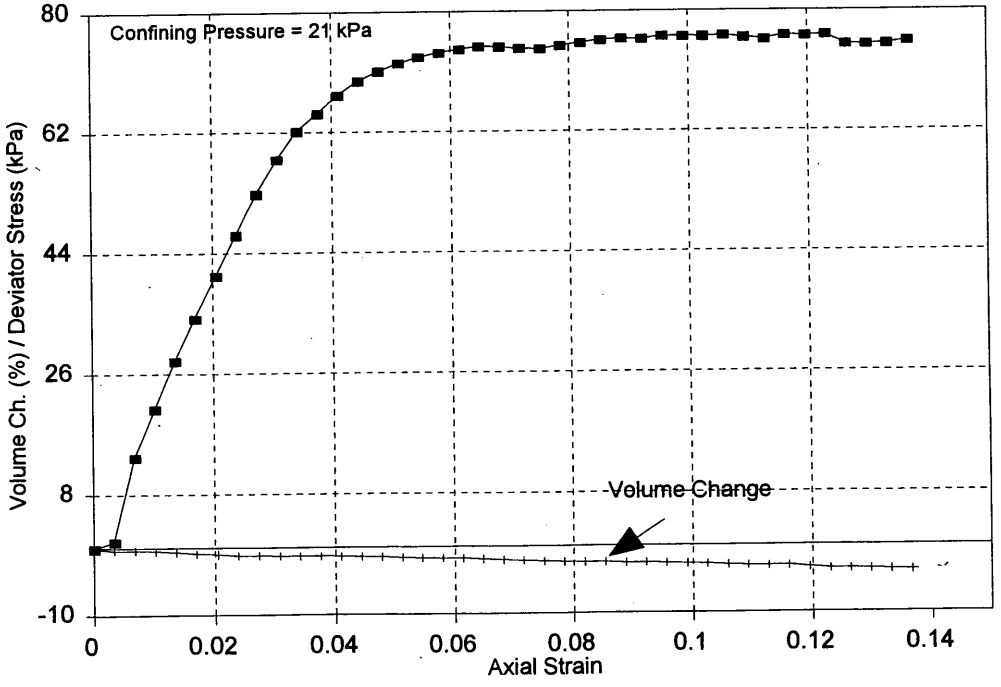

FIGURE 2 Undrained triaxial test on 1.5-pcf EPS.

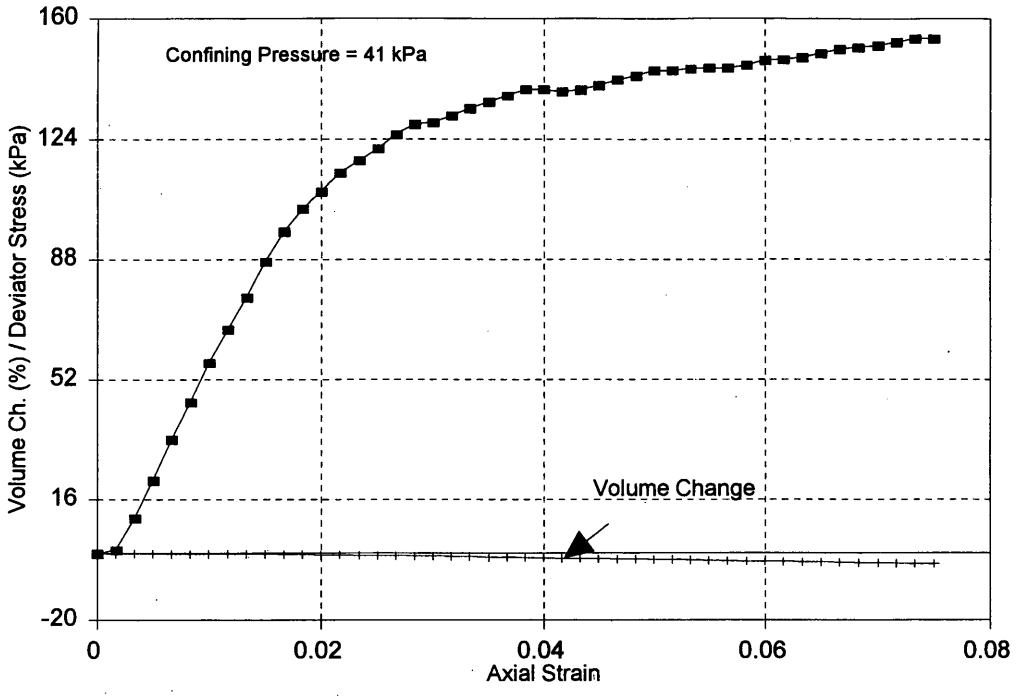

FIGURE 3 Undrained triaxial test on 2.0-pcf EPS.

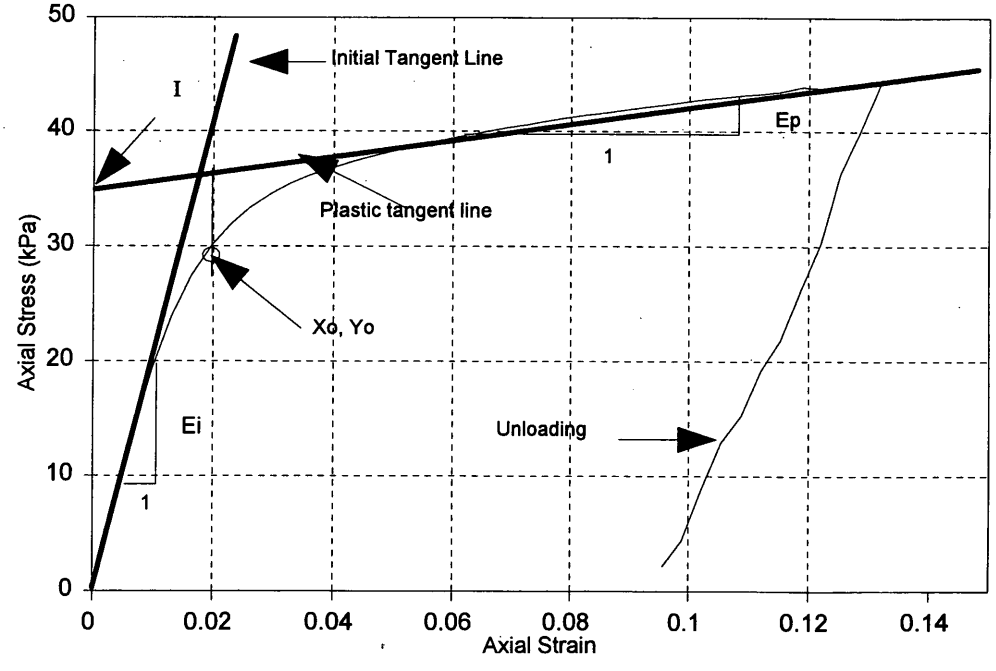

FIGURE 4 Parameters describing constitutive relationship.

E_i = Initial modulus.
E_p = Plastic modulus.
I = Intersection of the axial stress axis and the plastic tangent line.
Y_o = Axial stress value corresponding to strain X_o.

In addition, X_o is the strain value at the intersection of the initial tangent line and the plastic tangent line. This can be determined analytically from E_i, E_p, and I.

The axial stress-strain relationship of the EPS blocks is proposed to follow

$$\sigma = (I + E_p \epsilon)\left[1 - \exp\left(-C\epsilon^2 - \frac{E_i \epsilon}{I}\right)\right] \quad (1)$$

where σ is axial stress and ϵ is axial strain.

$$C = -\frac{E_i}{I X_o} - \frac{1}{X_o^2}\ln\left[1 - \frac{Y_o}{(I + E_p X_o)}\right]$$

This expression satisfies all the requirements specified previously: the initial modulus, the asymptote defined by the plastic modulus, the yield stress, and the stress-strain data coordinate. This mathematical expression is chosen on the basis of the shape of the observed stress-strain curves.

From this stress-strain expression, the instantaneous tangent modulus of the EPS material can be obtained by differentiating the axial stress with respect to the axial strain. The following steps describe how the four parameters can be evaluated as functions of the EPS material density and the confining pressure.

1. Determine the values of each parameter from the stress-strain curves obtained from the undrained triaxial tests, as shown in Tables 2 through 5.
2. Plot the values of the parameters determined in Step 1 as a function of the confining pressure for each unit weight of the EPS blocks (Figures 5 through 8).
3. Establish the curves corresponding to the highest and the lowest unit weights of the EPS material, representing each parameter. These are shown in Figures 5 through 8 as the limiting curves (solid lines).
4. Interpolate the limiting curves determined in Step 3 for intermediate unit weights of the EPS material (dotted lines).

Though the actual variations of the parameters are somewhat scattered, straight lines have been used in the figures to show the variations. The generalized equations for each parameter are as follows:

$$\begin{aligned} I &= (-107 + 910\gamma) + (0.63 - 6.32\gamma)\sigma_3 \\ E_i &= (-4{,}180 + 39{,}000) + (-6.2 - 53\gamma)\sigma_3 \\ E_p &= (104 + 440\gamma) + (-3.6 + 150\gamma)\sigma_3 \\ Y_o &= (1.4 + 905\gamma) + (-1.1 + 4.5\gamma)\sigma_3 \end{aligned} \quad (2)$$

where γ is the unit weight of EPS material (kN/m^3) and σ_3 is the confining pressure (kPa).

Poisson's Ratio

Poisson's ratio of the EPS material has been evaluated by measuring the volume change of the EPS samples during the undrained tri-

TABLE 2 I Values from Triaxial Tests (kPa)

Confining Pressure (kPa)	Type of EPS			
	1.0 pcf	1.25 pcf	1.5pcf	2.0 pcf
0	22.4	68.3	39	165.5
	47.7	61.4	36.9	191.7
21	31.7	49.0	73.8	151.8
	30.3	50.3	72.1	154.4
41	16.2	31.7	58.6	122.7
	17.9	37.9	52.4	124.1
62	10.0	12.4	37.2	100.0
	15.2	21.4	31.7	82.7

TABLE 3 E_i Values from Triaxial Tests (kPa)

Confining Pressure (kPa)	Type of EPS			
	1.0 pcf	1.25 pcf	1.5pcf	2.0 pcf
0	1536	4073	3505	6791
	4183*	4036	2176	9464
21	2234	3335	4597	7388
	4313*	3418	1970	7968
41	2955*	2501	4867	7335
	2555*	7661	5910	6895
62	1207	2758	4413	6015
	660	2236	4186	7454

*Unused data in regression analysis

TABLE 4 E_p Values from Triaxial Tests (kPa)

Confining Pressure (kPa)	Type of EPS			
	1.0 pcf	1.25 pcf	1.5pcf	2.0 pcf
0	297*	212	556	422*
	195	284	509	253
21	169	246	164	362
	168	207	42	181*
41	254	189	138	517
	241	286	241	431
62	261	302	207	506
	207	260	280	716

*Unused data in regression analysis

TABLE 5 Y_o Values from Triaxial Tests (kPa)

Confining Pressure (kPa)	Type of EPS			
	1.0 pcf	1.25 pcf	1.5pcf	2.0 pcf
0	20.8	56.9	35.2	157.2
	36.9	57.2	42.1	180.6
21	28.4	43.4	65.5	144.8
	20.0	45.9	64.5	153.1
41	12.4	26.9	50.3	118.6
	15.2	23.8	49.0	113.8
62	9.3	9.0	28.6	88.3
	10.7	15.2	27.6	79.3

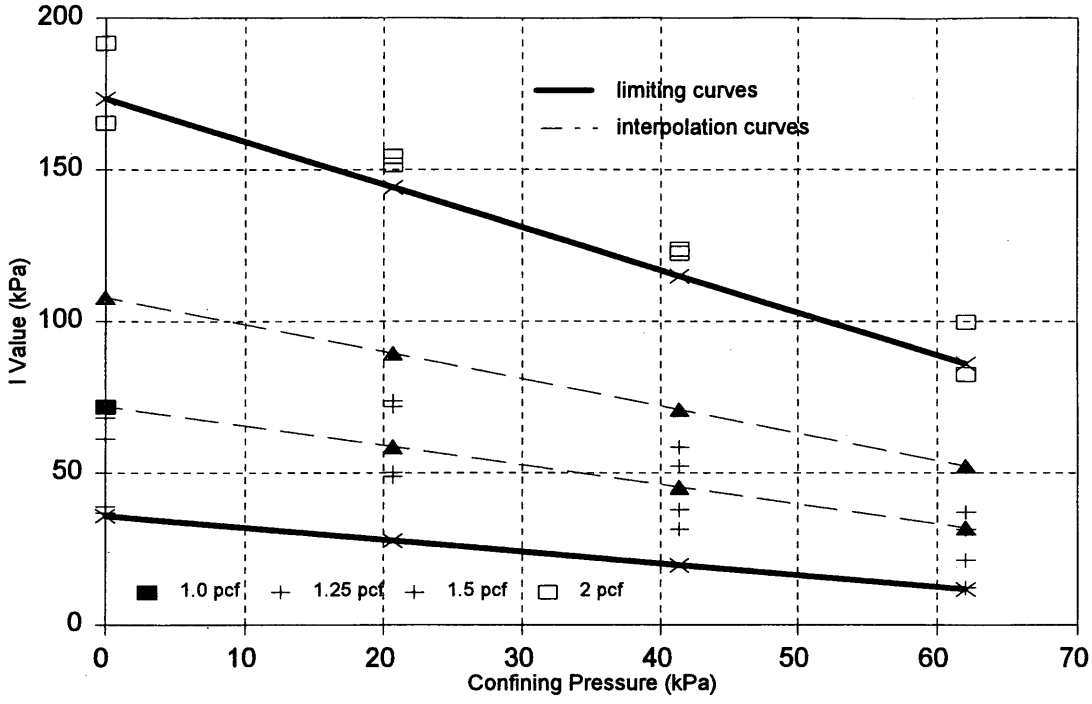

FIGURE 5 Variation of *I* value.

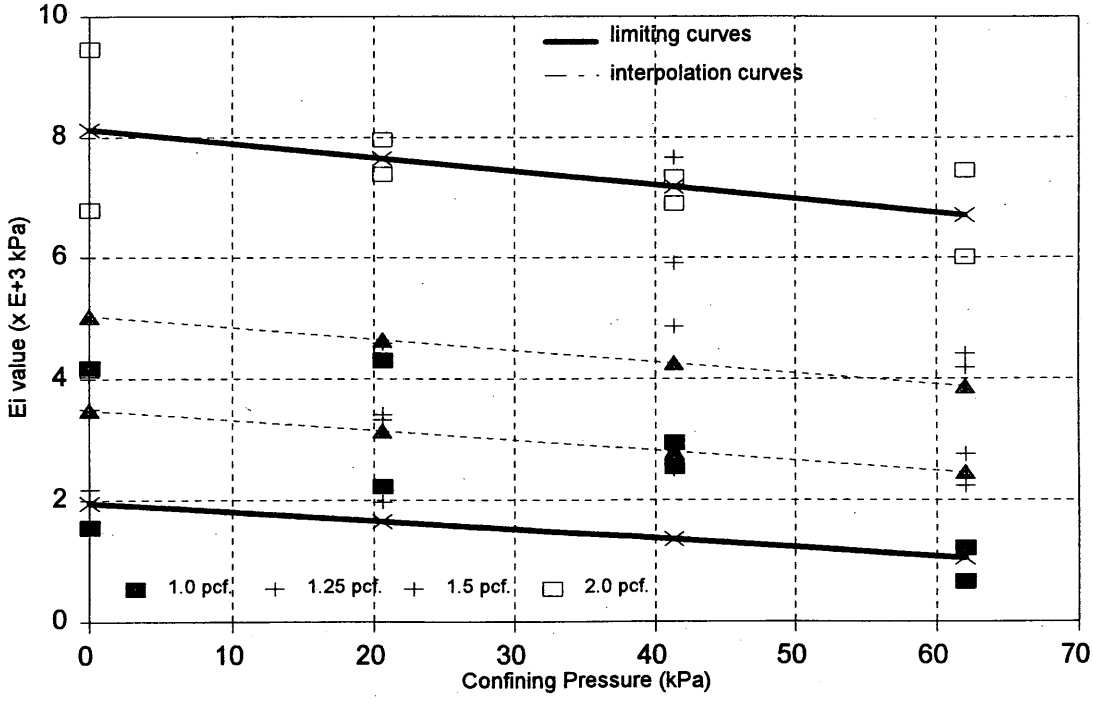

FIGURE 6 Variation of E_i value.

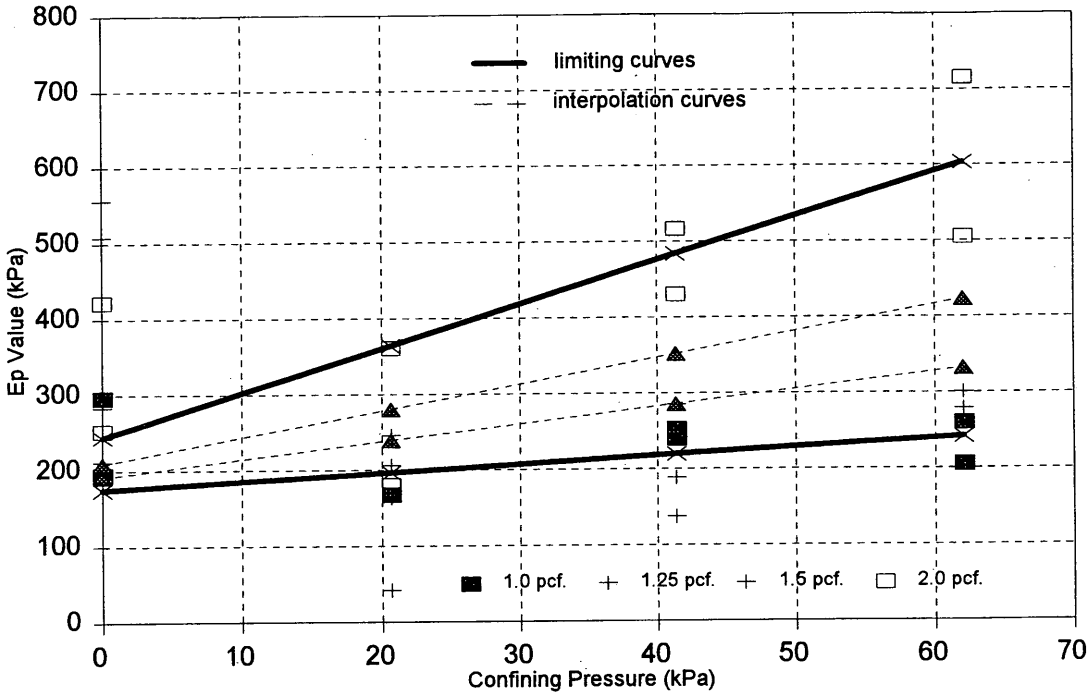

FIGURE 7 Variation of E_p value.

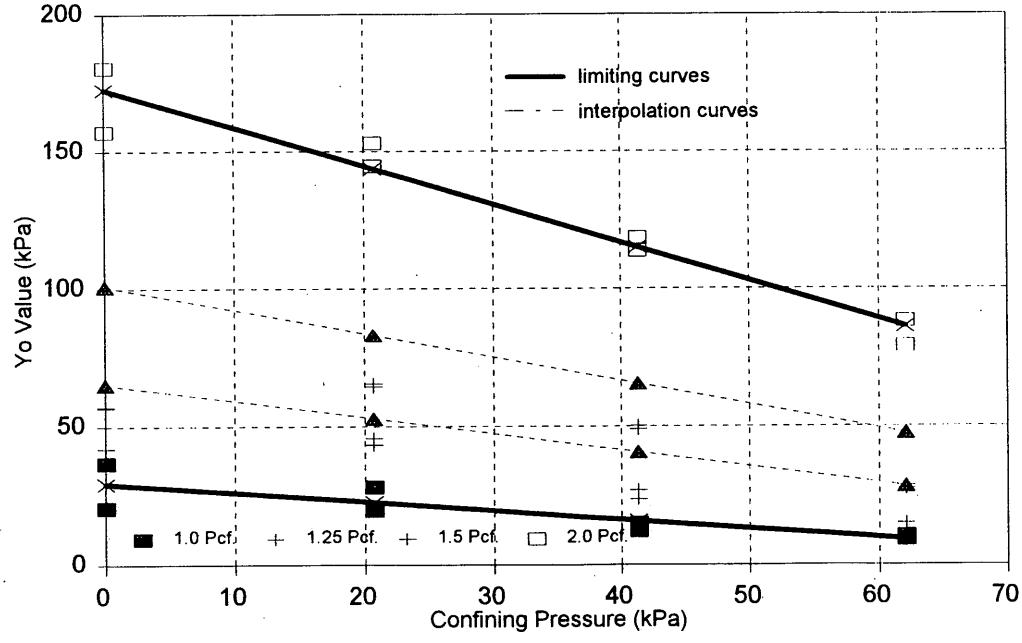

FIGURE 8 Variation of Y_o value.

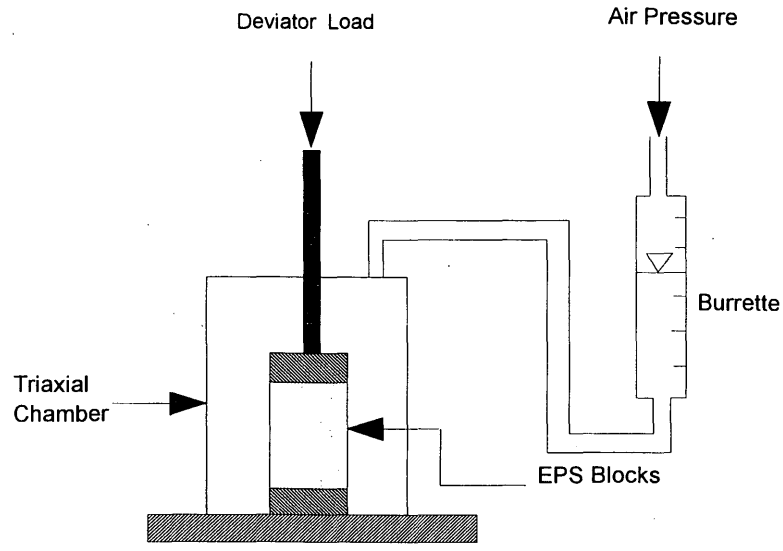

FIGURE 9 Schematics of undrained triaxial test on EPS blocks.

axial tests. The samples were separated from the surrounding chamber water by a thin rubber membrane. The volume change of the EPS samples was determined by measuring the amount of water flowing into or out of the triaxial chamber during the test. The test setup is shown in Figure 9.

The Poisson's ratios were calculated at the intersection of two tangent lines of the stress-strain curves and at large stress values as shown in Tables 6 and 7. The procedure of computing the Poisson's ratio from the measured volume change follows.

TABLE 6 Poisson's Ratio at Intersection

Confining Pressure (kPa)	Type of EPS			
	1.0 pcf	1.25 pcf	1.5pcf	2.0 pcf
0	.175	.301	.142	.381
	.332	.295	.163	.380
21	-.440	-.110	.075	.250
			-.270	.005
41	-.420	-.250	.052	.170
	-.330	-.420	-.142	.240
62	-.750	-.420	-.149	.037
	-.610	-.285	-.029	.065

TABLE 7 Poisson's Ratio at Failure

Confining Pressure (kPa)	Type of EPS			
	1.0 pcf	1.25 pcf	1.5pcf	2.0 pcf
0	.131	.204	.107	.256
	.199	.231	.115	.240
21	-.237	-.102	-.091	.010
			-.182	-.051
41	-.110	-.238	-.140	-.342
	-.182	-.206	-.187	-.004
62	-.440	-.366	-.239	-.081
	-.336	-.248	-.239	-.132

Poisson's ratio is defined by Desai and Siriwardane (*8*) and Gere and Timoshenko (*9*) as

$$\text{Poisson's ratio} = -\frac{\text{lateral strain}}{\text{axial strain}} = \frac{H\,\Delta R}{R\,\Delta H} \tag{3}$$

The total volume of the original sample is the same as that of the deformed sample plus the change in volume of water, as shown in Figure 10:

$$\text{Total volume} = V_w + \frac{\pi R^2}{4} H$$

$$= V_w + \Delta V_w + \frac{(R + \Delta R)^2}{4}(H - \Delta H) \tag{4}$$

By combining Equations 3 and 4 and neglecting the second-order terms, one obtains

$$\text{Poisson's ratio} = \frac{\pi R^2 \Delta H - 4\Delta V_w}{2\pi R^2 \Delta H} \tag{5}$$

As can be seen in Figures 11and 12, Poisson's ratio starts with approximately 0.2 at zero confining pressure. It decreases as the confining pressure increases and finally falls below zero as the confining pressure increases further. The figures indicate that this observation is more or less the same for both cases, that is, Poisson's

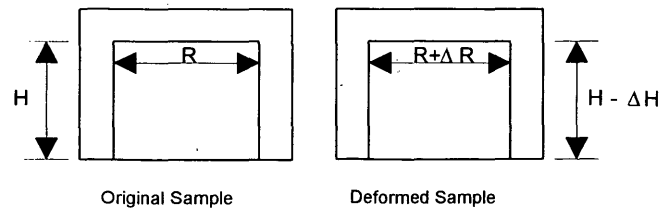

FIGURE 10 Simplified deformation under triaxial condition.

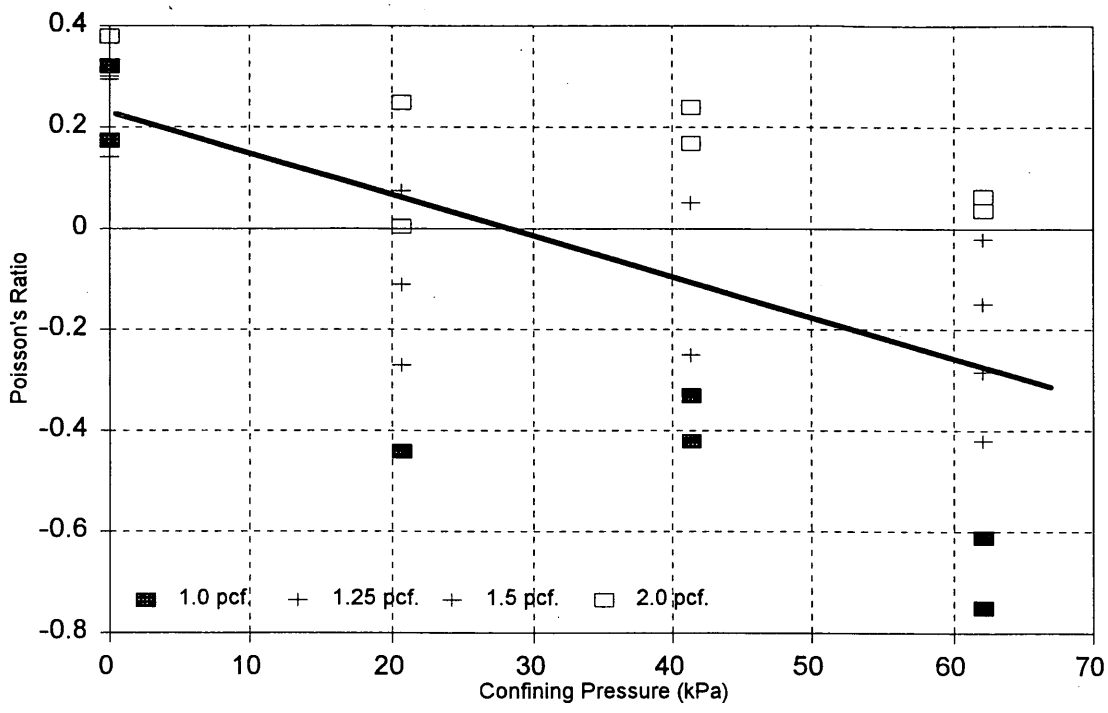

FIGURE 11 Poisson's ratio at intersection.

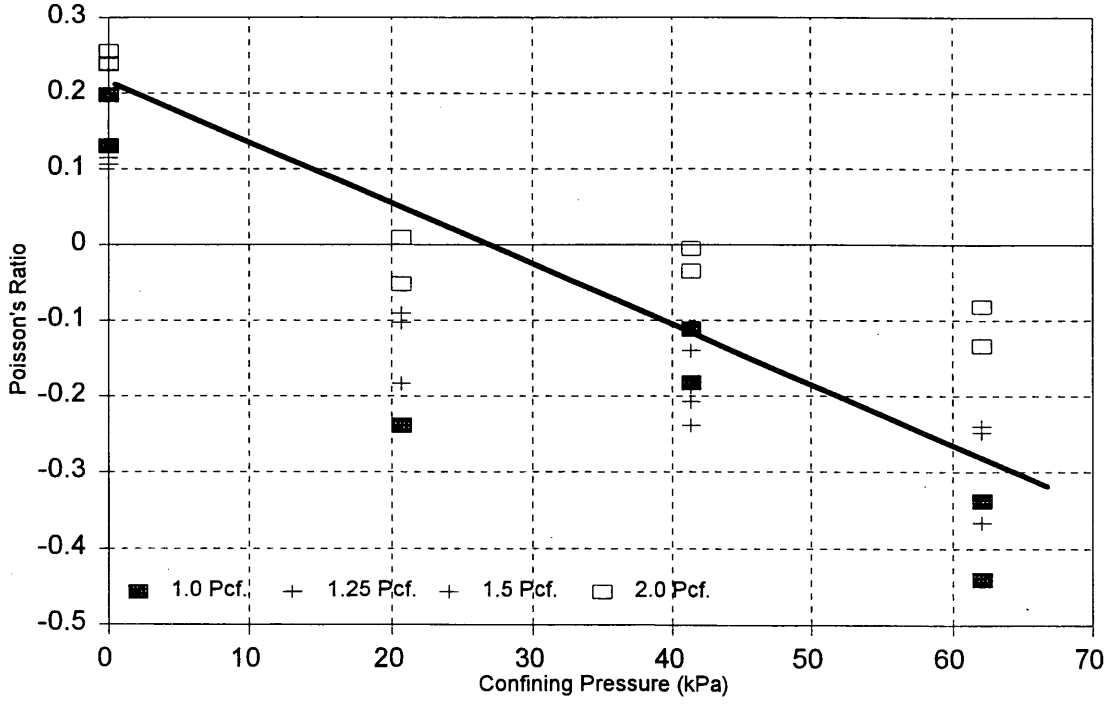

FIGURE 12 Poisson's ratio at failure.

ratio at the intersection point and at failure, although the samples with lower unit weights tend to exhibit lower Poisson's ratios. On the basis of the limited data obtained, the volume change behavior of the EPS material can be approximated as

$$\mu = 0.2 - 0.5\frac{\sigma_3}{62\ \text{kPa}} \qquad \text{for } 0 \le \sigma_3 \le 62\ \text{kPa} \tag{6}$$

where μ is Poisson's ratio and σ_3 is confining pressure (kPa).

It is noted that the past observations of reduced lateral earth pressures acting on retaining walls when the EPS blocks were used as backfills can be explained from the negative values of the Poisson's ratio. If Poisson's ratio indeed becomes negative, parts of the sides of the EPS blocks that have been in contact with the retaining walls may cave inward as the stress increases, resulting in partial separation from the retaining wall. Full-scale field instrumentation study is needed to verify this postulation.

Punching Shear Tests

In many geotechnically engineered structures, shear stresses combine with normal stresses, developing especially at and near the edges of the structures. Hence this combined stress condition needs to be simulated in laboratory testing. The punching shear test is one possible method of simulating this condition, since it produces both shear and normal stresses simultaneously. Figures 13 and 14 show the results of two typical punching shear tests. The stress-strain relationship curves are nonlinear. The punching shear strength increases rapidly at small strain, but its increasing ratio reduces gradually as the shear strain increases.

The punching shear strength of the EPS material increases about 300 percent from 1- to 1.25-pcf EPS material. However, the percent increase in punching shear strength decreases as the unit weight increases further. The maximum punching shear strengths are approximately 83, 275, 410, and 550 kPa for EPS samples of 1, 1.25, 1.5, and 2 pcf, respectively.

Repeated Loading Test

EPS blocks have been used frequently beneath pavement as either a frost-proofing layer or a load-bearing subgrade layer. For this reason, a simple repeated loading test was conducted on a 1.5-pcf EPS sample under a repeating axial stress of 72 kPa in a one-dimensional consolidometer.

The test results show that virtually zero permanent, nonrecoverable axial strain remains after 300 cycles of axial stress application, indicating that the resilient modulus of the EPS material is almost identical to the elastic modulus. This indicates that the EPS blocks can perform well under the repeated loading condition as long as the maximum stresses are less than its yield strength. However, testing for a higher number of load cycles may be necessary to confirm this behavior.

Creep Test

Figure 15 shows the results of a creep test on a 1.5-pcf EPS sample under a constant axial stress of 24 kPa. Through extrapolation, one can estimate the creep strain rate of less than 0.6 percent a year, indicating the relative insensitivity of the EPS material to creep.

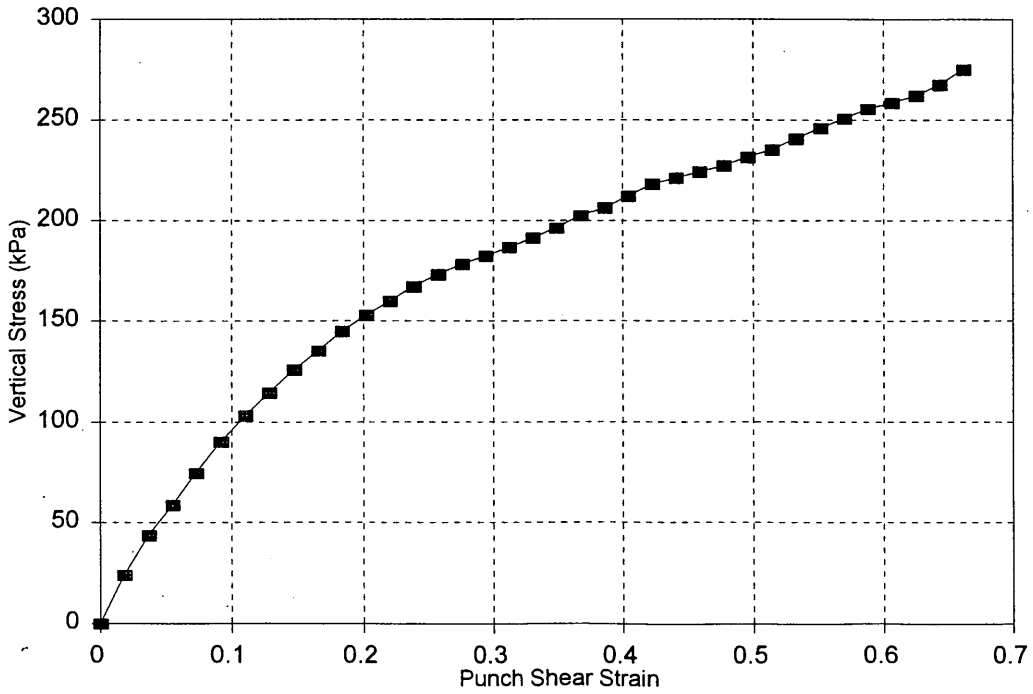

FIGURE 13 Punch shear test on 1.25-pcf EPS.

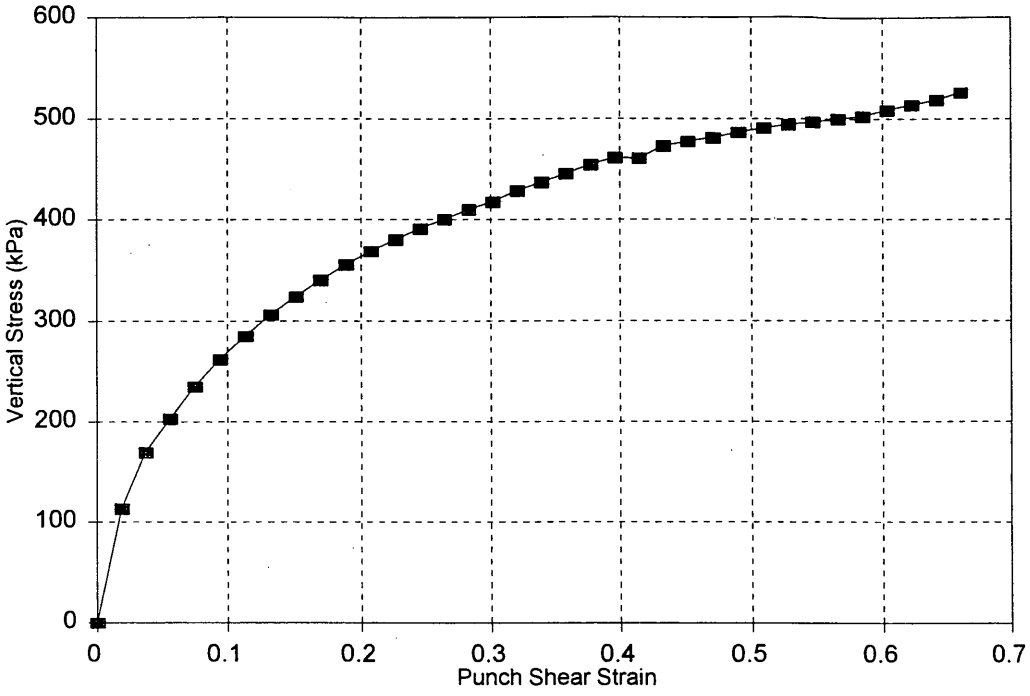

FIGURE 14 Punch shear test on 2.0-pcf EPS.

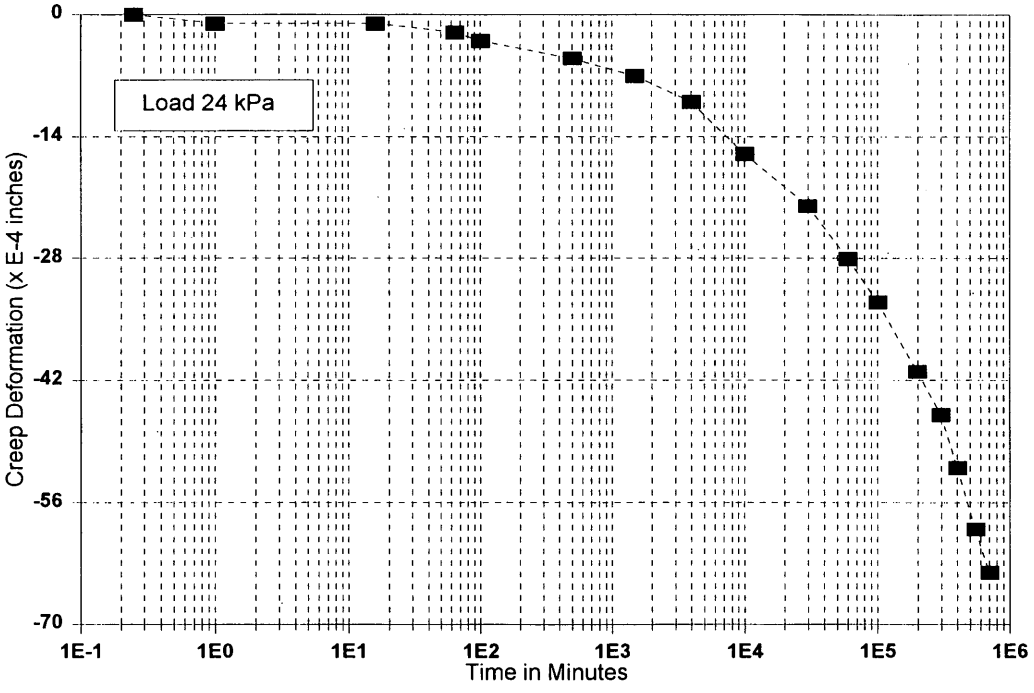

FIGURE 15 Creep test on 1.5-pcf EPS.

CONCLUSION

Various laboratory tests on EPS samples have been conducted to characterize behavior under constant and repeated loading conditions. Although there is some scatter in the test data, a general distinctive behavior of the EPS material has been observed. One possible explanation of the data scatter is sample inhomogeneity created during the manufacturing process. The EPS blocks are produced by a sudden expansion, which usually creates nonuniform material properties, possibly leaving localized dense or loose pockets.

In general, as the unit weight of the EPS material increases, both the initial and plastic moduli increase, with the plastic modulus in-

creasing at a slower rate. The EPS material becomes stronger as the unit weight increases. With an increase in confining pressure, the initial modulus decreases while the plastic modulus increases. Poisson's ratio remains greater than zero at low confining pressures but starts to decrease and eventually drops below zero as the confining pressure further increases.

The EPS blocks have been tested and found reliable under working stress conditions against both creep and repeated stresses.

Straight lines have been used to show Poisson's ratio and the parameters defining the nonlinear stress-strain relationship of the EPS material. This linearization is mainly due to the limited number of data available. Further refinement of the EPS material characterization needs to be made considering wider ranges of stress and strain magnitudes.

ACKNOWLEDGMENTS

This paper presents information on work done under joint developmental agreement with Benchmark Foam, Inc., and South Dakota School of Mines and Technology. It contains information relating to the results of a process that is proprietary to Benchmark Foam, Inc., under whose auspices this paper was written.

REFERENCES

1. Skuggedal, H., and R. Aaboe. *Temporary Overpass Bridge on Expanded Polystyrene.* Seminar on the Use of EPS in Road Construction, Oslo, Norway, June 1991.
2. Coleman, T. A. Polystyrene Foam is Competitive, Lightweight Fill. *Civil Engineering,* ASCE, Feb. 1974.
3. Frydenlund, T. E. *Expanded Polystyrene—A Lighter Way Across Soft Ground.* Internal Report, Norwegian Road Research Laboratory, May 1991.
4. Myhre, O. *Regarding Possible Standardization of Polystyrene Blocks.* Seminar on the Use of EPS in Road Construction, Oslo, Norway, June 1991.
5. BASF Corporation. Technical Bulletin E-3, Chemicals Division, Parsippani, N.J., 1993.
6. Rutz, L. *Expanded Polystyrene as an Embankment Alternative for Highway Slope Failures.* Project No. MP20-0160–30. Colorado State Department of Transportation, 1987.
7. Bang, S., and T. Preber. *Geotechnical Application of Expanded Polystyrene Blocks.* Research Proposal to South Dakota Governor's Office of Economic Development, July 1991.
8. Desai, C. S., and H. J. Siriwardane. *Constitutive Laws for Engineering Materials with Emphasis on Geologic Materials.* Prentice-Hall, Inc., Englewood Cliffs, N.J., 1984.
9. Gere, J. M., and S. P. T. Timoshenko. *Mechanics of Materials,* 3rd ed. PWS-KENT Publishing Company, Monterey, Calif., 1990.

Publication of this paper sponsored by Committee on Transportation Earthworks.

Investigation of Road Widening on Soft Soils Using a Small Centrifuge

H.G.B. ALLERSMA, L. RAVENSWAAY, AND E. VOS

Increasing traffic in the Netherlands increases the demand for roads to be widened. In several cases the sand body of the roads is founded on soft soils. To widen these roads, the width of the sand body has to be increased. The widening process can cause cracks in the asphalt layer of the original road, which has to be prevented as much as possible. To investigate the effect of different methods of road widening, a test program was carried out in the small geotechnical centrifuge of the University of Delft. Two different methods of widening were simulated: the horizontal method and the gap method. The excess pore water pressure was taken into account, and the deformation of the clay layer and sand body was measured by means of image processing. Although the differences in deformations measured were small, it could be seen clearly that the horizontal widening method caused more horizontal displacements than the gap method. This indicates that cracking of the asphalt layer could be minimized by using the gap method of construction.

In the western Netherlands the subsoil consists of a thick layer of soft soils, such as peat and clay. In some cases traditional road widening on these soft soils causes serious problems, such as large settlements. For example, the motorway from Rotterdam to Antwerp was widened during 1988–1990. In the sections close to the Van Brienenoord Bridge, embankments higher than 5 m were needed. The subsoil at that location consists of peat and soft clay layers with a thickness of more than 10 m. The subsoil was already covered with a thick layer of sand to obtain an embankment as a base for the asphalt pavement. It was decided to construct the widening of the embankment in stages of horizontal sand layers of 0.5 m a month. During construction it was found that serious longitudinal cracking occurred in the existing asphalt pavement. To eliminate or reduce this cracking, it was decided to modify the construction method, first constructing an embankment close to the existing embankment and then filling the remaining gap. It was expected that this so-called gap method would lead to a reduction in horizontal deformations in the existing embankment and consequently a reduction in the cracking of the asphalt pavement. The gap method was applied in the last sections of this widening project. The consensus is that a reduction in the cracking can indeed be achieved.

Because more roads in the Netherlands have to be widened, the Road and Hydraulic Engineering Division of Rijkswaterstaat initiated a research project to study this subject in a more consistent and systematic way. It was decided to study this problem both numerically (*1*) and experimentally. The experimental approach, discussed in this paper, focuses on a comparison of the two construction methods in well-defined experimental conditions using scale models in a centrifuge. Very little centrifuge research has been done on the widening of embankments. Most of the embankments investigated in a centrifuge were embankments stabilized by reinforcement (*2*) or founded on consolidated clay (*3*)

A test program was carried out in the small geotechnical centrifuge of the University of Delft to investigate the effect of different methods of widening embankments founded on soft soil. Most tests were performed on a clay layer with a thickness of approximately 0.07 m. At 100 *g* the same shear stresses can be simulated as in a clay layer of 7 m, so a small model in the centrifuge behaves in a manner similar to the prototype. The soft clay sample was prepared by consolidating a clay slurry in a centrifuge. The widening of the original sand body was performed in flight by means of a sand pluviation machine. The position of the hopper and the amount of sand to be sprinkled during translation of the hopper was controlled from the keyboard of a personal computer (PC). Different widening methods were simulated and the excess pore water pressure was taken into account. In centrifuge tests the same pore water pressure can be generated as in reality. Because the real dimensions of the model are a hundred times smaller than the prototype problem, the consolidation time is reduced by the square of the artificial gravity. The deformation of the clay layer and sand body was measured by means of image processing on the PC. A special technique was developed to copy a grid on the surface of a black or white clay without removing boundaries, and the reproducibility of the samples was extremely good, which was essential for visualizing the slight differences caused by the different widening procedures. As far as possible the test results were compared with numerical calculation methods.

The soil parameters were determined in the laboratory by compression tests and triaxial tests, and in-flight vane tests were used to investigate whether the clay was homogeneous and whether all clay samples had the same strength. Embankment tests were performed to validate the soil parameters found and investigate whether the clay model behaved as expected. From these embankment tests the maximum embankment height was found. To investigate the two widening methods, several tests were performed. The pore pressure measurements were used to determine the waiting time between the construction of the different layers.

EQUIPMENT

Investigations of the different methods of embankment widening were conducted using the small geotechnical centrifuge at the University of Delft (*4*). One disadvantage of a small centrifuge is the limitation in the use of sensors during a test. This restriction, however, is partly compensated for by applying image processing techniques to the video images obtained from the onboard video camera (*5,6*). Image processing software digitizes the coordinates of the nodes of a grid on a clay surface. Because the grid can be copied on

H.G.B. Allersma and L. Ravenswaay, University of Delft, Faculty of Civil Engineering, Stevinweg 1, 2628CN Delft, The Netherlands. E. Vos, Ministry of Public Works, Post Box 5044, 2600GA Delft, The Netherlands.

the clay surface without removing the transparent boundaries, the deformation of soft clay layers can be monitored accurately.

Sand Sprinkler

A computer-controlled sand sprinkler was developed to make embankments in flight (Figure 1). The sand hopper and sprinkler system can be translated over a range of 150 mm. Several options can be assessed in the control program, and it is possible to sprinkle sand layer by layer or at one particular location. The disturbing effect of the Coriolis forces is minimized by means of hinged sheets that guide the sand grains. The sand sprinkler's control program also reads the output of pore water pressure transducers, which can be placed in the clay layer. The pore water pressure changes in the clay layer are plotted on the PC screen while the embankment is under construction. The emergence of a dike during sand suppletion can be monitored by a video camera.

In-Flight Vane Apparatus

To correlate test results with calculation methods, information is needed about the properties of the soil types used. In the case of clay, the way in which the undrained shear strength changes with the depth during the test must be known. Information about the shear strength can be obtained by means of an in-flight vane apparatus. The undrained shear strength is calculated from the torque and the surface of the cylindrical soil unit, which is rotated by the vane. In this particular investigation the rotation speed of the vane was approximately the same as the speed in the slip circle in the clay during failure of a dike in the centrifuge. The position of the vane can be adjusted over a range of 250 mm during flight so that several tests can be performed without stopping the centrifuge.

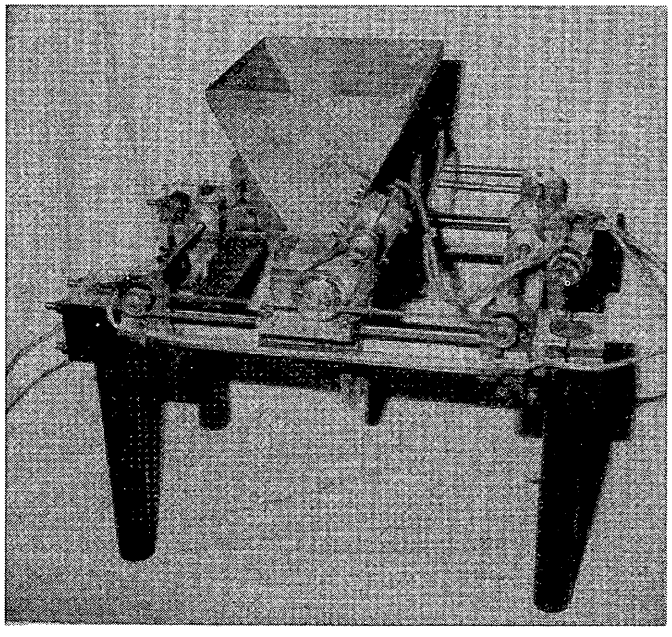

FIGURE 1 In-flight sand sprinkler.

CLAY PREPARATION

Clay slurry with a water content of approximately 100 percent is homogenized in a mixer before it is put into sample boxes. A new technique has been developed to obtain an air-free mixture of clay powder and water under normal atmospheric conditions. The best way to obtain a soft, normally consolidated soil with a smooth and realistic gradient of water content and strength over the height of the sample is to consolidate the slurry in the centrifuge at the same *g*-level as will be used in the tests. The sedimentation and consolidation of Kaolin clay takes approximately 8 hr. Because the centrifuge will be occupied during that time, no other tests can be performed. Therefore a special centrifuge was built exclusively to consolidate the clay layers.

RESULTS

Embankments

Embankment tests were performed to determine the maximum height of an embankment founded on a layer of Kaolin clay. The embankment was made in flight, at 100 *g*, by means of the computer-controlled sprinkler device. After the sample was fully consolidated in the centrifuge, the sand was dropped at one place, and the slope of the embankment appeared to be 30 degrees. The sand was dropped until the clay collapsed. Because this procedure took less than 1 min, the test was considered to be performed under undrained conditions. The slip circles could be seen clearly by the grid made on the clay.

In Figure 2 the slip circle can be seen going almost through the center of the embankment. This is in agreement with the Bishop theory. The maximum height was 0.043 m, which translates to 4.3 m in reality.

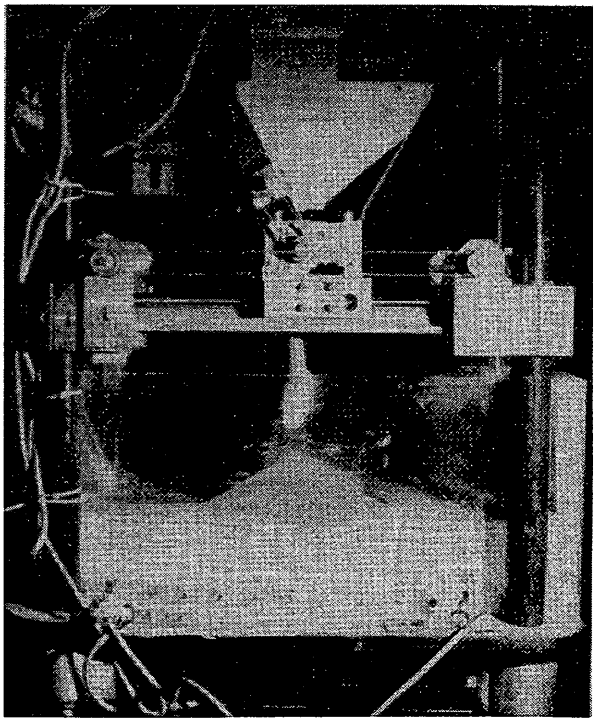

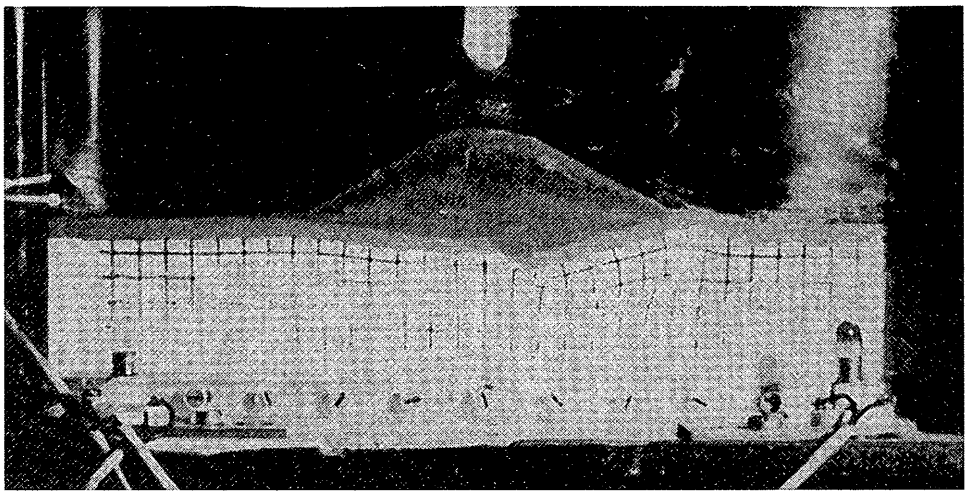

FIGURE 2 Collapsing embankment.

The safety factor of this embankment was calculated with two computer programs, Stabil and PLAXIS. Table 1 presents the soil parameters used for the calculations. These soil parameters were determined by compression tests and triaxial tests. The undrained shear strength at some depth was determined with the in-flight vane test.

Stabil calculates the safety factor of a slip circle according to the modified Bishop method. The soil parameters needed are the specific weight and the cohesion for every layer. Figure 3 shows the most critical slip circle as calculated by Stabil. The safety factor was 0.771.

PLAXIS (*7*) is a finite element program for soil construction calculations. All parameters presented in Table 1 are needed in this program. The incremental displacements of the final step calculated by this program are shown in Figure 4. The safety factor calculated with this program was 0.859.

Both calculation methods gave lower safety factors than did the test results. This could be because of simplifications in the computer simulations; for example, in Stabil the cohesion cannot be varied with the depth, and in PLAXIS the cohesion cannot be taken as equal to zero. A time effect could be another reason for the deviation. After the embankment has reached the critical height, it appears to take several seconds before the soil collapse. In this time

TABLE 1 Soil Parameters Used in Analytical and Numerical Calculations

SAND			
unit weight	γ_{wet}	20.5	kN/m^3
friction angle	ϕ	31°	
cohesion	c	0	kPa
CLAY			
unit weight	γ_{wet}	17	kN/m^3
Poisson ratio	ν	0.35	
Ko		0.57	
cohesion versus depth	Cu/σ'_v	0.40	
elastic shear versus depth	G/σ'_v	4.81	
permeability	k	$2.5*10^{-9}$	m/s

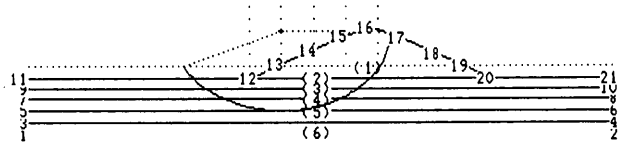

FIGURE 3 Critical slip circle, derived with Bishop method.

interval the hopper still continues to drop sand, so the embankment becomes oversized. The development of a slip circle takes some time because water has to flow to the slip circle surface to permit dilatation. Because of this time effect it is difficult to find the exact moment of failure.

From these embankment tests it can be concluded that the centrifuge is a good testing tool; the soil collapsed according to a slip circle, as expected. The calculated safety factor based on the dimensions of this test was close to 1, which is also an indication of the reliability of the test method.

Embankment Widening

Widening tests are performed at 100 *g* on a clay layer with a thickness of 0.07 m and embankment heights of approximately 0.04 m. This conforms with a prototype condition of 7-m clay and an embankment with a height of 4 m. Two different methods to widen embankments were investigated and compared: the horizontal method and the gap method. In the horizontal method the widening is made of horizontal layers. In the gap method, first a new embankment is constructed at some distance from the existing embankment, and then the gap is filled. These tests were performed to investigate the existence of differences in the deformations of the existing embankments and to determine whether the differences could be made visible. Such deformations, especially horizontal displacements, can be the cause of horizontal cracks in asphalt roads.

The existing embankment was made at 1 *g* and was 0.04 m high. This height was measured to be sure that the existing embankment did not collapse, as happened at 0.043 m at 100 *g*. Beads were placed in the embankment, and on the clay layer a grid was connected to follow the deformations. Two pore-pressure transducers were

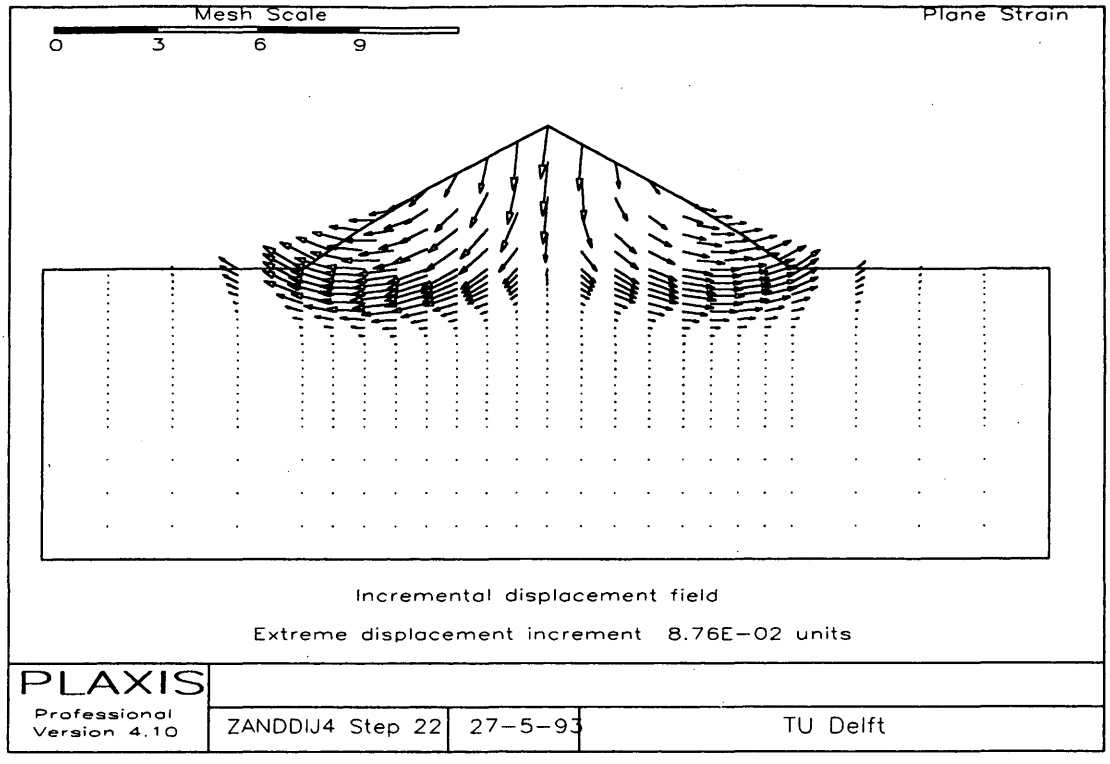

FIGURE 4 Result of numerical calculation.

placed in the clay layer, one located where the top of the widening would occur and one located under the existing embankment. To prevent the excess pore pressures from becoming too high, the acceleration was brought up to 100 *g* in steps of 1 *g* every minute.

After the clay layer was fully consolidated, the widening process was started. The widenings were made in flight with the help of the sand sprinkler. The test was observed from the control room by means of a camera. The widening part had a maximum height of 0.05 m, depending on the drainage during the test.

Three tests were conducted to investigate the stability of an existing embankment when a new embankment is constructed nearby. In the first test the new embankment was constructed at some distance from the existing embankment. In the second test the new embankment was constructed at the toe of the existing embankment, and in the third test the top of the new embankment was located at the slope of the existing embankment. All the embankments were constructed as quickly as possible, in approximately 30 sec (roughly 83 hr in prototype conditions).

Figure 5 shows the results of the first test. The top of the new embankment was made at 0.02 m from the toe of the existing embankment. As can be seen, the soil collapses according to a slip circle. It can also be seen that only the new embankment collapsed, and that nothing happened to the existing embankment. The displacements of the beads in the existing embankment were followed during the test, and they also showed no significant deformations. The most peculiar phenomenon is that not even a small part of the existing embankment collapsed. The other two tests, as described previously, were performed slightly closer to the existing embankment. The new embankments did not collapse and the influence on the existing embankment was not significant.

From these tests the conclusion can be drawn that the location of the new embankment is important. If there is a large overlap between the two embankments, the soil is too strong to collapse. If the embankment is constructed at some distance from the toe of the existing embankment, the new embankment collapses and the existing embankment is not affected dramatically.

Several tests were performed to compare the two widening methods. The pore pressure readings were used to determine the waiting time between the application of the different layers. The waiting time was 1,500 to 2,000 sec in the test, which is 173 to 230 days in reality.

The horizontal method (Figure 6) involved four layers of approximately 0.0125 m each. The first layer was constructed after the clay was fully consolidated. While sprinkling sand, the hopper moved two times between the outermost point of the widening and the toe of the existing embankment. After the layer was constructed, the pore pressures were measured and the readings used to determine when to construct the next layer. The process was repeated for the third and fourth layers. Figure 6 also shows the location of the two pore pressure transducers (PPTs).

Using the gap method (Figure 7) a new embankment was built at some distance from the top of the existing embankment. This embankment again consisted of four layers of 0.0125 m each. After the fourth layer was constructed, the gap was filled in one action.

The pore pressures were measured for all the tests. Figure 8 shows the excess pore pressures for the two widening tests. After the suppletion of the first layer, the next layer was supplied only after a reduction of the excess pore pressures to almost zero. This process was repeated for the next layers. The fifth peak that can be seen in Figure 8 (bottom) was the filling of the gap. PPT 1 was

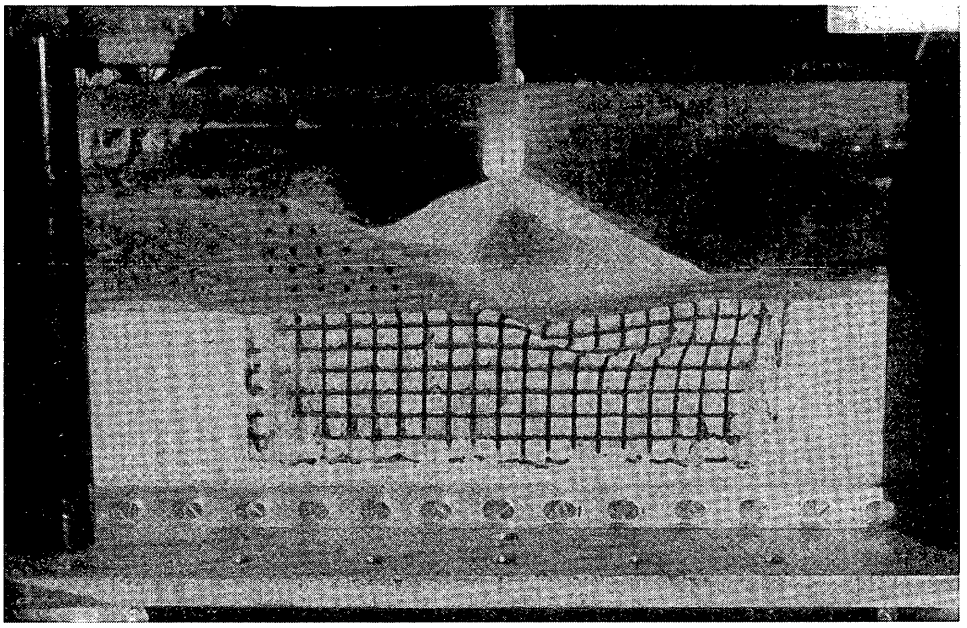

FIGURE 5 Collapse of new embankment.

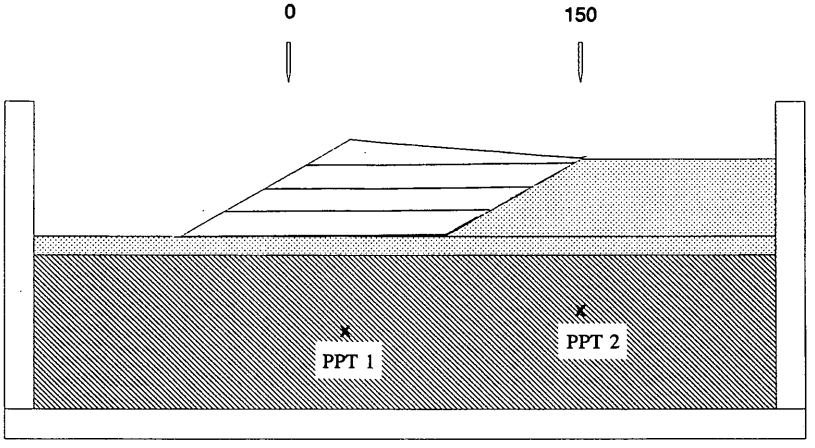

FIGURE 6 Horizontal widening method (dimensions of sample box: l = 410 mm, h = 165 mm, b = 150 mm).

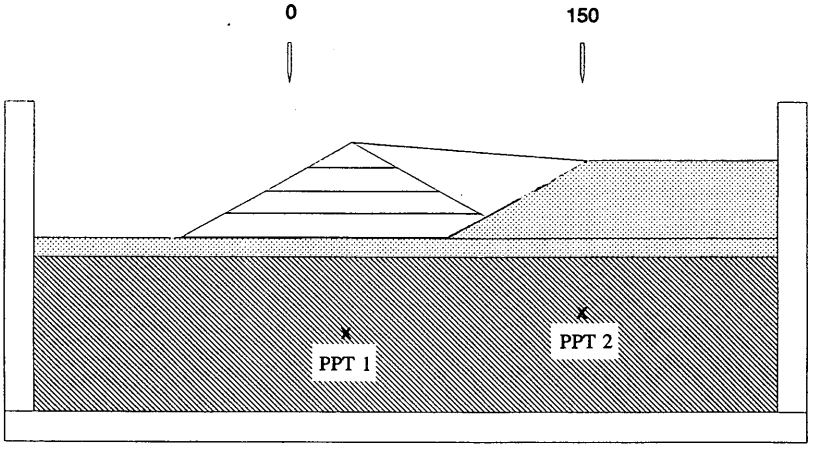

FIGURE 7 Widening by gap method.

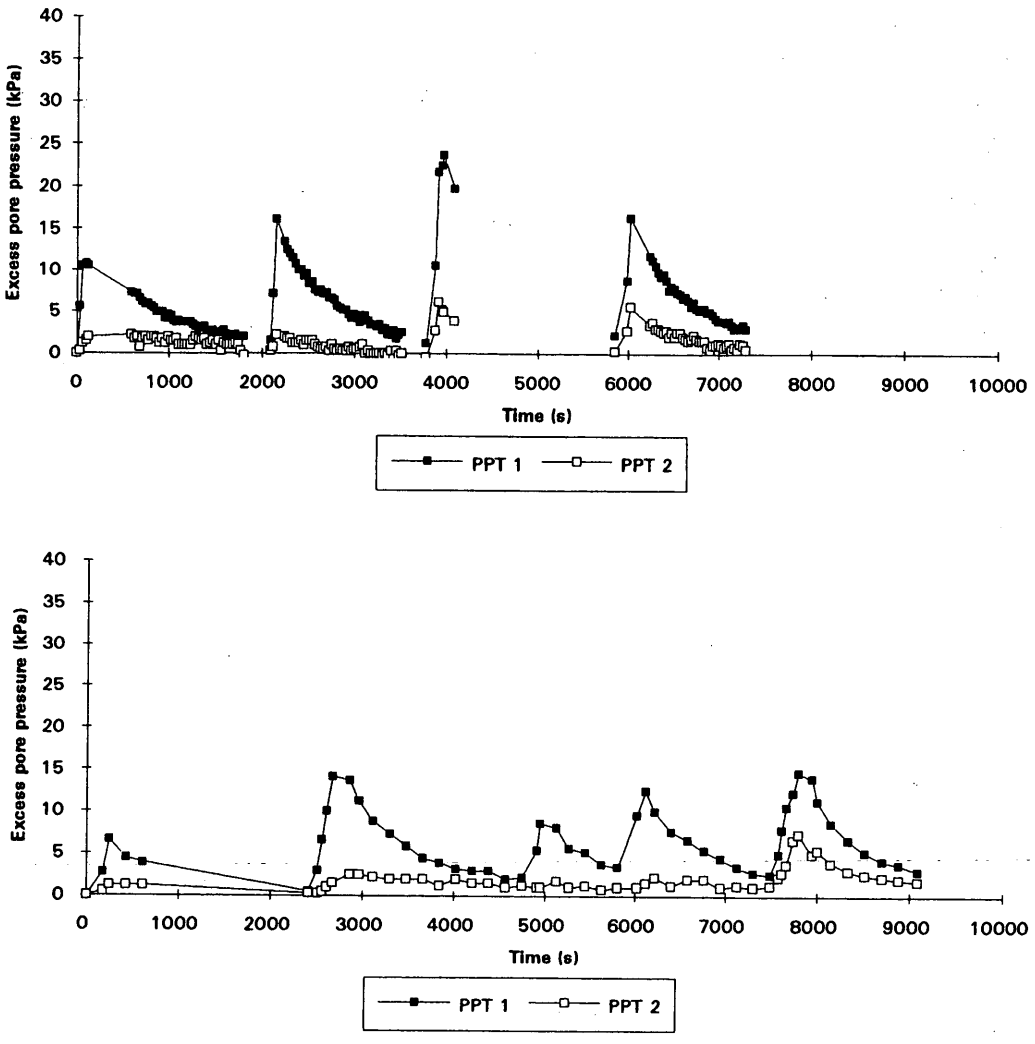

FIGURE 8 Course of excess pore pressure during widening, each peak representing a new layer (100 percent consolidation): horizontal method (*top*) gap method (*bottom.*)

located under the new embankment and PPT 2 was located under the slope of the existing embankment. This can be seen by noticing that the excess pore pressures of PPT 2 increased most when the gap was filled. The horizontal method causes larger peaks in the pore water pressure than the gap method, probably because more sand is added in a layer.

The displacements of the nodes of the grid on the clay layer and the displacements of the beads in the existing embankment can be measured with the help of image processing. Figure 9 presents the displacement fields of two tests visualized by processing the grid on the clay layer of two test stages and by improving the visibility of the beads in the embankment by image processing. From these tests two main differences can be observed:

- In addition to vertical displacements, the horizontal method caused more horizontal displacements, whereas the gap-method caused mainly vertical displacements. These differences in deformations could be seen particularly in the clay layer.
- The difference between vertical displacements at the toe of the existing embankment and those more to the center was much larger for the horizontal method than for the gap method. From this phenomenon a mechanism can be deduced that can cause horizontal cracks in the asphalt, as shown in Figure 10.

Both widening methods result in approximately the same loading conditions. The difference in deformation can be caused by several phenomena. With the gap method the new embankment has a potential failure mechanism that counteracts horizontal deformation of the existing embankment. Furthermore the same amount of sand is supplied over a larger time interval, so a more stable behavior can be expected because of lower excess pore water pressure. A more specific test program must be carried out to further investigate the influence of these and other factors.

CONCLUSIONS

The embankment testing produced results that came close to what was expected. The soil collapsed according to a slip circle and the safety factor was close to 1.

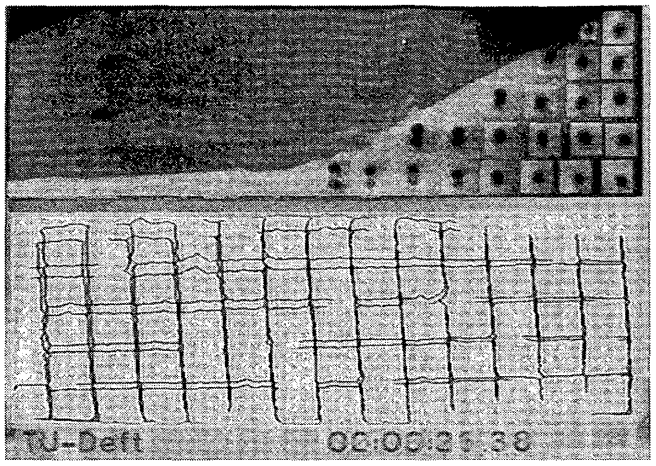

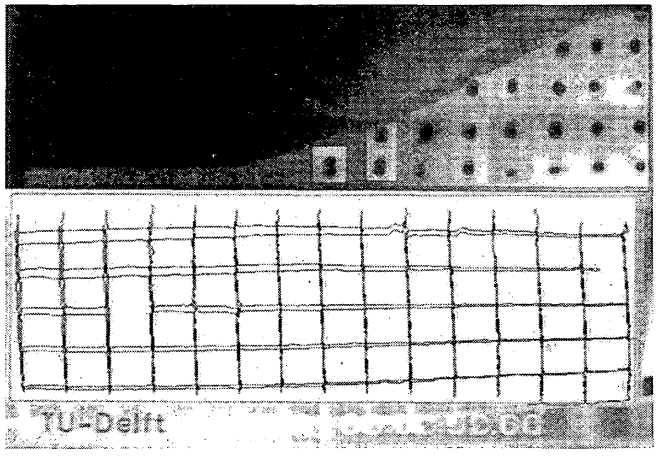

FIGURE 9 Visualized displacement fields after widening and consolidation (grid size 10 mm): horizontal method (*top*), gap method (*bottom*).

The location of the new embankment as constructed for the gap method was important. When there was a large overlap between the two embankments, both the existing embankment and the new embankment did not collapse if the critical height for normally consolidated clay was reached. If the new embankment was constructed at some distance from the existing embankment, the new embankment collapsed, but this had no significant consequences for the existing embankment.

The differences in deformations caused by the two widening methods were not great, but differences could still be observed. In addition to vertical displacements, the horizontal method also caused horizontal displacements. The gap method caused mainly vertical displacements. The difference between vertical displacements at the toe of the existing embankment and those more to the center was much larger for the horizontal method than for the gap method.

Kaolin clay is convenient in centrifuge tests because the consolidation time is short. On the other hand it is not a typical Dutch clay. Therefore a test program is planned to investigate the behavior of a more natural clay type.

Much attention has been given to techniques for preparing reproducible samples. Very good reproducible clay samples could be prepared with the new mixing method of powder and water and the in-flight consolidation of the slurry.

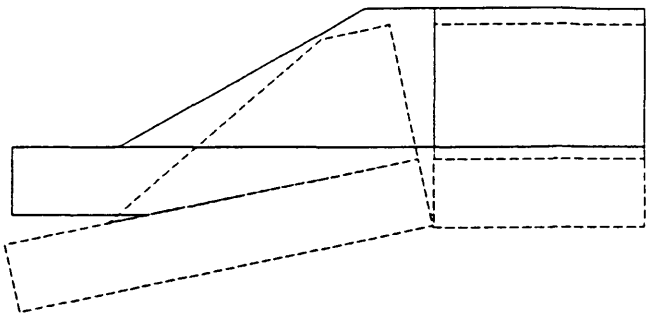

FIGURE 10 Schematic diagram of assumed mechanism that causes cracks in pavement if horizontal widening method is applied.

Because of the small size of the samples the centrifuge was flexible in operation and tests could be performed in a short time after the idea was developed. Advanced tests could be performed in flight using the most up-to-date electronics, measuring techniques, and miniature devices. The disadvantage of a small centrifuge is the limitation in sensors, which could be compensated for by using image-processing techniques.

ACKNOWLEDGMENTS

The centrifuges, electronics, soil preparation devices, and in-flight testing equipment were designed by the Geotechnical Laboratory of the Department of Civil Engineering at the University of Delft. Many thanks are given to the technicians of the laboratory, J. van Leeuwen, A. Mensinga, and J. J. de Visser, for their contribution to this research. This project was supported by the Dutch Ministry of Public Works.

REFERENCES

1. Vos, E., J. M. Couvreur, and M. Vermaut. Comparison of Numerical Analysis with Field Data of a Road Widening Project on Peaty Soil. *Proc., International Workshop on Advances in Understanding and Modelling the Mechanical Behaviour of Peat,* Balkema, Rotterdam, 1993.
2. Almeida, M. S. S., and R. H. G. Parry. Centrifuge Studies of Embankment Foundations Strengthened with Granular Columns. Presented at 3rd International Geotechnical Seminar, Singapore, 1985.
3. Davies, M. C. R., and R. H. G. Parry. Centrifuge Modelling of Embankments on Clay Foundations. *Soils and Foundations,* Vol. 25, No. 24, 1986, pp. 19–36.
4. Allersma, H. G. B. Development of Miniature Equipment for a Small Geotechnical Centrifuge. In *Transportation Research Record 1432,* TRB, National Research Council, Washington, D.C., 1994, pp. 99–105.
5. Allersma, H. G. B. On Line Measurement of Soil Deformation in Centrifuge Tests by Image Processing. *Proc., International Conference on Experimental Mechanics,* Copenhagen, 1990, pp. 1739–1748.
6. Allersma, H. G. B. Using Image Processing in Centrifuge Research. *Proc., International Conference on Centrifuge,* Boulder, 1991, pp. 551–558.
7. *PLAXIS Version 4.0 Manual.* Balkema, Rotterdam, 1991.

Publication of this paper sponsored by Committee on Modelling Techniques in Geomechanics.

PART 2

Resilient Modulus Testing

Resilient Moduli of Aggregate Materials: Variability Due to Testing Procedure and Aggregate Type

DAR-HAO CHEN, M.M. ZAMAN, AND J.G. LAGUROS

The variability of resilient modulus (RM) values is investigated for six aggregate materials that are commonly used in Oklahoma as subbases or bases. Six RM tests each under identical conditions for two aggregate types and three tests each for four aggregate types were performed according to the AASHTO T292–91I procedure to investigate the variability of the test results. All specimens were prepared at the same gradation that meets the Oklahoma Department of Transportation specifications for Type A materials. The effects of testing procedures on RM values were investigated for two selected aggregate types by conducting six tests each using the AASHTO T292–91I and T294–92I testing procedures. The variability of test data and consistency of the RM values are investigated within a statistical framework. The variability of RM values obtained ranges from 19 to 26 percent in terms of maximum coefficient of variation (MCOV). The results indicate that consistently higher RM values are obtained when using the T294–92I testing method than when using the T292–91I testing method, and the degree of increase depends on the type of aggregate. The variability of RM values due to testing procedure was found to be higher than that due to aggregate source. One aggregate type experienced a lower MCOV when using T294–92I than when using T292–91I, but the other aggregate type exhibited an opposite trend. Overall the RM values range from 41.3 to 261.8 MPa, depending on bulk stress, material type, and testing method, and they are slightly lower than those reported in the literature.

A reliable and economic design of pavement thickness relies on several factors, among which a proper characterization of the load-deformation response of the pavement materials is extremely important. AASHTO proposed a new pavement design procedure in 1986 (*1*) that incorporates the resilient modulus (RM) to properly describe the behavior of pavement materials subjected to moving traffic. Until now, however, no standardized test method has been adopted for measuring RM values. Since its introduction the T274–82 testing procedure (*2*) has been the target of widespread criticism (*3*), including the criticism that the required loading conditions are too severe and therefore a specimen may fail in the conditioning stage. For example, in documenting unsatisfactory experience with AASHTO T274–82, Vinson (*4*) stated that the heavy conditioning of the sample specimens, as required by T274–82, may cause different levels and types of stresses for both cohesive and cohesionless soils. Also, Ho (*5*) observed that the conditioning stage, as suggested by T274–82, was very severe for many soils. For these reasons various departments of transportation (DOTs), including those in Florida, New York, Illinois, and South Dakota, have developed their own testing procedures. A review of these methods reveals that they are similar to AASHTO T274–82 except for some factors pertaining to sample conditioning, load magnitude, and load application sequences (*6*). In 1991 AASHTO modified the T274–82 testing procedure and came up with the T292–91I testing procedure (*7*). In 1992 AASHTO adopted the Strategic Highway Research Program test method of determination of RM for soils and unbound aggregates, now known as T294–92I (*8*). The different testing procedures may result in different RM values. Also, the AASHTO *Guide for Design of Pavement Structures* (*1*) incorporates reliability in the design equation, which requires an understanding of the material strength variance. Therefore it is important to investigate the effects of pertinent factors on RM and the variability of the RM values due to the different testing procedures.

The need for nonlinear characterization of granular base/subbase in the pavement structure has received attention in recent years (*9,10*). The associated material parameters that are evaluated either in the field (e.g., falling weight deflectometer test) or in the laboratory (e.g., cyclic triaxial test) involve some degree of difficulty. For example Parker (*9*) stated that the granular base/subbase is the most difficult paving material to characterize because the modulus is sensitive to the state of stress and there may be influential seasonal variations. Rada et al. (*10*) reported that the results for the unbound granular base and subbase materials are considerably more variable than those for other layered materials.

In this paper the variability of RM test data is investigated for six different aggregate materials under repeated dynamic loading by using the AASHTO T292–91I testing procedure. Two of the aggregate types were selected for RM testing by using T294–92I, and the results were compared with those obtained with T292–91I as well as with those reported by various agencies. Research is under way to investigate the variability of the RM test results under various moisture contents (soaked and dried conditions) and the effect of stabilizing agents (fly ash, lime, and cement).

RESILIENT MODULUS CONCEPT

Design of roadway pavements relies on proper characterization of the load-deformation responses of the associated materials from base, subbase, and subgrade. Subgrade soils undergo deformation when subjected to repeated loads from moving traffic. Laboratory results indicate that part of this deformation is resilient or recoverable (ϵ_r) and part is permanent or plastic (ϵ_p). The property that describes this behavior of subgrade materials is RM, defined as the deviatoric dynamic stress σ_d divided by the resilient strain ϵ_r:

$$RM = \sigma_d/\epsilon_r \quad (1)$$

The basic differences among test methods T274–82, T292–91I, and T294–92I are sample conditioning before testing, number of

School of Civil Engineering and Environmental Science, University of Oklahoma, Norman, Okla. 73019.

loading cycles, and applied waveform and sequence. Test methods T292–91I and T294–92I were used in this study and their comparisons are summarized in Table 1. The testing parameters, such as the stresses applied and their duration and the selection of dynamic wave form and the number of repetitions, may affect RM values, as discussed in the following sections.

Applied Stress and Duration

Dynamic response of aggregate-based materials can be significantly influenced by the applied confining pressure (*11*). To better characterize such materials, it is desirable to evaluate RM tests under a wide range of confining pressures expected within the subgrades or bases/subbases. The AASHTO procedures (T274–82, T292–91I, and T294–92I) use a variety of constant confining pressures and dynamic deviatoric stresses; therefore, the test data comprise a set of RM values corresponding to the different bulk stresses. However Khedr (*12*) argued that tests involving constant confining pressure do not simulate the in situ conditions properly because the lateral pressure (confining pressure in this case) changes simultaneously with vertical stresses caused by traffic loading. In addition, tests involving the constant confining pressure instead of the cyclic confining pressure may lead to an overestimation of the RM values (*12,13*). In contrast Thompson (*14*) reported that for practical purposes the triaxial RMs are similar under constant and variable confining pressures. TRB (*15*) reported that when a wheel load passes over an element of pavement structure there is a simultaneous increase in both the major and minor principal stresses. However only the variation in the major principal stress is considered essential in testing.

The AASHTO testing procedures (T292–91I and T294–92I) require bulk stresses θ (defined by $\theta = \sigma_1 + \sigma_2 + \sigma_3$) as high as 551.2 to 689.0 kPa (80 to 100 psi). These values appear to be much higher than the stresses prevailing in the field (*3,5,16*). As reported by Thompson and Smith (*17*), 137.8 kPa is a representative value of the bulk stress in the mid-depth of a granular base with a thickness of 30.48 cm below a 7.62-cm asphalt concrete surface.

RM is only minimally affected by variations in stress pulse duration. In fact, Kalcheff and Hicks (*18*) demonstrated that the RM values are not greatly influenced in a case in which the stress pulse is applied rapidly and then sustained compared with the case in which the stress pulse is applied rapidly and released for a short duration, provided that the magnitude of the stress pulse is equal in both cases.

TABLE 1 Comparison of Testing Procedures

AASHTO (T292-91I [5])			AASHTO (T294-92I [6])		
σ_C kPa	σ_d kPa	No. of Cycles	σ_C kPa	σ_d kPa	No. of Cycles
137.8*	103.4*	1000*	103.4*	103.4*	1000*
137.8	68.9	50	20.7	20.7	100
137.8	137.8	50	20.7	41.3	100
137.8	206.7	50	20.7	62.0	100
137.8	275.6	50	34.5	34.5	100
103.4	68.9	50	34.5	68.9	100
103.4	137.8	50	34.5	103.4	100
103.4	206.7	50	68.9	68.9	100
103.4	275.6	50	68.9	137.8	100
68.9	34.5	50	68.9	206.7	100
68.9	68.9	50	103.4	68.9	100
68.9	137.8	50	103.4	103.4	100
68.9	206.7	50	103.4	206.7	100
34.5	34.5	50	137.8	103.4	100
34.5	68.9	50	137.8	137.8	100
34.5	103.4	50	137.8	275.6	100
20.7	34.5	50			
20.7	48.2	50			
20.7	62.0	50			

* The load sequence constitutes sample conditioning, that is, minimizing the effects of initially imperfect contact between the end platens and the test specimen.

σ_C and σ_d denote chamber confining pressure and deviator stress, respectively.

The conversion factor (1 psi = 6.89 kPa) was used in this Table.

Dynamic Waveform and Number of Repetitions

Seed and McNeill (*19*) made one of the earliest attempts to duplicate the stress-state history by considering the actual variation in vertical stress on a soil element at a depth of 27 in. below the surface of the pavement at the Stockton test track. Because of the limitations of their test equipment they did not use the actual form of the vertical stress that was observed; instead they chose a square wave. Terrel et al. (*20*) also studied the influence of the shape of the wave pulse on the total and resilient strains induced in an asphalt-treated base material. They found that the triangular and the sinusoidal stress pulses produce similar effects on the resilience characteristics of the materials. It was also concluded that a square vertical stress pulse is a reasonable approximation of the actual conditions within a pavement structure.

AASHTO T292–91I suggests that the triangular and rectangular wave forms are applicable to RM testing of subgrade soils and base/subbase materials for simulating traffic loading. However T294–92I recommends that the haversine-shaped load pulse with a 0.1-sec load followed by a 0.9-sec rest period be used for both soil and granular materials. T292-91I specifies a fixed load duration of between 0.1 and 1.0 sec and a fixed cycle duration of between 1.0 and 3.0 sec.

To determine the number of repetitions necessary to reach the stable permanent deformation, AASHTO T292–91I suggests comparing the recoverable axial deformation at the 20th and 50th repetition. If the difference is greater than 5 percent, an additional 50 repetitions are necessary at that stress state. Thompson (*14*) reported that for granular materials the RM response after a limited number of load repetitions, such as 100, is representative of the response determined after several thousand repetitions because generally granular materials will achieve a stable permanent deformation after about 100 load repetitions.

MATERIAL ORIGIN AND ENGINEERING INDEX PROPERTIES

Six aggregate types used in Oklahoma as bases/subbases were selected for this study: three limestones, one sandstone, one granite, and one rhyolite. The engineering properties—liquid limit (LL), plasticity index (PI), maximum dry density (MDD), optimum moisture content (OMC), specific gravity (SG), cohesion (C), friction angle (ϕ) and California bearing ratio (CBR)—for these six types of aggregates were evaluated. A summary of the test results is presented in Table 2. It may be noted that following the repeated triaxial testing, static triaxial compression tests were performed to

TABLE 2 Summary of Index Properties

County	Material	LL (%)	PI	MDD g/cm^3 (pcf)	OMC (%)	SG	C kPa (psi)	ϕ (°)	CBR
Comanche	Limestone	16	1	2.40 (150)	5.6	2.66	124 (18)	41	67
Cherokee	Limestone	16	1	2.39 (149)	5.2	2.64	96.5 (14)	45	132
Creek	Limestone	15	NP*	2.42 (151)	5.5	2.78	124 (18)	43	116
Choctaw	Sandstone	14	NP*	2.35 (147)	5.9	2.53	82.7 (12)	46	284
Johnston	Granite	15	NP*	2.34 (146)	5.4	2.62	75.8 (11)	46	226
Murray	Rhyolite	16	NP*	2.40 (150)	6.0	2.72	110.2 (16)	46	150

* NP denotes nonplastic material

obtain the cohesion (C) and friction angle (ϕ) of the material (aggregate). The repeated triaxial tests served as a "conditioning" of the sample for triaxial compression tests that could be imposed by moving vehicles. Thompson and Smith (*17*) reported that the shear strength of an unconditioned specimen does not represent the strength of an in-service compacted granular base material subjected to traffic loading.

TRIAXIAL SPECIMEN PREPARATION

Although the method of compaction is important for fine-grained soils because of soil structure considerations, the primary factor affecting the stiffness characteristics of granular materials is water content (degree of saturation) (*7,11*). Accordingly any method of compaction that produces the desired dry density is suitable. Vibratory compaction, for example, has been used successfully by Hicks (*21*) and Laguros et al. (*22*) and recommended by AASHTO T292-91I and T294–92I. AASHTO T294–92I suggests using the OMC and MDD for a given aggregate type in accordance with T180–90D (*23*), then using the OMC and 95 percent of the MDD for specimen preparation.

A split mold was designed and fabricated for this study with provisions to apply a desired amount of vacuum to fit the membrane tightly on the inner surface of the mold. The internal diameter of the completed mold is 15.24 cm, the thickness of the wall is approximately 0.635 cm, and the height of the finished specimen is 30.48 cm. The base of the mold is firmly bolted onto the vibrating table so the mold will not move during vibration. A vacuum pump provides the required suction to stretch the membrane around the wall of the mold to aid in the compaction of the specimen.

The compaction method involves a trial-and-error adjustment in the weight of aggregate materials per layer, the number of compacted layers, and the vibrating period for each layer to produce specimens of the desired densities. On the basis of this trial-and-error approach a suitable sample preparation procedure was devised. With this method the specimens are prepared in 10 layers having approximately 1600 g of aggregate mixes per layer. A steel rod is used to enhance the effectiveness of compaction. The vibrating time is approximately 30 sec per layer for the first eight layers and 4 min per layer for the last two layers. This method yields specimens more uniform than those prepared by using equal vibrating times for each layer, in which case the bottom layer becomes more dense as a result of vibrating times accumulating from bottom to top. All specimens investigated were compacted to 95 percent of maximum dry density at optimum moisture content as determined from T180–90D, as shown in Table 2.

To meet the Oklahoma DOT 1988 specifications (*24*) and to ensure consistent gradation for each specimen among various aggregate types, a gradation curve was selected for the purpose of sample preparation. Gradation of aggregate materials can also be an important factor when comparing the RM values. The selected gradation curve used in this study and the gradation required by ODOT is presented in Figure 1.

EQUIPMENT SETUP FOR RM TESTING

The load frame, triaxial cell, pressure gauge, load cell, and the overall setup used in this study are shown schematically in Figure 2 (*top*). A 5-kip (2 270-kg) load cell mounted inside the triaxial chamber and attached to the loading piston is used to monitor the applied deviatoric load. The MicroProfiler is programmed to conduct a test under the desired loading. A data acquisition software system reads and stores the desired data in the form of voltages that are emitted from the transducers. Air is used as the cell fluid and confining medium instead of water because water might get into the specimen through tiny leaks or breakage of the membrane. An air pressure gauge installed onto the triaxial cell measures the confining pressure, as shown in Figure 2 (*top*). The advantage of this system is that the load cell is housed within the triaxial cell to allow in-vessel load measurement and to overcome the detrimental effects of friction

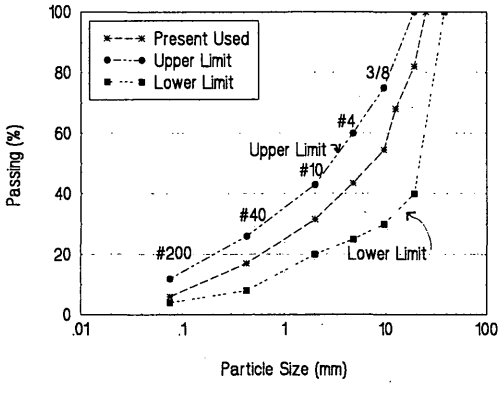

FIGURE 1 Gradation required by Oklahoma DOT and used in this study.

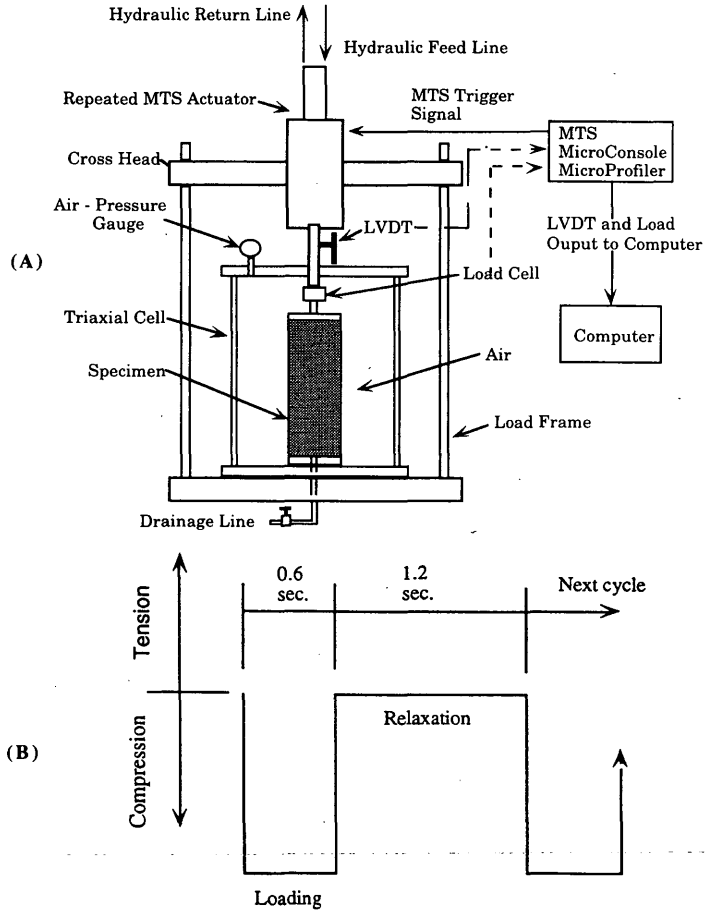

FIGURE 2 Test setup for RM testing (*top*) and rectangular wave (*bottom*) used in this study.

caused by the push rod. The quality of test results is generally improved by monitoring the in-vessel load and confining pressures.

A fixed cycle duration of 1.8 sec was selected in this study to provide a 0.6-sec loading duration and 1.2 sec of relaxation between the end and beginning of consecutive load repetitions, as shown in Figure 2 (*bottom*). An oscilloscope is used to monitor the applied cyclic loading to achieve the desired rectangular waveform by adjusting the gain controller in the MicroConsole.

DISCUSSION OF RESULTS

Variability Due to Aggregate Types

The six aggregate types were selected, compacted, and tested at OMC and 95 percent of MDD under testing procedure T292–91I to evaluate the effect of aggregate source variation and to investigate the variability of the results. According to testing procedure T292–91I, the RM values (in psi) for granular materials can be conveniently reported by using the relationship given in Equation 2, which requires determination of the regression constants K_1 and K_2.

$$RM = K_1 \theta^{K_2} \quad (2)$$

The constants K_1 and K_2 for these six aggregate types were obtained for every test and are presented in Table 3. Six RM tests were performed for the aggregates from Choctaw and Murray Counties and three RM tests each were performed for the aggregates from Comanche, Cherokee, Creek, and Johnston Counties. The standard deviation (SD) was also computed for each aggregate source and is given in Table 3. Table 3 shows that under testing procedure T292–91I some aggregate types experience a lower SD than other aggregate types. The ranges of K_1 and K_2 for untreated granular materials reported by several agencies are given by Shook et al. (*25*). Although the values of K_1 and K_2 obtained in this study are in the ranges reported by other agencies, it is inappropriate to make a direct comparison of the RM values by means of K_1 and K_2. Thus, in an effort to investigate the effects on RM values due to varying aggregate sources, the average (mean) RM values for each aggregate type are grouped together and presented in Figure 3. The details of the RM results in terms of bulk stress are given in Table 4, and the coefficient of variation (COV) is computed for each bulk stress and also presented in that table. An attempt was made to find the effect of confining stress on the RM values. Figure 4 shows that the RM values of all six aggregate types increased with increasing confining pressure, as expected. As shown in Table 4, the RM values obtained ranged from 51 to 195 MPa (7 to 28 ksi, values varying with

TABLE 3 Summary of K^1 and K^2 for Six Aggregate Types

County	Material	K_1 (psi)	SD*	K_2	SD*
Comanche	Limestone	4151	1082	.3918	.1175
		3908		.3683	
		2168		.5825	
Cherokee	Limestone	2283	2465	.5017	.1133
		4685		.3472	
		7213		.2882	
Creek	Limestone	4449	518	.3698	.0246
		4317		.3858	
		3494		.4180	
Choctaw	Sandstone	1388	165	.5309	.0295
		1691		.5847	
		1427		.5734	
		1498		.6073	
		2029		.5364	
		1440		.5533	
Johnston	Granite	2041	173	.5242	.0449
		2366		.4350	
		2102		.4889	
Murray	Rhyolite	2747	580	.4338	.056
		2417		.4949	
		3099		.4612	
		2160		.4769	
		1673		.5230	
		1652		.5949	

* SD denotes the standard deviation

bulk stress θ), which is in the range reported by May and Witczak (*26*) but lower than that suggested by the Asphalt Institute (*27*) for the design of flexible pavement [RM for untreated granular material vary from fewer than 103.4 MPa (15 ksi) to more than 344.5 MPa (50 ksi)].

Thompson (*14*) reported that for a given gradation (for either crushed or uncrushed materials) the source (limestone, sandstone, granite, etc.) is usually not a significant factor in terms of RM. Thompson and Smith (*17*) also observed that the RM properties of various aggregates are similar and the type of aggregates used as

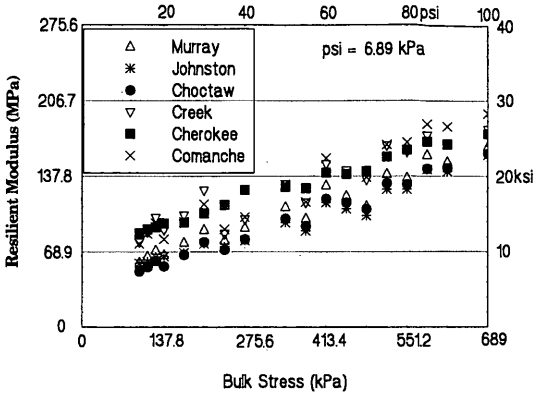

FIGURE 3 Comparison of average RMs for six aggregate types using AASHTO T292–91I.

base courses of roadway pavement (crushed stone/gravel) has limited effect on the RM. In fact, as shown in Figure 3, the differences of the RM values due to variation of aggregate types are approximately in the range of 20 to 50 percent. Table 4 shows that the maximum coefficient of variation (MCOV) for these six aggregate types is 20.8 percent, which suggests that the source of aggregate has some effect on the RM values.

In order to study the variability of the test results from the same aggregate type, aggregates from Choctaw and Murray Counties were selected for further investigations. It is assumed that Equation 2 adequately represents the granular material behavior. Accordingly the overall K_1 and K_2 (including results from the six tests) was computed and the predicted RM values were evaluated based on Equation 2 and compared with the corresponding experimental values. The relative error between the prediction (P) and the experimental results (T) was evaluated. The maximum relative error (MRE) thus obtained was defined as follows:

$$MRE = \left\{ \left| \frac{T1 - P}{P} \right|, \left| \frac{T2 - P}{P} \right|, \left| \frac{T3 - P}{P} \right| \right\} \left\{ \left| \frac{T4 - P}{P} \right|, \left| \frac{T5 - P}{P} \right|, \left| \frac{T6 - P}{P} \right| \right\}, \quad (3)$$

TABLE 4 Average RM for Six Aggregate Types Using AASHTO T292–91I

Bulk Stress (kPa)	Resilient Modulus (MPa)						MRE (%)	COV (%)
	Coma. County	Cher. County	Cree. County	Choc. County	John. County	Murr. County		
482.3	137.1	142.6	134.4	108.2	102.0	110.9	24.4	14.2
551.2	168.8	161.9	159.8	130.2	126.1	136.4	17.7	12.5
620.1	183.3	166.7	168.1	145.4	141.9	150.9	21.0	10.0
689.0	195.0	176.4	180.5	158.5	157.1	164.7	22.7	8.5
379.0	114.4	126.8	113.7	92.3	88.2	99.2	27.0	14.1
447.8	140.6	139.9	143.3	113.7	108.2	119.9	17.0	12.1
516.8	166.7	155.7	166.0	131.6	126.1	139.9	19.7	11.9
585.7	185.3	169.5	175.0	144.7	144	157.1	25.6	10.3
241.1	89.6	111.6	85.4	71.0	73.7	79.2	27.7	17.3
275.6	100.6	125.4	98.5	80.6	79.2	90.9	24.0	17.7
344.5	130.2	128.2	130.2	99.2	95.8	109.6	17.1	13.9
413.4	154.3	141.2	148.8	117.1	113.7	129.5	22.8	12.5
137.8	80.6	95.1	88.9	55.8	64.8	66.1	26.4	20.4
172.3	96.5	95.8	102.0	66.1	68.2	77.2	21.3	18.6
206.7	112.3	104	124.7	77.9	76.5	88.9	36.4	20.0
96.5	76.5	86.1	77.9	51.0	58.6	59.3	33.8	20.2
110.2	85.4	89.6	86.8	55.1	59.9	64.8	30.8	20.8
124.0	95.1	91.6	99.9	60.6	64.1	70.3	38.2	21.4

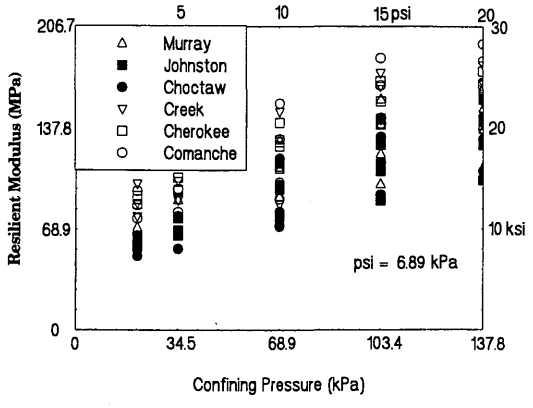

FIGURE 4 Effects of confining pressure on average RMs for six aggregate types using AASHTO T292–91I.

where $T1, T2, T3, T4, T5$, and $T6$ represent the experimental results from Tests 1, 2, 3, 4, 5, and 6, respectively. Since MRE fluctuates with bulk stress, a weighted maximum relative error (WMRE) becomes an important parameter in investigating the variability of the test results. Thus it is proposed that the calculations be performed in the form of

$$WMRE = \sqrt{\frac{\Sigma MRE^2}{n}} \tag{4}$$

It may be noted that here n is 18 for AASHTO testing procedure T292–91I and 15 for T294–92I because there are 18 and 15 RM values, respectively, for these two testing procedures. The computed WMRE for these two aggregate sources is presented in Table 5. The WMRE values of 28 percent and 26.4 percent were found for the aggregates from Choctaw and Murray Counties, respectively. The closeness of the WMRE values for these two aggregate types indicates that the testing procedure used gave consistent results.

In addition to the aforementioned comparisons, another attempt was made to determine the COV for the same aggregate source. The COV values were computed from the six RM tests along with the bulk stresses for the specimens from Choctaw and Murray Counties, as shown in Table 6. The maximum coefficient of variation (MCOV) for the aggregates from Choctaw and Murray Counties is presented in Table 5. The MCOV values were found to be 19.7 percent and 20.6 percent for the aggregates from Choctaw and Murray Counties, respectively.

TABLE 5 Summary of WMRE and MCOV

County	WMRE(%)	MCOV(%)
Choctaw (T292-91I)	28.0	19.7
Murray (T292-91I)	26.4	20.6
Choctaw (T294-92I)	23.0	18.9
Murray (T294-92I)	30.2	26.0
Aggregate Source		20.8
Testing Procedure		
Choctaw		25.8
Murray		36.0

TABLE 6 MRE and COV for Aggregates from Choctaw and Murray counties Using AASHTO T292–91I

Bulk Stress	Choctaw		Murray	
(kPa)	MRE (%)	COV (%)	MRE (%)	COV (%)
482.3	27.8	14.8	35.4	20.6
551.2	25.5	19.7	23.3	18.0
620.1	27.4	18.7	24.0	14.7
689.0	25.9	17.1	25.2	12.9
379.0	31.2	14.8	30.0	17.6
447.8	25.6	16.8	18.2	13.7
516.8	22.3	17.1	22.7	12.5
585.7	27.2	16.0	26.3	10.9
241.1	35.6	17.4	29.7	18.8
275.6	30.7	17.8	25.5	16.0
344.5	25.3	19.2	19.1	11.9
413.4	29.5	18.9	24.7	10.8
137.8	32.4	19.3	25.8	17.4
172.3	22.1	16.6	20.4	12.9
206.7	29.6	17.6	26.2	11.8
96.5	28.6	14.6	33.8	17.3
110.2	24.2	12.5	30.8	14.6
124.0	28.6	13.1	26.7	11.9

Variability Due to Testing Procedures

An attempt was made to investigate the effects of the applied stress sequence on the RM values. AASHTO test procedures T292–91I and T294–92I were chosen for this purpose because the T292–91I testing procedure starts with a higher confining pressure and deviatoric dynamic stress and ends with a lower confining pressure and deviatoric dynamic stress, whereas the T294–92I procedure suggests the reverse order. To eliminate another unknown in the comparison, the rectangular waveform shown in Figure 2 (bottom) was used for both the T292–91I and T294–92I methods. Aggregates from Choctaw and Murray Counties were selected and tested under both methods using six tests each. The results presented in Figure 5 suggest that the T294–92I procedure gives RM values higher than those obtained from T292–91I for both aggregate types. The higher RMs yielded by the T294–92I testing procedure may be attributed to the cyclic stress having a stiffening effect on the specimen structure because the stress application follows the low-to-high sequence. The amount of difference in the RM values due to testing method varies with aggregate type as shown in Figure 6. For example, aggregates from Murray County experience a higher degree of increase (about 35 to 55 percent) when using T294–92I than the aggregates from Choctaw County (about 15 to 34 percent).

Because the same aggregates have been tested using different testing procedures, it is expected that in using other testing procedures (such as the procedure suggested by the Florida, New York, Illinois, and South Dakota DOTs) the RM values would also fall in the ranges obtained in this study. When both T292–91I and T294–92I were used, the RM values ranged from 41.3 to 206.7 MPa (6 to 30 ksi) and from 48.2 to 261.8 MPa (7 to 38 ksi) (depending on bulk stress) for aggregates from Choctaw and Murray Counties, respectively (refer to Figure 5). These values are close to the values reported by Elliott (*28*) [ranging from 96.5 MPa (14 ksi, at θ = 14

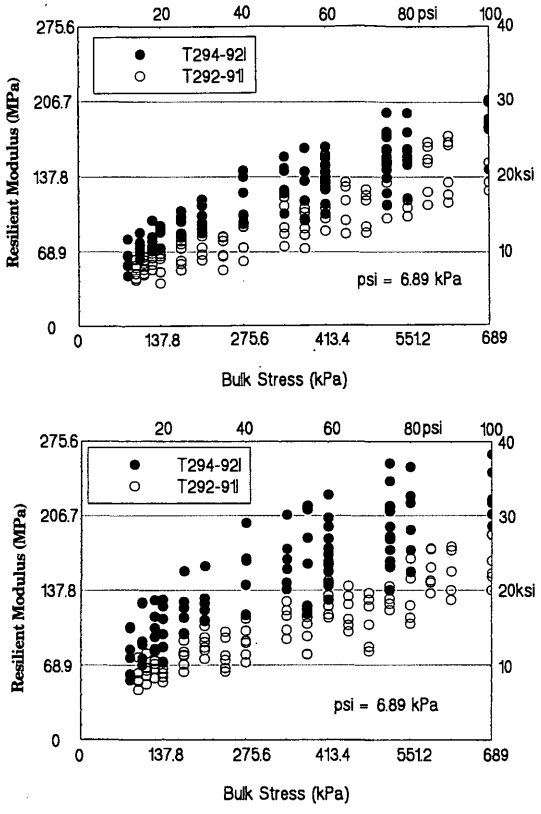

FIGURE 5 Effects of the testing procedure (AASHTO T292–91I and T294–92I) on RMs for the aggregates from Choctaw (*top*) and Murray (*bottom*) counties.

psi) to 255 MPa (37 ksi, at θ = 100 psi) with a relationship of RM (in psi) = 4,120 * $\theta^{0.47}$] but are lower than the values suggested by Monismith (*29*). A design modulus of 248 MPa (36 ksi) was recommended by Monismith for the crushed stone base.

Similarly, the COV values were computed along with bulk stress for the aggregates from Choctaw and Murray Counties on the basis of the results from six RM tests using the T294–92I procedure. The

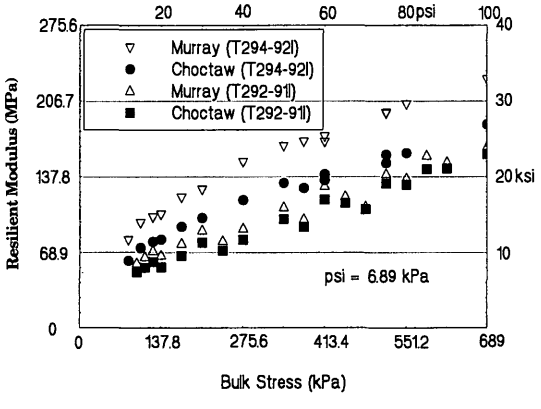

FIGURE 6 Comparison of average RM for different testing procedures (AASHTO T292–91I and T294–92I) and aggregate sources (Murray and Choctaw counties).

obtained WMRE and MCOV are given in Table 5. It was found that when using the T294–92I method the aggregates from Murray County experience a higher variability in the RM values (with WMRE 30.2 percent and MCOV 26 percent) than when using the T292–91I method (with WMRE 26.4 percent and MCOV 20.6 percent). In contrast, aggregates from Choctaw County exhibit a lower variability in the RM values (with WMRE 23.0 percent and MCOV 18.9 percent) when using T294–92I than when using T292–91I (with WMRE 28.0 percent and MCOV 19.7 percent). Thus, on the basis of the available data, it is premature to say that one test method is better than the other.

To investigate the variability of RM values due to testing procedure for the same aggregate source, six RM test data using T292–91I and six RM test data using T294–92I at the same level of bulk stress were grouped together and the COVs were computed. MCOVs of 25.8 percent and 36.0 percent were found for Choctaw County and Murray County aggregates, respectively, as evident from Table 5. Table 5 also shows that the variability of RM values due to the testing procedure was higher than the variability due to the aggregate source.

CONCLUSIONS

The AASHTO T292–91I testing procedures were used in this study to conduct the RM tests of six selected aggregate types and to investigate the variability of the test results. The variability of RM values due to testing procedures (T292–91I and T294–92I) and aggregate type was investigated. The following observations are made on the basis of the data obtained:

1. The RM values (ranging from 41.3 to 261.8 MPa, depending on bulk stress, material type, and testing method) obtained in this study are lower than those reported in the literature.
2. The variability of RM values obtained in this study ranges from 19 percent to 26 percent in terms of MCOV.
3. For a given gradation, the differences in RM values due to aggregate sources are found to be from 20 to 50 percent and the MCOV for these six aggregate types is 20.8 percent.
4. For both aggregate types investigated in this study, the T294–92I testing procedure yields higher RM values than those obtained by using the T292–92I testing procedure, possibly because the stress sequence in T294–92I has a stiffening and strengthening effect on the specimen structure as the stress level increases. The amount of increase in RM values due to testing method varies with the type of aggregate. For example, aggregates from Murray County exhibited a higher degree of increase (about 35 to 55 percent) when using the T294–92I testing method than the aggregates from Choctaw County (about 15 to 34 percent).
5. When using the T294–92I method, the aggregates from Murray County experience a higher variability in RM values (with WMRE 30.2 percent and MCOV 26 percent) than when using the T292–91I method (with WMRE 26.4 percent and MCOV 20.6 percent). In contrast, aggregates from Choctaw County exhibit a lower variability in RM values (with WMRE 23 percent and MCOV 18.9 percent) when using T294–92I than when using T292–91I (with WMRE 28 percent and MCOV 19.7 percent). Thus, on the basis of the available data, it is premature to say that one test method is better than the other.
6. The variability of RM values due to testing procedure was found to be higher than that due to aggregate source.

ACKNOWLEDGMENTS

Financial support for this study was provided by FHWA in cooperation with the Oklahoma DOT and by the Oklahoma Center for Advancement of Technology and Science. The assistance of Lawrence Senkowski, James Nevels, and Curt Hayes of Oklahoma DOT is gratefully acknowledged. R.L. Patten of the Mathematics Department, University of Oklahoma, provided advice on the statistical analysis and Steve Crain and Luping Yi helped with the specimen preparation and testing.

REFERENCES

1. *AASHTO Guide for Design of Pavement Structures.* AASHTO, Washington, D.C., 1986.
2. *Standard Method of Test for Resilient Modulus of Subgrade Soils.* AASHTO, Washington, D.C., 1986.
3. Pezo, R. F., G. Claros, W. R. Hudson, and K. H. Stoke. *Development of a Reliable Resilient Modulus Test for Subgrade and Non-granular Subbase Materials for Use in Routine Pavement Design.* Research Report 1177–4f, project 2/3/10-8-88/0-1177. Center for Transportation Research, The University of Texas, Austin, Jan. 1992.
4. Vinson, T. S. *Fundamentals of Resilient Modulus Testing.* Workshop on Resilient Modulus Testing, Oregon State University, Corvallis, Oreg., 1989.
5. Ho, Robert K. H. *Repeated Load Tests on Untreated Soils: A Florida Experience.* Workshop on Resilient Modulus Testing, Oregon State University, Corvallis, Oreg., 1989.
6. Zaman, M. M., J. Laguros, and R. Danayak. *Assessment of Resilient Modulus Testing Methods and Their Application to Design of Pavements.* Report No. FHWA/OK 91(08). University of Oklahoma, Norman, 1991.
7. *Interim Method of Test for Resilient Modulus of Subgrade Soils and Untreated Base/Subbase Materials.* AASHTO, Washington, D.C., 1991.
8. *Interim Method of Test for Resilient Modulus of Unbound Granular Base/Subbase Materials and Subgrade Soils.* AASHTO, Washington, D.C., 1992.
9. Parker, F. Estimation of Paving Materials Design Moduli from Falling Weight Deflectometer Measurements. In *Transportation Research Record 1293,* TRB, National Research Council, Washington, D.C., 1991, pp. 42–51.
10. Rada, G. R., C. A. Richter, and P. J. Stephanos. Layer Moduli from Deflection Measurements: Software Selection and Development of Strategic Highway Research Program's Procedure for Flexible Pavements. In *Transportation Research Record 1377,* TRB, National Research Council, Washington, D.C., 1993, pp. 77–87.
11. Rada, C., and W. M. Witczak. Comprehensive Evaluation of Laboratory Resilient Moduli Results for Granular Material. In *Transportation Research Record 810,* TRB, National Research Council, Washington, D.C., 1981, pp. 23–33.
12. Khedr, S. Deformation Characteristics of Granular Base Course in Flexible Pavements. In *Transportation Research Record 1043,* TRB, National Research Council, Washington, D.C., 1985, pp. 131–138.
13. Allen, J. *The Effect of Non-Constant Lateral Pressures of the Resilient Response of Granular Materials.* Ph.D. dissertation. University of Illinois at Urbana-Champaign, 1973.
14. Thompson, M. R. *Factors Affecting the Resilient Moduli of Soil and Granular Materials.* Workshop on Resilient Modulus Testing, Oregon State University, Corvallis, Oreg., 1989.
15. *Special Report 162: Test Procedures for Characterizing Dynamic Stress-Strain Properties of Pavement Materials.* TRB, National Research Council, Washington, D.C., 1975.
16. Jackson, N. C. *Thought on AASHTO T-274-82, Resilient Modulus of Subgrade Soils.* Workshop on Resilient Modulus Testing, Oregon State University, Corvallis, Oreg., 1989.
17. Thompson, M. R., and K. L. Smith. Repeated Triaxial Characterization of Granular Bases. In *Transportation Research Record 1278,* TRB, National Research Council, Washington, D.C., 1990, pp. 7–17.
18. Kalcheff, I. V., and R. G. Hicks. A Test Procedure for Determining the Resilient Properties of Granular Materials. *Journal of Testing and Evaluation, ASTM,* Vol. 1, No. 6, 1973.
19. Seed, H. B., and R. L. McNeill. *Soil Deformation Under Repeated Stress Applications.* STP 32, ASTM, Philadelphia, Pa., 1958, pp. 177–197.
20. Terrel, R. L., I. S. Awad, and L. R. Foss. *Techniques for Characterizing Bituminous Materials Using a Versatile Triaxial Testing System.* STP 561, ASTM, Philadelphia, Pa., 1974, pp. 47–66.
21. Hicks, R. G. *Factors Influencing the Resilient Properties of Granular Materials.* Ph.D. dissertation. University of California, Berkeley, 1970.
22. Laguros, J., M. M. Zaman, and Dar-Hao Chen. *Resilient Modulus of Select Aggregate Bases and Their Correlations with Other Engineering Properties.* Report 2189, ORA 125–6073. School of Civil Engineering and Environmental Science, University of Oklahoma, Norman, 1993.
23. *Moisture-Density Relations of Soils Using a 10-lb Rammer and an 18-in. Drop.* AASHTO, Washington, D.C. 1990.
24. *Standard Specifications for Highway Construction.* Oklahoma Department of Transportation, 1988.
25. Shook, J. F., F. N. Finn, M. W. Witczak, and C. L Monismith. Thickness Design of Asphalt Pavement—The Asphalt Institute Method. *Proc., 5th International Conference on the Structure Design of Asphalt Pavements,* Vol. 1, 1982, pp. 17–44.
26. May, R. W., and W. M. Witczak. Effective Granular Modulus to Model Pavement Responses. In *Transportation Research Record 810,* TRB, National Research Council, Washington, D.C., 1981, pp. 1–17.
27. *Thickness Design—Asphalt Pavements for Highways and Streets.* Manual Series No. 1 (MS-1). Asphalt Institute, Lexington, Ky., Sept. 1981.
28. Elliott, R. P. Selection of Subgrade Modulus for AASHTO Flexible Pavement Design. In *Transportation Research Record 1354,* TRB, National Research Council, Washington, D.C., 1992, pp. 39–44.
29. Monismith, C. L. Analytically Based Asphalt Pavement Design and Rehabilitation: Theory to Practice, 1962–1992. In *Transportation Research Record 1354,* TRB, National Research Council, Washington, D.C., 1992, pp. 5–26.

Publication of this paper sponsored by Committee on Soil and Rock Properties.

Accuracy Improvement of External Resilient Modulus Measurements Using Specimen Grouting to End Platens

DONG-SOO KIM AND SERGEY DRABKIN

To eliminate the source of errors in deformational measurements at small to intermediate strains (0.01 percent to 1.0 percent), a local strain measurement system inside the triaxial cell has been adopted in the resilient modulus (M_R) test. However because of complexities inherent in the local measurement, there are difficulties in using this technique in routine tests. As an alternative solution, external M_R measurement with the specimen grouted to the end platens with hydrostone paste was used. The effects of specimen grouting and the stiffness range on reliable external M_R measurements were investigated using six synthetic specimens of known stiffnesses ranging from that approximating a soft subgrade to that approximating stiff base material [from 20.7 MPa (3 ksi) to 552 MPa (80 ksi)]. For stiffness below about 345 MPa (50,000 psi), M_R values determined by external measurements with grouted specimens are identical to the known values from torsional testing. However for the stiffer specimens, M_R values of the grouted specimens are less than those from torsional testing, and the deviation increases with the increasing stiffness of the specimen. The secant static moduli determined by both loading and unloading curves closely matched the cyclic M_R at the same strain rate (or loading frequency), proving the feasibility of using the static testing scheme instead of the more expensive cyclic test. Finally the effects of specimen grouting were investigated using compacted subgrade soils.

AASHTO has adopted the use of resilient modulus (M_R) in pavement design to represent the deformational characteristics of pavement materials (*1*). Standard testing procedures for determining M_R were updated in AASHTO T-294–92I (*2*). However experience gained in applying these testing procedures has shown that great care must be exercised in evaluating resilient modulus at small to intermediate strains (0.01 percent to 1.0 percent) where the soil-pavement system is subjected to traffic loading, or significant inaccuracies can occur.

The axial strain is usually overestimated when the axial deformation is measured externally from the movement of the loading piston outside the triaxial cell (*3,4*). When stiffer specimens are tested at smaller strain amplitude under lower confining pressures, the degree of error is more pronounced. To eliminate the source of errors many local strain measurement systems inside the triaxial cell have been developed (*3–5*). However because of complexities inherent in the local measurement, there are difficulties using local measurement techniques in routine testing. Either compressed air or silicone oil, which is inert to a linear variable differential transformer, should be used as a confining fluid to accommodate the equipment inside the triaxial cell (*6*). Furthermore, even with on-specimen local deformation measurement, errors can still occur as a result of movement of the membrane relative to the specimen during a high-frequency cyclic test such as an M_R test.

S. Drabkin, Department of Civil and Environmental Engineering, Polytechnic University, 6 Metrotech Center, Brooklyn, N.Y. 11201. D.-S. Kim, Department of Civil Engineering, Korea Advanced Institute of Science and Technology, 373–1, Kusung-Dong, Yuoung -Ku, Taejon, Korea.

As an alternative solution, external M_R measurement with the specimen grouted to the end platens with hydrostone paste can be used without introducing the technical difficulties involved in internal measurement. Moduli of the grouted specimens determined by cyclic triaxial testing have been compared closely with those obtained by resonant column and torsional shear tests (*7–9*). Specimen grouting improves the contact between the specimen and the top cap and bottom plate, eliminating bedding errors. Use of hydrostone paste also has beneficial results because the evenness of the top cap can be adjusted to accommodate unevenness in the specimen end. However the reliability of external measurement depends on the stiffness of the specimen. Consequently before application for routine M_R testing, the effects of specimen grouting and stiffness range on reliable external M_R measurements should be investigated.

In this study, the effects of specimen grouting on external M_R measurements were investigated and quantified using six synthetic specimens of known stiffnesses. Both static modulus and cyclic M_R measurements were performed on the same specimen to investigate the feasibility of using the static testing scheme instead of the more expensive cyclic test. Static secant moduli determined by both loading and unloading curves were compared with cyclic M_R values. To investigate the reliability of external M_R measurements, both static modulus and cyclic M_R values of grouted specimens were compared with the known stiffness determined by torsional testing for a wide range of stiffness. Finally the effects of specimen grouting were investigated using compacted subgrade soils.

METHOD OF ANALYSIS

In the cyclic M_R test the modulus becomes nearly constant and the response can be assumed to be approximately elastic after about 100 cycles of loading for soil specimens (*2,10*). M_R values of soil specimens were determined using the average value of the last five cycles about the 100th cycle. M_R values of synthetic specimens were determined using the average value of three cycles about the 10th cycle because M_R values of synthetic specimens are independent of the number of loading cycles (*11*). The resilient strain and the deviator stress are measured as shown in Figure 1 (top), and the modulus is calculated from

$$M_R = (\sigma_1 - \sigma_3) / \epsilon_a = \sigma_d / \epsilon_a \quad (1)$$

where σ_1 is the major principal stress, σ_3 is the minor principal stress, σ_d is the deviator stress, and ϵ_a is the resilient axial strain.

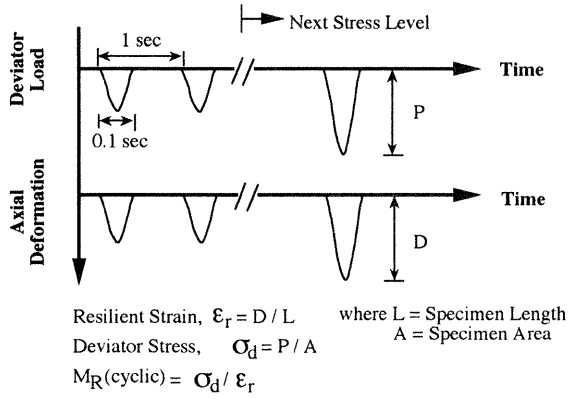

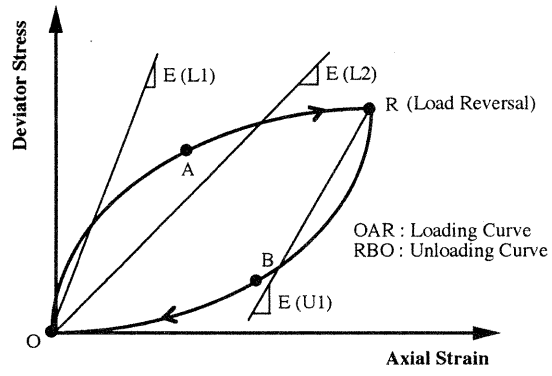

FIGURE 1 Determination of cyclic resilient modulus *(top)* and static secant modulus *(bottom)*.

In the static test the stress amplitudes increased linearly up to the maximum stress level used in the series of cyclic tests and decreased linearly to the zero level. The corresponding stress-strain relationships under loading and unloading conditions were determined as shown in Figure 1 (bottom). The secant moduli were calculated from the slope of a line connected from the origin to the stress-strain curve at various strain amplitudes. When the secant moduli were determined from the unloading curve the origin was translated to the reversal point as shown in Figure 1 (bottom). Variation in static modulus with strain amplitude can be obtained by performing only one static test, whereas more than one cyclic test would be required.

TEST MATERIALS

Six synthetic specimens with M_R values ranging from that approximating a soft subgrade to that approximating stiff base material [from 20.7 MPa (3 ksi) to 552 MPa (80 ksi)] were constructed at The University of Texas at Austin. The construction procedures and stiffness characteristics of synthetic specimens were well documented by Stokoe et al. (*11*). Synthetic specimens have physical characteristics that remain constant with time and thereby can be repeatedly tested using different testing schemes. The stiffness of synthetic specimens is essentially independent of strain amplitude and confining pressure in the range of M_R tests. The shear moduli of synthetic specimens were determined by torsional testing, and the measured shear modulus (G) was converted to Young's modulus (E) using the elastic equation.

$$E = 2\,G\,(1 + \upsilon) \tag{2}$$

where υ is Poisson's ratio. In M_R testing, E and M_R are assumed equal because the stiffness of the synthetic specimen is independent of loading history.

Two compacted subgrade soils were prepared and compacted at the optimum moisture content by dropping a hammer weighing 2.5 kg (5.5 lb) from a height of 30 cm (12 in.) with compaction energy based on the AASHTO T99 compaction method. Specimens were trimmed to approximately 10 cm (4 in.) in diameter and 20 cm (8 in.) in height. Table 1 presents the basic engineering properties of the test soils.

PROPERTIES OF HYDROSTONE PASTE

Hydrostone is a white, plaster-like material that is mixed with water and gains stiffness during the curing process. Because hydrostone paste is highly workable and has a rapid setting time, it is an appropriate material with which to grout the specimen to end platens. In addition, once cured, it is quite stiff. After the workability and setting time were checked, the water-hydrostone cement (W/C) ratio by weight was determined as 0.4.

In order to investigate the properties of hydrostone paste, a specimen with a W/C ratio of 0.4 was constructed with dimensions of 7.1 cm (2.8 in.) in diameter and 14.2 cm (5.6 in.) in height. Resilient modulus tests were performed at various curing times, then an unconfined compression test was performed at a curing time of 270 min. (*10*). The stiffness of the hydrostone paste increased from 1.04 GPa (150 ksi) to 1.73 GPa (250 ksi) at curing times of 50 min and 250 min, respectively. Pezo (*10*) recommended 120 min of curing time because the stiffness of hydrostone grout is strong enough [M_R of hydrostone grout is 1.38 GPa (200 ksi)] not to introduce problems on the M_R measurement of compacted subgrade soils with stiffnesses ranges up to about 345 MPa (50 ksi). The stress-strain curve of hydrostone paste obtained from the unconfined compression test showed the linear relationship up to a strain amplitude of 0.6 percent, within the range of most M_R tests.

TEST PROCEDURES

Synthetic Specimens

Synthetic specimens were tested under three different end conditions: grouted, ungrouted without seating pressure, and ungrouted with seating pressure. A seating pressure (static deviator pressure) of 69 kPa (10 psi) was used for ungrouted specimens to achieve bet-

TABLE 1 Basic Properties of Compacted Subgrade Soils

Soil ID	AASHTO Class.	Passing No. 200 (%)	Liquid Limit	Plasticity Index	Optimum Moisture Content (%)	Sample Moisture Content (%)	Wet Unit Wt. (pcf)
1	A-7-6	87.3	56	29	19.3	19.3	112.7
2	A-4	34.9	25	10	10.6	10.5	129.8

ter contact between the specimen and the end platens and to simulate the conditioning effect for the soil specimen. All of the tests were performed at zero confinement.

Both cyclic and static tests were performed on the same specimen. The cyclic tests were performed with increasing deviator stress amplitude up to approximately 207 kPa (30 psi). A harversine waveform was used with a load duration and cycle duration of 0.1 sec and 1.0 sec, respectively. Once the cyclic tests were completed, static tests were performed. The deviator stress was loaded linearly to the maximum stress level [207 kPa (30 psi)] during cyclic tests and unloaded to the original stress level, with a typical load duration of 10 sec.

Compacted Subgrade Soil

The compacted clay specimens were tested under three different end conditions: grouted, ungrouted without conditioning, and ungrouted with conditioning. Both cyclic and static tests were performed on the same specimen. The specimen was tested at a confining pressure of 41.4 kPa (6 psi). The cyclic tests were performed with increasing deviator stress from 6.9 kPa to 83 kPa (1 psi to 12 psi). After completion of the cyclic test at the highest stress amplitude, a low stress modulus was measured again and compared with the previous value to ensure that the specimen was not damaged. If the specimen was not damaged during cyclic tests (the moduli difference was within 5 percent), which was true for most cases, static tests were performed using the same waveform used on synthetic specimens.

After M_R tests with a grouted specimen were finished the specimen was carefully detached from the end platens. Both ends of the specimen were trimmed flat and the specimen was placed without grouting. At first the specimen was tested under cyclic and static loadings at 41.4 kPa (6 psi) of confining pressure without any conditioning. During the test the specimen was subjected to numerous load repetitions of various amplitudes more than specified in current conditioning stage (*2*). Conditioning was considered achieved during the first set of tests. The specimen was then tested following the same procedures used on the grouted specimen.

EFFECTS OF GROUTING ON SYNTHETIC SPECIMENS

Cyclic Resilient Modulus

The typical variation in cyclic resilient modulus with axial strain is shown in Figure 2 at three different end conditions. The moduli measured in the cyclic tests are almost independent of strain amplitude, but are substantially affected by the end conditions. The moduli of the grouted specimen are larger than those of the ungrouted one, and for the ungrouted specimen the moduli with seating pressure are larger than those without seating pressure. M_R values obtained from torsional testing are also plotted for comparison purposes and closely match the moduli of the grouted specimen.

It is difficult to make the specimen ends perfectly flat, hence an irregular air gap exists between the specimen and the end platens when placing the specimen without grouting. Because of these irregular gaps and nonuniform distribution of contact pressures (bedding errors), excessive deformation was monitored during the testing. Even if this measured erratic deformation is small, it can destroy

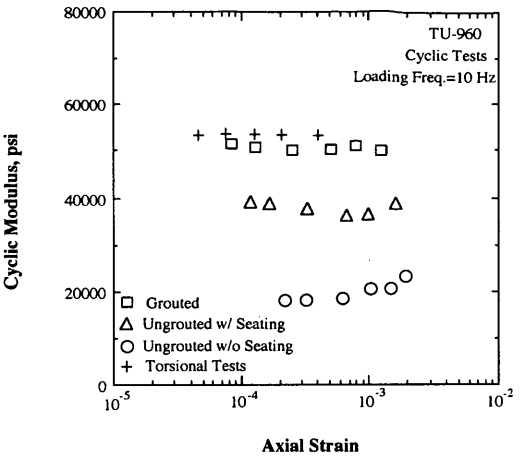

FIGURE 2 Typical variations in cyclic resilient moduli of synthetic specimens with axial strain determined at different end conditions.

the M_R measurements for relatively stiff specimens. For example, an error of approximately 2 thousandths of an inch (0.005 cm) in the deformation measurement (assuming the load is properly measured) provides a 0.025 percent error in strain measurement of a specimen 20 cm (8 in.) in height. If the real stiffness of this specimen is 345 MPa (50 ksi), only the M_R value of 112 MPa (16.2 ksi) would be measured when applying deviator stress of 41.4 KPa (6 psi).

Once the specimen ends are grouted to the end platens with hydrostone paste, the air gap is filled with hydrostone and uniform contact between specimen and end caps can be achieved. Because the erratic measurement of deformation is eliminated by specimen grouting, the moduli determined by a grouted specimen are much more reliable than those of an ungrouted one. The bedding error can also be reduced by applying seating pressure, but the improvement in the M_R measurement due to seating pressure is much less than the improvement due to grouting, as shown in Figure 2. Moreover, excessive seating pressure applied to the soil specimen may cause changes in the stress history of the specimen.

Cyclic M_R values of synthetic specimens measured at a strain amplitude of about 0.02 percent are summarized in Table 2; cyclic moduli obtained from torsional testings are included. To quantify the effect of specimen grouting on stiffness measurements, the moduli of the ungrouted specimen were normalized by the value of the grouted one. Figure 3 shows the variations in normalized modulus, M_R(ungrouted)/M_R(grouted), with the stiffness of the grouted specimen. The normalized moduli of ungrouted specimens varied from 100 percent to 25 percent of those of grouted specimens without seating pressure and from 100 percent to 50 percent of those of grouted specimens with seating pressure when the grouted M_R values varied from 21.4 MPa (3.1 ksi) to 497 MPa (72 ksi). Specimen grouting improves the M_R measurement significantly, and the amount of improvement increases as the stiffness of the specimen increases.

To investigate the effects of the stiffness range on reliable external M_R measurements with specimen grouting, moduli obtained from M_R tests were compared with moduli obtained from torsional testing, as shown in Figure 4. Within the range of stiffness below about 345 MPa (50 ksi), M_R values determined by external measurements with grouted specimens were identical with the cyclic

TABLE 2 Cyclic Moduli of Synthetic Specimens Determined at Different End Conditions

Specimen ID	Cyclic Modulus[1] (psi)			Cyclic[2] Modulus by RCTS (psi)
	Grouted	Ungrouted with Preload	Ungrouted without Preload	
TU 700	3100	2970	2950	3060
TU 900	10200	8900	5500	10100
TU960	50700	39800	16000	53500
D50	20100	18100	11300	20200
D60	50300	27100	15400	58600
D70	71900	37000	16800	89800

[1] Determined at a load duration of 0.1 sec and cycle duration of 1.0 sec, and at a strain amplitude of about 0.02%.

[2] Determined by resonant column and torsional shear test at a loading frequency of 10 Hz

moduli from torsional testing. The typical range of the resilient modulus of subgrade soils and unbound granular materials used in pavement design is less than 310 MPa (45 ksi) (*1*). Therefore the resilient modulus can be reliably determined for pavement design using external measurements of the axial strains of the grouted specimen. However in the stiffness ranges above about 345 MPa (50 ksi), M_R values of the grouted specimen are less than those from torsional testing, and the deviation increases with the increasing stiffness of the specimen.

Static Modulus

Typical stress-strain relationships obtained by static loading are shown in Figure 5 (top). The stress-strain behaviors of synthetic specimens are linear regardless of end condition. However the slopes of the stress-strain curves are substantially different depending on the end conditions. The slope for the grouted specimen is much steeper than those for ungrouted specimens. For the ungrouted specimens, the slope for the specimen with seating pressure

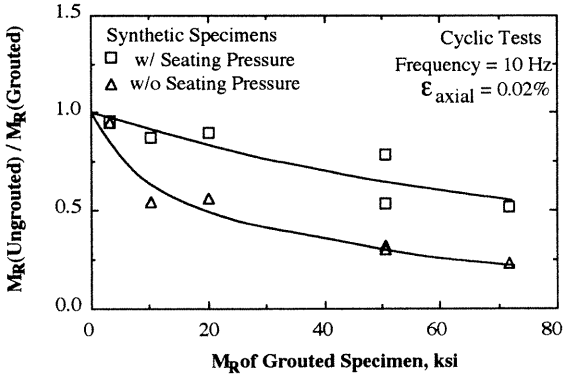

FIGURE 3 Variation in normalized moduli of synthetic specimens, M_R (ungrouted)/M_R (grouted), with stiffness of grouted specimen.

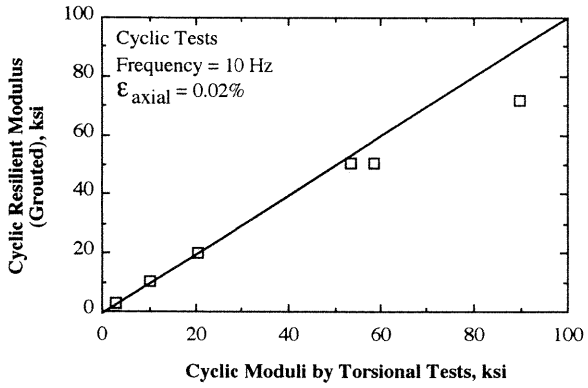

FIGURE 4 Comparison of resilient modulus of synthetic specimens determined by external measurement with specimen grouting and cyclic moduli determined by torsional testing.

is steeper than the slope for the specimen without seating pressure. It is interesting to note that strain amplitudes are different at the same corresponding deviator stress depending on the end conditions. The deformation of ungrouted specimens is overestimated because of the irregular gap that exists between the specimen ends and end platens. These erratic deformation measurements adversely influence the stress-strain behavior.

Typical stress-strain relationships measured from static unloading are shown in Figure 5 (bottom). The stress-strain behavior of the

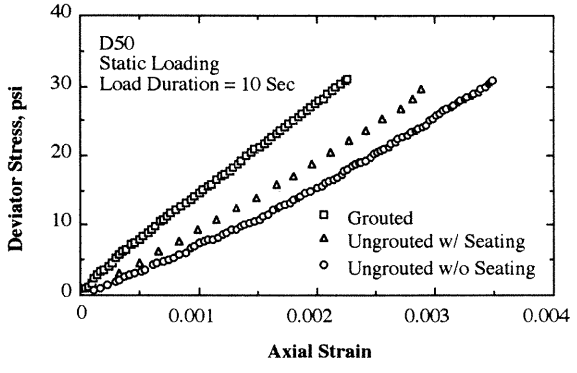

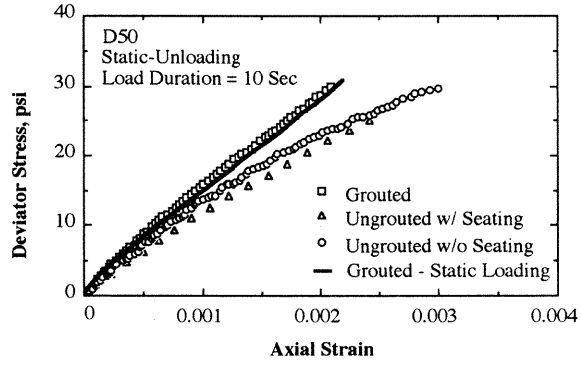

FIGURE 5 Typical stress-strain relationships of synthetic specimens under static loading (*top*) and unloading determined at different end conditions (*bottom*).

grouted specimen obtained from static loading is also included for comparison. The behaviors of grouted specimens measured from static loading and unloading tests are almost identical; however, the behaviors of the ungrouted specimens are quite different from those determined by static loadings. At strains below about 0.0005, all stress-strain curves match well. At higher strains, however, the strain amplitudes determined by ungrouted specimens are overestimated compared with those of the grouted specimen, and the difference increases with strain amplitude. This indicates that an irregular gap between the specimen ends and platens was closed during the static loading, and uniform contact was achieved before unloading. In the early stage of unloading, uniform contact remained even for ungrouted specimens, but at higher strains the irregular gap occurred again and influenced the measurements.

Static moduli of synthetic specimens determined by both loading and unloading tests under different end conditions are summarized in Table 3. Static moduli are determined at a load duration of 10 sec and at a strain amplitude of about 0.02 percent. To quantify the effect of specimen grouting on the static measurement, the moduli of the ungrouted specimen were normalized by the value of grouted specimen, and the variation in the normalized modulus with the stiffness of the grouted specimen is shown in Figure 6. The static modulus determined from loading tests is substantially affected by end conditions: the normalized values of ungrouted specimens without seating pressures varied from 98 percent to 26 percent of grouted specimen values, and values of ungrouted specimens with seating pressures varied from 102 percent to 46 percent of grouted specimen values when those values varied from 18.6 MPa (2.7 ksi) to 308 MPa (44.7 ksi), respectively. Specimen grouting significantly improves the accuracy of measurements, and the higher improvement rate is achieved for the stiffer specimens. The improvement rate achieved in the static loading test is similar to that in cyclic M_R tests at a given stiffness. However the static modulus determined from unloading tests is much less affected by the end conditions than that determined from static loading tests: the maximum difference of moduli between grouted and ungrouted specimens is less than 30 percent.

To investigate the reliability of static measurements, the moduli of grouted specimens determined by loading and unloading tests are

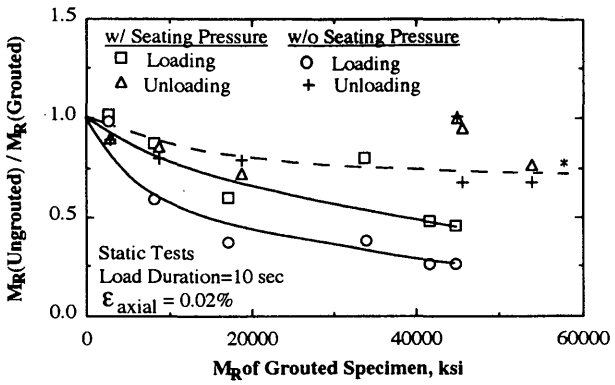

FIGURE 6 Variation in normalized static moduli of synthetic specimens, M_R (ungrouted)/M_R (grouted), with stiffness of grouted specimen.

compared with moduli determined by torsional testing, as shown in Figure 7. Because the stiffness of the synthetic specimen is affected by the loading rate (*11*), M_R values are compared at a similar loading rate: torsional testing was performed at a loading frequency of 0.05 Hz and static testing was performed using a load duration (equivalent to a half period in the cyclic test) of 10 sec. Within the ranges of stiffness below about 290 MPa (42 ksi), static moduli obtained from both loading and unloading curves were almost identical to the values obtained from torsional testing. This indicates an interesting feature: a reliable moduli can be measured using a static testing scheme if the M_R values are corrected to consider the loading rate. More important, if the specimen ends are grouted to the end platens using hydrostone paste, a static triaxial loading scheme with external measurement, which is common for conventional triaxial testing, provides an alternative M_R testing method without introducing the technical difficulties involved in internal measurement. In addition, the need for expensive cyclic testing equipment is avoided. At higher stiffness ranges, however, static moduli of grouted specimens are less than the values from torsional testing.

TABLE 3 Static Moduli of Synthetic Specimens Determined at Different End Conditions

End Condition / Loading Condition / Specimen ID	Static Modulus[1] (psi)						Cyclic[2] Modulus by RCTS (psi)
	Grouted		Ungrouted with Preload		Ungrouted without Preload		
	Load	Unload	Load	Unload	Load	Unload	
TU 700	2700	3020	2750	2720	2650	2700	2650
TU 900	8150	8800	7120	7550	4820	7030	8800
TU960	33900	45000	26500	45100	12800	42700	32700
D50	17100	18800	10200	13500	6300	14800	17300
D60	41600	45600	20100	43500	10700	31200	42100
D70	44700	53900	20400	40900	11700	36800	69600

[1]Determined by loading and unloading curves at load duration of 10 sec.
[2]Determined by resonant column and torsional shear test at a loading frequency of 0.05 Hz

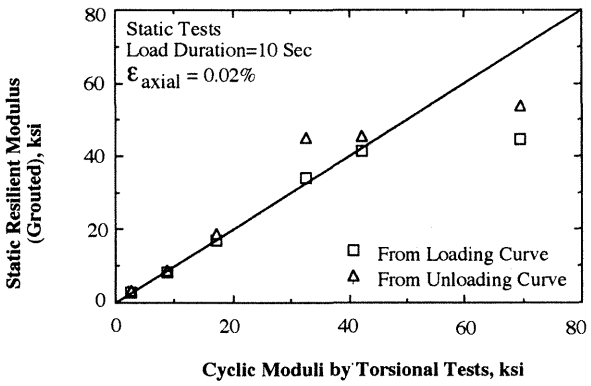

FIGURE 7 Comparison of static modulus of synthetic specimens determined by external measurement with specimen grouting and cyclic moduli determined by torsional testing (0.05 Hz).

EFFECTS OF GROUTING ON COMPACTED SUBGRADE SOILS

Cyclic Resilient Modulus

The variations in cyclic resilient moduli of two compacted subgrade soils with their strain amplitudes are shown in Figure 8. M_R values of grouted specimens are generally larger than those of ungrouted specimens. Modulus difference between the grouted and ungrouted specimens is greater for higher values of M_R and decreases as M_R decreases. At M_R values below about 69 MPa (10 ksi), both the moduli of the grouted and of the ungrouted specimens are almost identical regardless of end conditions. This behavior indicates that improvements in the cyclic M_R measurements due to specimen grouting are greater when the stiffness of the specimen is higher.

To show the effect of conditioning on M_R measurements, moduli of Sample 2 determined without conditioning are included in Figure 8. Moduli without conditioning are significantly lower than the grouted values, whereas moduli determined after conditioning are much closer to the grouted values, indicating that conditioning significantly improves the test results, particularly at low strain measurements, by making better contacts between the specimen and end platens. After conditioning the normalized moduli of compacted subgrade soils, M_R (ungrouted)/M_R (grouted), are approximately from 80 percent to 85 percent when M_R values vary from 207 MPa (30 ksi) to 138 MPa (20 ksi). These values are considerably higher than those on synthetic specimens without seating pressure (45 percent to 50 percent) and similar to those with seating pressures (76 percent to 83 percent) as shown in Figure 3. Specimen conditioning improves M_R measurements on compacted subgrade soils by reducing bedding errors, but it does not provide the same level of improvement achieved by specimen grouting.

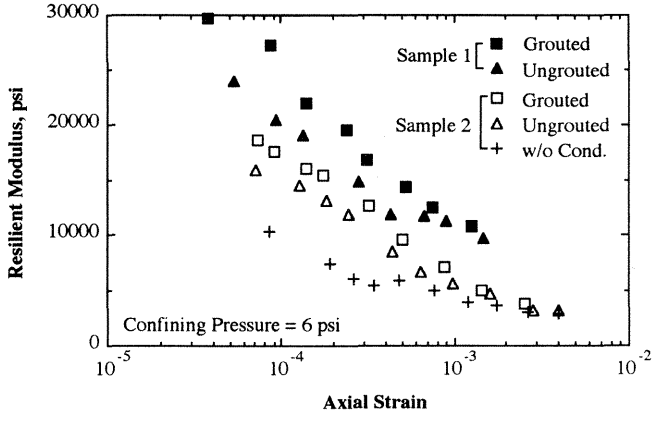

FIGURE 8 Variations in cyclic resilient modulus of two compacted subgrade soils with axial strain under different end conditions.

Static Modulus

Typical variations in static moduli with strain amplitude determined by loading and unloading tests are shown in Figure 9. Static moduli determined by loading tests are affected by end conditions as shown in the top portion of Figure 9: moduli of grouted specimens are greater than the values of ungrouted specimens. However specimen end condition does not influence the static modulus determined by unloading tests, as shown in the bottom portion of Figure 9, where the moduli of grouted and ungrouted specimens are almost identical.

For comparison of the M_R values determined by static and cyclic tests, cyclic moduli of grouted specimen are included in Figure 9.

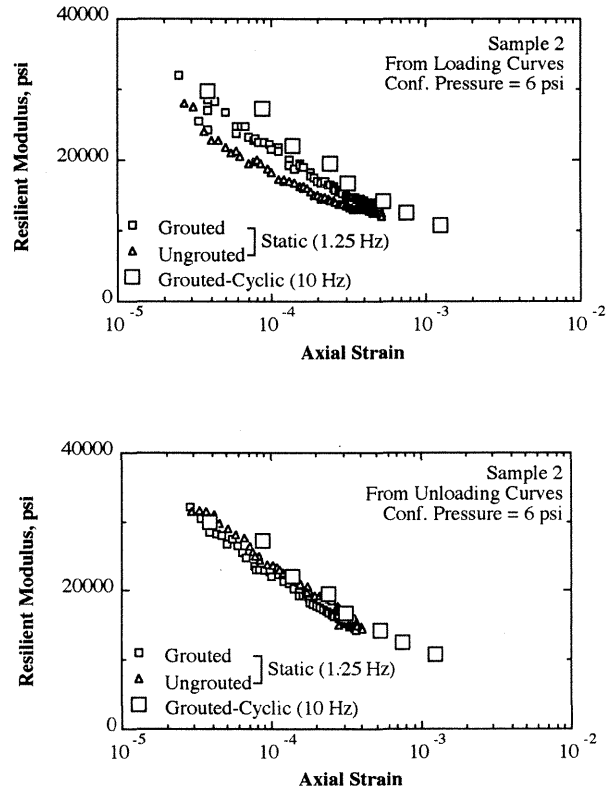

FIGURE 9 Typical variation in static modulus of compacted subgrade soil with strain amplitude determined by static loading (*top*) and unloading (*bottom*) curves at different end conditions.

With an identical specimen, the static modulus is determined at a load duration of 0.4 sec (equivalent of 1.25 Hz) and a cyclic modulus is determined at a loading frequency of 10 Hz. All static moduli match fairly well except for those of the ungrouted specimen measured by the loading curve but they are somewhat smaller than the cyclic moduli. This difference can be explained by the difference in loading frequency between both tests, because the resilient modulus of compacted subgrade soil is affected by the loading frequency (*12*). This suggests the feasibility of using an alternative static loading scheme for a resilient modulus measurement if the measured value is properly corrected to consider the loading frequency. Further study is being conducted by the authors.

CONCLUSIONS

The reliability of external M_R measurements with specimens grouted to end platens was investigated using synthetic specimens of known stiffness and compacted subgrade soils. Both static and cyclic tests were performed on the same specimens. The following conclusions were drawn:

1. Specimen grouting provides better contact between the specimen and end platens and improves the external M_R measurements by eliminating bedding errors. The amount of improvement increases as the stiffness of the specimen increases. For synthetic specimens, the moduli of ungrouted specimens varied from 100 percent to 25 percent of grouted specimen values without seating pressure and from 100 percent to 50 percent of grouted specimen values with seating pressure when the grouted specimen M_R values varied from 21.4 MPa (3.1 ksi) to 497 MPa (72 ksi).
2. Static secant moduli are obtained from both static loading and unloading curves. The improvement achieved in static loading tests due to specimen grouting was similar to that in the cyclic M_R tests at a given stiffness. However static modulus obtained from the unloading curve was much less affected by the end conditions.
3. Reliable M_R can be determined for pavement design by external M_R measurements with specimen grouting in the range of stiffness below about 290 MPa (42 ksi) for static tests and below about 345 MPa (50 ksi) for cyclic tests. However at higher stiffness ranges, external M_R measurements underestimate the M_R values and the deviation increases with the increasing stiffness of the specimen.
4. Static moduli of synthetic specimens and compacted subgrade soils determined by external measurements match fairly well with the cyclic M_R values at a corresponding strain amplitude if the loading rate is considered in the comparison. A static triaxial loading scheme with an external measurement may provide an alternative M_R testing method without introducing the technical difficulties involved in internal measurement and without the need for expensive cyclic testing equipment.

ACKNOWLEDGMENTS

The authors would like to thank Kenneth H. Stokoe II and his students at the University of Texas at Austin who constructed the synthetic specimens and calibrated the specimens using resonant column/torsional shear equipment.

REFERENCES

1. *AASHTO Guide for Design of Pavement Structures.* AASHTO, Washington, D.C., 1986.
2. *Resilient Modulus of Unbound Base/Subbase Materials and Subgrade Soils*—SHRP Protocol P46 AASHTO, T-294-92I. AASHTO, Washington, D.C., 1992, pp. 52–65.
3. Burland, J. B. Ninth Lauritis Bjerrum Memorial Lecture: Small is Beautiful—The Stiffness of Soils at Small Strains. *Canadian Geotechnical Journal,* 26, 1989, pp. 499–516.
4. Tatsuoka, F., S. Shibuya, S. Goto, T. Sato, and X. J. Kong. Discussion on the Paper by Clayton et al. *Geotechnical Testing Journal,* Vol. 13, No. 1, 1990, pp. 63–67.
5. Goto, S., F. Tatsuoka, S. Shibuya, Y. S. Kim, and T. Sato. A Simple Gauge for Local Small Strain Measurement in the Laboratory. *Soils and Foundations,* Vol. 31, No.1, March 1991, pp. 169–180.
6. Nataatmadja, A., and A. K. Parkin. Axial Deformation Measurement in Repeated Load Triaxial Testing. *Geotechnical Testing Journal,* Vol. 13, No. 1, March 1990, pp. 45–48.
7. Ladd, R. S., and P. Dutko. Small-Strain Measurements Using Triaxial Apparatus. *Proc., Advances in the Art of Testing Soils Under Cyclic Conditions,* Detroit, Mich. ASCE, 1985, pp. 148–165,
8. Pezo, R. F., D. S. Kim, K. H. Stokoe, and W. R. Hudson. Developing a Reliable Resilient Modulus Testing System. In *Transportation Research Record 1307,* TRB, National Research Council, Washington, D.C., 1991, pp. 90–98.
9. Kim, D. S. *Deformational Characteristics of Soils at Small to Intermediate Strain From Cyclic Tests.* Ph.D dissertation. The University of Texas at Austin, 1991.
10. Pezo, R. F. *Development of Reliable Resilient Modulus Test for Subgrade and Subbase Materials for Use in Routine Pavement Design.* Ph.D dissertation. The University of Texas at Austin, 1991.
11. Stokoe, K. H., D. S. Kim, and R. Andrus. Development of Synthetic Specimens for Calibration and Evaluation of M_R Equipment. In *Transportation Research Record 1278,* TRB, National Research Council, Washington, D.C., 1990, pp 63–71.
12. Kim, D. S., and K. H. Stokoe. Characterization of Resilient Modulus of Compacted Subgrade Soils Using Resonant Column and Torsional Shear Tests. In *Transportation Research Record 1369,* TRB, National Research Council, Washington, D.C., 1992, pp 83–91.

Publication of this paper sponsored by Committee on Soil and Rock Properties.

Factors Influencing Determination of a Subgrade Resilient Modulus Value

JAMES M. BURCZYK, KHALED KSAIBATI, RICHARD ANDERSON-SPRECHER, AND MICHAEL J. FARRAR

Factors influencing the determination of a subgrade resilient modulus value were evaluated. Nine test sites with cohesive subgrade soils were selected in the state of Wyoming, and laboratory testing was conducted on subgrade cores obtained in 1992 and 1993. Several fundamental soil properties of these cores were determined and deflection data from these nine sites were used to determine resilient modulus values with three back calculation programs. The data analysis resulted in several important conclusions about factors that influence the selection of a design subgrade resilient modulus value.

The 1993 *AASHTO Guide for Design of Pavement Structures* requires selecting a value for the design subgrade resilient modulus (M_R). Resilient modulus is a "measure of the elastic property of soil recognizing certain nonlinear characteristics" (*1*). Numerically, it is the ratio of the deviator stress to the resilient or recoverable strain ($M_R = \sigma_d/\epsilon_r$). This value may be based on laboratory testing, back-calculation programs using deflection measurements, resilient modulus correlation studies, or original design and construction data (*2*). In many cases, agencies lack the capital required for the laboratory equipment, or their pavement engineers are unfamiliar with this new subgrade soil property (*3*). As a result, equations have been developed to convert values from soil tests, such as California bearing ratio (CBR) and R-value, to resilient modulus values. Even though this method of obtaining M_R values is acceptable, AASHTO recommends that "user agencies acquire the necessary equipment to measure M_R" (*1*).

Several factors must be taken into consideration when selecting a design M_R value. According to Darter et al. (*2*), "Regardless of the method used, the design subgrade M_R value must be consistent with the value used in the design performance equation for the AASHO Road Test subgrade." The 1986 guide uses a value of 20 684 kPa (3000 psi), but does not justify its selection. Elliott, however, presented the findings of several researchers on the reason this value was chosen to represent the AASHO Road Test subgrade (*3*). Based on a study by Thompson and Robnett (*4*), this value is appropriate when the AASHO soil is about 1 percent wetter than optimum and is subjected to a deviator stress of about 41.4 kPa (6 psi) or more. Besides the usefulness of this observation in selecting a design M_R value from laboratory testing, it also plays an important role in determining a value from back-calculation programs using deflection data. To make these nondestructive testing (NDT) values consistent with the 20 684-kPa (3000-psi) value, the calculated M_R value is multiplied by a correction factor (C) less than or equal to 0.33 for cohesive soils (*3*). The need for a correction factor resulted from the fact that most NDT programs assume that the measured deflection, at a certain distance away from the loading plate, is attributable solely to the subgrade. In many cases, the amount of stress at this point is less than 41.4 kPa (6 psi), giving a higher resilient modulus value. Reducing the back-calculated resilient modulus value satisfies the underlying assumption in the overlay equation.

Because the intent of laboratory testing is to simulate conditions in the field, other factors, such as water content, soil type, and sample condition, must also be considered. First, water content is important because of its effect on M_R values obtained either above or below the optimum value. In 1989 Elfino and Davidson (*5*) reported variations in the resilient modulus value of 7 to 41 percent from soils at different water contents. Second, whether the sample is undisturbed or disturbed will influence the M_R. Third, soil type may influence the M_R because of the differences in quality and soil strength.

The University of Wyoming and the Wyoming Department of Transportation (DOT) conducted a joint research project, first to investigate the importance of several fundamental soil properties in determining a design subgrade resilient modulus value, and second to define the actual relationship between back-calculated and laboratory-based M_R values for typical subgrade soils in Wyoming. The main findings of this study are presented here.

EXPERIMENT DESIGN

Figure 1 shows the data collection process and overall evaluation strategies followed in this research. Initially, a large number of pavement test sections were selected in the state of Wyoming. During the summer of 1992 and spring of 1993, different types of field data were collected on all sections. This field evaluation included pavement and subgrade coring, deflection measurements, and condition surveys. Several laboratory tests were later conducted on the soil cores to determine the types of subgrade at each site. As a result of this laboratory testing, all sections with granular subgrade material were dropped from the study. More laboratory tests, including resilient modulus, were later conducted only on the sites that had cohesive subgrades. Table 1 shows the locations and thicknesses of the sections included in this experiment. In addition to the laboratory analysis, the deflection data collected in 1992 and 1993 were used to determine M_R values with the following three back-calculation programs: MODULUS (*6*), EVERCALC (*7*), and BOUSDEF (*8*). All data were summarized in a computerized data base. Statistical analyses were then performed to determine how fundamental soil properties, linear variable differential transducer (LVDT) placement during M_R testing, and sample condition influence the resilient modulus value. Further analyses were completed to examine the relationship between laboratory and back-calculated M_R values.

J.M. Burczyk, K. Ksaibati, and R. Anderson-Sprecher, University of Wyoming, Laramie, Wyo. 82071. M.J. Farrar, Wyoming Department of Transportation, P.O. Box 1708, Cheyenne, Wyo. 82002–9019.

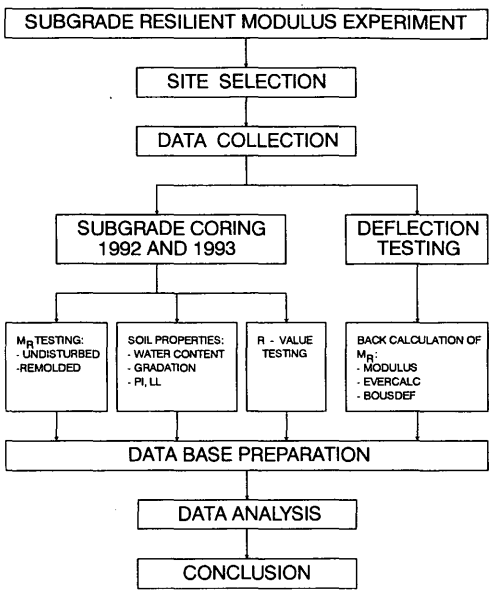

FIGURE 1 Data collection and analysis strategies.

DATA COLLECTION AND LABORATORY TESTING

Field Data Collection

Extensive field data were collected on all test sections included in this study. Pavement deflection measurements were obtained by using standard loads on the Wyoming DOT Kuab 2-m falling weight deflectometer. Then, three pavement cores were obtained from each section to examine the characteristics of the asphalt layers and to verify the thicknesses. This information was used later in determining the back-calculated resilient modulus values. Next, pavement condition surveys were completed to record each section's surface condition. Finally, three Shelby tubes were taken from the subgrade at each test section. The soil samples were used to conduct resilient modulus testing, obtain R-values, and perform other tests for certain fundamental soil properties.

Resilient Modulus Testing

Laboratory M_R values are normally obtained with repeated-load triaxial testing. The Interim Method of Test for *Resilient Modulus of Unbound Granular Base/Subbase Materials and Subgrade Soils—SHRP Protocol P46* (AASHTO: T 294–92 I) outlines the latest testing procedure. This specification separates subgrade material into two different categories: Type I (granular) and Type II (cohesive). Each type of soil has a different conditioning cycle and 15 loading sequences varying in confining and deviator stresses. Overall, Type I soils undergo higher stresses, both confining and deviator, because of their higher resistance to deformation. The amount of deformation in the soil sample is recorded using two LVDTs outside of the testing chamber. However, the original AASHTO T-274 specifications required two LVDTs within the test chamber. These LVDTs are placed at a specified gauge length depending on the size of the soil sample. Figure 2 shows the two different LVDT locations used in this study. The M_R value is then calculated by using the averaged deviator load and deformation from the last five cycles of each testing condition.

In this project, deformation readings were recorded at two different locations during the laboratory testing: from two LVDTs

TABLE 1 Locations and Thicknesses of Test Sections

Roadway	Milepost		Pavement Thicknesses	
	From	To	Surface (inches)	Base (inches)
US-30	67.063	76.819	5.5	6.0
US-30	45.984	48.786	12.0	12.0
US-287	411.890	419.270	6.0	6.0
US-26	105.642	109.677	5.0	6.0
US-20/26	10.360	21.237	5.0	8.0
US-20	162.120	164.094	3.0	2.5[1]
US-16	226.300	233.700	6.0	8.0[1]
US-16	241.990	246.590	2.3	3.5[1]
US-85	195.760	202.690	6.0	8.0[2]

[1]Asphalt Treated Base (ATB)

[2]Cement Treated Base (CTB)

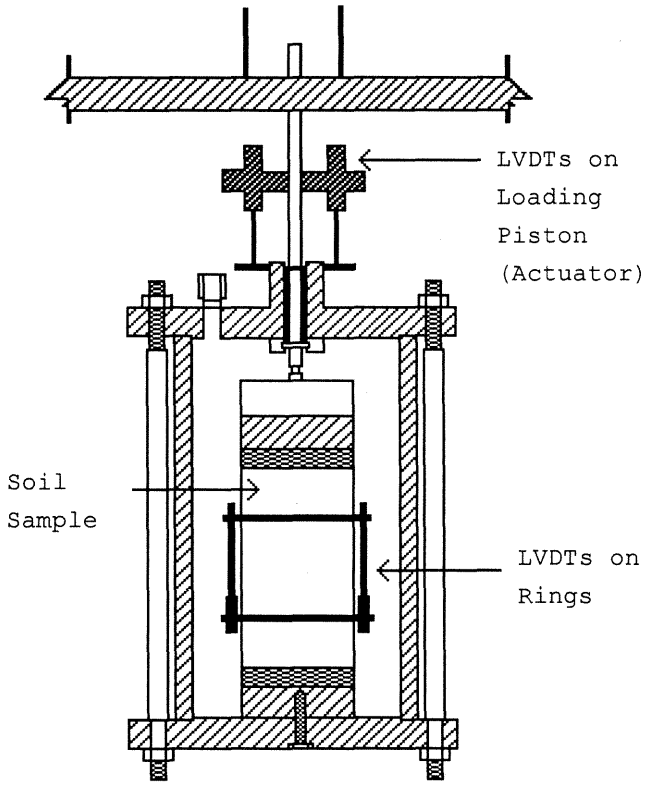

FIGURE 2 Location of LVDTs on testing equipment.

located outside the triaxial cell on the loading piston (referred to as the actuator in this paper) and from three LVDTs located on the rings inside the testing chamber. Even though some testing programs automatically average these signals during testing, readings were averaged after completion of testing. This procedure was useful in eliminating inconsistent readings. Three segments of subgrade soil from each Shelby tube were extracted for testing. All subgrade cores were tested in undisturbed and disturbed conditions, and each sample was 15.2 cm (6 in.) in length and 7.1 cm (2.8 in.) in diameter.

After laboratory testing was completed, deformation and applied load readings from the last five cycles of each loading condition were retrieved from the data files. Several spreadsheets were developed to accept these data as well as the length and diameter of each sample. After this information was entered the resilient modulus values were calculated automatically for each testing condition and test section.

Other Laboratory Tests

After completing the resilient modulus testing, each soil sample was tested to determine its R-value, liquid limit (LL), plasticity index, soil classification, group index, and water content. Table 2 shows some typical values observed in this study. The following equation, occasionally used by the Wyoming DOT, was used in estimating the optimum water content of each sample:

$$\omega = 0.477\ (LL) + 2 \qquad (1)$$

where ω is the optimum water content (percent) and LL is the liquid limit.

All laboratory tests were conducted in accordance with their respective ASTM and AASHTO specification.

Back Calculations of Resilient Modulus

Deflection data collected from the nine test sites were used to obtain M_R values with three back-calculation computer programs: MODULUS, EVERCALC, and BOUSDEF. These programs compare the deflection basins based on field data to theoretical basins in order to determine back-calculated M_R values. However each program computes these moduli using different methodologies and assumptions. The first program, MODULUS, was developed at Texas A&M University. MODULUS determines M_R values based on a layered elastic code called WES5. This code creates a large data base of theoretical deflection basins and matches, through interpolation, the best basin to the field data. The second program, EVERCALC, was developed at the University of Washington. In this program theoretical deflections are based on CHEVRON as the layered elastic solution. The third program, BOUSDEF, was developed at Oregon State University. This program uses the method of equivalent thicknesses, assuming one thick, uniform layer of material, and the Boussinesq theory to determine theoretical basins. Overall, by matching the deflection basin measured in the field, the M_R value is calculated for each section's layers (surface, base, and subgrade) (*9*).

DATA ANALYSIS

Data were gathered during two different periods, Period A (summer 1992) and Period B (spring 1993), at nine different sites. Five of these sites were common to both time periods; one was specific to Period A; and three were specific to Period B. Aside from designations of the sampling variables (period, site, tube, and layer), the measured variables included the resilient modulus (measured in various manners), R-value, and certain soil characteristics (soil classification, group index, actual and optimum water contents, and plasticity index). The inclusion of different sites made for some inconstancy in soil types between periods. The analyses below account for these differences as necessary. All analyses were based on $\log_{10}(M_R)$, abbreviated as LMR, instead of M_R itself.

Relationship Between Resilient Modulus and R-Values

Accurate values of LMR are expected to correlate fairly well with R-values. Because of this assumption correlations were obtained for measured R-values and the four measurements of LMR for Periods A and B. Table 3 shows the observed correlations. Within rows of this table correlations are comparable because they are based on the same soil samples. However differences in base soils between Periods A and B may distort comparisons between these rows. The most important aspect of Table 3 is that the disturbed soils' LMRs are not significantly correlated with the R-value, but undisturbed soils' LMRs are correlated with the R-value. Correlations between undisturbed and disturbed LMRs (not shown) were modest to nonexistent. Therefore samples should be retained intact if the resilient modulus is to be a meaningful measure for pavement design.

TABLE 2 Typical Soil Characteristics, Spring 1993

Water Content (%)	Optimum Water Content (%)	Soil Classification	Plasticity Index (PI)
14.2	13.9	A-4(1)	10
15.9	18.7	A-6(13)	22
11.9	14.4	A-6(1)	13
10.8	14.9	A-4(0)	7
11.5	14.4	A-4(0)	6
13.2	14.4	A-4(0)	8
13.9	14.4	A-4(0)	5
12.8	14.4	A-4(0)	7
15.5	17.7	A-6(9)	18
15.8	13.0	A-4(3)	9
16.8	15.4	A-6(6)	14
15.4	20.1	A-6(13)	23
19.7	25.9	A-7-6(26)	26
20.1	28.2	A-7-6(30)	28
18.7	26.3	A-7-6(29)	29
20.7	22.0	A-7-6(16)	16
20.6	23.5	A-7-6(23)	22
20.8	22.5	A-7-6(15)	15
15.9	17.7	A-6(7)	17
23.7	19.6	A-6(7)	13
20.7	24.4	A-7-6(21)	23
25.3	19.6	A-6(3)	11
21.1	17.3	A-7-6(26)	28
20.9	24.4	A-7-6(23)	26
19.8	26.3	A-7-6(27)	29
11.3	21.1	A-6(16)	23
17.4	22.5	A-7-6(20)	25
12.8	21.6	A-7-6(17)	23
15.5	22.0	A-7-6(17)	23
19.3	21.1	A-6(16)	22
16.2	22.0	A-7-6(16)	22
15.2	23.5	A-7-6(21)	25
13.8	14.9	A-4(5)	9
17.4	25.9	A-7-6(25)	31
12.7	15.4	A-4(4)	7

TABLE 3 Correlations Between LMR[1] and R-Value

	Undisturbed		Disturbed		Sample
	Ring	Actuator	Ring	Actuator	Size
Period A[2]	0.630	0.749	-0.041	-0.089	16
Period B[3]	0.334	0.437	-0.219	-0.273	23
Pooled[4]	0.380	0.509	-0.136	-0.142	39

[1]Log_{10} (Resilient Modulus Values)

[2]Summer 1992

[3]Spring 1993

[4]Pooled (1992 & 1993)

Only undisturbed LMRs were used in the remaining analyses unless noted otherwise.

Effect of Sensor Location on M_R Measurements

The correlations shown in Table 3 also suggest that the placement of LVDTs outside the testing chamber may be more suitable than placement on the ring. Observed differences in the correlations with R-value are not, however, extreme, and placements were also compared on the basis of measurement precision. To ensure that all variability measured was attributable to differences in measurement methods, values were adjusted for site, period, and sample tube. The test for differences in variances for paired data (*10*) showed the ring variance to be greater than the actuator variance ($t = 2.238$, $df = 20$, $p = 0.0368$): The greater variation in ring measurements is a result of the difficulty in obtaining good contact between the LVDTs on the ring and the soil sample. Analyses are henceforth made using actuator measurements only.

Although measurements at the actuators appear to be preferable, the relationship between actuator and ring measures is of interest. Actuator and ring measurements of LMR are highly correlated, as shown in Table 4. A *t*-test of paired differences indicates that ring measures are consistently higher than actuator measures. Repeated measures analysis indicates that differences between ring and actuator measurements are similar for undisturbed samples ($p = 0.206$), and the pooled analysis is consequently considered acceptable.

Effect of Sample Location on M_R Values

An issue relevant to M_R measurement is the selection of samples from tubes. If layers systematically differ from each other, with surface layers having consistently higher or lower values than deeper layers, one would expect that surface-layer measures would differ in quality from lower-layer measures. Available data do not yield evidence of such differences (repeated measures analysis $F_{2,\ 13} = 1.27$, $p = 0.3126$). Assuming that layers are in fact similar to each other, averaging LMR values will give more reliable results than will readings from any single layer. It may still be that M_R values at one level of the soil are particularly important for highway considerations, but it is not possible with available data to select one layer over another without additional reference criteria.

Relationships Between Back-Calculated and Laboratory M_R Values

M_R values can be obtained indirectly, via back calculations from nondestructive testing instead of laboratory tests. As mentioned earlier, the following three back-calculation programs were used in this research: MODULUS (MP), EVERCALC (EP), and BOUSDEF (BP). To consider the quality of these three programs, logs of back-calculated values (designated as LMR-MP, LMR-EP, and LMR-BP, respectively) were compared with laboratory LMR values. The site-by-period mean LMR from undisturbed samples measured on the actuator was used as the best available value for the "true" resilient modulus, the one exception being a single site for which only ring measurements were available in Period A. Because means were calculated from different numbers of observations, a weighted analysis was used (weight = sample size). Results are shown in Table 5. Note that the EVERCALC program appears to be slightly superior to the other two back-calculation methods. All back-calculated values match each other better than they do the laboratory measurements.

Assuming constant differences between logs of back-calculated and "true" values, the best estimated differences appear in Table 6, along with implied relationships between laboratory and back-calculated values of M_R. A 95 percent confidence interval for the appropriate correction factor (C) for subgrade soils in Wyoming, based on the EVERCALC program, is (0.20, 0.32) where $M_R = C*$ (back calculated value).

Relationship Between M_R Values and Soil Properties

The final question considered was the relationship between soil characteristics and the resilient modulus. The possible relationship between LMR and four factors, moisture (actual water content − optimum water content), soil classification, group index, and plasticity index were analyzed. Because the group and plasticity indices were highly correlated, only the group index was ultimately considered for describing soil–M_R relationships.

TABLE 4 Relations Between LMRR[1] and LMRA[2]

	Correlation	Mean Diff.	t	df	p-value
Period A[3]	0.858	0.0987	2.94	17	0.009
Period B[4]	0.906	0.1576	5.11	22	<0.0001
Pooled	0.885	0.1317	5.75	40	<0.0001

[1]Log_{10} (Resilient Modulus Value for Ring Measurements)

[2]Log_{10} (Resilient Modulus Value for Actuator Measurements)

[3]Summer of 1992

[4]Spring of 1993

TABLE 5 Back Calculation Correlations (N = 13)

	Weighted Correlations with LMR[1]	Cross-correlations		
		LMR-MP	LMR-EP	LMR-BP
LMR-MP[2]	0.526	1.000	0.744	0.941
LMR-EP[3]	0.735	0.744	1.000	0.799
LMR-BP[4]	0.590	0.941	0.799	1.000

[1]Log_{10} (Resilient Modulus Values)

[2]Log_{10} (Resilient Modulus Values from MODULUS Program)

[3]Log_{10} (Resilient Modulus Values from EVERCALC Program)

[4]Log_{10} (Resilient Modulus Values from BOUSDEF Program)

Moisture and LMR are related, and their relationship depends on soil type. Similar strengths in the relationship between soil factors and responses were found for both undisturbed and remolded samples, and also for R-values (see Table 7). All of the test sections had one or more of the following types of subgrade soil: A-4, A-6, and A-7. For each of these soil classifications correlations were developed to determine the effect of moisture on the measured values. Overall values for undisturbed and remolded M_R values and R-values from A-4 and A-6 soils decreased as water content increased. The A-7 subgrade soils showed little change in the measured values (see Table 8).

CONCLUSIONS AND RECOMMENDATIONS

On the basis of data analysis performed in this project, the following conclusions are drawn:

1. Layers within Shelby tubes do not differ significantly from one another. Averaging the resilient modulus values from all layers will give more reliable results than measuring the value from one layer.
2. Some fundamental soil properties influence the measured M_R value. Resilient modulus values for type A-4 and A-6 subgrade soils decreased as water content increased.

TABLE 6 Back Calculation Relationships (N = 13)

Computer Program	Diff.	Standard Error	95% CI	Relation	Bounds on C (M_R = C * [X])
MODULUS (MP)	0.408	0.073	(0.249, 0.567)	M_R = 0.39MP	(0.27, 0.56)
EVERCALC (EP)	0.599	0.049	(0.492, 0.706)	M_R = 0.25EP	(0.20, 0.32)
BOUSDEF (BP)	0.503	0.059	(0.374, 0.632)	M_R = 0.31BP	(0.23, 0.42)

TABLE 7 Coefficients of Determination for Soil–M_R Relations

Models (linear models with interaction)	Undisturbed samples LMR[1]	Remolded samples LMR[1]	R-value
Moisture and Soil Classification	0.427	0.436	0.478
Moisture and Group Index	0.479	0.286	0.321

[1]Log_{10} (Resilient Modulus Values)

TABLE 8 Parameter Estimates ± Standard Error for Model with Group Index

Soil Classification	Parameter Estimates	Undisturbed Samples LMR[1]	Remolded Samples LMR[1]	R-value
A-4	Intercept	4.50 ± 0.0740	4.35 ± 0.0893	47.1 ± 1.21
	Slope(Moisture)	-0.102 ± 0.0286	-0.0803 ± 0.0383	-0.845 ± 0.619
A-6	Intercept	4.38 ± 0.0548	4.685 ± 0.0524	37.9 ± 1.96
	Slope(Moisture)	-0.0682 ± 0.0148	-0.0401 ± 0.0162	-2.04 ± 0.570
A-7	Intercept	4.54 ± 0.151	4.73 ± 0.0435	31.0 ± 1.97
	Slope(Moisture)	0.0110 ± 0.0250	-0.00492 ± 0.00699	-0.762 ± 0.316

[1]Log_{10} (Resilient Modulus Values)

3. M_R measurements made with LVDTs on the ring inside the testing chamber consistently gave higher values than the actuator LVDTs located on the loading piston.
4. The EVERCALC back-calculation program appears to give more accurate M_R values than do the other two computer programs.
5. The recommended correction factor (C) of 0.33 or less appears to be adequate for subgrade soils in Wyoming.

ACKNOWLEDGMENTS

This cooperative study was funded by the U.S. DOT's University Transportation Program through the Mountain-Plains Consortium, the Wyoming DOT, and the University of Wyoming. The authors would like to express their appreciation to Benjamin Adkison, Wyoming DOT, for conducting the laboratory tests and Michael Whelan, University of Wyoming, for providing support and advice throughout the study.

REFERENCES

1. *AASHTO Guide for Design of Pavement Structures.* Washington, D.C., 1993.
2. Darter, M. I., R. P. Elliott, and K. T. Hall. *Revision of AASHTO Pavement Overlay Design Procedures, Appendix: Documentation of Design Procedures, Final Report.* Prepared for NCHRP, TRB, National Research Council, Washington, D.C., 1992.
3. Elliott, R. P. Selection of Subgrade Modulus for AASHTO Flexible Pavement Design. In *Transportation Research Record 1354,* TRB, National Research Council, Washington, D.C., 1992.
4. Thompson, M. R., and Q. L. Robnett. *Resilient Properties of Subgrade Soils, Final Report–Data Summary.* Transportation Engineering Series No. 14. Illinois Cooperative Highway Research and Transportation Program Series No. 160. University of Illinois, Urbana-Champaign, 1976.
5. Elfino, M. K., and J. L. Davidson. Modeling Field Moisture in Resilient Moduli Testing. Special Technical Publication *Resilient Moduli of Soils: Laboratory Conditions.* ASCE, 24: 1989.
6. MODULUS: A Microcomputer Based Procedure for Back Calculating Layer Moduli from FWD Data. Cooperative Research Program: TTI, Texas A&M University System, Texas DOT, 1988.
7. *EVERCALC: Pavement Evaluation Program.* Washington State Transportation Center, University of Washington; Washington DOT.
8. Zhou, H., R. G. Hicks, and C. A. Bell. BOUSDEF: A Back Calculation Program for Determining Moduli of a Pavement Structure. In *Transportation Research Record 1260,* TRB, National Research Council, Washington, D.C., 1990.
9. Mahoney, J. P., et al. Pavement Moduli Back Calculation Shortcourse. Presented in Reno, Nev., 1991.
10. Snedecor, G. W., and W. G. Cochran, *Statistical Methods,* 8th ed. Iowa State University Press, Ames, 1989.

Publication of this paper sponsored by Committee on Soil and Rock Properties.

Resilient Modulus of Subgrade Soils: Comparison of Two Constitutive Equations

B. LANKA SANTHA

The concept of resilient modulus has been used to explain the nonlinear stress-strain characteristics of subgrade soils. During the past few decades, several constitutive models have been developed for the resilient modulus of subgrade soils. No stress or deformation analysis can be useful unless a correct constitutive equation that describes the actual behavior of material has been used in the analysis. When the correct form of constitutive equation is selected, there is a need for the accurate k parameters, which vary from soil to soil. Under a Georgia Department of Transportation research project, subgrade soil samples were tested in the laboratory using AASHTO T274–82 to determine their resilient moduli. Results were used to compare two widely used constitutive equations and to study the effect of material and physical properties of subgrade soils on the k values of these equations. Two well-known constitutive equations (bulk stress and universal model) are compared for their capability of modeling granular subgrade soils. This comparison shows that the resilient modulus of granular subgrade soils are better described by the universal model, where resilient modulus is a function of bulk stress and deviator stress. The universal model and the semi-log model, where the resilient modulus is a function of deviator stress, were selected to model granular and cohesive soils, respectively, to study the effect of material and physical properties of subgrade soils on their resilient modulus. Results show that the k parameters in the constitutive equations can be calculated using material and physical properties of the soil, and the values of k parameters vary within wide ranges for cohesive and granular subgrade soils.

In recent years highway engineers have devoted considerable effort to determining the nonlinear stress-strain characteristics of subgrade soils. During the past few decades several constitutive models have been developed and used by pavement design engineers. These developments have provided powerful tools for research and design engineers to conduct pavement analysis in a more realistic manner. However stress or deformation analysis cannot be useful unless a correct constitutive equation that describes the actual behavior of material has been used in the analysis.

Each time a load passes in a pavement structure, the pavement rebounds less than it was deflected under load. After repeated loading and unloading sequences, each layer accumulates only a small amount of permanent deformation, with recoverable or resilient deformation. To explain this behavior, researchers have used the concept of resilient modulus, which can be defined as

$$M_R = \frac{\sigma_d}{\epsilon_R} \tag{1}$$

where

M_R = resilient modulus,
σ_d = repeated deviator stress ($\sigma_1 - \sigma_3$) as defined in Figure 1,
ϵ_R = recoverable axial strain in the direction of principal stress σ_1, and
$\sigma_1, \sigma_2, \sigma_3$ = principal stresses as shown in Figure 1.

Office of Materials and Research, Georgia Department of Transportation, 15 Kennedy Drive, Forest Park, Ga. 30050.

Soil samples collected from 35 test sites throughout Georgia were tested in the laboratory using AASHTO T274–82 to determine their resilient modulus. Four replicate samples were run for each soil. A set of these resilient moduli test data was used in this study.

The objectives of this study were to compare two widely used constitutive equations (bulk stress and universal model) and study the effect of material and physical properties of subgrade soils on k parameters of the constitutive equations.

BACKGROUND

Granular Soils

Research (*1,2*) has shown that the resilient modulus of granular materials increases with increasing confining stress. There are several relationships to describe the nonlinear stress-strain characteristics of granular materials. The following bulk stress model is currently used by most pavement design engineers (*3,4*):

$$M_R = k_1 P_a \left[\frac{\Theta}{P_a}\right]^{k_2} \tag{2}$$

where

M_R = resilient modulus of granular soils,
Θ = bulk stress or first stress invariant ($\sigma_1 + \sigma_2 + \sigma_3$),
$\sigma_1, \sigma_2, \sigma_3$ = principal stresses as shown in Figure 1,
k_1, k_2 = material and physical property parameters, and
P_a = atmospheric pressure, expressed in the same unit as M_R and Θ, used to make the constants independent of the units used.

The main disadvantage of this model is that it does not adequately model the effect of deviator stress. In 1981 May and Witczak (*5*) suggested the following equation to describe the resilient modulus of granular materials:

$$M_R = K_1 k_1 \Theta^{k_2} \tag{3}$$

where K_1 is a function of pavement structure, test load, and developed shear strain, and k_1, k_2 are constants.

In 1985 Uzan (*6*) demonstrated that Equation 2 cannot adequately describe the nonlinear behavior of granular soils. In 1988, he suggested Equation 4 to describe the nonlinear behavior found in repeated load triaxial tests, which was obtained from empirical ob-

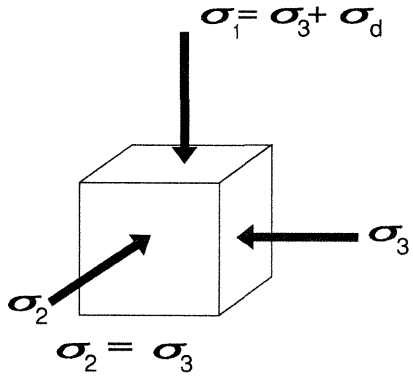

FIGURE 1 Illustration of principal stresses acting on a soil element.

servations. This model includes the influence of deviator stress on resilient modulus.

$$M_R = k_1 P_a \left[\frac{\Theta}{P_a}\right]^{k_2} \left[\frac{\sigma_d}{P_a}\right]^{k_3} \quad (4)$$

where σ_d is deviator stress ($\sigma_1 - \sigma_3$) as defined in Figure 1, and k_1, k_2, k_3 are material and physical property parameters.

In 1987 Lade and Nelson (*7*) presented a constitutive model that shows that modulus of granular materials is a function of the first stress invariant (bulk stress) and the second invariant of the stress deviator tensor. This development provides support for the validity of Equation 4 instead of Equation 2. Brown and Pappin's (*8*) nonlinear stress-strain relationship also agrees with Equation 4 instead of Equation 2.

Cohesive Soils

Sneddon (*9*) conducted resilient modulus tests for sand and fine-grained soils. Results indicated that the resilient modulus of sandy soils is a function of the applied deviator stress and the confining stress. However the resilient modulus of fine-grained soils is mainly a function of the applied deviator stress, when single confining stress level is considered. In general the resilient modulus of these soils decreases with increasing deviator stress. In 1976 Thompson and Robnett (*10*) introduced an arithmetic model (Equation 5) to describe the resilient properties of fine-grained soils. This model was successfully used in the ILLI-PAVE (*11,12*) computer program.

$$M_R = k_2 + k_3 (k_1 - \sigma_d) \qquad k_1 > \sigma_d$$
$$M_R = k_2 + k_4 (\sigma_d - k_1) \qquad k_1 < \sigma_d \quad (5)$$

where

M_R = resilient modulus of the fine-grained soil,
σ_d = deviator stress ($\sigma_1 - \sigma_3$), and
k_1, k_2, k_3, k_4 = material and physical property parameters.

Another successful model often used to describe the behavior of cohesive soils is the semi-log model (Equation 6). This model has the advantage of having fewer material constants than the arithmetic model.

$$M_R = k_1 P_a \left[\frac{\sigma_d}{P_a}\right]^{k_3} \quad (6)$$

As mentioned by Uzan and Scullion (*13*), Equation 4 can be used as a universal model for all types of soils. For a constant modulus or linear elastic material, both k_2 and k_3 are set to zero (*14*). Also the bulk stress model (Equation 2) can be obtained by setting k_3 to zero. The semi-log model (Equation 6) can be obtained by setting k_2 to zero.

LABORATORY TESTS

Subgrade soil samples collected from different locations in Georgia were classified and separated into cohesive and granular categories according to the AASHTO soil classification. Each soil was subjected to laboratory tests such as sieve analysis, Atterberg limits, percent swell and shrinkage, optimum moisture, maximum dry unit weight, and California Bearing Ratio.

Resilient modulus tests were carried out according to the AASHTO T 274–82 (1986) test procedure. The tested samples had a diameter of 73 mm (2.875 in.) and a height of 142.2 mm (5.6 in.) and were statically compacted in three layers. A sample is placed in a triaxial device and subjected to the repetitive loads and stresses expected in a pavement system. These tests were performed on four replicate samples of each soil. One of these samples was compacted to 95 percent compaction; the other three were compacted to 100 percent. The ratio of sample dry unit weight to maximum dry unit weight of soil was taken as the measure of compaction. Low compacted samples had a moisture content of approximately 3 percent above the optimum moisture content. Two of the other three samples had moisture contents approximately 1.5 percent below and 1.5 percent above the optimum moisture. The moisture content of the fourth sample was kept close to optimum. Practical difficulties prevented obtaining the exact intended compactions and moisture contents. The results of the tests were recorded along with the other soil properties.

STUDY DATA

Data used in this study were obtained from a data base created from the aforementioned laboratory test results. To avoid inaccuracies, data were selected according to the following criteria, based on research findings and observations:

1. All soils, fine and coarse grained, that have decreasing resilient modulus with increasing deviator stress at least at lower deviator stresses (*6–8,15,16*).
2. All soils, fine and coarse grained, that have increasing resilient modulus with increasing confining stress (*1,2*).
3. All soils, fine and coarse grained, that have decreasing resilient modulus with increasing moisture content in the vicinity of optimum moisture (*16*) when other soil properties are kept constant.

Fourteen cohesive and 15 granular data sets that satisfied the criteria were used for the study. Some of these soils did not have resilient modulus test results for low-compacted, high-moisture samples. Therefore the resilient modulus test results of low-compacted, high-moisture samples were not included in this study.

DATA ANALYSIS

Granular Soils

The measured resilient moduli values corresponding to confining stresses of 6.89 and 34.45 kPa (1 and 5 psi) and deviator stresses of 13.78, 34.45, 51.68, 68.9, and 103.35 kPa (2, 5, 7.5, 10, and 15 psi) were used to obtain a close representation of stress conditions of the subgrade. These stress conditions and the measured resilient moduli were used to develop relationships for each soil sample in which the resilient modulus is a function of both the bulk stress and the deviator stress. The form of this relationship is given in Equation 4, the universal model, which was transformed to linear form as shown in Equation 7 to carry out linear regressions:

$$\text{Log}(M_R) = \text{Log}(k_1 P_a) + k_2 \text{Log}\left[\frac{\Theta}{P_a}\right] + k_3 \text{Log}\left[\frac{\sigma_d}{P_a}\right] \quad (7)$$

Linear regressions were performed for each set of data and k_1, k_2, and k_3 were found for each soil sample. These developed relationships and the stress conditions of soil samples were then used to back-calculate the resilient moduli for each stress condition of each soil sample. These resilient moduli values were referred to as the predicted resilient moduli. Atmospheric pressure used in these analyses was 101.3 kPa (14.7 psi). The same data were used to develop relationships for each soil sample in which the resilient modulus is a function of bulk stress. The form of this relationship is given in Equation 2, the bulk stress model. Equation 8 gives the linear form of the bulk stress model used for regression analysis.

$$\text{Log}(M_R) = \text{Log}(k_1 P_a) + k_2 \text{Log}\left[\frac{\Theta}{P_a}\right] \quad (8)$$

The predicted resilient moduli obtained from the bulk stress model gave a poor correlation to actual resilient moduli (Figure 2). Figure 3 shows a close correlation between predicted resilient moduli obtained from the universal model and the actual resilient moduli. Symbols A, B, C, and D in the figures refer to one, two, three, and four overlapping data points, respectively. The statistics given in Table 1 provide evidence of better predictability in describing behavior of granular soils using the universal model than using the bulk stress model. Fifty percent of the predicted resilient moduli obtained using the bulk stress model were within ±16.6 percent of the actual values, whereas the predicted moduli were within ±5 percent using the universal model. The universal model also provided better predictions than Equation 2 for the 25th, 75th, and 90th percentiles (Table 1). The universal model is therefore more suitable to represent the relationship between resilient modulus and stress levels of granular soils used in this study. The coefficients k_1, k_2, and k_3 obtained from least-square regressions of the universal model for each sample are listed in Table 2 with moisture content (MC), percent saturation (SATU), and compaction (COMP) of the sample. The values of these coefficients were used in further analyses. Table 2 also gives the optimum moisture content (MOIST) of each soil and the ratio of MC and MOIST (MCR).

A multiple regression analysis approach was used to obtain the relationships among k parameters (dependent variables) and other soil properties such as percent passing #40 sieve (S40), percent passing

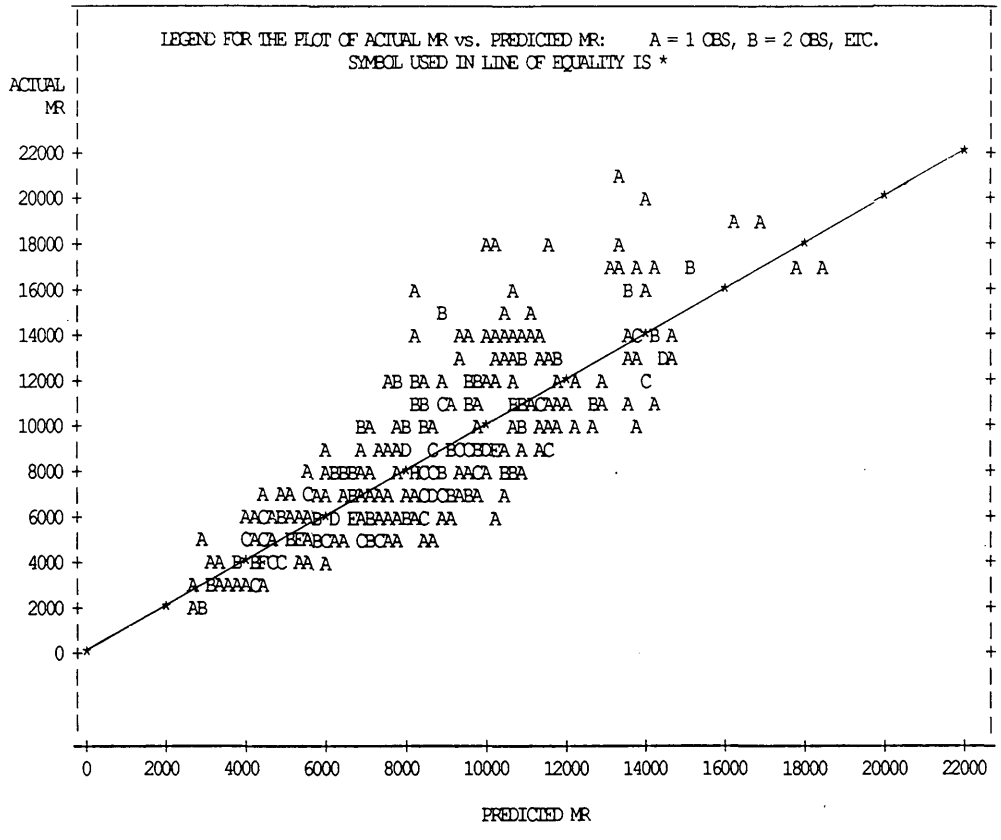

FIGURE 2 Actual resilient moduli versus predicted resilient moduli obtained from bulk stress model.

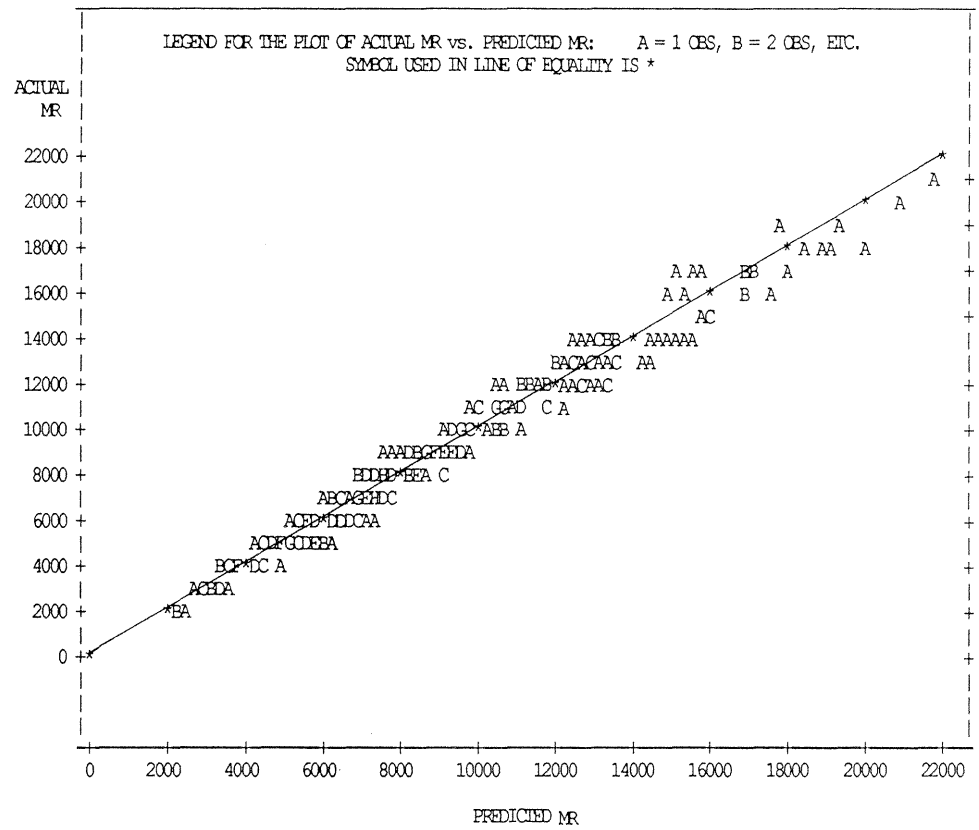

FIGURE 3 Actual resilient moduli versus predicted resilient moduli obtained from universal model.

#60 sieve (S60), percentage of clay (CLY), percentage of silt (SLT), percent swell (SW), percent shrinkage (SH), maximum dry unit weight (DEN), optimum moisture content (MOIST), California Bearing Ratio (CBR), sample moisture content (MC), sample compaction (COMP), and percent saturation (SATU). Table 3 gives the index properties of each soil used for the study. Three separate regression analyses were done for the three coefficients k_1, k_2, and k_3.

To select the best subset of these variables and their interaction terms, The "PROC STEPWISE" procedure in SAS (*17*) was used with maximum R-square improvement technique (MAXR). This regression procedure does not settle on a single model, but tries to find the best one-variable model, the best two-variable model, and so forth. The stepwise procedure with the MAXR method begins by finding the one-variable model producing the highest R^2. Then another variable, the one that yields the greatest increase in R^2, is added. Once the two-variable model is obtained, each variable in the model is compared to each variable not in the model. For each comparison, MAXR determines whether removing one variable and replacing it with the other variable increases R^2. After comparing all possible switches, MAXR makes the switch that produces the largest increase in R^2. By doing this MAXR finds the best two-variable model. Another variable is then added to the model and the comparing and switching process is repeated to find the best three-variable model, and so forth. The number of parameters that correspond to the lowest coefficient of performance value (C_P) was selected to describe the data (*18*). In each model developed, the multicolinearity effect of independent variables was evaluated and interaction terms were selected to minimize the multicolinearity effect.

The difference between the forward or backward stepwise technique and the MAXR technique is that all switches are evaluated before any switch is made in the MAXR method. In the forward or

TABLE 1 Difference in Actual Resilient Moduli and Predicted Resilient Moduli as a Percentage of Actual Resilient Moduli for Granular Soil Data

Percentile	25	50	75	90
Using Equation 2 (Bulk stress model)	9.0	16.6	27.6	35.4
Using Equation 4 (Universal model)	3.0	5.0	7.3	10.4

TABLE 2 Physical Properties of Granular Soil Samples and Their Least-Square Regression Results

ID	MOIST	MC	MCR	COMP	SATU	k_1	k_2	k_3	R^2
1-I	12	11.2	0.93	1.00	80.3	392	0.291	-0.487	0.97
1-II	12	12.5	1.04	1.00	91.0	349	0.316	-0.531	0.89
1-III	12	9.7	0.81	1.00	70.1	543	0.268	-0.402	0.98
2-I	18	17.0	0.94	1.01	78.7	401	0.239	-0.484	0.98
2-II	18	19.5	1.08	0.98	82.6	326	0.328	-0.627	0.93
2-III	18	14.9	0.83	1.02	69.8	715	0.175	-0.330	0.94
3-I	16	16.0	1.00	1.00	91.0	451	0.301	-0.501	0.97
3-II	16	17.4	1.09	1.00	99.4	413	0.316	-0.574	0.94
3-III	16	14.8	0.93	1.00	83.8	642	0.199	-0.403	0.97
4-I	25	24.5	0.98	1.01	82.2	528	0.304	-0.364	0.94
4-II	25	25.9	1.04	1.01	87.0	403	0.318	-0.385	0.84
4-III	25	22.9	0.92	1.01	77.1	703	0.292	-0.259	0.93
5-I	16	15.2	0.95	1.01	78.3	356	0.285	-0.304	0.93
5-II	16	17.0	1.06	1.01	86.8	335	0.293	-0.369	0.90
5-III	16	13.8	0.86	1.01	70.9	547	0.203	-0.213	0.75
6-I	17	15.7	0.92	1.02	80.8	573	0.201	-0.272	0.82
6-II	17	17.2	1.01	1.02	88.5	423	0.250	-0.317	0.83
6-III	17	14.0	0.82	1.02	72.4	832	0.145	-0.152	0.68
7-I	19	19.3	1.02	1.00	81.5	214	0.404	-0.343	0.91
7-II	19	20.6	1.08	1.00	87.2	173	0.412	-0.403	0.98
7-III	19	17.1	0.90	1.03	73.3	299	0.319	-0.351	0.95
8-I	16	15.7	0.98	1.01	80.0	241	0.379	-0.319	0.95
8-II	16	17.0	1.06	1.01	86.7	211	0.441	-0.340	0.92
8-III	16	14.0	0.88	1.01	71.3	284	0.295	-0.292	0.91
9-I	11	13.4	1.22	0.99	69.3	280	0.328	-0.336	0.90
9-II	11	14.3	1.30	0.99	78.8	252	0.349	-0.322	0.94
9-III	11	11.1	1.01	1.00	61.6	324	0.267	-0.301	0.91
10-I	16	15.7	0.98	1.01	71.5	430	0.457	-0.340	0.95
10-II	16	16.6	1.04	1.01	76.8	338	0.479	-0.373	0.90
10-III	16	13.4	0.84	1.01	62.2	534	0.368	-0.298	0.91
11-I	14	13.1	0.94	1.01	70.2	458	0.401	-0.353	0.96
11-II	14	14.4	1.03	1.01	78.7	384	0.444	-0.385	0.89
11-III	14	11.6	0.83	1.02	63.0	573	0.345	-0.294	0.94
12-I	14	13.6	0.97	1.01	78.3	668	0.398	-0.302	0.94
12-II	14	15.2	1.09	1.00	87.2	494	0.469	-0.363	0.94
12-III	14	12.1	0.86	1.01	69.7	918	0.326	-0.159	0.93
13-I	12	11.5	0.96	0.99	66.6	354	0.484	-0.403	0.95
13-II	12	12.7	1.06	0.99	74.4	334	0.498	-0.459	0.90
13-III	12	9.8	0.82	0.99	57.3	446	0.436	-0.367	0.94
14-I	16	14.7	0.92	1.01	70.5	440	0.429	-0.382	0.95
14-II	16	16.3	1.02	1.01	78.1	346	0.454	-0.446	0.90
14-III	16	13.4	0.84	1.01	64.1	507	0.397	-0.330	0.96
15-I	20	19.8	0.99	1.01	76.4	183	0.400	-0.450	0.89
15-II	20	21.4	1.07	1.01	82.4	130	0.430	-0.451	0.90
15-III	20	18.2	0.91	1.01	70.3	201	0.342	-0.437	0.93

backward stepwise method, the worst variable may be removed without considering what adding the best remaining variable might accomplish. The MAXR method could require much more computer time than the stepwise method.

Cohesive Soils

The measured resilient moduli values corresponding to the confining stress of 20.67 kPa (3 psi) and the deviator stresses of 13.78, 27.56, 55.12, and 68.9 kPa (2, 4, 8, and 10 psi) were used to obtain a close representation of stress conditions of subgrade. The stress conditions and the measured resilient moduli were used to develop relationships in which the resilient modulus is a function of deviator stress. The form of this relationship is given in Equation 6, the deviator stress model, which was transformed into the following linear form to carry out linear regressions:

$$\text{Log}(M_R) = \text{Log}(k_1 P_a) + k_3 \text{Log}\left[\frac{\sigma_d}{P_a}\right] \quad (9)$$

TABLE 3 Index Properties of Granular Soils

ID	SLT	CLY	CBR	SW	SH	S40	DEN
1	8	22	2.5	4	4	72	121
2	9	16	4.4	13	2	50	108
3	8	13	8.7	19	2	38	113
4	19	52	8.1	7	4	96	92
5	13	23	2.5	15	7	69	108
6	9	32	4.7	7	10	75	108
7	15	23	4.3	19	2	82	103
8	12	17	9.8	24	1	68	110
9	8	15	2.8	20	4	68	114
10	28	27	4.7	18	2	97	106
11	21	26	8.1	17	2	99	111
12	12	22	2.5	4	2	71	112
13	13	19	13.5	13	3	69	114
14	19	24	13.0	12	4	98	107
15	3	16	32.4	1	0	50	123

Linear regressions were performed for each set of data and k_1 and k_3 were found for each cohesive soil sample. Atmospheric pressure of 101.3 kPa (14.7 psi) was also used. The coefficients k_1 and k_3 that were obtained from least-square regressions of the deviator stress model for each sample are listed in Table 4 with sample MC, SATU, and COMP of the samples.

The multiple regression analysis approach, described in the discussion of granular soils, was used to obtain relationships for k_1 and k_3. In these regressions, the independent variable CBR, which was used in granular soil regressions, was replaced by liquid limit (LL) and plasticity index (PI). Table 5 gives the index properties of each soil used for the study.

RESULTS

Granular Soils

Table 6 presents the descriptive statistics of the k values. Mean and median of each k value were close. Mean, maximum, and minimum values of k_1 were 421, 918, and 130, respectively. These results show that the k values of granular soils are subject to a great degree of variability. Equations 10–12 represent the regression equations found for k_1, k_2, and k_3, respectively, from the multiple regression procedure. Complete regression results, including analysis of variance tables, are given in the Georgia Department of Transportation Special Report 91001 (*19*).

$$\text{Log}(k_1) = 3.479 - 0.07 * MC + 0.24 * MCR + 3.681 * COMP + 0.011 * SLT + 0.006 * CLY - 0.025 * SW - 0.039 * DEN + 0.004 * (SW^2/CLY) + 0.003 * (DEN^2/S40) \qquad R^2 = 0.94 \qquad (10)$$

$$k_2 = 6.044 - 0.053 * MOIST - 2.076 * COMP + 0.0053 * SATU - 0.0056 * CLY + 0.0088 * SW - 0.0069 * SH - 0.027 * DEN + 0.012 * CBR + 0.003 * \{(SW^2/CLY)\} - 0.31 * (SW + SH)/CLY \qquad R^2 = 0.96 \qquad (11)$$

$$k_3 = 3.752 - 0.068 * MC + 0.309 * MCR - 0.006 * SLT + 0.0053 * CLY + 0.026 * SH - 0.033 * DEN - 0.0009 * (SW^2/CLY) + 0.00004 * (SATU^2/SH) - 0.0026 * (CBR * SH) \qquad R^2 = 0.87 \qquad (12)$$

The success of multiple regression analysis to obtain relationships for k_1, k_2, and k_3 is shown in Figures 4–6. Actual material and physical properties of soils (given in Tables 2 and 3) were used to calculate k_1, k_2, and k_3 from Equations 10–12, respectively. These k values were labeled as predicted k values. The plots of predicted k values against actual k values with the line of equality clearly indicate the good fit of the regressions. The coefficients of determination for each regression (also given in the figures) were 0.94, 0.96, and 0.87 for k_1, k_2, and k_3, respectively.

As a measure of model evaluation, predicted k values and the stress levels were used to back-calculate the resilient moduli values using the universal model. These resilient moduli values were labeled as predicted resilient moduli values. These predicted resilient moduli values versus actual laboratory-observed resilient moduli values and the line of equality are shown in Figure 7. This plot shows a close correlation between actual and predicted resilient moduli values.

The descriptive statistics for the actual and predicted resilient moduli values show that 50 percent of the predicted resilient moduli values were within ±8 percent of actual values. They also show that 25 percent, 75 percent, and 90 percent of the predicted values were within ±4 percent, ±15 percent, and ±21 percent of the actual values, respectively. Thus these results show that for granular soils the k parameters of Equation 4 have a direct relationship to material and physical properties of each soil.

Cohesive Soils

Table 7 gives the descriptive statistics of the k values. Mean and median of each k value were very close. Mean, maximum, minimum, and standard deviation of k_1 were 645, 1263, 188, and 252, respectively. These results show that the k values of cohesive soils are also

TABLE 4 Physical Properties of Cohesive Soil Samples and Their Least-Square Regression Results

ID	MOIST	MC	MCR	COMP	SATU	k_1	k_3	R^2
1-I	20	19.2	0.96	1.01	89.3	382	-0.466	0.94
1-II	20	21.7	1.09	1.00	98.7	287	-0.478	0.97
1-III	20	18.4	0.92	1.01	84.3	574	-0.322	0.89
2-I	20	20.2	1.01	1.00	93.0	276	-0.511	0.98
2-II	20	20.8	1.04	1.01	97.7	188	-0.598	0.98
2-III	20	17.5	0.88	1.01	82.7	450	-0.368	0.96
3-I	20	19.9	1.00	1.00	86.3	657	-0.188	0.80
3-II	20	21.1	1.06	1.00	92.1	431	-0.261	0.80
3-III	20	18.1	0.91	1.00	79.0	745	-0.128	0.51
4-I	19	18.1	0.95	1.00	88.7	608	-0.264	0.95
4-II	19	19.9	1.05	1.00	96.8	423	-0.272	0.97
4-III	19	16.4	0.86	1.00	80.8	774	-0.251	0.88
5-I	20	19.2	0.96	1.00	89.5	641	-0.219	0.99
5-II	20	20.6	1.03	1.00	96.1	442	-0.312	0.90
5-III	20	17.7	0.89	1.00	82.6	657	-0.134	0.78
6-I	17	16.6	0.98	1.00	85.0	777	-0.169	0.71
6-II	17	18.2	1.07	1.00	93.1	473	-0.235	0.74
6-III	17	14.6	0.86	1.01	75.1	913	-0.079	0.70
7-I	19	18.4	0.97	1.01	84.8	651	-0.273	0.94
7-II	19	19.1	1.01	1.01	89.2	549	-0.260	0.90
7-III	19	16.6	0.87	1.01	76.6	943	-0.136	0.98
8-I	18	17.7	0.98	1.01	85.0	460	-0.323	0.90
8-II	18	18.6	1.03	1.01	90.7	299	-0.424	0.97
8-III	18	15.9	0.88	1.01	77.0	599	-0.177	0.78
9-I	15	14.2	0.95	1.00	78.1	650	-0.243	0.93
9-II	15	15.5	1.03	1.00	85.6	474	-0.366	0.97
9-III	15	12.2	0.81	1.01	68.0	823	-0.072	0.97
10-I	16	15.6	0.98	1.01	83.3	917	-0.204	0.98
10-II	16	16.3	1.02	1.01	89.0	685	-0.211	0.90
10-III	16	13.6	0.85	1.01	73.9	1169	-0.074	0.97
11-I	21	20.2	0.96	1.00	77.1	916	-0.184	0.95
11-II	21	21.5	1.02	1.00	90.3	748	-0.216	0.84
11-III	21	18.5	0.88	1.01	77.8	1263	-0.090	0.99
12-I	16	15.5	0.97	1.01	83.1	541	-0.414	0.89
12-II	16	17.1	1.07	1.01	91.3	310	-0.501	0.98
12-III	16	13.6	0.85	1.01	73.7	808	-0.274	0.86
13-I	18	19.1	1.06	0.99	83.0	967	-0.109	0.89
13-II	18	20.5	1.14	0.99	89.1	734	-0.176	0.82
13-III	18	17.7	0.98	0.99	76.8	1181	-0.068	0.98
14-I	22	19.9	0.90	1.02	82.5	560	-0.221	0.91
14-II	22	21.7	0.99	1.02	89.5	442	-0.262	0.93
14-III	22	18.5	0.84	1.02	76.7	691	-0.206	0.95

TABLE 5 Index Properties of Cohesive Soils

ID	SLT	CLY	LL	PI	SW	SH	S40	DEN
1	14	52	40.3	20.9	3	9	79	105
2	11	29	35	10.8	5	7	67	107
3	14	55	38.9	19.2	3	11	90	106
4	10	36	36	17.5	6	8	84	108
5	43	39	40.5	17.8	13	8	89	106
6	6	32	46.5	30.4	10	12	88	109
7	11	39	43	18	7	5	73	104
8	14	31	40	13.1	16	7	72	107
9	10	27	33	11.3	17	4	64	112
10	12	32	49	32	9	10	95	111
11	10	51	59	18	3	14	83	103
12	11	31	30	12	7	4	50	110
13	7	40	34	14	2	5	87	111
14	10	43	39	14	3	1	95	101

TABLE 6 Mean, Median, Standard Deviation, Maximum, and Minimum of k Values of Granular Soils

	Samples	Mean	Median	Std.Dev.	Maximum	Minimum
k_1	45	421	401	173	918	130
k_2	45	0.34	0.33	0.089	0.50	0.15
k_3	45	-0.37	-0.36	0.095	-0.15	-0.63

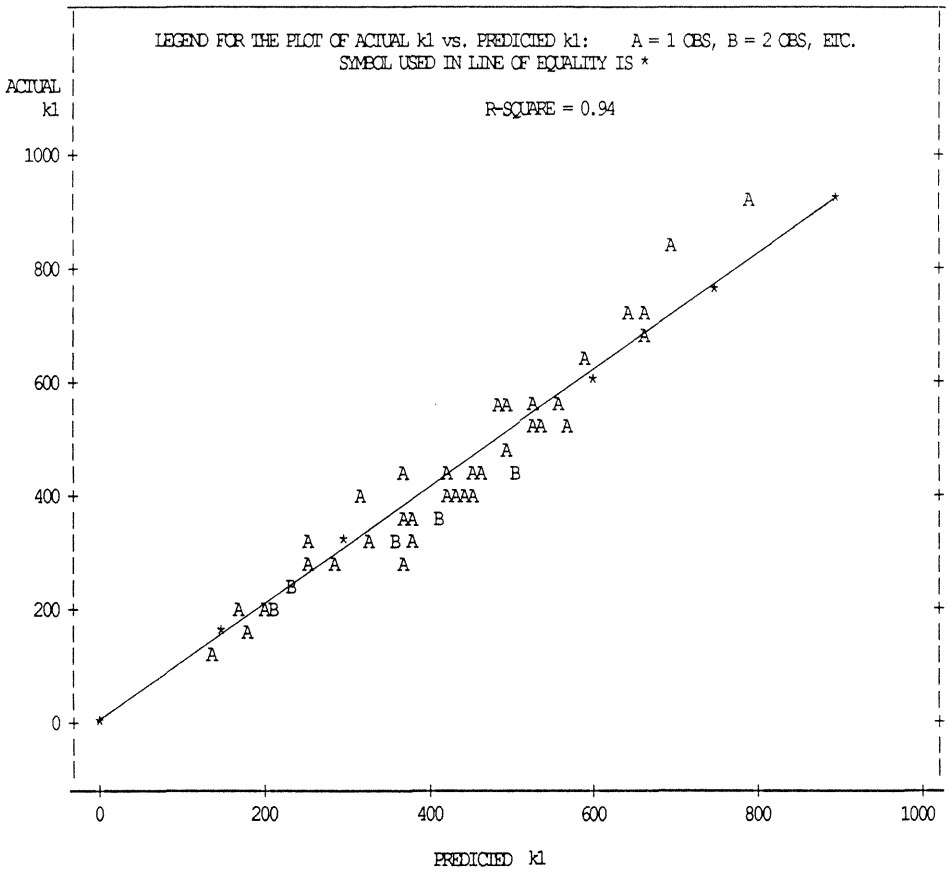

FIGURE 4 Actual k_1 versus predicted k_1 for granular soils.

subject to a great degree of variability. Equations 13 and 14 represent the regression equations found for k_1 and k_3, respectively, from the multiple regression procedure. Complete regression results, including analysis of variance table are presented elsewhere (*19*). Results of an evaluation of the success of multiple regression analysis to obtain the relationships between k_1 and k_3 are shown in Figures 8 and 9. Actual material and physical properties of soils (given in Tables 4 and 5) were used to calculate k_1 and k_3 from Equations 13 and 14, respectively. These k values were labeled as predicted k values. The plots of predicted k values against actual k values show the effectiveness of the regressions. The coefficients of determination for each regression (also given in the figures) are 0.95 and 0.88 for k_1 and k_3, respectively.

$$\text{Log}(k_1) = 19.813 - 0.045 * MOIST - 0.131 * MC - 9.171 * COMP + 0037 * SLT + 0.015 * LL - 0.016 * PI - 0.021 * SW - 0.052 * DEN + 0.00001 * (S40 * SATU) \qquad R^2 = 0.95 \tag{13}$$

$$k_3 = 10.274 - 0.097 * MOIST - 1.06 * MCR - 3.471 * COMP + 0.0088 * S40 - 0.0087 * PI + 0.014 * SH - 0.046 * DEN \qquad R^2 = 0.88 \tag{14}$$

As a measure of model evaluation, predicted k values and the stress levels of soil samples were used to back-calculate the resilient

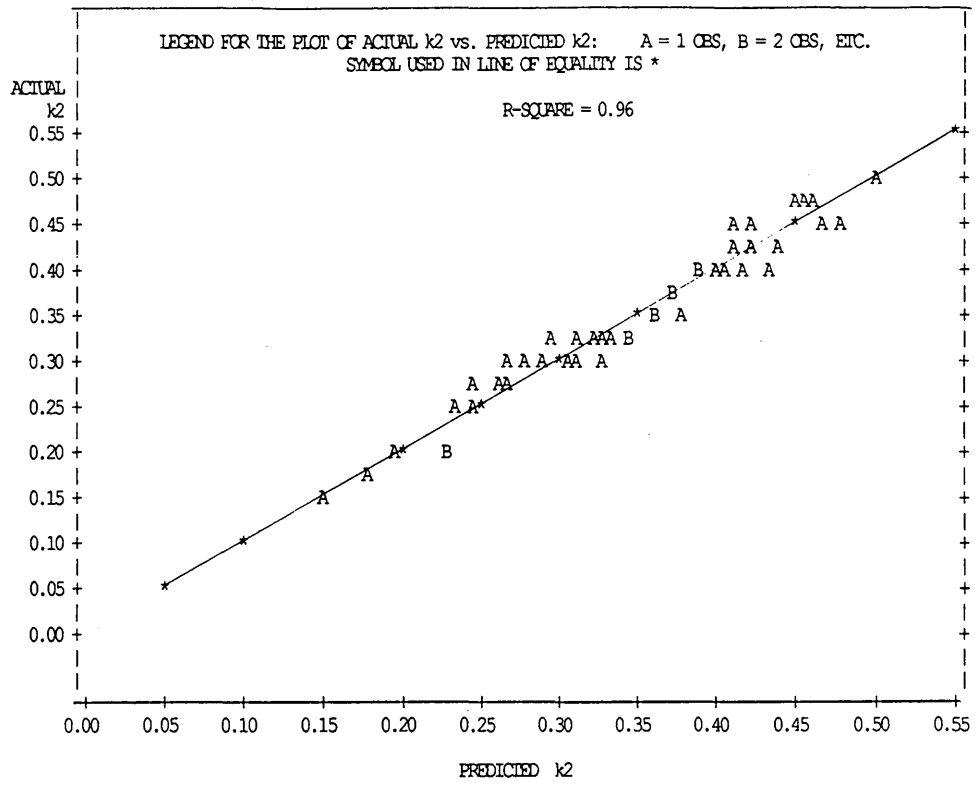

FIGURE 5 Actual k_2 versus predicted k_2 for granular soils.

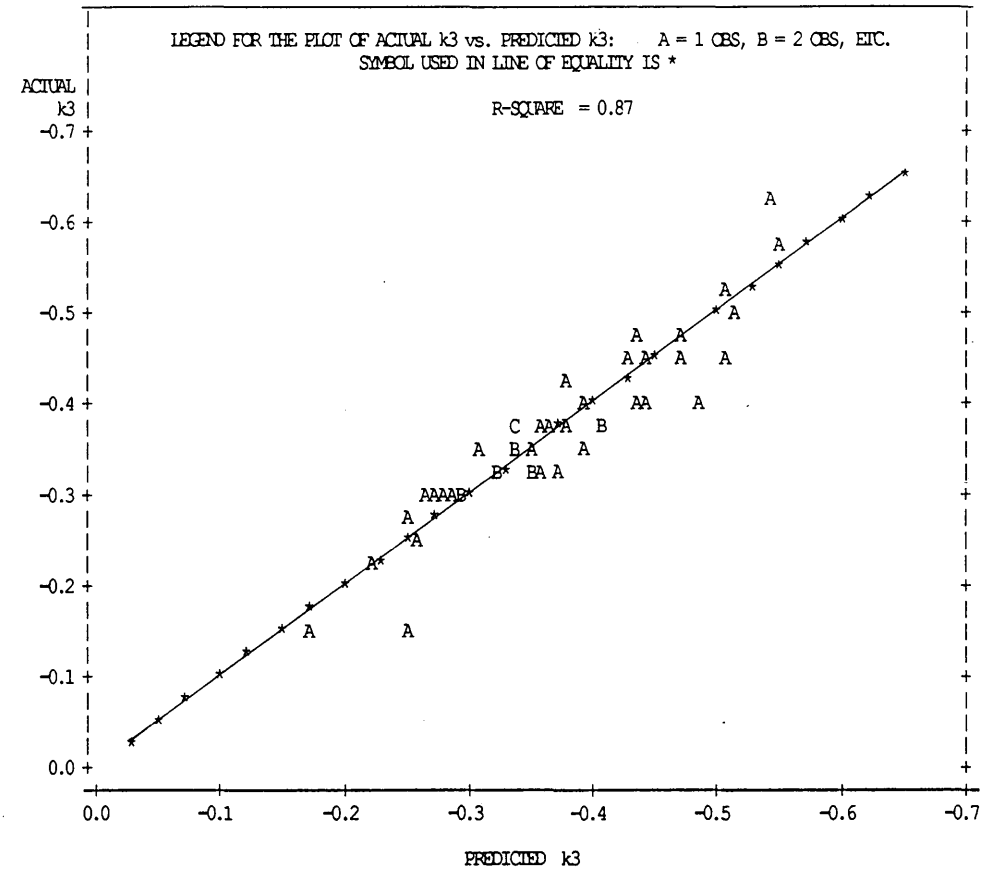

FIGURE 6 Actual k_3 versus predicted k_3 for granular soils.

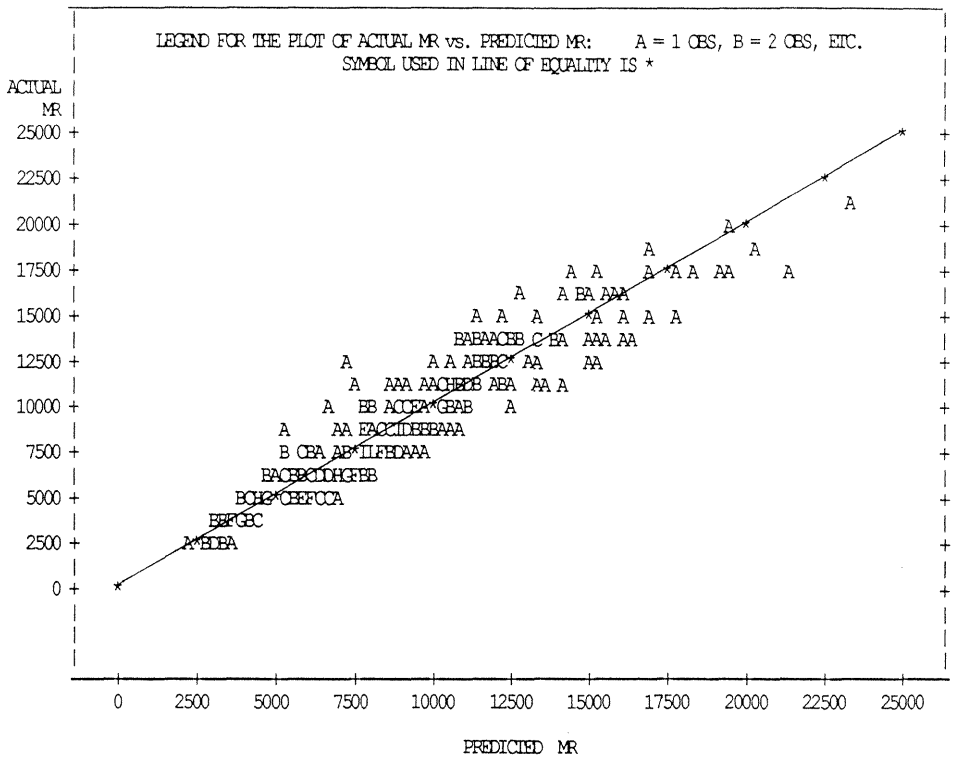

FIGURE 7 Actual resilient moduli versus predicted resilient moduli for granular soils.

moduli values using the deviator stress model. These values, named as predicted resilient moduli values, and the line of equality are shown in Figure 10. This plot shows a close correlation between actual and predicted resilient moduli values.

The descriptive statistics for actual and predicted resilient moduli values show that 50 percent of the predicted resilient moduli values were within ±7 percent of actual values. They also show that 25 percent, 75 percent, and 90 percent of the predicted values were within ±3 percent, ±11 percent, and ±18 percent of the actual values, respectively. Thus these results show that the k parameters of Equation 6 have a direct relation to the material and physical properties of each soil.

CONCLUSIONS AND RECOMMENDATIONS

Conclusions

1. Equation 4 (the universal model) is capable of describing the behavior of granular soils better than Equation 2 (the bulk stress model).
2. Both granular and cohesive soils have a wide spread in their k parameters. These k parameters depend on the material and physical properties of soil.

Recommendations

1. When a complete data base of resilient modulus test results and material and physical properties of soils is available, it is possible to develop a regression model to predict resilient modulus.
2. The universal model is recommended for use with cohesive soils if the model development data have more than one confining stress level.
3. It is important to omit any incorrect data from the data base.

ACKNOWLEDGMENTS

The data used for this study were obtained from Georgia Department of Transportation (DOT) Research Project 8801, sponsored by FHWA. The author would like to express his sincere appreciation

TABLE 7 Mean, Median, Standard Deviation, Maximum, and Minimum k Values of Cohesive Soils

	Samples	Mean	Median	Std.Dev.	Maximum	Minimum
k_1	42	645	645	252	1263	188
k_3	42	-0.26	-0.24	0.13	-0.07	-0.60

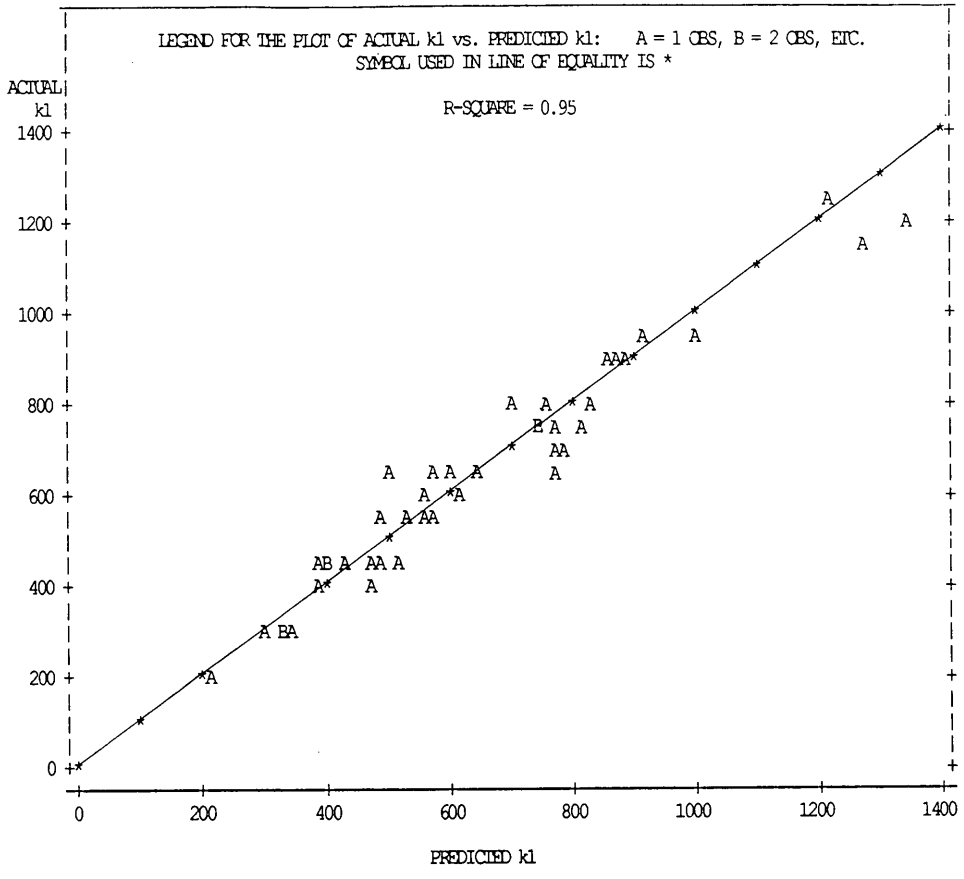

FIGURE 8 Actual k_1 versus predicted k_1 for cohesive soils.

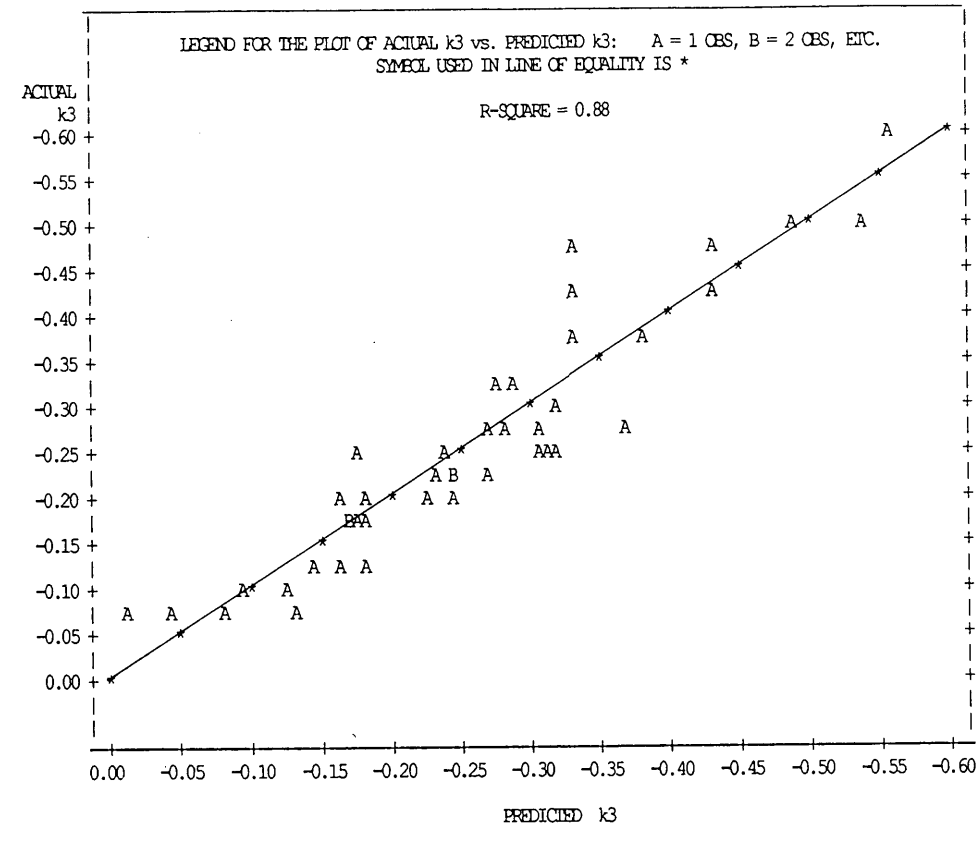

FIGURE 9 Actual k_3 versus predicted k_3 for cohesive soils.

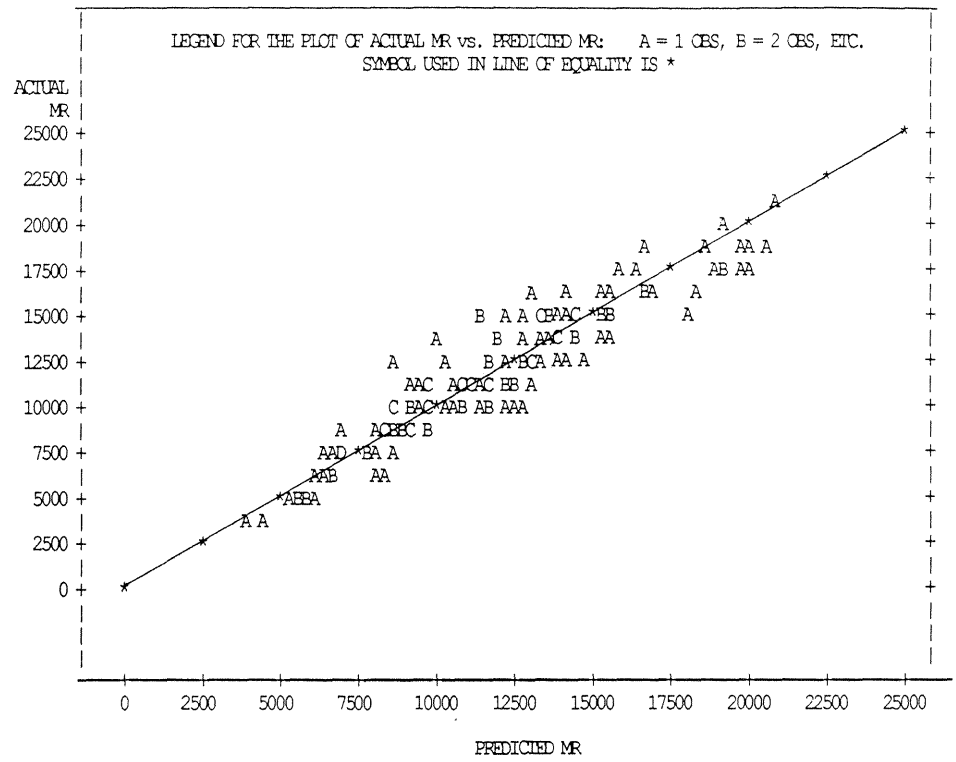

FIGURE 10 Actual resilient moduli versus predicted resilient moduli for cohesive soils.

for this support. The author gratefully acknowledges the assistance and encouragement given by Wouter Gulden, Lamar Caylor, Steve Valdez, Gerald Bailey, and staff of the Office of Materials and Research of Georgia DOT.

REFERENCES

1. Witczak, M. H., and J. Uzan. *The Universal Airport Design System, Report I of IV: Granular Material Characterization.* Department of Civil Engineering, University of Maryland, College Park, 1988.
2. Barksdale, R. D. *Repeated Load Testing Evaluation of Base Course Materials.* GHD Research Project 7002, Final Report. FHWA, U.S. Department of Transportation, 1972.
3. Hicks, R. G., and C. L. Monismith. Factors Influencing the Resilient Response of Granular Materials. In *Highway Research Record 345,* HRB, National Research Council, Washington, D.C., 1971.
4. Shook, J. F., F. N. Finn, M. W. Witczak, and C. L. Monismith. Thickness Design of Asphalt Pavement—The Asphalt Institute Method. Presented at 5th International Conference on the Structural Design of Asphalt Pavements, Delft, The Netherlands, 1982.
5. May, R. W., and M. W. Witczak. Effective Granular Modulus to Model Pavement Responses. In *Transportation Research Record 810,* TRB, National Research Council, Washington, D.C., 1981, pp. 1–9.
6. Uzan, J. Characterization of Granular Materials. In *Transportation Research Record 1022,* TRB, National Research Council, Washington, D.C., 1985, pp. 52–59.
7. Lade, P. V., and R. B. Nelson. Modelling the Elastic Behavior of Granular Materials. *International Journal for Numerical and Analytical Methods in Geomechanics,* Vol. 11, No. 5, Sept.-Oct. 1987, pp. 521–542.
8. Brown, S. F., and J. W. Pappin. Analysis of Pavement with Granular Bases, Layered Pavement System. In *Transportation Research Record 810,* TRB, National Research Council, Washington, D.C., 1981, pp. 17–23.
9. Sneddon, R. V. *Resilient Modulus Testing of 14 Nebraska Soils.* Research Project RESI (0099). University of Nebraska, Lincoln, 1988.
10. Thompson, M. R., and Q. L. Robnett. Resilient Properties of Subgrade Soil. *Transportation Engineer Journal,* Jan. 1979, pp. 1–89.
11. Figueroa, J. L., and M. R. Thompson. Simplified Structural Analysis of Flexible Pavements for Secondary Roads Based on ILLI-PAVE. In *Transportation Research Record 776,* TRB, National Research Council, Washington, D.C., 1980, pp. 5–10.
12. *ILLI-PAVE User's Manual.* Transportation Facilities Group, Department of Civil Engineering, University of Illinois, Urbana-Champaign, May 1982.
13. Uzan, J., and T. Scullion. Verification of Backcalculation Procedures. *Proc., 3rd International Conference on the Bearing Capacity of Roads and Airfields,* Trondheim, Norway, 1990.
14. Rodhe, G. T. *The Mechanistic Analysis of FWD Deflection Data on Sections with Changing Subgrade Stiffness with Depth.* Ph.D. dissertation. Texas A&M University, College Station, 1990.
15. Crockford, W. W., K. M. Chua, W. Yang, and S. K. Rhee. *Response and Performance of Thick Granular Layers.* Draft Interim Report, USAF Contract F08635-87-C-0039. Texas A&M University, College Station, May 1988.
16. Wilson, B. E., S. M. Sargand, G. A. Hazen, and R. Green, Multiaxial Testing of Subgrade. In *Transportation Research Record 1278,* TRB, National Research Council, Washington, D.C., 1990, pp. 91–95.
17. *SAS User's Guide: Statistics.* Version 5 Edition.
18. Neter, J., W. Wasserman, and M. H. Kutner. *Applied Linear Regression Models,* 2nd ed. Richard D. Irwin, Inc., Homewood, Ill., 1989.
19. Santha, B. Lanka. *An Alternative Procedure to Estimate Resilient Modulus of Subgrade Soils Using Their Materials and Physical Properties.* Special Report 91001. Georgia Department of Transportation, 1991.

The views expressed in this paper are those of the author, who is responsible for the facts and accuracy of the data analysis. The contents do not necessarily reflect the official views or policies of Georgia DOT. The paper does not constitute a standard, specification, or regulation.

Publication of this paper sponsored by Committee on Soil and Rock Properties.

Influence of Testing Procedure and LVDT Location on Resilient Modulus of Soils

LOUAY N. MOHAMMAD, ANAND J. PUPPALA, AND PRASAD ALAVILLI

Several transportation agencies use the AASHTO-recommended resilient modulus (M_r) as the fundamental parameter in the mechanistic analysis and design of pavements. At present there are several types of dynamic testing devices calibrated to measure resilient modulus. The repeated triaxial device is popular because of its repeatability, reliability, and ease of operation. Testing procedures and internal deformation measurements play a crucial role in testing. A statistically designed experiment was used to compare the influence of these factors. Two testing procedures, AASHTO T-294-1992 and AASHTO T-292-1991, were evaluated, and two separate measurement systems inside the triaxial cell were used to measure the axial deformations. Both cohesive and granular soils were tested. The influence of testing procedures and measurement systems are presented in the form of normalized factors, which are discussed with respect to the test variables and confining and deviatoric stresses. The testing procedure appears to influence test results for sand specimens, possibly due to the variation in magnitudes of testing stresses. The measurement system has a greater influence on clay specimens due to a combination of several factors such as soil fabric, stress dependency behavior, and end friction effects. The type of soil, testing procedures, and location of the internal, linear variable differential transformers and their influence on the regression model constants are discussed and graphically presented.

In 1986 AASHTO recommended the use of resilient modulus as a fundamental property for characterizing highway materials in the mechanistic design of flexible pavements (*1*). Many state transportation agencies use empirical procedures involving soil support, California bearing ratio, and *R*-values for estimating the resilient modulus. These approaches do not adequately represent the response of pavement materials to the dynamic loading to which they are exposed under actual service conditions. Therefore dynamic testing methods are needed to determine realistic resilient modulus values.

The resilient modulus (M_r) is defined as the ratio of deviatoric stress to recoverable axial strain and is presented in the following equation:

$$M_r = \sigma_d/\epsilon_r \quad (1)$$

where σ_d is the deviatoric stress and ϵ_r is the resilient strain.

Most of the recent research on resilient modulus testing is concentrated on the use of various dynamic testing equipment for determining the resilient modulus (*2,3*), influence of soil characteristics (*3–9*), and instrumentation effects on M_r (*9–16*). This research has contributed significantly to understanding of the resilient properties of soils.

AASHTO has recommended several procedures (T-274, T-292, and T-294) for determining resilient modulus of subgrade soils. The most recent procedure, T-294, is a modification of the old procedures and was published by AASHTO in the interim specifications in 1992 (*17*). Since their introduction, all the above procedures have been subjected to criticism and discussion. For example, many investigators, questioned the need for extensive sample conditioning (*6,11,14*). Their investigations showed that severe conditioning may result in disturbance to the soil sample and sometimes may result in the breaking of samples during testing. However it was reported by Houston et al. (*11*) that conditioning is needed to eliminate the plastic strains before obtaining measurements for determining the resilient modulus. Other reasons for this conditioning are given in the Conditioning and Testing Procedure section of this paper.

The sequence of applying the confining pressure and deviatoric stress to the specimen in AASHTO T-292-1991 has raised many concerns (*12,13*). The new protocol, T-294-1992, is a modified version of the sequence of stresses of T-292-1991. This protocol is more conducive to testing and does not have any sudden jumps in test stresses from one sequence to another. Furthermore some transportation agencies and organizations have adopted their own testing procedures based on investigations conducted on locally available soils (*14*). The procedure influence is investigated by conducting resilient tests on two different soils using two AASHTO procedures (T-292 and T-294).

The location of linear variable differential transformers (LVDTs) on the specimen for resilient displacement measurements is a crucial element in this investigation. Two locations, the middle and the end of the specimen, were selected for this study. The results of the tests using all these variables are presented in the form of coefficients or multipliers.

OBJECTIVE AND SCOPE

The main objective of this paper is to develop an understanding of the influence of AASHTO T-292-1991 and T-294-1992 testing procedures on measured resilient modulus. The testing was conducted on both cohesive and cohesionless soils (A-7 silty clay and A-3 sand). Another objective is to investigate the influence of the location of internal LVDTs on the specimen in measuring the resilient deformations. To achieve these objectives, an extensive resilient modulus testing program was initiated at the Louisiana Transportation Research Center (LTRC). As part of this study, fully automated test software, data acquisition, and equipment control were also developed.

EXPERIMENTAL SETUP

Loading System and Data Acquisition

An MTS model 810 closed-loop servo-hydraulic material testing system was used. The major components of this system are an ana-

Louisiana Transportation Research Center, Louisiana State University, 4101 Gourrier Avenue, Baton Rouge, La. 70808.

log controller, a load frame, a hydraulic actuator, and a function generator. The loading system consists of a load frame and a hydraulic actuator. Fully automated test software for equipment control and data acquisition was developed to perform tests and acquire, analyze, and present data. These units and software are described in detail elsewhere (*13*).

Measurement Systems

In existing testing procedures, LVDTs are placed outside the chamber for measuring displacements. This external measurement system is easy to install and provides a simplified procedure to externally rezero the initial LVDT readings without having to remove the chamber of the cell. However the influence of external LVDT location is significant on M_r results due to the nonuniform strain distributions at the ends, the result of end friction effects as well as instrumental and system compliance errors (*2*). One suggestion is to use internal LVDTs in the place of external LVDTs to minimize these errors (*2*). It should be mentioned that T-294 uses an external LVDT system and T-292 uses both external and internal LVDT systems. However, due to the reasons mentioned, internal LVDT systems were selected for this study. The internal system is subjected to fewer system compliance errors than the externally mounted LVDT system because the internal system is mounted directly on the specimen.

One system is used to measure deformations with respect to ends, whereas the other is used to measure the deformations at the middle one-third of the specimen (Figure 1). These systems are hereafter referred to as end and middle systems, respectively. The LVDTs of the middle system have a full-scale stroke of ±3.05 mm (±0.12 in.) with a nonlinearity of ±0.00762 mm (±0.0003 in.). The LVDTs of the end system have a full-scale stroke of ±6.35 mm (±0.25 in.) with a nonlinearity of ±0.0158 mm (±0.000625 in.).

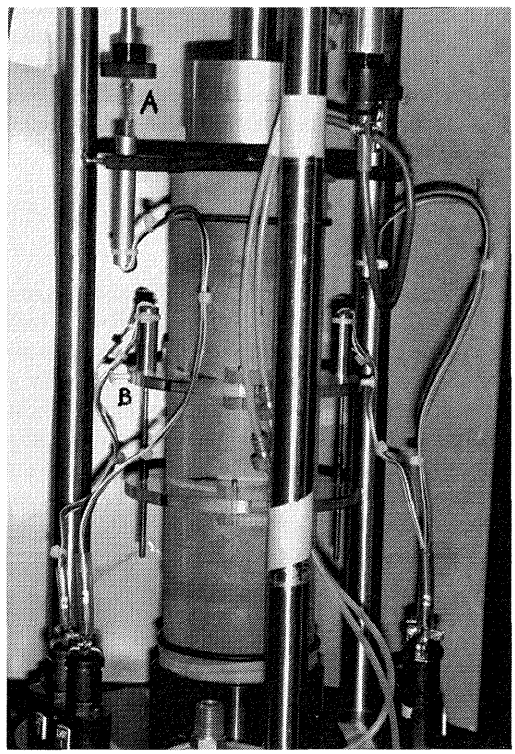

FIGURE 1 Specimen with LVDTs: (*a*) end system and (*b*) middle system.

Specimen Preparation

Tests were conducted on two locally available soils: a blasting sand and a silty clay. Properties of these soils are given in Table 1. Specimens tested were 71.1 mm (2.8 in.) in diameter and 142.2 mm (5.6 in.) in height. This produces a height-to-diameter ratio of 2, which is required in this type of testing to reduce end effects due to friction. Both types of soil specimens were compacted close to the optimum water content–dry density combination.

Quality Assessment and Control

The influence of sample preparation on the target design water content and density was examined for each soil type. No significant difference in densities were observed among samples for each soil type, indicating that similar specimens were tested in each category. For sand specimens, the influence of fine migration due to compaction and testing procedures was examined. After testing, the sand specimen was carefully removed, cut into two slices, and dried for grain size distribution tests. Results of these tests are shown in Figure 2, including the results for untested sand. No significant variation in grain size distributions was observed, indicating that the compaction procedures did not result in any fine migration, layering, or crushing of the aggregates.

The moisture migration check is important for fine-grained cohesive soils because variations in moisture content could result in variations in partial saturation of the specimen. This partial saturation induces suction pressures that cause some confinement, which in turn increases the total strength of the specimen and thereby influences the final M_r values. Moisture migration was therefore checked by measuring the water content of different slices of a freshly prepared silty clay specimen before testing. The moisture content of these slices varies between 20.8 and 21.6 percent, which implies that moisture migration was not present in these samples.

TABLE 1 Properties of Soils Tested

PROPERTY	BLASTING SAND	SILTY CLAY
Specific Gravity, G_s	2 .75	2.6
Optimum Density (kN/m^3)	17.5	16.0
Optimum Moisture Content (%)	12.0	21.2
Plasticity Index (PI)	--	22
AASHTO Classification	A-3	A-7

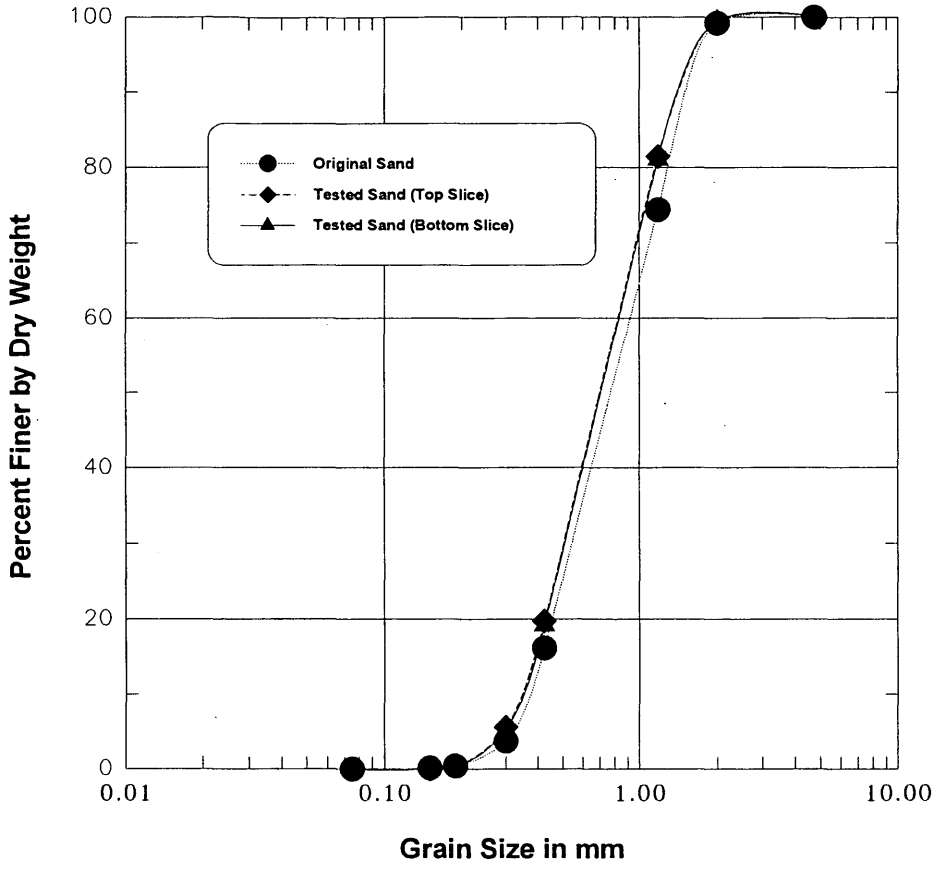

FIGURE 2 Fine migration check in sands.

Conditioning and Testing Procedure

The tests on both soil samples were performed at the confining and deviatoric stress levels recommended in AASHTO T-292-91 and T-294-92. Few additional testing stresses were added to T-294 and T-292 testing sequences for sands. These stresses are selected to fit in between the provided successive testing sequences.

The samples were first conditioned by applying 1,000 repetitions of a specified deviatoric stress. Conditioning eliminates the effects of specimen disturbances due to sampling, compaction, and specimen preparation procedures, and also aids in minimizing the effects of imperfect contacts between end platens and the specimen. Once the conditioning is completed, the specimen is subjected to different stress sequences of confining and deviatoric stresses. One hundred cycles were used for each sequence. The stress sequence was selected to cover the expected in-service range that a pavement or subgrade material experiences as a result of traffic loading.

Figure 3 presents the stress sequences of both AASHTO procedures in the form of bar charts for both soils, representing the maximum amount of deviatoric stress applied to each specimen at each confining pressure. It should be noted that granular soils under T-292 were subjected to a higher variation of stresses in each testing sequence than those under T-294.

Cohesive soil samples were subjected to lower magnitudes of stresses than granular samples. The stress sequence for clays under T-294 shows that they are subjected to a higher confining pressure in the beginning of a testing sequence (42 kPa) and a lower confining pressure in the end (0 kPa). It is well known that this type of phenomenon will cause over-consolidation of the clays and may result in strengthening of the specimen, which may give higher M_r values at lower confining stresses. The stress sequence for clays under T-292 depicts only one set of confining pressure (21 kPa).

All tests were conducted with a haversine-type loading waveform with a peak load equivalent to the specified deviatoric stress. The loading period and the relaxation periods were 0.1 and 0.9, respectively.

EXPERIMENTAL DESIGN

A statistically designed experiment was used to examine the influence of the testing procedure and LVDT location. The number of samples (n) for each soil type can be computed as follows:

$$n = (z_{\alpha/2}\sigma/e)^2 \quad (2)$$

where

$z_{\alpha/2}$ = upper $\alpha/2$ critical value for the standard normal distribution,
σ = population standard deviation, and
e = error in estimation.

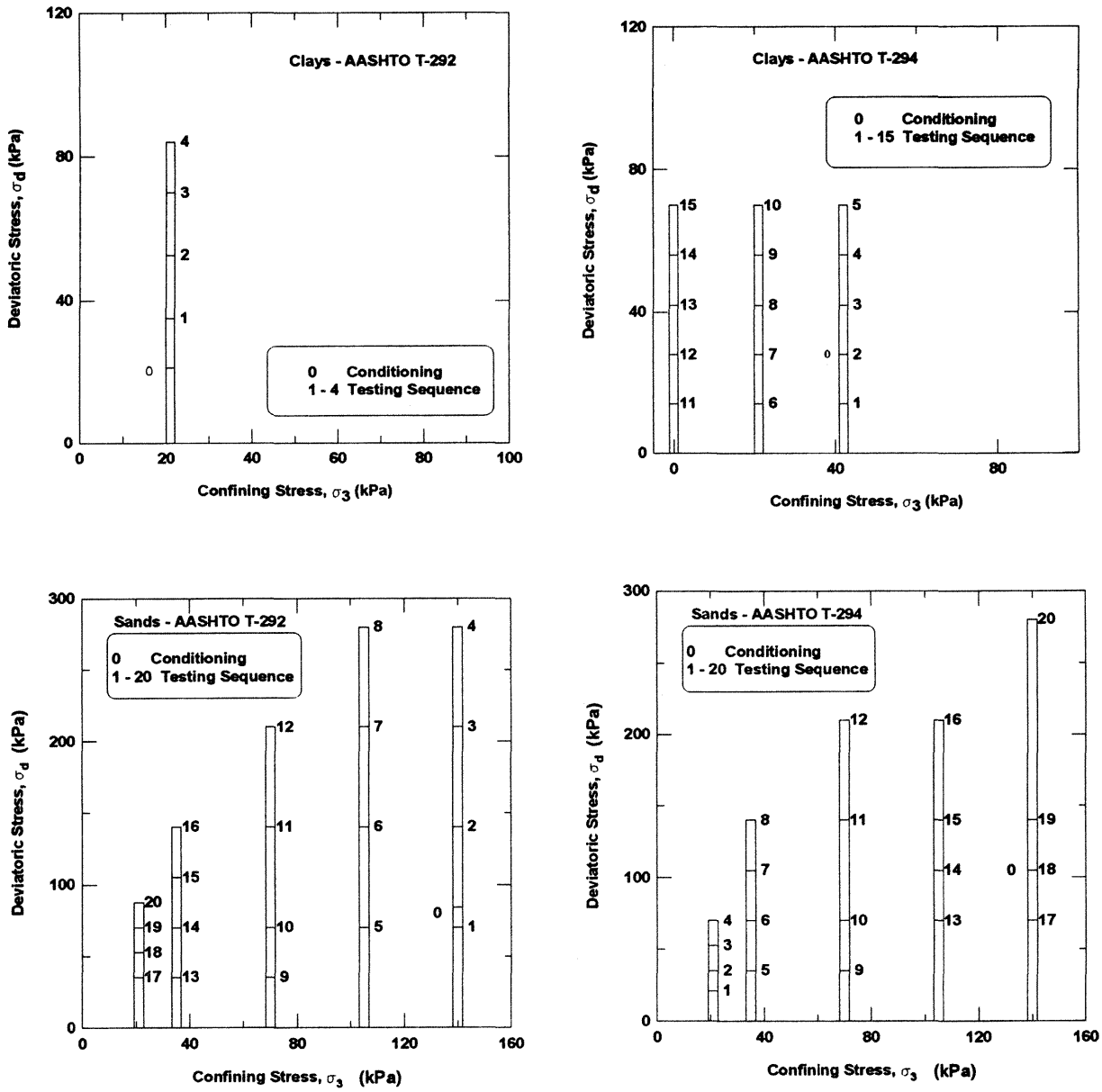

FIGURE 3 AASHTO procedures for sands and clays.

The variables σ and e were initially unknown, and in such a case statisticians have established that a sample size of 30 would define the pattern of the variation of the variable. Thus 30 specimens were used in the preliminary testing phase, which involved testing both soils under the T-292 procedure. The test results were statistically analyzed using the analysis of variance procedure. A multiple comparison procedure with a risk level of 5 percent was performed on the means. The independent variables are assumed to have populations with normal distributions. In addition operator errors are insignificant because all tests were conducted by a single operator. The number of samples for the subsequent testing based on the statistics obtained from the first-phase 30 sample test results total approximately 7, however 10 samples were selected and tested to produce more reliable results.

ANALYSIS OF RESULTS

The test results were analyzed using the analysis of variance procedure provided in the Statistical Analysis System (SAS) program. Tables 2 and 3 present the mean resilient modulus (in MPa) of the test results of sands and silty clay samples, respectively, along with standard deviation (σ), coefficient of variation (C_v), and test repeatability. The coefficient of variation, an indicator of the variation of the results, lies between 0.9 and 10.3 for sands and 5.10 and 24.0 for clays. Even though the range is wider for clays, most of the results have C_v values around 10. These variations are insignificant and therefore the test results are considered repeatable as per ASTM C670. Higher C_v values were obtained for samples tested under T-292 because the samples under T-292 were subjected to a wider

TABLE 2 M_r Results from Blasting Sand

S3	Sd	AASHTO Procedure								AASHTO Procedure							
		T–292				T–294				T–292				T–294			
		MRE	SD	CV	R	MRE	SD	CV	R	MRM	SD	CV	R	MRM	SD	CV	R
21	21					159.2	4.7	3.0	Y					189.0	8.6	4.6	Y
21	35	153.0	8.4	5.5	Y	164.2	6.7	4.1	Y	189.0	12.6	6.7	Y	193.2	10.7	5.5	Y
21	52.5	162.1	10.1	6.2	Y	173.6	5.6	3.3	Y	195.0	11.1	5.7	Y	206.5	6.1	2.9	Y
21	70	168.7	9.7	5.8	Y	180.1	4.3	2.4	Y	200.9	11.6	5.8	Y	212.1	8.7	4.1	Y
21	87.5	173.6	10.9	6.3	Y					205.5	11.9	5.8	Y				
35	42	168.0	9.6	5.7	Y	209.0	4.9	2.4	Y	194.6	12.1	6.2	Y	250.6	10.3	4.1	Y
35	70	183.8	9.6	5.3	Y	220.5	6.1	2.8	Y	217.0	9.5	4.4	Y	259.0	7.4	2.9	Y
35	105	199.5	10.1	5.0	Y	220.5	4.3	2.0	Y	231.7	9.9	4.3	Y	255.5	9.6	3.8	Y
35	140	206.5	12.3	6.0	Y	219.0	3.0	1.4	Y	237.3	13.9	5.8	Y	254.5	11.3	4.4	Y
70	35	226.1	11.9	5.3	Y	283.9	4.8	1.7	Y	269.9	16.6	6.1	Y	345.8	18.7	5.4	Y
70	70	238.0	10.1	4.3	Y	293.3	3.3	1.1	Y	275.8	12.9	4.7	Y	341.6	16.5	4.8	Y
70	140	257.6	10.0	3.9	Y	302.6	3.7	1.2	Y	295.4	11.5	3.9	Y	345.8	12.3	3.6	Y
70	210	274.1	9.6	3.5	Y	295.4	3.0	1.0	Y	309.8	11.8	3.8	Y	336.7	11.0	3.3	Y
105	70	287.0	12.0	4.2	Y	337.6	6.2	1.8	Y	336.7	21.4	6.4	Y	386.4	18.4	4.8	Y
105	105					346.5	4.6	1.3	Y					394.1	16.0	4.1	Y
105	140	304.5	12.4	4.1	Y	353.5	3.7	1.0	Y	347.2	19.3	5.6	Y	399.7	14.3	3.6	Y
105	210	317.8	11.6	3.7	Y	356.3	3.3	0.9	Y	358.4	17.6	4.9	Y	403.2	14.4	3.6	Y
105	280	327.3	10.7	3.3	Y					365.4	14.6	4.0	Y				
140	70	352.5	17.8	5.1	Y	380.8	4.8	1.3	Y	423.5	43.6	10.3	Y	445.9	26.1	5.9	Y
140	105					392.0	4.9	1.2	Y					448.7	23.2	5.2	Y
140	140	366.8	16.5	4.5	Y	396.2	3.3	0.8	Y	424.9	35.2	8.3	Y	456.1	22.4	4.9	Y
140	210	369.6	13.9	3.8	Y					420.0	28.1	6.7	Y				
140	280	372.4	11.8	3.2	Y	406.0	4.4	1.1	Y	417.9	21.9	5.3	Y	465.5	26.6	5.7	Y

S3 : Confining Pressure (in kPa)
Sd : Deviatoric Pressure (in kPa)
MRE : Resilient Modulus from End Measurement System (in MPa)
MRM : Resilient Modulus from Middle Measurement System (in MPa)
SD : Standard Deviation
CV : Coefficient of Variation
R : Repeatability
Y : Indicates Test is Repeatable as per ASTM C670.

variation of stresses from test to test, which might have resulted in some change in the structure of the specimen.

Influence of Testing Stresses

The influence of confining and deviatoric stresses on the moduli of sands and clays is depicted in Figure 4. The trends represented in this figure are similar to those obtained in previous investigations (*5,6,8,11*). Granular materials exhibit an increase in M_r value with an increase in confining and deviatoric stresses. This is attributed to the dilatational characteristics and stiffness properties of the soils (*13*). Higher confining pressures tend to resist the dilatational behavior during shearing, which results in lower axial strain measurements and subsequently higher M_r values. For cohesive materials, however, M_r decreases with an increase in deviatoric stress. This is attributed to the pore pressure development, which increases with an increase in deviatoric stress and also in the number of cycles (*11*). This development of pore pressures results in a decrease in effective stresses and in the overall strength of the specimen. Therefore lower M_r values were obtained.

The traditional break in the curve with deviatoric stress as seen in cohesive specimen results was not observed during this study. Silty clay materials tested have significant strength even under unconfined conditions, and this is probably the reason for clays not displaying the breaking behavior at a certain deviatoric stress.

TABLE 3 M_r Results from Silty Clay

S3	Sd	Measurement System								Test Procedure
		End				Middle				
		MR	SD	CV	R	MR	SD	CV	R	
42	14	243.2	23.0	9.5	Y	293.4	42.2	14.4	Y	
42	28	216.9	14.2	6.5	Y	266.4	26.9	10.1	Y	T-294
42	42	195.9	10.1	5.1	Y	234.9	24.8	10.6	Y	
42	55	179.8	10.1	5.6	Y	214.2	26.1	12.2	Y	
42	69	152.7	10.0	6.1	Y	194.4	27.3	14.1	Y	
21	14	204.3	17.9	8.8	Y	265.9	33.5	12.6	Y	
21	28	186.2	9.9	5.3	Y	244.7	31.6	12.9	Y	T-294
21	42	171.7	11.6	6.8	Y	226.1	28.7	12.7	Y	
21	55	157.7	11.3	7.2	Y	204.5	27.9	13.7	Y	
21	69	145.9	12.5	8.6	Y	187.3	26.0	13.9	Y	
21	35	171.9	17.6	10.2	Y	240.6	57.5	23.9	Y	
21	52	158.4	18.9	11.9	Y	213.5	44.1	20.7	Y	T-292
21	69	141.7	19.6	13.8	Y	180.3	35.2	19.5	Y	
21	86	127.4	19.8	15.5	Y	154.8	31.9	20.6	Y	
0	14	161.5	15.5	9.6	Y	257.2	22.9	8.9	Y	
0	28	141.4	14.6	10.3	Y	223.3	26.8	12.0	Y	
0	42	129.9	13.8	10.6	Y	206.8	23.1	11.2	Y	T-294
0	55	122.4	13.0	10.6	Y	189.1	23.9	12.6	Y	
0	69	116.8	14.6	12.5	Y	172.9	23.9	13.8	Y	

S3 : Confining Pressure (in kPa)
Sd : Deviatoric Pressure (in kPa)
MR : Resilient Modulus (in MPa)
SD : Standard Deviation
CV : Coefficient of Variation
R : Repeatability
Y : Indicates Test is Repeatable as per ASTM C670.

Testing Procedure

The results on both sands and clays are presented in the form of a simplifying normalized factor, termed the procedure coefficient (PC). The PC is defined as the ratio of the M_r value obtained from the AASHTO T-294 procedure to that obtained from the AASHTO T-292 procedure. The T-292 procedure value was taken as the reference value to which the comparisons were made. In other words, the PC values represent the variation of M_r of the T-294 procedure with respect to the same from the T-292 procedure. The PC values for confining and deviatoric stresses are determined for each measurement system.

Figure 5 shows the results for sand specimens using both measurement systems. The PC values are as high as 1.28 at low confining stresses (35 to 105 kPa) and deviatoric stresses (less than 70 kPa) and are reduced to around 1.15 with the increase in these stresses. Both measurement systems produced similar results. At low confining stresses (35 to 105 kPa) and deviatoric stresses (less than 70 kPa), the previous sequence of the testing had a certain influence on the moduli, which resulted in higher PC values. This influence, however, is not observed at higher deviatoric stresses (greater than 70 kPa), which implies that test procedures have only minor influence on M_r values at these stresses. This is probably because the higher deviatoric stresses applied to the specimen will overcome the stress dependency effects due to previous testing stress sequences. Surprisingly for both measurement systems, however, lower PC values with an average value of around 1.08 are observed for the tests conducted at the lowest (21 kPa) and the highest (140 kPa) confining pressures. The lower values at higher confining pressures can be reasoned from the previous explanations, but cannot be explained in the case of lowest confining pressure (21 kPa) results. After additional examinations it can be assumed that one of the reasons for the lower values is that both procedures tested the samples at this confining stress, 21 kPa, either at the end of the testing, as in the case of T-292, or at the beginning, as with T-294, in which this test was preceded by conditioning at a high deviatoric

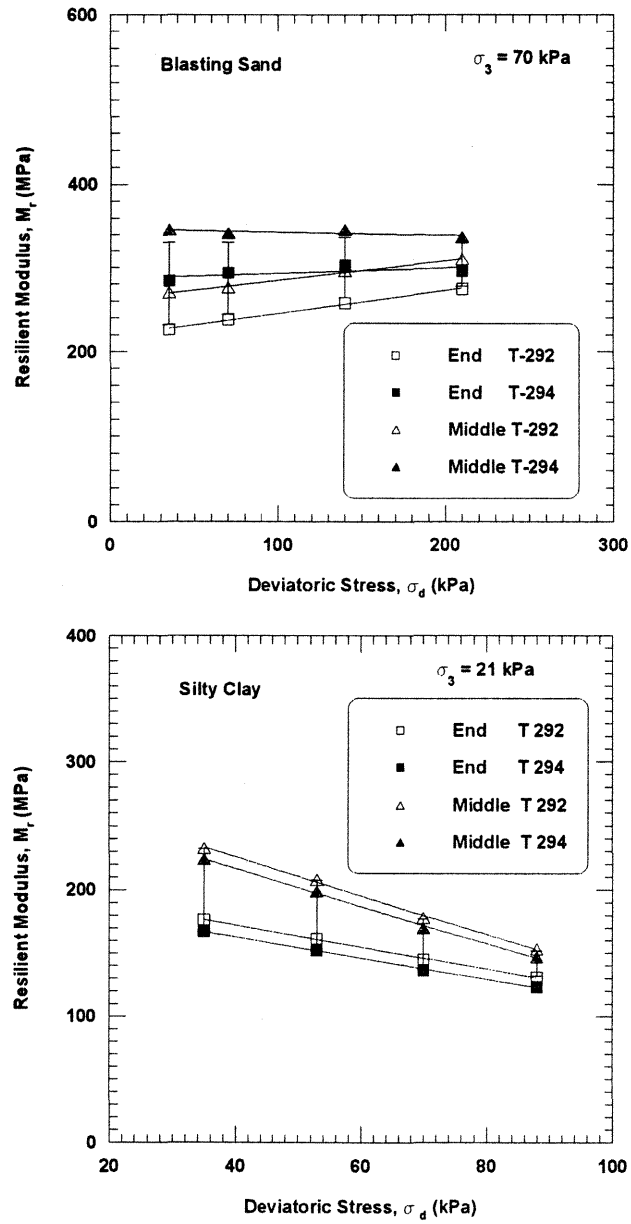

FIGURE 4 Influences of test stresses on M_r values of both soils (*13*).

stress (140 kPa). In both procedures, therefore, previous conditioning (T-294) and testing (T-292) stabilized the sample and reduced the stress dependency behavior to an extent beyond which the testing procedures did not contribute to any significant variation in the results.

Equation 3 is derived based on the results reported in Figure 5. This equation, which provides the procedure coefficients, is valid for both measurement systems and confining pressures of magnitudes 35, 70, and 105 kPa. For other confining pressures of 21 and 140 kPa, the coefficients remain constant for all deviatoric stresses and are around 1.08.

$$PC = 1.28 - 0.00115 * \sigma_d \quad (3)$$

where σ_d is the deviatoric stress in kPa.

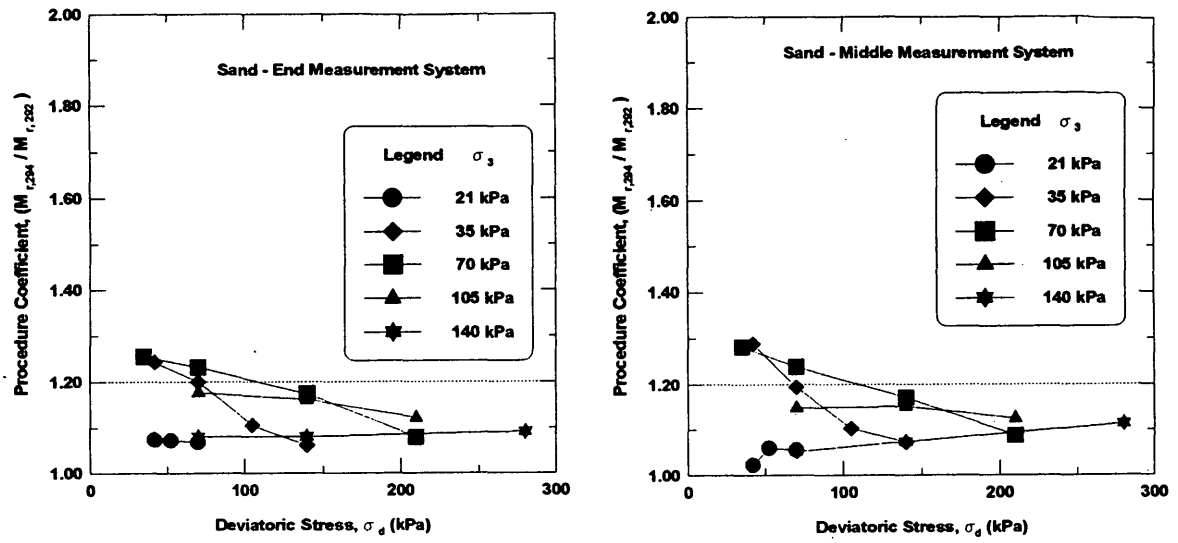

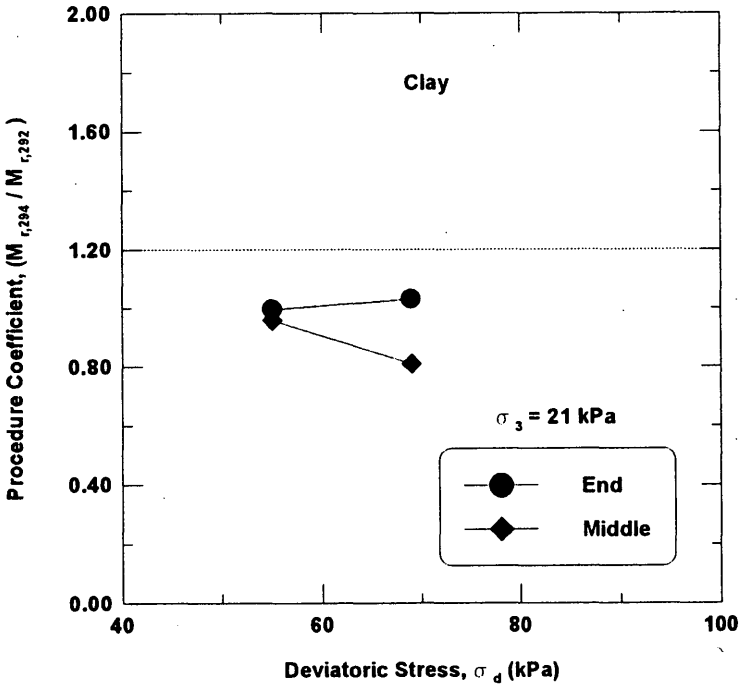

FIGURE 5 Procedure coefficients (sands and clays).

Figure 5 also depicts the procedure variation on clays but does not provide enough information for discussion because, for testing on clays, both procedures have different confining pressure and deviatoric stress sequences. The only common test stresses are the confining pressure of 21 kPa and the deviatoric stress of 72 kPa. To determine another PC value, results from the deviatoric stress of 55 kPa in T-294 and 52 kPa in T-292 are assumed to be equivalent. The PC values of these two deviatoric stresses are calculated and are also shown in Figure 5. These coefficients from both measurements are around 1.0, except at the middle system, which has a value of 0.8 at 72 kPa deviatoric stress and 21 kPa confining pressure. Swelling phenomenon and stress dependency may have occurred for the specimens tested under T-294 at 21 kPa confining pressure as a result of a drop from the previous confining stress, which was 42 kPa. These phenomena appear to have more influence on middle measurement results, therefore, lower M_r and PC values are calculated by the middle measurement system at 72 kPa deviatoric stress. Overall the procedure variation on M_r values for clay specimens is not as significant as in the case of sands because the procedures for clay specimens do not have a wide range of testing stresses and the lower magnitudes of confining pressures (0 to 42 kPa range).

Measurement System

The influence of the measurement system is presented in the form of a measurement coefficient (MC), which is defined as the ratio of the resilient modulus or axial strain measured by the middle system to that measured by the end system. These coefficient values are determined for both procedures and test stresses. The coefficient can be used to convert the end measurement system results to more realistic middle measurement system results.

Figure 6 presents the variation of MC values of sands for both AASHTO procedures. The MC values range from 1.20 at lower confining and deviatoric stresses to 1.08 at higher confining and deviatoric stresses. The lower value is due to the perfect contacts between the end plates, porous stones, and the specimen ends at higher stresses. This is the reason that both measurement systems measured relatively similar values. An average measurement coefficient value of 1.14 is recommended for converting M_r values for the end system to M_r values for the middle system.

Figure 6 also presents the MC values obtained from results on clay specimens. The influence of the measurement system can be clearly seen from this figure. MC values ranging from 1.5 to 1.6 are observed for unconfined conditions. These significantly higher coefficients are due to the complex behavior of clay specimens that can result from specimen preparation, stress history caused by the stress sequence of the testing (note that T-292 shows only loading sequence and T-294 has both loading and unloading sequences),

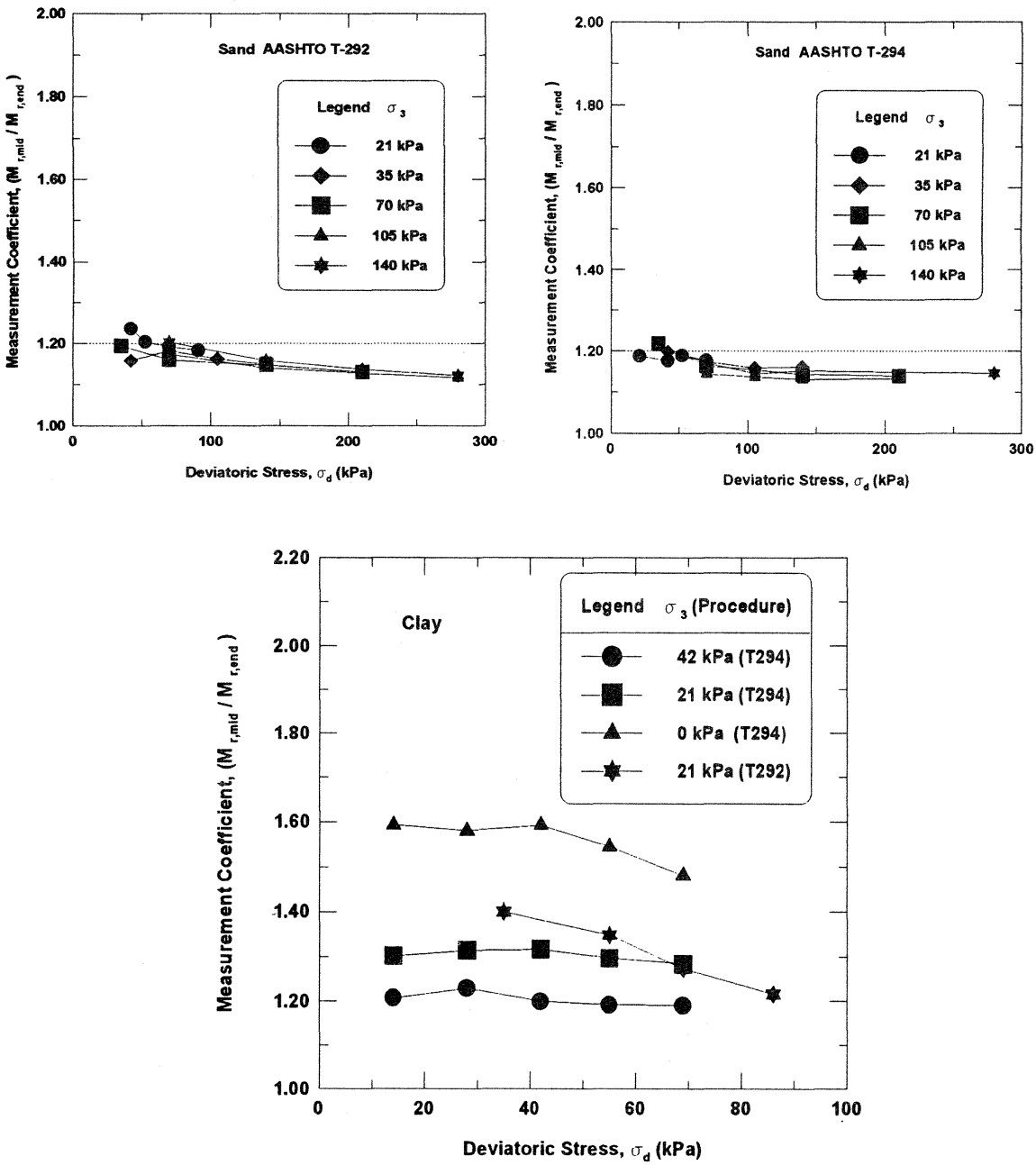

FIGURE 6 Measurement coefficients (sands and clays).

imperfect end contacts, and system compliance errors. Specimen preparation using a standard Proctor test may not produce the same soil fabric in all layers. The bottom layer is subjected to more blows or energy than the top layer, even though each layer is subjected to a similar number of blows. This, coupled with the variations due to test stress sequences that cause stress dependency behavior and errors due to instrumentation, will significantly influence the displacement measurements. The end system that measures the displacements over the full length of the specimen will be more influenced by these problems than the middle system. The end system therefore measured significantly higher displacements, which resulted in lower M_r values and higher measurement coefficients.

These MC values decrease with an increase in confining stress and, to some extent, with deviatoric stress. The MC values from both test procedures, which match at 21-kPa confining pressure, are compared in Figure 6. These values are similar and vary between 1.2 to 1.52, with most around 1.3.

The following measurement coefficient equation for clays is derived from the results shown in Figure 6. The deviatoric stress is not taken into account in the equation because its influence on MC value is relatively insignificant.

$$MC = 1.52 * e^{-0.00594 * \sigma 3} \quad (4)$$

Regression Models

Regression models are used in the form of equations for predicting the moduli. The theta (θ) or the bulk stress and the deviatoric stress are used as predictors in these models on the basis of whether the soil is cohesionless or cohesive (*8,9,12*). These models were recommended in AASHTO T-292, T-294, and Strategic Highway Research Program Protocol P-46. The model can be expressed as

$$M_r = k_1 * \theta^{k2} \quad \text{granular soils} \quad (5)$$

$$M_r = k_3 * \sigma_d^{k4} \quad \text{cohesive soils} \quad (6)$$

where k_1 and k_2 (granular soils) and k_3 and k_4 (cohesive soils) are regression coefficients.

The regression coefficients were determined from the test results for both soils (Figure 7) and are given in Table 4. It is interesting to note that $k_2$and k_4, which are slopes of the lines in the respective models, appear to be mainly dependent on the type of soil tested and to some extent on conditioning and testing procedure. In the case of sands, the variation of k_2 obtained from both AASHTO procedures (0.49 to 0.47) is negligible; however, the same is not true in the case of clay soils. The k_4 values from both procedures are significantly different from one another because of the variations in the conditioning and testing procedures. The other constants, k_1 and k_3, which are intercepts in the figures, depend both on the testing procedures and on the measurement systems. As expected, higher k_1 and k_3 values are obtained for the middle system than for the end system because of higher measurements of resilient moduli. Figure 8 shows the influence of the type of soil, the testing procedure, and the measurement system on the regression coefficients.

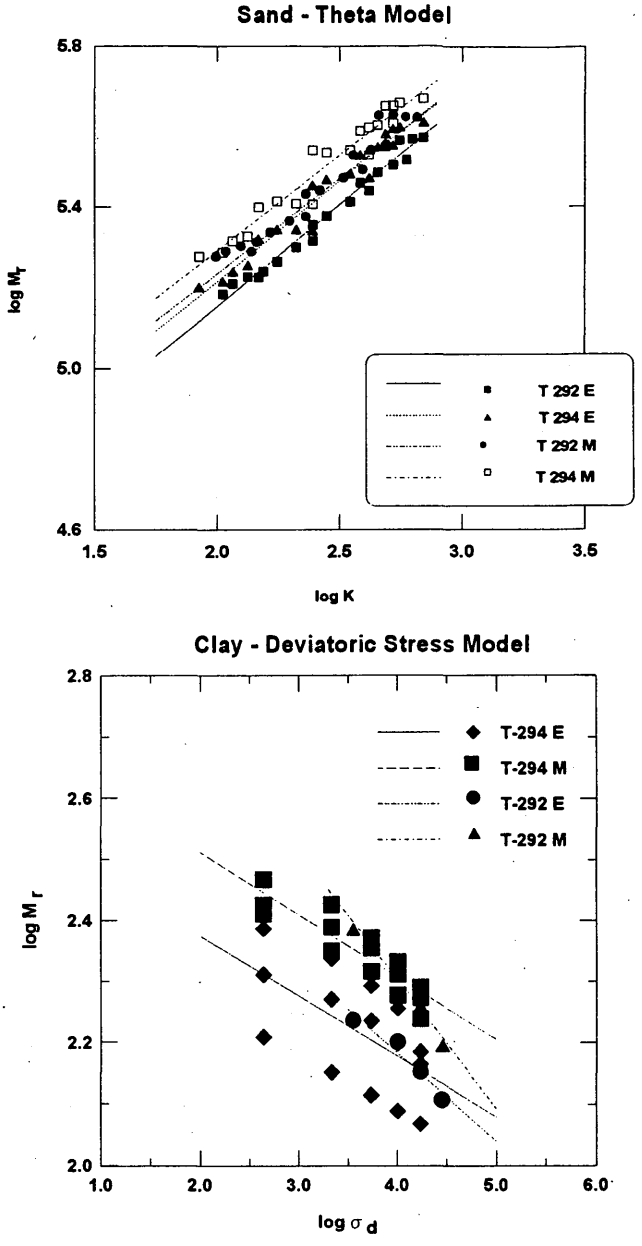

FIGURE 7 Regression models: sands (θ model) and clays (deviatoric stress model).

DISCUSSION OF RESULTS

The testing procedure influenced the resilient moduli of sands more significantly than those of clays. This can be attributed to the sequences involved in the conditioning and testing that make the specimens stress dependent and in some cases may cause some disturbance to the sample. The ranges of stresses for sands are also significantly larger than those for clays. T-294 is more conductive for testing sands because it has less variation in the deviatoric stress magnitudes in the successive test sequences (Figure 3). Moreover in the testing phase the deviatoric stress increases at each confining pressure. Therefore results from the T-294 procedure are unaffected by the specimen stress dependency phenomenon at higher stresses. The T-294 procedure for clays has both loading (deviatoric) and unloading (both deviatoric and confining stresses) phases. The range and magnitudes of confining stresses for both procedures for clays are significantly low, which may be the reason for clays not showing significant procedure variation.

TABLE 4 Regression Constants: θ and Deviatoric Stress Models

	Sand		Silty Clay	
Procedure & Measurement System	k_1	k_2	k_3	k_4
T-292E	4.15	0.49	2.75	-0.14
T-292M	4.30	0.47	3.15	-0.21
T-294E	4.23	0.49	2.57	-0.10
T-294M	4.35	0.47	2.71	-0.10

Note: E - End System; M - Middle System; T-292 and T-294 - AASHTO Procedures.

The following PC can be used to determine the moduli values of T-294 procedure:

$$M_{r,294} = PC * M_{r,292} \quad (7)$$

where

PC = 1.08 (sands—both measurement systems, σ_3 = 21 and 140 kPa; all σ_d values),
PC = 1.28 − 0.0015 * σ_d (sands—both measurement systems, σ_3 = 35 to 105 kPa), and
PC = 1.00 for clays at all measurement systems and stresses; and 0.8 for σ_3 = 21 kPa and σ_d = 72 kPa for middle measurement system.

Because the resilient moduli values were computed based on a uniform state of stresses and strains, the middle internal measurement system will be the appropriate one to use. As explained earlier, however, the end internal measurement system is easier to use routinely than the middle system. Whenever end measurement systems are used, the measurement coefficients must be multiplied with the end measurement resilient moduli to get realistic resilient moduli that can be used in the design of flexible pavements. The measurement coefficient is presented for both soils in the following equation:

$$M_{r,\text{mid}} = MC * M_{r,\text{end}} \quad (8)$$

where

MC = 1.14 (sands—both procedures, for all σ_3 and σ_d values) and
MC = 1.41 $e^{-0.0365\,\sigma 3}$ (clays—both procedures).

These factors are only recommended for the soils tested. Additional research needs to be conducted to develop such factors for other soils.

SUMMARY AND CONCLUSIONS

Several resilient modulus tests were conducted using two AASHTO procedures on both granular and cohesive soils (A-3 sand and A-7 silty clays). Two types of internal systems were used for displacement measurements. The following conclusions were obtained from this study:

1. Procedures have some influence on sands because of the differences in the stress sequences. The T-292 procedure causes more stress dependency and disturbance to the specimen than the T-294 procedure because of the sudden stress jumps of significant magnitudes.
2. For clays tested, the resilient modulus from both procedures is not significantly different. This is thought to be due to the smaller magnitudes of confining stresses used in these procedures. Data used for understanding the procedure variation of clays are not sufficient to provide meaningful conclusions.
3. Measurement systems have more influence on clays than on sands. This is attributed to changes in the fabric of the specimen due

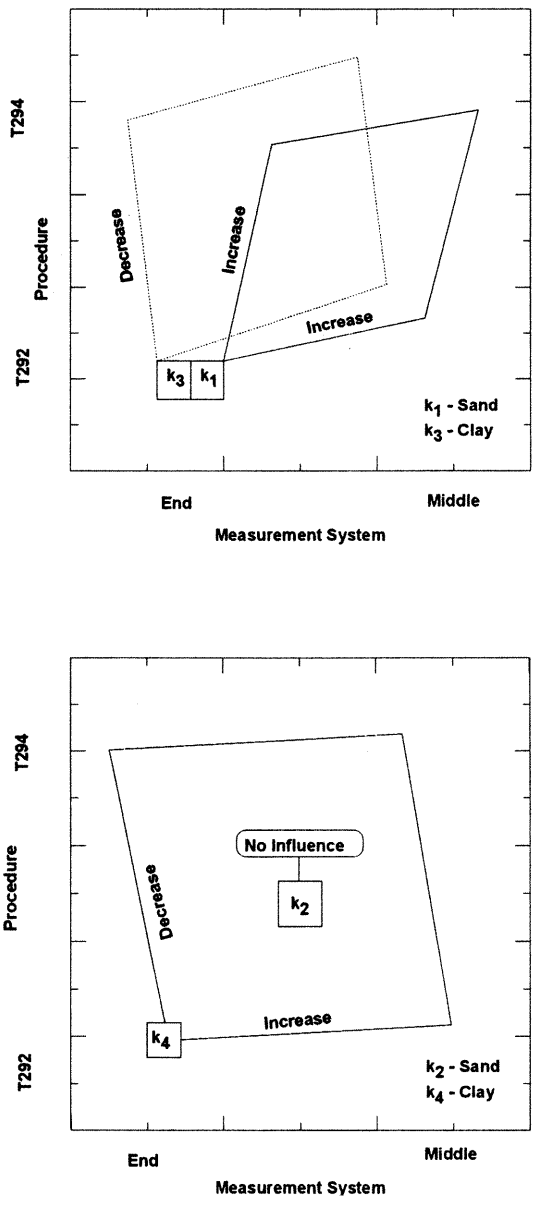

FIGURE 8 Regression model: a graphical picture about constants.

to the preparation procedures; the test stress sequence, which may have resulted in stress dependency behavior; the visco-elastic behavior of the clays; and the imperfect contacts at the ends of the specimen. Even though some of these problems are present, the primary reason for obtaining lesser measurement coefficients for sands is the perfect contacts between porous stones and the specimen ends. These perfect contacts may have occurred as a result of the higher magnitudes of the stresses at which the sands are tested.

4. A multiplier of 1.5 to 1.6 is recommended for M_r values of the end system to obtain M_r values at the middle system in an unconfined test on clays. An equation for the measurement coefficient of clays is also provided as a function of confining pressure. The same coefficient is approximately 1.12 for sands.

5. The theta and deviatoric stress models are used to determine the constants for both soils. The constants k_2 and k_4 depend mainly on the type of soil and to some extent on the testing stresses. Constants k_1 and k_3, however, depend on the measurement system and testing procedure. The middle system produced higher k_1 and k_3 values for both soils because of higher resilient modulus determinations.

ACKNOWLEDGMENTS

This work was supported by LTRC under the Louisiana Department of Transportation and Development. The authors wish to express their appreciation for this support.

REFERENCES

1. *Guide for Design of Pavement Structures.* AASHTO, Washington, D.C., 1986.
2. Barksdale, R. D., et al. *Laboratory Determination of Resilient Modulus For Flexible Pavement Design.* NCHRP Report 1–28. Georgia Institute of Technology, 1990.
3. Kim, D. S., K. H. Stokoe. Characterization of Resilient Modulus of Compacted Subgrade Soils Using Resonant Column and Torsional Shear Tests. In *Transportation Research Record 1369,* TRB, National Research Council, Washington, D.C., 1992.
4. Sneddon, R. V. *Resilient Modulus Testing of 14 Nebraska Soils.* Project RES1(0099)P404. University of Nebraska, Lincoln, 1988.
5. Elliott, R. P., S. I. Thornton, K. Y. Foo, K. W. Siew, and R. Woodbridge. *Resilient Properties of Arkansas Subgrades.* Report FHWA/AR-89/004. Arkansas Highway and Transportation Research Center, University of Arkansas, Fayetteville, 1988.
6. Ho, R. Repeated Load Tests on Untreated Soils: A Florida Experience. *Proc., Workshop on Resilient Modulus Testing State-of-the-Practices,* Oregon State University, Corvallis, 1989.
7. Seim, D. A Comprehensive Study on the Resilient Modulus of Subgrade Soils. *Proc., Workshop on Resilient Modulus Testing State-of-the-Practices,* Oregon State University, Corvallis, 1989.
8. Thompson, M. Factors Affecting the Resilient Moduli of Soils and Granular Materials. *Proc., Workshop on Resilient Modulus Testing State-of-the-Practices,* Oregon State University, Corvallis, 1989.
9. Thompson, M. Resilient Modulus of Subgrade Soils. *Proc., Workshop on Resilient Modulus Testing State-of-the-Practices,* Oregon State University, Corvallis, 1989.
10. Baladi, G. Resilient Modulus. *Proc., Workshop on Resilient Modulus Testing State-of-the-Practices,* Oregon State University, Corvallis, 1989.
11. Houston, W. N., S. L. Houston, and T. W. Anderson. Stress State Considerations for Resilient Modulus Testing of Pavement Subgrade. Presented at 71st Annual Meeting of the Transportation Research Board, Washington, D.C., 1992.
12. Mohammad, L. N., A. J., Puppala, and P. Alavilli. Effect of Strain Measurements on Resilient Modulus of Sands. *In Special Technical Publication 1213: Dynamic Geotechnical Testing: Second Volume* (R. J. Ebelhar, V. P. Drnevich, and B. L. Kutter, eds.), ASTM, Philadelphia, Pa., 1994.
13. Mohammad, L. N., P. Alavilli, and A. J. Puppala. Data Acquisition System for Determining the Resilient Modulus of Soils. *In Geotechnical Special Publication 37: Advances in Site Characterization: Data Acquisition, Management and Interpretation,* ASCE, Dallas, Tx., 1993, pp. 27–41.
14. Pezo, R. F., G. Claros, and W. R. Hudson. An Efficient Resilient Modulus Testing Procedure for Subgrade and Non-Granular Subbase Materials. Presented at the 71st Annual Meeting of the Transportation Research Board, Washington, D.C., 1992.
15. Vinson, T. Fundamentals of Resilient Modulus Testing. *Proc., Workshop on Resilient Modulus Testing State-of-the-Practices,* Oregon State University, Corvallis, 1989.
16. Wilson, B. E., et al. Multiaxial Testing of Subgrade. *In Transportation Research Record 1278,* TRB, National Research Council, Washington, D.C., 1990.
17. *Interim Specifications for Transportation Materials and Methods of Sampling and Testing, Part II: Interim Test Methods.* AASHTO, Washington, D.C., 1992.

Publication of this paper sponsored by Committee on Soil and Rock Properties.

Analysis of Procedures for Establishing In Situ Subgrade Moduli

JEROME F. DALEIDEN, BRIAN M. KILLINGSWORTH, AMY L. SIMPSON, AND RICHARD A. ZAMORA

Through the efforts of the Strategic Highway Research Program Long-Term Pavement Performance study, a vast amount of data has been collected on hundreds of pavement test sections across North America. As part of this effort, extensive subgrade data have been collected, including Atterberg limits, gradations, moisture contents, deflection data, laboratory resilient moduli, and subgrade profiles. With this wealth of information on the subgrade and its associated properties, it becomes possible to evaluate previously proposed methods for determining the subgrade resilient moduli and possibly to develop new models to improve the ability to estimate soil support conditions for pavement design purposes. Three methods for determining the subgrade resilient moduli are considered: laboratory testing, backcalculation using deflections measured from nondestructive testing (NDT), and an estimation equation contained in the 1986 *AASHTO Guide*. There is currently no consensus as to which moduli value should be used for pavement design. An attempt is made to develop relationships between the various sources for moduli prediction. Based on the data currently available, there appears to be little if any relationship between these various methods for determining the resilient modulus of a subgrade. Efforts were made to develop moduli prediction equations based on various subgrade properties and NDT. The subgrades were separated into basic soil classifications (clay, sand, and silt) and models were developed for each subgrade type. Each model contains the load and sensor 7 reading from falling weight deflectometer test results. Other properties that proved to be significant were the thicknesses of the pavement layers, percent saturation of the subgrade, dry densities, and specific gravities.

A pavement structure is designed to distribute the vehicle loadings to which it is exposed. If that pavement structure is not designed appropriately for its underlying support, it will fail. Pavement designers must take into account the properties of the subgrade on which the road is built to ensure that sufficient pavement structure is provided to adequately distribute the anticipated loading.

Taking these fundamentals of pavement design into account, the stiffness of the subgrade is obviously an important parameter in pavement design. Many unique methods have been developed over the years for representing the subgrade support and estimating the subgrade stiffness, but to date there is no consensus on how to best establish the stiffness of the subgrade for pavement design purposes.

Through the efforts of the Strategic Highway Research Program (SHRP) Long-Term Pavement Performance (LTPP) Program, considerable data have been collected on pavement subgrades. In addition to the fundamental subgrade properties (e.g., Atterberg limits, gradation, and in situ moisture content), deflection data, lab resilient moduli, and data on the subgrade profile to a depth of 20 ft have also been accumulated. With this wealth of information on the subgrade and its associated properties, relationships that exist among all of these various properties should be established to provide a more comprehensive understanding of subgrade support for future pavement design work. Several researchers have reported on various facets of this complicated subject (*1,2*). The LTPP data base, however, provides such a vast array of data types for so many sections (more than 700) that some of the methods previously prescribed for estimating soil support conditions can now be evaluated and modifications established that will ultimately enhance predictive capabilities. Data from only the North Atlantic and Southern SHRP regions were available for this analysis.

As part of the LTPP Program, backcalculation of test section deflection data has been conducted using the MODULUS program to establish the layer moduli for each test section. Subgrade moduli from these backcalculation procedures were evaluated in conjunction with the lab-determined moduli and estimated subgrade moduli on the basis of procedures prescribed in the 1986 *AASHTO Guide to the Design of Pavement Structures* (*3*). Comparisons of these three sources of subgrade moduli were used along with the other subgrade properties in an attempt to identify where relationships exist among these various sources of subgrade moduli data and to identify methods for estimating subgrade stiffness in the absence of resilient modulus or deflection testing. Although there has been some debate as to which source of subgrade stiffness data is best suited for pavement design, no efforts are made here to prove or disprove the merits of either source.

SHRP-LTPP DATA BASE

Under SHRP, many different types of data have been collected on various test sections within the United States and Canada, including information about traffic, pavement materials, and structural parameters, as well as monitoring information. All of these data are stored in a data base in the form of tables using the Oracle program. Under SHRP, the United States and Canada were divided into four regions, with each region responsible for all of the data collection and monitoring within its respective area. Each region also controls the data base for that region and semiannually uploads its data to a national data base in Washington, D.C. The data used in this analysis were obtained from that data base, and the statistics for the data set are presented in Table 1. Because of testing limitations at SHRP, however, only lab resilient moduli values for the Southern and North Atlantic regions were available for this analysis.

MODULI PREDICTION PROCEDURES

For this analysis, subgrade resilient moduli from three sources were used. The first source was laboratory resilient modulus testing.

J. F. Daleiden, B. M. Killingsworth, and A.L. Simpson, Brent Rauhut Engineering, 8240 Mopac, Suite 220, Austin, Tex. 78759. R.A. Zamora, FHWA, 8240 Mopac, Suite 250, Austin, Tex. 78759.

TABLE 1 Statistical Values of Data Set Used in Analysis

Variable	Units	No. of Values	Mean Value	Standard Deviation	Low Value	High Value	Range
Back calculated Modulus	psi	534	29214	29778	0	292000	292000
Laboratory Resilient Modulus	psi	671	9694	3882	0	54023	54023
AASHTO Estimated Resilient Modulus	psi	546	40132	25759	0	260596	260596
In Situ Moisture	%	671	14.8	7.7	1.2	43.4	42.2
Plasticity Index		671	7.8	10	0	61	61
Liquid Limit		671	20.1	18.8	0	81	81
Plastic Limit		671	12.2	11	0	51	51
% passing #200 Sieve	%	671	43.7	28.1	0	99	99
Effective Depth to Rigid Layer	in	523	316	235	43.8	600	556.2
Specific Gravity		671	2.68	0.07	2.49	3.1	0.6
Wet Density		671	123.3	9.0	92.8	150.8	58.0
Saturation		671	67.7	19.7	6.0	162.1	156.1
Dry Density		671	108	10.5	76.6	135.8	59.2
Sensor 7 Deflection	mils	284	1.33	0.64	0.08	4.03	3.45
FWD Load	lbs	284	9335	441	7528	10475	2947
Base Thickness	In	664	8.5	8.91	0	47.1	47.1
Surface Thickness	In	664	11.5	6.01	1.1	34	32.9

"Undisturbed" samples were collected in Shelby tubes where possible. Where undisturbed samples could not be obtained, bulk samples were obtained and samples remolded for testing. The second source was a backcalculation process using measured deflections from all seven sensors of a falling weight deflectometer (FWD). The third source was an estimation procedure using the load and the measured deflection from the seventh sensor of an FWD. The following is a brief explanation of these three sources of subgrade moduli.

Laboratory Estimation of Subgrade Moduli

Laboratory moduli included in this analysis were determined using SHRP protocol P46, "Resilient Modulus of Unbound Granular Base/Subbase Materials and Subgrade Soils." The modulus from this test is determined from the results of repeated-load triaxial compression tests. The resilient modulus is expressed as the ratio of the amplitude of the repeated axial deviator stress to the amplitude of the resultant recoverable strain, and each value is related to a specific stress state.

The test method consists of applying a repeated axial deviator stress of fixed magnitude, load duration, and cycle duration to a cylindrical test specimen. The specimen is subjected to a constant (static) lateral stress by means of the triaxial test chamber where the specimen is placed for testing. The recoverable axial deformation of the specimen is measured and used to calculate the resilient modulus. For this analysis the resilient modulus values were determined using a deviator stress of 2 psi and a confining pressure of 2 psi (M_{R22}). It was believed that these values best represented the average stress and pressure values that occur in the subgrade under traffic loading and surcharge.

Backcalculated Estimation of Subgrade Moduli

Backcalculation of the subgrade moduli was conducted using a microcomputer-based procedure called MODULUS 4.0 (*4*), which was selected by SHRP for LTPP after careful study of available backcalculation software. This procedure estimates the layer moduli using deflections for seven sensors measured by an FWD. The objective of any backcalculation routine is to process the deflection data and estimate the pavement material properties on the basis of these data and the applied load. This can be accomplished by employing a procedure that predicts a set of parameters that corresponds to the best fit of the measured deflection bowl. Best fit is achieved when the percent error between the measured deflection bowl and the calculated deflection bowl is minimized. A data base of calculated deflection bowls can be generated by elastic layer theory (assuming ranges of material properties) and then used as a comparative tool by which the error is minimized.

Once the error between measured and calculated deflection bowls is minimized, the calculated modulus for each layer of the pavement structure associated with the calculated deflection bowl that best fits

the measured bowl together are used as the layer moduli of the existing pavement. In summary, the steps followed by MODULUS to backcalculate pavement layer moduli are as follows:

1. Input measured deflection data obtained from FWD testing, the applied load, and other pavement properties (layer thickness, estimated range of layer moduli, and Poisson's ratio).
2. Generate calculated deflection bowls using elastic layer theory.
3. Minimize the percent error between calculated and measured deflection bowls.
4. Determine layer and subgrade moduli on the basis of calculated deflection bowl that corresponds to lowest percent error.

It should be noted that the MODULUS program is only one of many backcalculation programs available. These programs are developed on basically the same theory, but they can and will generate different results when supplied with the same input. This point is made because the analysis process could also include the results from these other programs, but no effort is made here to do this.

Estimation of Subgrade Moduli from Deflection Testing

The 1986 *AASHTO Guide to the Design of Pavement Structures* (*3*) includes a procedure that uses deflection testing results to estimate the subgrade resilient modulus. Figures 1 and 2 show a typical deflection profile and corresponding stress "bulb" in a pavement structure as it is loaded at a specific point. The stress bulb, or conical zone, represents the way in which the load application is spread through the pavement system under a steady state or impulse NDT load. The slope of the line that projects through each pavement layer reflects the relative modulus, or stiffness, of the material within the layer, with a fundamental being that as the modulus increases, the stress within the layer is spread over a greater area (*3*).

It is generally accepted that deflections measured far enough away from the center of the load can be used to characterize the subgrade stiffness. As shown in Figure 1, at the distant sensors the pavement surface deflection that is occurring is due only to the stresses or deformations from the subgrade itself, and therefore the outer readings primarily reflect the stiffness of the subgrade soil.

As reported in the AASHTO Guide, using deflection measurements collected from the sensor located at a distance of $1 < r/a_e < 6$ (where r is the outer geophone radial distance from the applied load and a_e is the radius of the stress bulb at the interface of the subgrade and bottom layer of the pavement), the subgrade modulus may be estimated from the following equation:

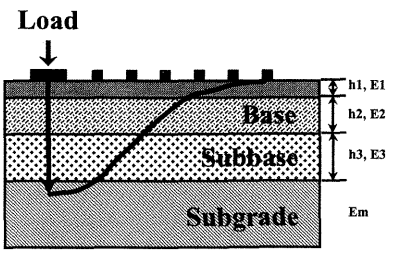

FIGURE 1 Exaggerated deflection basin from FWD.

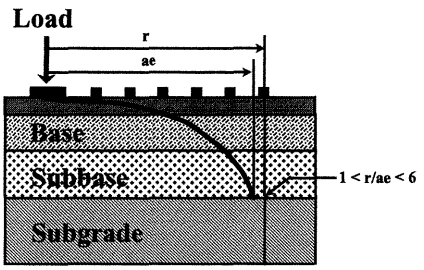

FIGURE 2 Stress "bulb" under FWD load.

$$E_{sg} = \frac{P S_f}{d_r r} \quad (1)$$

where

E_{sg} = in situ modulus of elasticity of the subgrade (psi).
P = plate load of the NDT device (lb),
d_r = measured NDT deflection at radial distance r from the center of the plate load (mils),
r = radial distance from plate load center to the point of the deflection measurement (in.) and
S_f = prediction factor based on the soil's Poisson's ratio as shown in Table 2.

Other values for the prediction factor may be obtained from the Guide with the use of a figure that plots the prediction factor versus the radial offset ratio for varying Poisson's ratio values. As the ratio increases the prediction factor also increases until it becomes constant past a ratio of one.

Using this process, the subgrade modulus may be directly estimated without costly computing time and software; however, prediction accuracy may be lost due to the varying nature of subgrade properties.

COMPARISONS

An unprecedented wealth of data on subgrade properties for more than 300 test sections offers many possibilities for the evaluation of subgrade stiffness. The following studies were considered in this analysis:

1. Straightforward comparison between the various moduli estimation procedures (i.e., determining ratios between predicted moduli values from each estimation procedure);

TABLE 2 Prediction Factors Based on Poisson's Ratio

u	S_f
0.50	0.2686
0.45	0.2792
0.40	0.2892
0.35	0.2874
0.30	0.2969

2. Determination of direct relationships between the moduli estimation procedures using regression techniques;
3. Determination of relationships between moduli estimation procedures using regression techniques and including other known properties that influence the resilient modulus; and
4. Development of new procedures to estimate the subgrade moduli on the basis of the subgrade data available.

Results of these studies are provided here to highlight where relationships were and were not found. It is also anticipated that the results noted here may lend insight to those who wish to explore these data further.

Direct Comparisons of Moduli Values from Various Sources

The first comparison explored here was a straightforward comparison using ratios of the various subgrade moduli values. As shown in Table 3, there is a wide range of ratios between the estimated moduli from the AASHTO equation and the backcalculated moduli from the MODULUS program, and between both the backcalculated and estimated moduli and the moduli determined by laboratory testing. The wide scatter of ratios between the backcalculated moduli and the moduli from laboratory testing is consistent with previously published reports and tends to highlight the noted concerns about which values are most appropriate for pavement design purposes (*1,2*).

Regression Analyses Between Various Moduli Sources

Acknowledging that no simple relationship exists, the next step was to explore other relationships that might exist. These studies were conducted by performing linear regression analysis between each of the moduli sources. As one might expect review of ratios mentioned previously revealed no significant relationship between the laboratory and backcalculated moduli. The coefficients of determination (R^2) for this regression analysis did not rise above 0.10, and the root mean square error (RMSE) was generally as large as the moduli values.

Researchers recognized that the relationship between lab and backcalculated moduli must be a function of the subgrade properties, among other things, and expanded the regression analysis to include Atterberg limits, gradations, depth to rigid layer, moisture contents, and other data as available. Even with this additional data, however, a significant relationship could not be found.

One relationship that did prove to be somewhat significant occurred between the estimated and the backcalculated moduli. The estimated value was calculated using Equation 1 and an assumed Poisson's ratio of 0.45. A linear regression analysis of the moduli prediction sources yielded $R^2 = 0.37$ and RMSE = 23,404.

The analysis of estimated versus backcalculated moduli was then expanded to include various subgrade properties in an attempt to improve on this relationship. The inclusion of subgrade properties did improve the relationship, but the results were still somewhat less than favorable ($R^2 = 0.50$, RMSE = 20,949). This is particularly intriguing when one considers that both of these subgrade moduli values are based on essentially the same basic data. From this observation it was established that development of a better estimation procedure may be warranted.

Modification of the Moduli Estimation Equation

Modification of the estimation equation was attempted using a linear regression analysis between the backcalculated moduli and the constant term from Equation 1, $P/d_r r$. The resulting coefficient from this analysis could be used as a new value for S_f. It should be noted that the regression for this particular analysis was performed with the no intercept option, which forces the y-intercept through the origin. This analysis procedure produced a new $S_f = 0.1508$ with an R^2 of 0.56 and an RMSE of 20,601. This appears to indicate, at least for the data available, that a slightly improved estimation equation has been formulated with which subgrade moduli can be predicted solely from the seventh sensor deflections and load from NDT.

Predictions of Backcalculated Moduli

As noted previously, use of the equation form shown in the AASHTO Guide for predicting backcalculated subgrade moduli provided reasonable results, but it was believed that a better relationship must exist. To further explore the data, efforts were made to predict the backcalculated moduli using the various data elements noted with a variety of different equation forms.

In initial attempts to establish a relationship no distinctions were made among the various subgrade types. As one might expect, however, the Atterberg limits and gradation information were significant to these relationships. On the basis of this information the sections were sorted and separated by subgrade type to facilitate these analyses. Sections with greater than 50 percent passing the number 200 sieve were considered fine subgrades (clay or silt). The fine subgrades were further distinguished using the plasticity index (PI); subgrades with PIs of greater than 10 were considered clays. Good relationships were ultimately established for each of the three subgrade types in these analyses (clay, silt, and sand). Only seven sections had gravel subgrades, so these sections were not included in

TABLE 3 Direct Comparison Among Moduli from Different Sources

Ratio	Mean	Standard Deviation	Maximum	Minimum
Laboratory / Back calculated	0.57	0.67	10.34	0.01
Estimated / Laboratory	4.65	3.81	58.09	1.10
Estimated / Back calculated	2.34	2.94	36.56	0.20

the analysis. The equations are shown below and the associated statistics are presented in Table 4.

Clay:

$$M_R = 0.88\left(\frac{ld}{S7}\right) + 90.13\left(\frac{b^2}{S7}\right) - 4.88 \times 10^{-3}(b)^2(ld) + 1.47 \times 10^{-4}(sat)^2(ld) - 0.08(b)^2(t)^2 + 116{,}774\left(\frac{b^2}{sat^2}\right) + 94{,}749\left(\frac{t^2}{sat^2}\right) - 2{,}707.99$$

Silt:

$$M_R = 30.17\left(\frac{b^2}{S7^2}\right) + 3.84 \times 10^{-4}(ld^2) + \frac{611{,}120}{spgr} + 630.12\left(\frac{b^2}{t^2}\right) - 23.54\,(b)^2(spgr) + 2{,}439.62\left(\frac{t}{spgr}\right) - 258{,}797$$

Sand:

$$M_R = \frac{-2{,}834{,}967}{dd} + 1.31 \times 10^{-4}(ld)^2(S7) + 15.04(b)^2(S7) + 371.33\left(\frac{dd}{S7}\right) - 3.01 \times 10^{-6}(ld)^2(dd) - 2{,}751.43\left(\frac{t^2}{dd}\right) + 22{,}372$$

where

$S7$ = Sensor 7 reading from FWD (mils),
ld = load from FWD (lb),
t = asphalt or concrete thickness + treated base thickness (in.),
b = untreated granular base thickness (in.),
$spgr$ = specific gravity of the subgrade,
sat = percent saturation, and
dd = dry density of the subgrade.

Common to each of these models is the load and deflection at Sensor 7. Because only Sensor 7 deflection readings were included in this analysis (at a spacing of 60 in. from the load), the distance from the load to the sensor was not needed as a variable. Similarly the area of the loading was constant for each section (using a 12-in.-diameter plate), hence the area also was not a function in the analysis. Variables that did prove significant were the thicknesses of the pavement layers, in situ moisture contents, dry densities, and specific gravities.

Sensitivity Analysis

A simple set of factorial tables was designed using a wide range of input values for each variable to determine the validity of the models. Testing the equation in this way can establish how the equation performs for input values outside the inference space from which it was developed, but still within practical limits. Table 5 presents the ranges used in this analysis.

The model for a sand subgrade appears to yield reasonable values for the backcalculated subgrade moduli for the input ranges considered. Subgrade moduli values generated ranged from 6200 to 153,000 psi. Values greater than 100,000 psi appear high; however, for deflections of 0.25 mils (typically associated with "rock" subgrades) this is not all that surprising.

TABLE 4 Statistics for the Three Subgrade Moduli Prediction Equations

Equation	R^2	Adjusted R^2	Root Mean Square Error
Clay	0.8886	0.8739	6,997
Silt	0.7809	0.7238	11,419
Sand	0.8371	0.8276	15,033

The model for silt seems to falter at the high end of the specific gravity range. Specific gravities in excess of 2.7 tend to produce negative values. This is not a realistic value for specific gravity, however, and if the range of specific gravities is narrowed to a range of around 2.3 to 2.6, moduli generated values begin to appear more consistent with expectations.

The clay model fails at the low end of the percent saturation range. For saturation levels of 10 percent, subgrade moduli values can exceed 700 ksi. Saturation levels of 10 and 20 percent do not seem unreasonable, but they are outside the inference space from which these equations were developed. If the saturation level remains above 30 percent, the equation appears to provide reasonable estimates of backcalculated subgrade moduli.

CONCLUSIONS

The SHRP LTPP program has produced a considerable amount of information characterizing pavement structures. These data were used to attempt to improve existing procedures and develop new procedures to predict subgrade resilient moduli. Equations generated from this analysis can be used to predict subgrade backcalculated resilient moduli based on NDT data and other subgrade properties. These equations have relatively high correlation coefficients (from .78 to .89) and low root mean square errors.

In addition to developing new prediction equations, an attempt was made to redevelop the prediction factor, S_f, used in the AASHTO Guide's subgrade moduli prediction equation. A new factor was established on the basis of the data set with reasonable statistics. It appears that the layer structure has a greater impact on estimations of subgrade moduli than is commonly accepted. However each of the equations generated using all available data were heavily dependent on the layer structure. This could also indicate that Sensor 7 is not sufficiently distant from the load in the SHRP sensor setup.

Evaluations were conducted to explore relationships among the various sources of subgrade moduli. With the volumes of data avail-

TABLE 5 Ranges Used for Sensitivity Analysis

Variable	Range
Load	8,000 - 10,000 (lbs)
Sensor 7	0.25 - 2 (mils)
Untreated Base	4 - 20 (inches)
Treated Base + Asphalt/Concrete	4 - 12 (inches)
Percent Saturation	10 - 100 (%)
Specific Gravity	2 - 3
Dry Density	85 - 115

able one would expect that some relationship between laboratory and backcalculated subgrade moduli could be established; however, these evaluations did not generate any useful relationships.

RECOMMENDATIONS FOR CONTINUING RESEARCH

This limited analysis has raised many opportunities for further research. Some studies that warrant further pursuit are as follows:

- Continue to seek relationships between laboratory and backcalculated subgrade moduli.
- Develop other moduli prediction equations that include subgrade properties but do not include deflection data.
- Continue to pursue a relationship for estimating laboratory subgrade moduli.

Nonlinear modeling or other modeling techniques may be used to better represent these data and the relationships sought. It is evident, however, that the disparity between these methods of estimating subgrade moduli is fairly substantial. Pavement designers should be particularly cautious when estimating subgrade moduli to ensure that the values used are consistent with those on which their pavement design equations are developed.

REFERENCES

1. Houston, W. N., M. S. Mamlouck, and R. W. S. Perera. Laboratory Versus Nondestructive Testing for Pavement Design. *ASCE Journal of Transportation Engineering,* Vol. 118, No. 2, March/April 1992.
2. Akram, T., T. Scullion, and R. E. Smith. Comparing Laboratory and Back Calculated Layer Moduli On Instrumented Pavement Sections. Prepared for the ASTM Symposium on Nondestructive Testing of Pavements and Back Calculation of Moduli, June 1993.
3. *AASHTO Guide for Design of Pavement Structures.* AASHTO, Washington, D.C., 1986.
4. Uzan, J., T. Scullion, C. H. Michalek, M. Paredes, and R. L. Lytton. *A Microcomputer Based Procedure for Backcalculating Layer Moduli from FWD Data."* Texas Transportation Institute, Report FHWA/TX-88/1123–1, 1988.

Publication of this paper sponsored by Committee on Soil and Rock Properties.